Perturbed Brain Energy Metabolism in Alzheimer's Disease and Diabetes

By

Long Wu

Submitted to the graduate degree program in Pharmacology and Toxicology and the Graduate Faculty of the University of Kansas in partial fulfillment of the requirements for the degree of Doctor of Philosophy.

Liqin Zhao, Ph.D., Chairperson

Shirley ShiDu Yan, Ph.D., Co-Chairperson

Rick Dobrowsky, Ph.D.

Elias Michaelis, M.D., Ph.D.

Nancy Muma, Ph.D.

Michael Wolfe, Ph.D.

Date Defended: May 24th, 2017

The dissertation committee for Long Wu certifies that this is the approved version of the following dissertation:

Perturbed Brain Energy Metabolism in Alzheimer's Disease and Diabetes

Liqin Zhao, Ph.D., Chairperson

Date Approved: May 24th, 2017

Abstract

The brain has high energy demands, which are met by the complete oxidation of glucose, the obligatory energy substrate for the brain under physiological conditions. Glucose oxidative metabolism consists of cytosolic processes that generate pyruvate, TCA cycle that provides reducing equivalents, and mitochondrial oxidative phosphorylation that converts energy to ATP. Consistent with the crucial role of energy metabolism in the maintenance of brain function, impaired glucose metabolism, and mitochondrial dysfunction have been implicated in the pathobiology of many brain disorders, including Alzheimer's disease (AD) and diabetes. In this dissertation, the molecular mechanisms underlying altered glucose metabolism in the brains at genetic risk for AD and perturbed mitochondrial function in diabetes-associated brain dysfunction are studied.

In the first study, the impact of human ApoE isoforms, which confer differential risk for AD, on brain glucose metabolism were investigated in human ApoE gene-targeted replacement mice (hApoE-TR). Gene expression profiling of the cortical RNA extracted from hApoE-TR mice revealed that ApoE2-bearing brains exhibited the most robust, while ApoE4 brains were associated with the most, deficient profile on both the uptake and metabolism of glucose. In particular, the three ApoE brains differed in the expression of hexokinase, which acts as the "gateway" enzyme by catalyzing the conversion of glucose to glucose-6-phosphate, a branch point metabolite that can be directed to glycolysis, glycogen synthesis, and the pentose phosphate pathway. Ingenuity pathway analysis (IPA) predicted that PPAR-γ/PGC-1α signaling pathway could be enhanced in the ApoE2 brain and attenuated in the ApoE4 brain. In line with the prediction, PGC-1α overexpression ameliorated ApoE4-associated bioenergetic deficits. Furthermore, forced

expression of ApoE2 counteracted the detrimental effects induced by ApoE4 as demonstrated by the marked improvement in glycolytic function, mitochondrial respiration, and the concurrent increase in ATP levels in ApoE4-expressing cells transfected with ApoE2 as compared to those transfected with mock control. Taken together, in the first study, we discovered a key cytosolic point in glucose metabolism that is differentially modulated by human ApoE isoforms, which could serve as a potential mechanism underlying their discrete risk impact in AD.

In the second study, the potential roles of cyclophilin D (CypD), a critical regulator of mitochondrial permeability transition (mPT), in diabetes-related mitochondrial abnormalities and cognitive dysfunction were investigated using mice injected with streptozotocin (STZ), a mouse model of type 1 diabetes. Brain mitochondria from STZ-treated mice exhibited a significant increase in CypD expression, a marked decrease in mitochondrial respiratory function, as well as deficits in spatial learning and memory. Notably, genetic deletion of CypD significantly attenuated diabetes-associated defects in mitochondrial function and cognitive deficits. By contrast, upregulation of CypD and defects in mitochondrial respiration were greatly exacerbated in the brains of AD transgenic mice, suggesting AD and diabetes may have synergistic effects on CypD expression and mitochondrial dysfunction. As a result of an exacerbation of mitochondrial dysfunction, cognitive decline was greatly accelerated in AD transgenic mice injected with STZ. Collectively, results obtained from the second study provide new insights into the mechanisms underlying brain mitochondrial malfunction and cognitive impairment, both of which are common pathological features in AD and diabetes.

Acknowledgement

Throughout my graduate studies at the University of Kansas, I have received help from many others, without whom this dissertation would not have been possible. Thus, I would like to express my heartfelt thanks to all of them.

First of all, I would like to express my deepest appreciation to my mentor, Dr. Liqin Zhao, for her persistent guidance, constant support and enduring encouragement in the past two years. Her passion for science and commitment to research have always inspired me. She always wants the best for her students, both on an academic and personal level, for this, I am extremely grateful. I am also thankful for the opportunity she gave me to think freely and explore the directions in my research, which prepared me to be an independent researcher. I would like to extend my thanks to my co-mentor, Dr. Shirley ShiDu Yan, who provided me an opportunity to be involved in several research projects which exposed me to a variety of research techniques. She also taught me the importance of hard-work.

I am grateful to my committee members Drs. Rick Dobrowsky, Nancy Muma and Elias Michaelis for their valuable suggestions and critical advice on my dissertation. Additionally, I would like to express my gratitude to Dr. Michael Wolfe for serving as the outside member on my committee despite his busy schedule. Further, I am thankful to all the faculty in the department of Pharmacology and Toxicology, from whom I learnt to be a scientist.

I owe my gratitude to several members from my previous lab, especially Dr. Lan Guo, who has trained me on most of the biochemical techniques that I'm familiar with. I learnt

the behavior analysis from Dr. Qinru Sun. I would like to thank Drs. Xueqi Gan, Shengbin Huang, Gang Hu, Shijun Yan, Dina Zhu, Qing Yu and Fang Du for their encouragement and companionship. Likewise, I am thankful to my current lab members, Sarah Woody, Anindit Chhibber and Xin Zhang for their friendship and moral support. I am also grateful to several former graduates. Drs. Pan Pan and Ziyan Zhang have helped me tremendously to get through the first two years of graduate school. Dr. Jade Franklin provided me with some helpful suggestion on passing the oral exam.

I would also like to thank people outside the department for their help in my research project. I am thankful to Jennifer Hackett from the genome sequencing core for her help in measuring RNA concentrations. It was very kind of Dr. Xinkun Wang to teach me how to evaluate RNA integrity using the Agilent bioanalyzer.

Lastly, I would like to thank my parents for their perpetual love and unequivocal support. Most importantly, I am fortunate to have such a wonderful mom who understands, respects my decisions and always believes in me. Without her, I would not have made this far. I am also indebted to my fiancé, Ken, for his constant encouragement, great help in improving my English as well as some insightful suggestions and interesting scientific debates on my research.

This work was supported by grants from the National Institutes of Health, the Alzheimer's Association, and University of Kansas internal funds.

Table of contents

Chapter 2 Cyclophilin D-Mediated Mitochondrial Perturbation Underlies Diabetes-Associated Cognitive Dysfunction

List of Figures

List of Tables

List of Abbreviations

2-DG	2-Deoxy-D-glucose
AcAc	acetoacetate
ACAT	acetyl-CoA acetyltransferase
AD	Alzheimer's disease
ADAS-Cog	AD Assessment Scale-Cognitive subscale
ADNI	Alzheimer's Disease Neuroimaging Initiative
AG	aerobic glycolysis
ALS	amyotrophic lateral sclerosis
ANT	adenine nucleotide translocator
ApoE	apolipoprotein E
ApoJ	apolipoprotein J
Aβ	amyloid beta
BBB	blood brain barrier
BDH	β-hydroxybutyrate dehydrogenase
BHB	β-hydroxybutyrate
CMRglc	cerebral glucose metabolic rate
CNS	central nervous system
CREB	cAMP response element binding protein
CsA	cyclosporine A
CSF	cerebrospinal fluid
CypD	cyclophilin D
DMN	default mode network
ECAR	extracellular acidification rate
EPR	electron paramagnetic resonance
ER	endoplasmic reticulum
ERR	estrogen-related receptor
ETC	electron transport chain

FC	fold change
FDG-PET	[^{18}F] fluorodeoxyglucose-positron emission tomography
FRET	fluorescence resonance energy transfer
Glc-1-p	glucose-1-phosphate
Glc-6-p	glucose-6-phosphate
GLUTs	facilitated glucose transporters
GP	glycogen phosphorylase
GSH	reduced glutathione
GSSG	glutathione disulfide, oxidized glutathione
GYS	glycogen synthase
hApoE-TR	human ApoE gene-targeted replacement mice
HD	Huntington's disease
HDL	high-density lipoproteins
HK1	hexokinase I
HK2	hexokinase II
Igf1	insulin-like growth factor 1
IMM	inner mitochondrial membrane
IPA	ingenuity pathway analysis
LDH	lactate dehydrogenase
LDL	low-density lipoprotein
LOAD	late-onset AD
LRP	LDL-receptor-related protein
LTP	long-term potentiation
MAM	mitochondria-associated ER membranes
MAPK	mitogen-activated protein kinases
MCI	mild cognitive impairment
MCTs	monocarboxylate transporters
MDH	malate dehydrogenase

MMSE	Mini-Mental State Examination
MnSOD	manganese superoxide dismutase
mPT	mitochondrial permeability transition
mPTP	mitochondrial permeability transition pore
MRI	magnetic resonance imaging
MS	multiple sclerosis
MWM	Morris water maze
NFT	neurofibrillary tangles
NO	nitric oxide
NRF1	nuclear respiratory factor 1
OCR	oxygen consumption rate
OMM	outer mitochondrial membrane
OSCP	oligomycin sensitivity-conferring protein
PARP-1	poly (ADP-ribose) polymerase-1
PCC	posterior cingulate cortex
PD	Parkinson's disease
PGC-1α	peroxisome proliferator-activated receptor gamma coactivator 1-alpha
PHB	polyhydroxybutyrate
PiC	mitochondrial phosphate carrier
PKA	cAMP-dependent protein kinase A
PP1	protein phosphatase 1
PPAR-γ	peroxisome proliferator-activated receptor gamma
PPP	pentose phosphate pathway
ROS	reactive oxygen species
SCOT	succinyl-CoA: 3-oxoacid CoA transferase
SNP	single nucleotide polymorphism
SPR	surface plasmon resonance
STZ	streptozotocin
TCA	tricarboxylic acid

TFAM	transcription factor A, mitochondrial
TNF-α	tumor necrosis factor-alpha
TOM	translocase of the outer mitochondrial membrane
VDAC	voltage-dependent anion channel
VLDL	very-low-density lipoproteins

Introduction

Alzheimer's disease (AD) and diabetes are chronic disorders that have a rapidly increasing prevalence worldwide and place an enormous burden on the healthcare system and society. According to the World Health Organization, AD and diabetes will be the 6th and 7th leading cause of death respectively by 2030 [1]. AD is a neurodegenerative disease clinically characterized by a progressive decline in memory and cognitive functions. Diabetes, characterized as a peripheral metabolic disorder, has been known to cause complications in the central nervous system, such as cognitive impairment and dementia [2-4]. Numerous epidemiological studies have shown that diabetes, and type 2 diabetes in particular, significantly increased the risk of developing AD [5-9]. Of note, a clinical study reported that over 80% of AD patients had type 2 diabetes or exhibited abnormal glucose levels [10]. These findings implicate a close relationship between AD and diabetes. Mechanistic studies of this connection reveal that perturbed brain energy metabolism, including impaired glucose metabolism and mitochondrial dysfunction, may serve as the common link between AD and diabetes.

Impaired glucose metabolism as a common pathological feature in AD and diabetes

Diabetes is characterized by chronic hyperglycemia resulting from defects in insulin production, insulin action or both. While the mechanisms underlying diabetes-associated complications are complex and involve multiple factors, the biological basis that drives these complications is impaired glucose metabolism. The effects of diabetes on brain glucose transport and utilization remain largely unexplored. Increased brain glucose concentration has been observed in the individuals with type 1 diabetes, which was

thought to result from an increase in glucose transport across the blood-brain barrier (BBB) and/or reduced glucose metabolism [11, 12]. In type 2 diabetic patients, insulin resistance and reduced cerebral glucose metabolic rate have been observed in several AD-affected brain regions including parietotemporal, frontal, and cingulate cortices [13]. The abnormalities in brain glucose transport and metabolism were also observed in rodent models of experimental diabetes. Mice with type 1 diabetes induced by streptozotocin (STZ) exhibited a decrease in glucose transporter in the BBB, and an increase in brain glucose concentration and glucose utilization [14-17]. In line with these findings, the activities of several key enzymes involved in glucose metabolism were significantly elevated [18]. However, these alterations occurred within the first month of diabetes induction. In the late stage, a marked reduction in glucose metabolism was found in multiple brain regions [17]. Overall, these findings suggest diabetes causes perturbations in cerebral glucose transport and metabolism. Given that glucose is the obligatory fuel for the brain, the disrupted glucose supply, transport or utilization could lead to energy failure and brain damage. In support of this notion, both chronic hyperglycemia and repeated occurrences of severe hypoglycemia have been associated with impaired cognition [19-22]. Studies on diabetic animal models also point out a link between disrupted glucose metabolism and learning and memory deficits [23-26]. Taken together, these findings suggest that the dysregulated glucose transport and metabolism may, at least in part, underlie diabetes-associated cognitive dysfunction.

Impaired glucose metabolism has also been observed in the preclinical and clinical AD brains. Positron emission tomographic studies with [^{18}F] fluorodeoxyglucose (FDG-PET) in AD patients indicate severe glucose hypometabolism in the cerebral cortex, with

posterior cingulate and parietotemporal regions mostly affected [27-29]. Reduced glucose metabolism has also been detected in individuals with mild cognitive impairment (MCI), which is the prodrome to AD [30, 31]. In fact, cerebral glucose hypometabolism may precede the clinical symptoms for decades, as abnormally low measurements of glucose metabolic rate have been reported in the AD-typical regions including hippocampus, posterior cingulate, parietal, temporal, and prefrontal cortex in young and middle-aged adults at genetic risk for AD [32-36]. The impaired glucose metabolism may be associated with perturbed glucose transport. In support of this notion, the expression of two major brain glucose transporters, GLUT1, which is responsible for the uptake of glucose across BBB, and GLUT3, which mediates glucose entry into neurons, were significantly decreased in the AD brain [37-39]. In addition to the defects in glucose transport, impaired intracellular glucose catabolism has been observed. Altered activity of glycolytic enzymes including hexokinase, aldolase, pyruvate kinase, lactate dehydrogenase and glucose 6-phosphate dehydrogenase have been observed in the AD-vulnerable brain regions [40, 41]. Decreased activity of two key enzymes in the tricarboxylic acid (TCA) cycle, pyruvate dehydrogenase, and α-ketoglutarate dehydrogenase were also documented in the AD brain [42, 43]. Similarly, reduced glucose metabolic rates, glucose transport dysfunction and disturbed intracellular glucose catabolism were detected in the brains of transgenic mouse models of AD [44-46]. The bioenergetic deficits resulting from perturbed glucose transport and metabolism may drive the molecular processes contributing to the formation of AD-related neuropathological hallmarks and cognitive decline [45-47].

In summary, accumulating evidence suggests abnormal glucose metabolism as the mechanistic link between AD and diabetes. Impaired cerebral glucose utilization due to insulin resistance or disturbed insulin signaling predisposes neurons to the energy crisis and functional deficits, which may contribute to the pathological alterations responsible for the cognitive dysfunction observed in the brains affected by AD and diabetes.

Mitochondrial dysfunction and oxidative stress are commonly shared by AD and diabetes

Apart from impaired glucose metabolism, mitochondrial dysfunction and oxidative stress have been implicated in AD- and diabetes-associated brain dysfunction. Multiple lines of evidence suggest mitochondrial dysfunction and oxidative stress are intimately involved in AD pathogenesis and progression. Reduced mitochondrial electron transport chain complex activity, particularly deficiency in cytochrome c oxidase activity, has been well documented [48-51]. As mitochondria are both the major source and direct victim of reactive oxygen species (ROS), mitochondrial dysfunction is usually associated with oxidative stress, as evidenced by the extensive lipid, protein, and nucleic acid oxidation observed in the AD brain [52-55]. While the cause of mitochondrial dysfunction in AD remains elusive, mounting evidence suggests amyloid beta peptide (Aβ) plays a crucial role. It has been shown that Aβ is imported into mitochondria via the translocase of the outer membrane (TOM) import machinery and localized to mitochondrial cristae [56], where it interacts with the mitochondrial proteins such as Aβ-binding alcohol dehydrogenase [57] and cyclophilin D [58], leading to mitochondrial respiratory dysfunction and mitochondrial reactive oxygen species (ROS) generation. Oxidative stress induces mitochondrial Ca^{2+} overload, resulting in mitochondrial membrane

potential collapse, ATP depletion, mitochondrial membrane permeability transition pore opening, cytochrome c leakage, and the activation of cell death signaling cascades [59-61]. In addition to perturbations in mitochondrial function, alterations in mitochondrial morphology have been observed in the AD brain [62]. Aβ has been demonstrated to facilitate mitochondrial fragmentation by disrupting mitochondrial fission/fusion balance in AD-affected neurons [63, 64]. Further, AD brain also demonstrated impaired mitochondrial motility [65]. It has been shown that Aβ oligomers decreased axonal mitochondrial transport, resulting in reduced mitochondrial density in the axons and synaptic terminals [66-68]. Together, these Aβ-related impairments in mitochondrial bioenergetics, dynamics, and trafficking could contribute to the synaptic loss and functional deficits correlated with cognitive dysfunction in AD [69, 70].

Emerging evidence suggests the involvement of mitochondrial dysfunction and oxidative stress in diabetes-induced brain damage. In an animal model of type 1 diabetes, brain mitochondria showed declines in oxidative phosphorylation, ATPase activity and ATP levels [71, 72]. Along with the defects in mitochondrial respiratory chain activities, levels of ROS, nitric oxide (NO), and mitochondrial nitric oxide synthase expression were found to be increased in the mitochondria, suggesting enhanced oxidative and nitrosative stress [73]. Additionally, STZ-induced diabetes promoted a reduction in glutathione (GSH) peroxidase activity and significant decreases in mitochondrial coenzyme Q9 and manganese superoxide dismutase (MnSOD) protein contents, suggesting impaired antioxidant capability [71-73]. Importantly, insulin treatment reversed diabetes-related mitochondrial alterations presumably via attenuating hyperglycemia-induced oxidative stress and improving oxidative phosphorylation efficiency. A similar decrease in

mitochondrial respiratory efficiency has been observed in the brains of Goto-Kakizaki rats, an animal model of type 2 diabetes [74]. Interestingly, diabetes-related mitochondrial dysfunction was exacerbated by aging and/or by the presence of Aβ, which supports the idea that diabetes and aging are risk factors for AD [74]. In addition to impaired mitochondrial respiratory function, diabetes has been associated with disrupted mitochondrial dynamics (imbalance of fission/fusion events). Reductions in mitochondrial density and mitochondrial length have been observed in the hippocampus of leptin receptor deficient mice (db/db), suggesting diabetes causes the balance shifting towards mitochondrial fission [75]. In line with the *in vivo* findings, treatment of human neuronal SK cell line with high glucose resulted in mitochondrial fragmentation by enhancing fission. Of note, restoration of mitochondrial dynamics ameliorated diabetes-induced defects in mitochondrial respiratory function and deficits in synaptic plasticity, suggesting defects in mitochondrial function may be responsible for the cognitive dysfunction related to diabetes [75]. Additional evidence for the implications of mitochondrial bioenergetics and oxidative status in the cognitive decline came from the studies on type 1 diabetic patients experiencing recurrent hypoglycemia. It was found that both STZ-induced diabetes and insulin-induced hypoglycemia decreased mitochondrial respiratory efficiency, increased ROS generation and suppressed antioxidant defense in the cortical and hippocampal mitochondria [76]. Additionally, a higher release of glutamate was observed in the diabetic and hypoglycemic synaptosomes [77]. Therefore, mitochondrial dysfunction, oxidative stress, and higher release of excitatory neurotransmitters may act synergistically, contributing to neuronal injury and cognitive impairments in type 1 diabetic patients receiving insulin treatment.

As mitochondria are the major site where the complete oxidation of glucose takes place, their functional defects may constitute a downstream event of impaired glucose metabolism. Oxidative stress induced by poor glycemic control or Aβ promotes abnormalities in mitochondrial respiratory function, dynamics, and motility, contributing to synaptic dysfunction and cognitive impairment, both are prominent in the AD- and diabetes-affected brains. In conclusion, I briefly reviewed the evidence for the perturbed glucose metabolism and mitochondrial dysfunction as common pathological features of AD and diabetes. Further investigations aiming at uncovering the molecular mechanisms underlying AD and diabetes interrelation may lead to the discovery of novel therapeutic approaches that could reverse brain damage associated with both disorders.

Purpose of the Dissertation

Alzheimer's disease and diabetes are aging-related chronic disorders affecting millions of people worldwide. The incidence of both has increased drastically in recent years due to the enhanced lifespan and population growth. Numerous epidemiological studies indicate that diabetes significantly increases the risk of dementia including the Alzheimer's type [5, 78, 79]. A rapidly growing body of evidence suggests insulin resistance, the major defect in type 2 diabetes, and impaired insulin signaling may contribute to AD neuropathology and cognitive impairment [80-83]. These findings suggest a commonly shared mechanism may be responsible for AD- and diabetes-related cognitive impairment. One of the several common abnormalities shared by the two disorders is the perturbed brain energy metabolism, including impaired glucose metabolism and mitochondrial dysfunction. Uncovering the molecular intersection of AD- and diabetes-regulated brain energy metabolism may provide insights into the etiologies of cognitive dysfunction associated with these disorders and lead to the development of novel therapeutic interventions.

Cognitively normal individuals at risk for AD, including those carrying ApoE4, showed reduced cerebral metabolism of glucose, the primary energy substrate for the brain [32, 84]. Treatment with a ketogenic agent did not improve cognitive function in ApoE4 carriers [85, 86], suggesting ApoE4 genetic status affects the brain's capability of metabolizing ketone bodies, the secondary fuel for the brain. Utilizing mouse models expressing human ApoE isoforms, we found that ApoE2 brain is associated with a most robust profile in insulin-like growth factor 1 signaling and glucose transport [87]. Together, these findings suggest human ApoE genetic status influences brain energy

metabolism. However, what substrate and which metabolic pathway are specifically regulated by ApoE isoforms remain to be elucidated. Therefore, the purpose of the first part of my study is to identify the specific substrates and metabolic pathways in the brain that are differentially modulated by human ApoE isoforms. The intracellular oxidative catabolism of glucose includes glycolysis and pentose phosphate pathway in the cytosol, and TCA cycle and oxidative phosphorylation in the mitochondria. Previous research has been primarily focused on mitochondrial bioenergetics, in particular, the detrimental effects of ApoE4 on mitochondrial respiratory chain. Comparatively, few studies have looked at the cytosolic metabolism. However, metabolic pathways occur in the cytosol are crucial for ATP production and maintenance of mitochondrial function by providing reducing equivalents and antioxidant defense against oxidative stress. Therefore, my study focused on pinpointing the cytosolic metabolic pathways that are potentially affected by ApoE genetic status.

To probe the metabolic pathways altered by ApoE genetic status, we first performed a gene expression profiling study on the brains of 6-month-old human ApoE gene-targeted replacement mice. Specifically, the custom array examined the expression of 43 genes involved in the cytosolic processes from energy substrate transport to the major cytosolic metabolic pathways leading to the generation of acetyl-CoA. Based on the findings from gene array analysis, we carried out functional studies of ApoE modulation of energy metabolism using an *in vitro* cell culture model. To further understand the biological implications of gene expression changes, we used a bioinformatics computing program, IPA, and conducted a regulatory pathway and molecular network analysis. IPA predicted the enhanced activity of peroxisome proliferator-activated receptor gamma coactivator 1-

alpha (PGC-1α) may underlie the bioenergetic robustness associated with ApoE2. Therefore, we proceeded with investigations of whether PGC-1α overexpression could ameliorate the detrimental effects induced by ApoE4 in brain energy metabolism using cell lines stably expressing human ApoE isoforms. Lastly, we examined whether the introduction of ApoE2 could counteract ApoE4-associated bioenergetic deficits.

Diabetes has been associated with an increased risk of synaptic injury and cognitive dysfunction [88-91], however, the underlying mechanism is not clear. Emerging evidence suggests mitochondrial dysfunction and oxidative stress are common events in the brains of animal models of type 1 and type 2 diabetes [71, 72, 75]. In addition to reduced mitochondrial respiratory efficiency and lower ATP production, brain mitochondria isolated from diabetic animals also presented impaired capacity to accumulate Ca^{2+} [71, 72]. A decrease in Ca^{2+} buffering capacity may lead to reduced threshold for mitochondrial permeability transition pore (mPTP) opening. In the presence of mPTP triggers, such as ROS generation, diabetic mitochondria may be more susceptible to the induction of mitochondrial permeability transition, which lead to loss of mitochondrial membrane potential, depletion of ATP, mitochondrial swelling, the rupture of the outer mitochondrial membrane and cell death. The structural and functional impairment of mitochondria may, in turn, promote ROS production, forming a vicious feedback loop. Therefore, mitochondrial mPTP may be implicated in mitochondrial dysfunction and oxidative stress observed in the diabetic brain. Previously, it has been shown that cyclophilin D (CypD), a critical regulator of Ca^{2+}-mediated opening of mPTP, is significantly increased in the brains of AD patients and in a transgenic mouse model of AD [58]. Intriguingly, CypD-deficient mitochondria have improved calcium buffering

capacity and are resistant to Aβ- and Ca^{2+}-induced mitochondrial permeability transition. Notably, genetic deletion of CypD protects neurons from oxidative stress-induced cell death. Further, the absence of CypD significantly attenuated synaptic injury and cognitive deficits in an AD mouse model. Given that mitochondrial dysfunction is a common abnormality in the AD- and diabetes-affected brain, we hypothesized that CypD deficiency attenuates diabetes-associated mitochondrial dysfunction and cognitive impairment.

To test this hypothesis, I first verified the expression levels of CypD in the brains of STZ-injected mice, a mouse model of type 1 diabetes. 3 month-old wild-type mice and CypD null mice were subjected to intraperitoneal injection of STZ for five consecutive days to induce diabetes. Then, I examined the effects of CypD deficiency on mitochondrial function by measuring mitochondrial electron transport chain (ETC) complex activities. Additionally, Morris water maze (MWM) task was performed to assess the effect of CypD deficiency on diabetes-induced learning and memory deficits.

It has been shown that diabetes-associated mitochondrial dysfunction is exacerbated in the presence of Aβ. Additionally, the CypD expression is enhanced in an Aβ-enriched environment. Further, the expression level of CypD is positively correlated with the probability of mPTP opening. Therefore, I asked the question, whether enhanced CypD expression induced by AD exacerbates diabetes-associated mitochondrial dysfunction and cognitive decline.

To address this question, we induced type 1 diabetes in an AD mouse model (J20) which has been demonstrated to express increased level of CypD in the brain. Then I evaluated

the synergistic effects of diabetes and AD on mitochondrial dysfunction by measuring mitochondrial ETC complex activities. Lastly, I performed MWM to determine whether diabetes and AD act synergistically to exacerbate cognitive impairment.

Chapter 1 Human ApoE Isoforms Differentially Modulate Brain Glucose and Ketone Metabolism: Implications for Alzheimer's Disease Prevention and Early Intervention

1.1 Abstract

Alzheimer's disease (AD) is an irreversible neurodegenerative disorder characterized clinically by progressive loss of memory and cognitive decline. There are two types of AD: early-onset and late-onset (LOAD); LOAD accounts for over 95% of all AD cases. Humans possess three genetic isoforms of apolipoprotein E (ApoE)—ApoE2, ApoE3, and ApoE4—that confer differential risk for LOAD; however, the underlying mechanisms are poorly understood. This study sought to investigate the impact of human ApoE isoforms on brain energy metabolism, an area significantly perturbed in preclinical AD. A TaqMan custom array was performed to examine the expression of a total of 43 genes involved in glucose and ketone body uptake, transport and cytosolic metabolism in the cortical tissues of human ApoE gene-targeted replacement mice (hApoE-TR). Consistent with our previous findings, ApoE2-bearing brains exhibited the most robust while ApoE4 brains were associated with the most deficient profile on both the uptake and metabolism of glucose, the primary energy substrate for the brain. In particular, the three ApoE genotypes significantly differed in the expression of facilitated glucose transporters, which mediate the entry of glucose into neurons, and hexokinase, which acts as the "gateway enzyme" in glucose metabolism by converting glucose to glucose-6-phosphate, the initial step in the glycolysis, glycogen synthesis and pentose phosphate pathway. Interestingly, on the uptake and metabolism of ketone bodies, the secondary energy source for the brain, ApoE2 and ApoE4 brains exhibited a similar level of

robustness, while ApoE3 brains presented a relatively deficient profile, which may provide a plausible explanation for the clinical observations that a ketogenic agent was found to benefit ApoE3 but not ApoE4 carriers. Moreover, Ingenuity Pathway Analysis predicted that PPAR-γ/PGC-1α signaling activity could be enhanced in the ApoE2 brain and attenuated in the ApoE4 brain. Consistent with the prediction, PGC-1α overexpression ameliorated ApoE4-associated deficits in glycolysis and mitochondrial respiration. Further, forced expression of ApoE2 counteracted the detrimental effects induced by ApoE4 as demonstrated by the significant improvement in glycolytic function, the elevation in mitochondrial respiration, and the concurrent increase in ATP production in ApoE4-expressing cells transfected with ApoE2 when compared to those transfected with mock control. Taken together, our data provide additional evidence that human ApoE isoforms differentially modulate brain energy metabolism, which could serve as a potential mechanism underlying their discrete risk impact in AD. Importantly, the introduction of ApoE2 may represent a promising therapeutic approach in AD prevention and early intervention by promoting bioenergetic robustness contributing to brain resilience against AD.

1.2 Introduction

1.2.1 Alzheimer's disease: current status

As one of the most common forms of dementia, Alzheimer's disease (AD) currently affects 35 million people worldwide, including 5.3 million Americans. By 2050, this number is predicted to nearly triple, projected to 13.8 million. This devastating disease creates a huge economic burden to the American society; an estimated overall payment for AD care in 2015 was $226 billion, which is projected to increase to more than $1 trillion by 2050 [92].

AD is manifested clinically as progressive loss of memory and cognitive function and is characterized pathologically by the formation of amyloid beta (Aβ) plaques and neurofibrillary tangles (NFT). Since its discovery in 1906, extensive research has been undertaken to delineate AD pathogenesis and to develop treatments; however, the cause of AD remains largely unknown and no success has been found from over 200 AD drug trials conducted in the past decade [93]. It has been estimated that a treatment that delays the onset of AD by just 5 years could reduce the number of individuals with the disease by 38% in 2050 [94]. Therefore, increased research should be directed to better understand AD-risk mechanisms that would allow the development of strategies aimed at AD prevention and early intervention.

1.2.2 Human apolipoprotein E (ApoE) in the brain: isoforms, expression, and function

Apolipoprotein E (ApoE) is a component of a wide spectrum of plasma lipoproteins found in almost all mammals. Human ApoE was first described in 1973 by Shore and Shore as "arginine-rich protein" present in the very-low-density lipoproteins (VLDL) [95]. Later in 1975, it was proposed that the defect in the regulation or the structure of ApoE is responsible for the type III hyperlipoproteinemia, which is a familial disorder characterized by premature atherosclerosis and accumulation of plasma cholesterol [96, 97]. In the half-century since its discovery, extensive research has been undertaken to delineate the role of the ApoE in cholesterol/lipid transport and metabolism under both physiological and pathological conditions. It is known that ApoE is a constituent of several plasma lipoproteins including chylomicrons, VLDL remnants, VLDL and a subclass of high-density lipoproteins (HDL). Lipoprotein-associated ApoE is a ligand for various members of the low-density lipoprotein (LDL) receptor family including LDL receptor, the very-low-density lipoprotein (VLDL) receptor, the ApoE receptor 2 (ApoER-2) and the LDL-receptor-related protein (LRP). The transport of ApoE-containing lipoproteins between the cells occurs through LDL receptor-mediated endocytosis. After internalization, ApoE can be degraded or recycled back to the cell surface.

The human ApoE gene localizes to the long arm of chromosome 19q13.2, is approximately 3.7 kb in length and contains four exons separated by three introns [98] (Fig.1.2.1). The promoter sequence TATAATT occurs at 33 nucleotides upstream of the transcription initiation site [99]. Analysis of human ApoE cDNA indicates that the

corresponding mRNA contains 1157 nucleotides and the primary translation product is a 317-amino acid precursor protein with an 18-amino acid signal peptide attached to the N-terminal [100, 101]. The cleavage of the signal peptide results in the mature ApoE, which is a 299-amino acid protein with a molecular mass of 34 kDa.

Human ApoE exists as three major isoforms, ApoE2, ApoE3 and ApoE4, which are the products of three alleles at a single gene locus. These isoforms differ structurally by two amino acid substitutions at residues 112 and 158: ApoE2 (Cys-112, Cys-158), ApoE3 (Cys-112, Arg-158), and ApoE4 (Arg-112, Arg-158). The difference in amino acids arises from two single nucleotide polymorphisms (SNP) in the ApoE gene on codon 112 (388 T > C) and 158 (526 C > T) (Fig. 1.2.1). ApoE consists of two major functional domains — an amino-terminal domain which has been shown to be a four-helix bundle that contains a highly positively charged receptor-binding region composed mainly of arginine and lysine residues and a carboxyl-terminal domain which includes a lipid-binding region — and these two domains are joined by a flexible hinge region (Fig.1.2.1). The characterization studies of the receptor binding properties of ApoE suggest positively charged residues are essential since chemical modifications of either arginine or lysine residues in the vicinity of the recognition sites abolished the bindings of lipoproteins to the LDL receptor [102, 103].

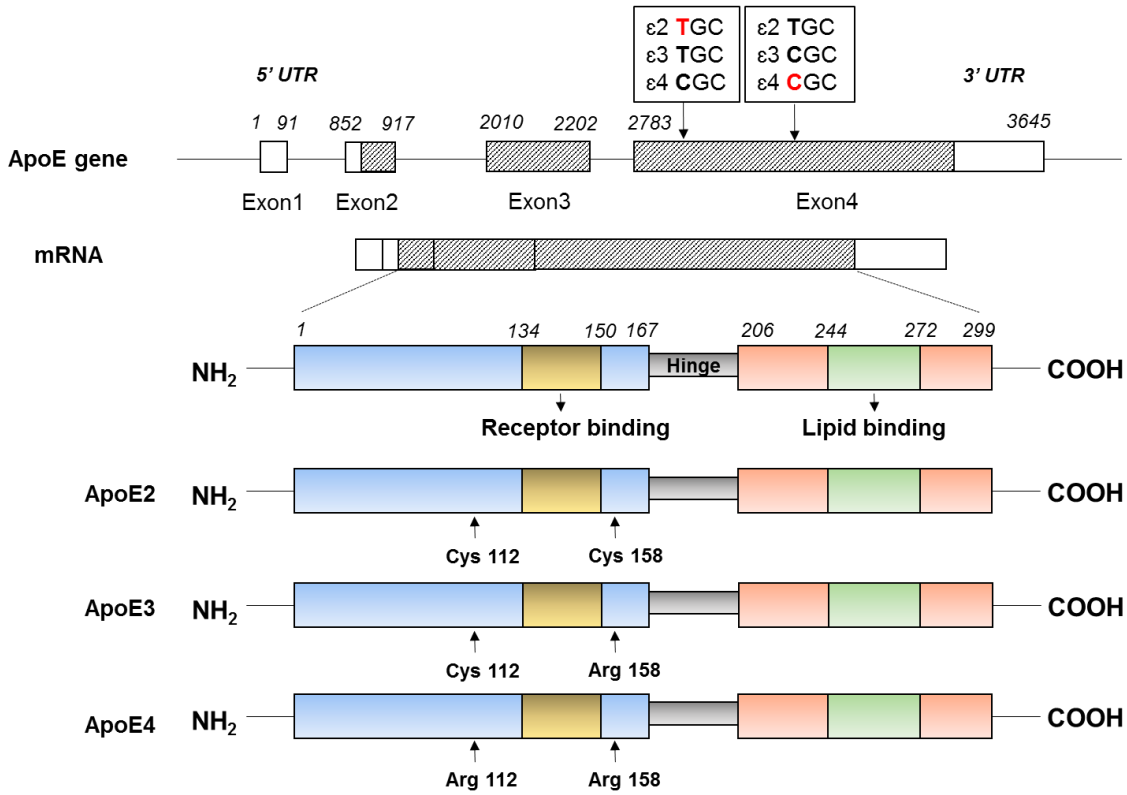

Figure 1.2.1

Fig.1.2.1 The schematic representation of the structural and functional domains of human ApoE isoforms. Human ApoE gene is composed of four exons interrupted by three introns (pattern box: coding region; open box: untranslated region). The ApoE2, ApoE3 and ApoE4 isoforms are coded by ε2, ε3 and ε4 alleles of the ApoE gene, respectively. The isoforms differ with each other in two amino acid substitutions at residues 112 or 158 resulting from C→T or T→ C point mutation in exon 4 as indicated. ApoE has two functional domains: the N-terminal domain containing the receptor-binding region (residues 134-150) and the C-terminal domain which includes the lipid-binding region (residues 244-272). Adapted from Wu, Long, and Liqin Zhao (2016) Neural Regeneration Research 11(3): 412–413.

Substitutions of two amino acid residues in the three ApoE isoforms significantly alters their structure and function, which is crucial for understanding their roles in AD pathogenesis [104]. Results from X-ray crystallography, fluorescence resonance energy transfer (FRET) and electron paramagnetic resonance (EPR) spectroscopy of human

ApoE isoforms reveal that ApoE4 displays a distinct conformation resulting from intramolecular domain interaction [105-108] (Fig.1.2.2). Specifically, Arg-112 in the amino-terminal domain of ApoE4 forms a salt bridge with Glu-109 and causes the Arg-61 side chain to extend away from the four-helix bundle, thus allowing an interaction with Glu-255 in the carboxyl-terminal domain, resulting in a more compact structure. In comparison, Cys-112 in ApoE2 and ApoE3 causes the Arg-61 side chain to be buried between two helixes, rendering it less accessible for the interaction with Glu-255 and resulting in a more extended structure. Indeed, *in vitro* studies indicate that mutation of Arg-61 to threonine or Glu-255 to alanine abolished domain interaction [106, 107]. Additionally, in mouse ApoE, which contains Arg-112 and Glu-255 that are equivalent to human ApoE4 but lacks Arg-61, substitution of Thr-61 with arginine introduced an ApoE4 domain interaction, making mouse ApoE to act like human ApoE4 [109]. This domain interaction appears to affect both the receptor- and lipid-binding affinities of ApoE. For instance, ApoE2 has a much lower binding affinity for LDL receptors compared to that of ApoE3 and ApoE4 [110]. While ApoE2 and ApoE3 preferentially bind to small, phospholipid-enriched HDL, ApoE4 preferentially binds to LDL and the large, triglyceride-enriched VLDL [106, 109]. Further, the structural difference renders ApoE4 more susceptible to protein misfolding and instability. It has been shown that ApoE2 is the most stable isoform whereas ApoE4 is the least stable and is prone to form a folding intermediate with the characteristics of a molten globule during guanidine-HCl, urea, and thermal denaturation [111, 112]. These altered properties of ApoE4 have been postulated to contribute to the neuropathological effects of ApoE4, including elevation in

Aβ production [113], increase in Aβ-induced lysosomal leakage and apoptosis [114], and enhanced proteolysis and the generation of neurotoxic fragments in neurons [115, 116].

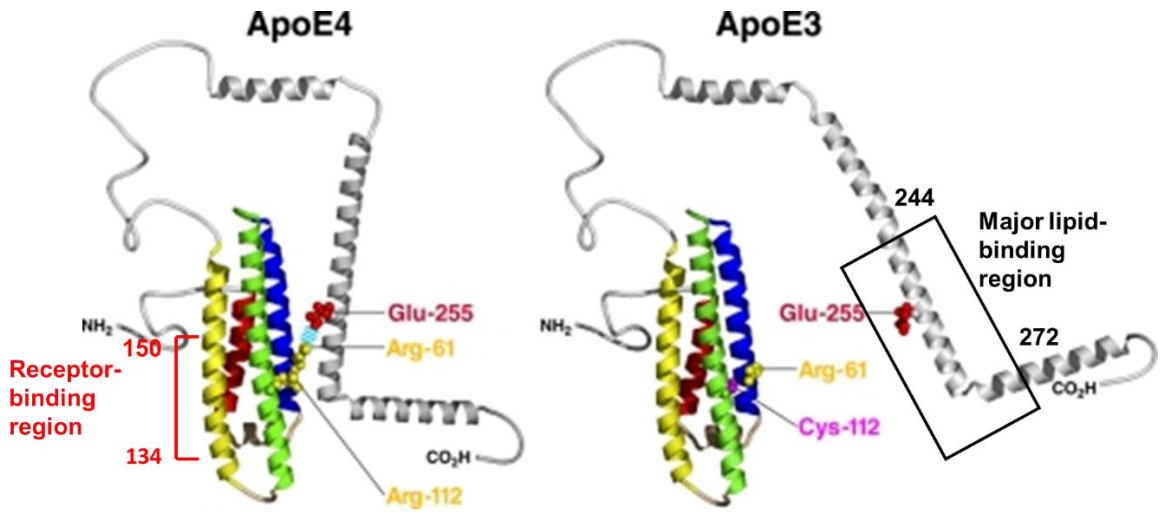

Figure 1.2.2

Fig.1.2.2 Influence of domain interaction on the structure of ApoE. In ApoE4, Arg-112 causes the Arg-61 side chain to extend away from the four-helix bundle, allowing an interaction with Glu-255. In ApoE3, Cys-112 causes the Arg-61 side chain to be tucked between helix 2 and helix 3, thus unable to interact with Glu-255. The secondary structure of the amino-terminal domain of ApoE was shown. red, helix 1; blue, helix 2; green, helix 3; yellow, helix 4 and the connecting loop. Adapted from Zhong, Ning, and Karl H. Weisgraber. (2009) Journal of Biological Chemistry 284(10): 6027–6031.

ApoE is found in a variety of organs. In the periphery, ApoE is abundantly expressed in liver, kidney, and to a lesser extent in spleen, lung and adipose tissues. The liver is the major source of plasma ApoE [117-121]. Interestingly, although the intestine is involved in lipoprotein synthesis, ApoE was not detected in intestinal mucosa [118]. A substantial

amount of ApoE mRNA was also detected throughout all regions of the brain. Initially, it was thought that ApoE is solely synthesized and secreted by glial cells, mainly astrocytes [122]. Later, it was found that neurons can produce ApoE in response to a variety of physiological or pathological stimuli, albeit at a much lower level compared to astrocytes [123-126]. Of note, ApoE is the major apolipoprotein in the human cerebrospinal fluid (CSF), where it may play an important role in mediating lipid transport and cholesterol metabolism in the central nervous system [127-129]. CSF ApoE concentration is only at 5% - 10% of its concentration in the plasma and it has been shown to vary in inflammatory neurological disorders [130]. Currently, the clinical significance of CSF ApoE concentration in AD is still under debate. Some suggest the CSF level of ApoE is associated with pathogenesis and progression of AD [131-136] whereas others did not find such association [137-141]. Recently, a meta-analysis which includes a total of 1064 AD patients and 1338 controls failed to identify a significant association between CSF ApoE levels and AD risk. However, the interpretation of the results may be confounded by the gender-specific and ApoE isoform-specific effects on ApoE level, the difference in age of onset as well as a lack of longitudinal CSF ApoE measurements [142]. Therefore, future studies, which take all the factors mentioned above into consideration, are warranted to address the clinical relevance of CSF ApoE concentrations in AD.

One of the primary functions of ApoE in the brain is cholesterol transport, mainly from astrocytes to neurons. Cholesterol is an essential component in the membrane and myelin sheaths and is of critical importance in the synaptogenesis and synaptic function [143]. A role for ApoE in central nervous system (CNS) reinnervation after neural injury has been described [144-147]. In response to damage, such as neuronal loss or terminal

deafferentation, astrocytes synthesize and release ApoE, which presumably takes up the cholesterol and phospholipids released from cellular membrane and myelin debris. Following LDL receptor-mediated endocytosis, cholesterol is released into the cytoplasm and transported to the dendritic field for dendritic remodeling or to the terminals for synapse formation. Additionally, ApoE is also responsible for other brain lipid transport and metabolism. For instance, sulfatide, a class of oligodendrocyte-synthesized lipids which mediate neuronal plasticity and myelin sheath integrity, is carried by ApoE containing HDL-like lipoproteins in the human CSF [148].

Accumulating evidence suggests ApoE interacts with LRP to modulate neurite outgrowth. The effect of ApoE-containing lipoproteins on neurite outgrowth has been shown to be isoform-specific with ApoE3-containing lipoproteins promoting neurite outgrowth whereas ApoE4-containing lipoproteins having no effect or suppressing neurite outgrowth [149-151]. Interestingly, the effects of ApoE-containing lipoproteins on neurite outgrowth is present only when β-migrating VLDL, which are cholesterol-enriched remnants of chylomicrons, or HDL are utilized as lipoprotein carriers [150]. Further, these effects can be abolished by the inhibitors that prevent the ligand binding to LRP [151, 152]. Together, these findings indicate that the interaction between ApoE and certain lipoproteins may facilitate their internalization via the LRP-dependent pathway.

Conflicting *in vivo* findings exist pertaining to the role of ApoE in synaptic integrity and plasticity. Results from some studies point out a critical role of ApoE in maintaining synaptic structure and function. Masliah et al. reported that ApoE null mice displayed an age-dependent loss of synapses and disruption of the dendritic cytoskeleton in the neocortex and limbic system [153]. Homozygous ApoE-deficient mice exhibited working

memory impairments in the MWM tasks, which has been correlated with cholinergic deficits in the basal forebrain [154-156]. Infusion of recombinant ApoE into the brain of ApoE-deficient mice resulted in a significant improvement in their learning capacity which was associated with the restoration of synapto-dendritic structure [157]. Others, however, suggest that ApoE is of no importance in the maintenance of normal synaptic integrity or plasticity. For instance, it has been shown that the ApoE-knockout mice have a normal cholinergic system during aging [158-160]. Additionally, mice lacking ApoE appear to be intact in spatial learning or reference memory as they performed similar to their wild-type littermates in the MWM tasks [161, 162]. Further, mice deficient in ApoE do not differ from aged-matched wild-type mice in synaptic plasticity, synaptic injury recovery or synaptic degeneration during aging [163-165]. One possible explanation for the lack of defects observed in ApoE-deficient mice could be that alternative apolipoproteins, for instance, apolipoprotein J (ApoJ), compensate for the loss of ApoE. ApoJ shares a number of similarities with ApoE: ApoJ is highly expressed in the brain and mainly synthesized and secreted by astrocytes. More importantly, like ApoE, ApoJ plays a role in synaptic remodeling, repair, and regeneration after brain injury [166-168]. Therefore, it is likely that ApoJ may replace the function of ApoE in the brain, although further investigations are warranted to validate this assumption.

1.2.3 ApoE polymorphisms in AD: clinical evidence for the neuroprotective properties of ApoE2

The genetic polymorphism of human ApoE was first discovered in 1977 from a German population, which was associated with the occurrence of type III hyperlipoproteinemia [169]. Three major ApoE alleles, ε2, ε3, and ε4, are determined by two single nucleotide polymorphisms. The expression of two of the three alleles gives rise to a total of six ApoE genotypes: three homozygous genotypes (ApoE ε2/ε2, ApoE ε3/ε3, and ApoE ε4/ε4) and three heterozygous genotypes (ApoE ε2/ ε3, ApoE ε3/ ε4, and ApoE ε2/ ε4). The allele frequencies of ApoE vary widely across the population with ApoE ε3/ε3 being the most common followed by ApoE ε3/ ε4 and ApoE ε2/ ε3. ApoE polymorphic alleles have been shown to confer differential susceptibility to AD [170]. As the most common allele, ApoE ε3 is present in approximately 75% of the population and is believed to play a neutral role in AD. ApoE ε2 is relatively rare, with only 5% incidence, and is recognized as a protective variant against AD. In contrast, as the most potent genetic risk factor for AD, ApoE ε4 exists in only about 20% of the population, however, it accounts for nearly 65% of total AD cases. Possession of ApoE4 not only increases the prevalence of AD but also lowers the age of onset in a gene dosage-dependent manner. It has been estimated that the mean age of onset is 84 years in individuals who do not have ApoE ε4, 76 for individuals with one copy of ApoE ε4, and 68 in subjects with both copies of ApoE ε4 [171].

ApoE4 was first identified as the major risk factor for developing late-onset AD in 1993 [171]. Over the past few decades, a plethora of studies have been done to examine the role of ApoE in AD pathogenesis. Most studies have primarily focused on identifying

AD-risk mechanisms conferred by ApoE4 through comparisons between ApoE4 and ApoE3 and between ApoE4 carriers and non-carriers. Clinically, ApoE4 has been associated with an accelerated rate of cognitive decline in aging and AD. Healthy ApoE4 homozygotes in their 60s have faster deterioration in several cognitive domains when compared to ApoE4 heterozygotes or non-carriers before the diagnosis of mild cognitive impairment (MCI), the prodromal stage of AD [172, 173]. Similarly, longitudinal studies reveal that ApoE4 carriers display memory decline even before the age of 60 and exhibit greater acceleration than non-carriers despite ongoing normal clinical status [174, 175]. ApoE4 carriers also show a higher rate of cognitive deterioration in verbal memory and abstract reasoning in the ninth decade of life [176]. More recently, it was found that ApoE4 exacerbated Aβ-related memory decline in cognitively normal older adults [177, 178]. Notably, ApoE4 carriers with high Aβ concentration in the brain demonstrated the most pronounced decline in learning and working memory. In subjects with MCI, ApoE4 was also associated with greater memory deficits and accelerated declines in the global measures of cognition [179-181]. Further, ApoE4 predicts a faster rate of cognitive decline in AD [182-185], although results obtained from some studies suggest no difference in the rate of deterioration in respect to ApoE4 genetic status [186-189]. These conflicting findings could be explained by methodologic differences in the measurements of cognitive function, subject's stage of AD and length of follow-up time. Comparatively, few studies have explored the role of ApoE2 in relation to AD, and overall the results of these studies suggest that ApoE2 is neuroprotective. For instance, ApoE2 has been positively associated with cognitive function in aging [190]. A longitudinal study in a large cohort of elderly dementia-free subjects demonstrated that individuals who possess

at least one ApoE2 allele (ε2/ε2 and ε2/ε3) exhibit improved episodic memory performance, which may be attributed to increased functional connectivity in the entorhinal cortex region [191]. In contrast, a decrease in episodic memory performance was found in the subjects with the ApoE3 (ε3/ε3) genotype and a faster-deteriorating rate in those with at least one ApoE ε4 allele [192]. Additionally, ApoE2 has been found to slow AD progression [183, 184]. Possession of one copy of ApoE2 allele has been associated with slower rate of cognitive decline, whereas possession of an ApoE4 allele predicted an earlier and faster cognitive decline in patients with probable AD. Together, these findings point to a protective role of ApoE2 in maintaining cognitive function under both physiological and neurodegenerative conditions.

Structural alterations may relate to cognitive impairments in the aging and AD brains. In subjects with MCI and AD, ApoE4 has been associated with an accelerated rate of hippocampal atrophy coupled with worsening memory performance [193-196]. In healthy non-demented individuals, possession of ApoE4 exacerbated the age-related decline in cortical thickness and hippocampal volume [197-199]. Recently, structural magnetic resonance imaging (MRI) of infants reveals that ApoE4 carriers have smaller gray matter volume in the brain areas that are most affected by AD, including precuneus, posterior middle cingulate, lateral temporal, and medial occipitotemporal regions [200]. It has been proposed that an age-related structural breaking down of myelin sheaths in the brain's later-myelinating regions may lead to progressive interruption of neural impulse transmission and the subsequent degradation of the widely distributed neural network, contributing to cognitive dysfunction. Indeed, ApoE4 carriers demonstrate accelerated rate of myelin breakdown with age in late-myelinating regions as compared to non-

carriers [201], which may underlie the faster rate of cognitive deterioration observed in the ApoE4 brain. In contrast, ApoE2 has been associated with the structural integrity of the brain during aging. For instance, ApoE2 carriers exhibit significantly less decline in age-related myelin breakdown [201]. Children and adolescents who possess ApoE2 have the thickest entorhinal and medial temporal cortex [202]. Results from the Alzheimer's Disease Neuroimaging Initiative (ADNI) study indicate that ApoE2 carriers have larger hippocampal volume and a reduced rate of hippocampal atrophy compared to non-carriers [203]. Collectively, these findings suggest that ApoE2 may play a positive role in preserving the structural integrity of the brain which may set a foundation for its cognition-favoring properties during physiological aging and the development of AD.

1.2.4 Brain energy substrate uptake and metabolism

The brain has a surprisingly high energy demand, despite its small size. While it only represents 2% of the body mass, it utilizes up to 20% of the oxygen and 25 % of the glucose consumed by the body. It has been estimated that neurons consumed 80% of the energy to support the activity of ion pumps, such as Na^+/K^+-ATPase, that re-establish the electrochemical gradients dissipated by signaling, namely action potentials, synaptic potentials and recycling of neurotransmitters [204-206]. In normal physiological conditions, glucose is the only significant energy substrate for the adult brain. However, under certain circumstances like starvation, ketone body can serve as a secondary energy source. Cerebral glucose metabolism includes glucose uptake, transport and intracellular oxidative catabolism (Fig.1.2.3). Brain glucose uptake and glucose entry into neurons are significantly dependent on the functions of glucose transporters. Intracellular oxidative

catabolism of glucose begins with the conversion of glucose to glucose-6-phosphate, which is a branch point metabolite that has different fates depending on the metabolic pathways. It is primarily processed via glycolysis, leading to the production of pyruvate, which can feed into TCA cycle and mitochondrial oxidative phosphorylation for the production of ATP. Alternatively, it is directed to the pentose phosphate pathway shunt for the generation of NADPH to support reductive biosynthesis, antioxidant defense and the synthesis of nucleic acids. In astrocytes, it is the precursor for glycogen. The entry of ketone bodies into neurons is mediated by monocarboxylate transporters. The metabolism of ketones occurs exclusively in the mitochondria. In the following sections, the transporters and major metabolic processes involving glucose and ketone bodies as energy substrates will be discussed with more details.

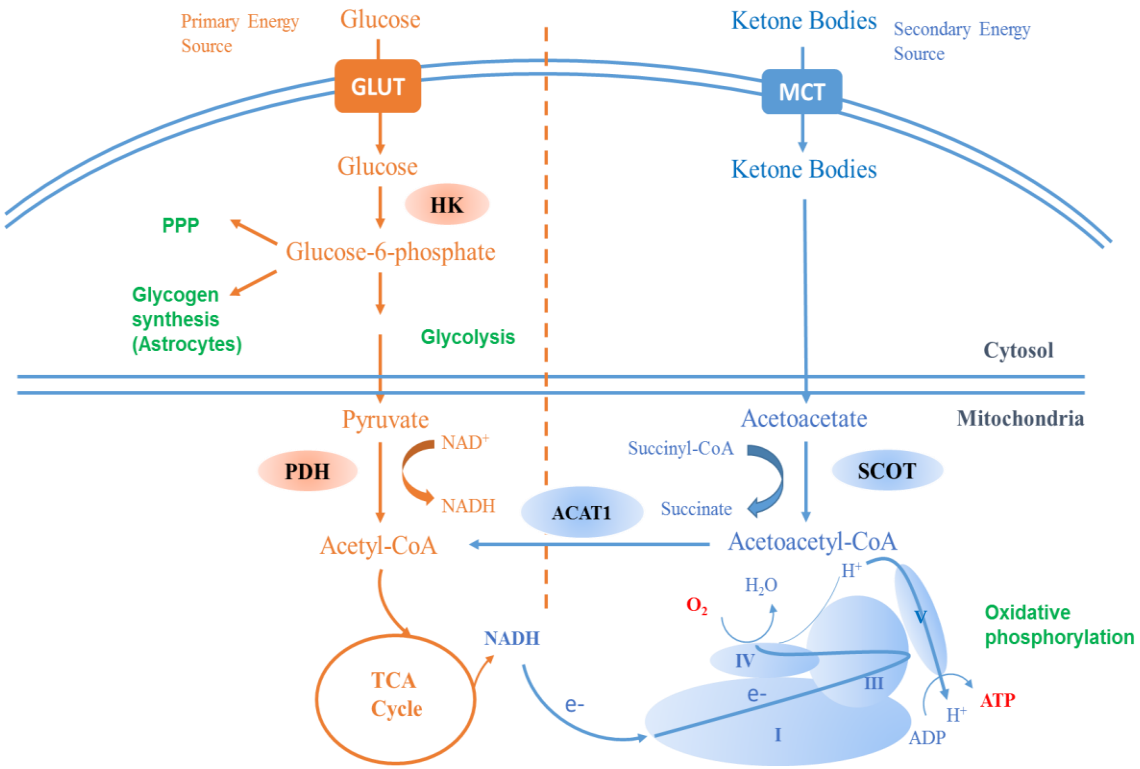

Figure 1.2.3

Fig.1.2.3 The schematic representation of the brain energy metabolism. Brain energy substrates include: 1) Glucose as the primary energy source under most conditions, and 2) ketone bodies as the secondary energy source in times of glucose shortage. Brain glucose and ketone body uptake are strictly controlled by their respective transporters, GLUTs and MCTs. The substrate metabolism includes cytosolic metabolism and mitochondrial bioenergetics. Glucose-6-phosphate can be processed through several metabolic pathways including glycolysis and pentose phosphate pathway (PPP) in neurons and glycogen synthesis in astrocytes. GLUT: glucose transporters; MCT: monocarboxylate transporters; HK: hexokinase; PDH: pyruvate dehydrogenase; ACAT1: acetyl-CoA acetyltransferase; SCOT: succinyl-CoA: 3-ketoacid CoA transferase.

1.2.4.1 Glucose uptake and metabolism in the brain

Brain glucose transporters

In the brain, glucose transport across the cell membrane or tissue barrier is primarily mediated by the facilitated glucose transporters (GLUTs). Table 1.2.1 summarizes the major GLUTs, their locations and main substrates in the brain. The most characterized glucose transporter in the brain is glucose transporter 1 (GLUT1). Brain GLUT1 exists as two isoforms: a highly glycosylated, 55 kDa form, expressed in the blood-brain barrier (BBB) endothelial cells [207-209] and a less glycosylated, 45 kDa form, localized to astrocytes [210-212]. The relationship between the extent of glycosylation and protein function remains to be defined. It has been shown that glucose concentrations modulate GLUT1 protein expression in the BBB and the glucose uptake in cerebral microvessels directly correlates with GLUT1 protein levels, suggesting GLUT1 plays a crucial role in overall glucose supply for the brain [210, 213].

Comparatively few studies have explored the role of glucose transporter 2 (GLUT2) in the CNS. To date, the expression pattern and function of GLUT2 in the brain remain controversial. Some studies reported that GLUT2 was exclusively expressed in the astrocytes in a limited number of brain nuclei including the paraventricular hypothalamic nucleus, the lateral hypothalamic area, and the arcuate nucleus, where it may function as a glucose sensor [214-216]. Other studies found that some cerebral neurons also expressed GLUT2 and may participate in glucose sensing, regulation of neurotransmitter release and glucose release by glial cells [217, 218]. Brant et al., however, found that GLUT2 was widely expressed in all brain regions, albeit at low levels [219]. Thus,

further investigations are warranted to validate the location and potential role of GLUT2 in the regulation of cerebral glucose homeostasis.

Apart from GLUT1, glucose transporter 3 (GLUT3) is another predominant transporter which mediates glucose uptake in the brain. It is recognized as a neuron-specific glucose transporter. GLUT3 is widely expressed throughout rat brain, including the cerebellum, striatum, cortex and hippocampus [210, 220]. A detailed examination of the location of GLUT3 by immunohistochemistry analysis revealed that GLUT3 was localized to neuropil and was largely absent from neuronal cell bodies [221, 222]. An additional electron microscopic study in rat brain further confirmed GLUT3 to be exclusively neuronal [211]. More importantly, on the subcellular level, GLUT3 was found localized mainly to the membranes of axon terminals, suggesting a functional role in energy supply that matched closely to synaptic transmission [211]. Despite its expression in neurons, how GLUT3 is regulated remains largely unknown. It has been shown that insulin facilitated GLUT3 translocation to the plasma membrane, and promoted neuronal glucose uptake [223].

Glucose transporter 4 (GLUT4), the insulin-sensitive glucose transporter, is primarily expressed in discrete neuronal populations in several brain regions including cerebellum, hypothalamus, hippocampus and cortex [224-227]. At the subcellular level, GLUT4 expression has been observed in neuronal cell bodies and dendrites [227]. Interestingly, there is a significant overlap between the cerebral areas where GLUT4 and insulin receptors are present [224, 228], suggesting GLUT4 may modulate the effects of insulin in the brain. In support of this hypothesis, altered cerebral expression of GLUT4 has been observed in rodent models with insulin resistance [225, 229, 230]. Additionally, it has

been shown that insulin induces the translocation of GLUT4 to the plasma membrane in human neuroblastoma cells [231]. Therefore, insulin may regulate neuronal glucose uptake by altering GLUT4 expressions on the cell surface. Further, since GLUT4 is highly expressed in the brain areas associated with motor function, such as sensorimotor cortex and cerebellum [227], GLUT4 may provide additional glucose to motor neurons under conditions of high energy demand. This notion is in line with the observation that heavy dynamic exercise markedly increased local cerebral glucose utilization in brain areas involved in motor function [232]. However, future studies are needed to delineate the molecular mechanisms by which GLUT4 modulates cerebral glucose homeostasis.

Glucose transporter 5 (GLUT5) has been identified as the fructose transporter in the brain as it exhibits high affinity to fructose but displays significantly lower transporter activity for glucose [233]. In the human brain, GLUT5 has been found in microglial cells [210] and endothelial cells of the microvasculature [234]. Expression of GLUT5 was also observed in the Purkinje cells in the rat cerebellum [235]. Given that GLUT5 is localized to the BBB, it may mediate brain uptake of fructose since fructose can serve as an alternative energy source for the brain. In support of this notion, short-term fructose feeding increased brain expression of GLUT5 in both young and aging adult rats [236]. Recently, it was reported that rat neocortical cells took up and metabolized extracellular fructose *in vivo* [237]. Despite these advances, the physiological role of GLUT5 in the brain remains to be determined.

Compared to the above-mentioned glucose transporters, other facilitative glucose transporters such as GLUT6, GLUT8, and GLUT10, are poorly studied. The exact location, biochemical characteristics, regulation and physiological functions of GLUT6

and GLUT10 remain to be determined. GLUT8, a novel insulin-sensitive glucose transporter, was found ubiquitously expressed in the rat brain, including hippocampus, hypothalamus, cortex, amygdala, and cerebellum [238-240]. Similar to GLUT4, the immunoreactivity of GLUT8 was detected exclusively in neurons, particularly in the neuronal cells bodies and the proximal apical dendrites [238, 240, 241]. Results from *in vivo* studies suggest insulin may stimulate the translocation of GLUT8 from the cytoplasm to the membranes of the rough endoplasmic reticulum (ER) in hippocampal neurons [242]. Notably, this subcellular trafficking was impaired in the diabetic rat hippocampus [243]. It was proposed that GLUT8 may control ER glucose homeostasis by transporting glucose molecules removed from glycoproteins during protein processing out of the rough ER lumen into the cytoplasm [242]. However, *in vitro* studies failed to show GLUT8 translocation in neurons in response to insulin, potassium- or glutamate-induced depolarization [244, 245]. Therefore, future work is necessary to resolve the discrepancy and determine the function of GLUT8 in both physiological and pathological conditions.

Table 1.2.1 GLUTs expressed in the central nervous system

Protein	Expression sites	Cell Types	Substrates	Comments
GLUT1	Blood brain barrier	Glia and endothelial	>> Glucose mannose galactose	Very abundant Basal glucose uptake
GLUT2	Hypothalamus	Neurons, glia, and tanycytes	Glucose, mannose, galactose, fructose	Limited
GLUT3	Cortex, hippocampus, cerebellum, striatum	Neurons and glia	Glucose, mannose, galactose	Very abundant
GLUT4	Hippocampus, hypothalamus, cerebellum, olfactory bulb	Neurons and glia	Glucose	Insulin-sensitive
GLUT5	Blood brain barrier cerebellum	Microglia and endothelial	>> Fructose	
GLUT8	Hippocampus, cortex, hypothalamus, cerebellum	Neurons	Glucose, fructose	Insulin-sensitive Widely expressed

Glycolysis

Glycolysis is the first stage of cellular glucose metabolism. Through a series of metabolic processes in the cytosol, one molecule of glucose is broken down into two molecules of pyruvate, with the net gain of 2 molecules of ATP and production of NADH from NAD^+ (Fig.1.2.4). The previously consumed NAD^+ can be replenished through the reactions catalyzed by lactate dehydrogenase (LDH) or malate dehydrogenase (MDH) in the

malate-aspartate shuttle. Hexokinases act as the pacemaker of glycolysis by converting glucose into glucose-6-phosphate (Glc-6-p). Several hexokinase isoforms have been identified in the brain, with hexokinase I (HK1) being the major brain isoform responsible for glycolysis. HK1 has a low half-saturation constant (Km) thus possesses a high binding affinity for glucose and is able to metabolize glucose efficiently even when glucose concentration is low [246]. The activity of HK1 is feedback inhibited by high concentration of Glc-6-p. Another hexokinase isoform, HK2 is also expressed in the brain, albeit at a much lower level. HK2 also has low Km, thus may also be involved in glucose metabolism by promoting glycolysis. Recently, a protective role of HK2 in preventing mitochondrial death pathway and cell apoptosis has been proposed [247], suggesting HK2 may control neuronal survival in response to cellular stress. In addition to hexokinases, phosphofructokinase is another key enzyme that regulates glycolysis depending on the energy state [248]. The activity of phosphofructokinase is inhibited by signals for the high-energy state, such as increased ATP level, and reduced pH, which indicates the excessive formation of lactic acid, as well as enhanced citrate, an early intermediate in the TCA cycle. The inhibitory effect of ATP can be reversed by a high concentration of AMP, which suggests energy charge falls, or fructose 2, 6-bisphosphate, a potent activator of phosphofructokinase. A third key regulatory point in the glycolytic pathway is pyruvate kinase, which catalyzes the third committed step, yielding ATP and pyruvate. Fructose 1, 6-bisphosphate activates whereas ATP and alanine allosterically inhibit pyruvate kinase. Recently, brain aerobic glycolysis (AG), which describes non-oxidative metabolism of glucose despite the presence of adequate oxygen, has received increasing attention. Regional differences in AG have been observed in the human brain

[249]. Local AG was found to increase when neuronal activity was elevated. Importantly, brain regions with high AG, showed upregulated expression of genes related to synapse formation and growth [250]. Further, AG has been found to play a role in synaptic plasticity during motor adaptation learning [251]. These findings point out the implication of AG in the synaptic development and functions in the brain.

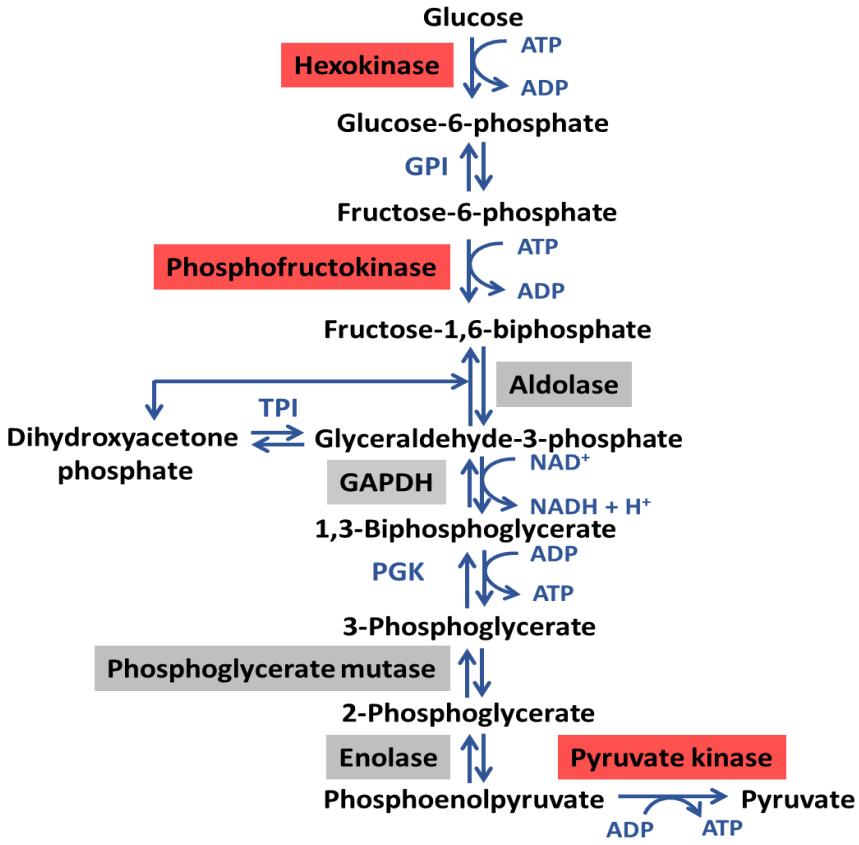

Figure 1.2.4

Fig.1.2.4 The glycolytic pathway. Enzymes and metabolic intermediates in the glycolytic pathway were shown. Three key regulatory points in the glycolytic pathway were highlighted in red. GPI: glucose-6-phosphate isomerase; TPI: triose-phosphate isomerase; GAPDH: glyceraldehyde 3-phosphate dehydrogenase; PGK: phosphoglycerate kinase

Pentose Phosphate Pathway (PPP)

Apart from being metabolized through the glycolytic pathway, Glc-6-p can be directed to the PPP shunt for the generation of NAPDH and five-carbon sugars, which are important for reductive biosynthesis, antioxidant defense, and nucleic acid synthesis. The PPP shunt consists of two phases: the oxidative phase and non-oxidative phase (Fig1.2.5). In the oxidative phase, glucose 6-phosphate is oxidized to ribose 5-phosphate, yielding NAPDH. In the non-oxidative phase, the interconversion of sugars with molecules containing different number of carbons occurs in a series of non-oxidative reactions, resulting in the synthesis of five-carbon sugars. Alternatively, excessive five-carbon sugars can be converted to the intermediates of glycolysis via transketolase and transaldolase. Glucose 6-phosphate dehydrogenase (G6PD) catalyzes the rate-limiting step in the PPP, thus serving as a critical regulatory point [252]. The rate of PPP is also controlled by the concentration of $NADP^+$ [252]. Low level of $NADP^+$ inhibits the activity of G6PD, whereas the high level of $NADP^+$ facilitates the oxidative phase of PPP shunt to replenish NADPH, which functions as a reductant for lipid and fatty acid synthesis. In the brain, the PPP shunt may represent an important antioxidant defense mechanism. It was suggested that NADPH generated by the PPP shunt can be used for regenerating antioxidant glutathione (GSH) from its oxidized form (GSSG) through a reaction catalyzed by glutathione reductase [253]. In support of this notion, oxidants such as hydrogen peroxide, cumene hydroperoxide, and peroxynitrite triggered a rapid activation of the PPP shunt and increased NADPH accumulation in both neurons and astrocytes [254-256]. Additionally, inhibition of glutathione peroxidase, GSH depletion, or the absence of glucose decreased oxidative stress-induced PPP activity and increased toxicity

[254, 255]. Further, D-glucose was found to protect rat cortical neurons against glutamate-mediated cell death likely through the stimulation of the PPP shunt, thus reversing glutathione oxidation and NADPH depletion induced by glutamate [257]. Together, these findings suggest the PPP shunt may play a major role in protecting brains against oxidative damage via the glutathione system.

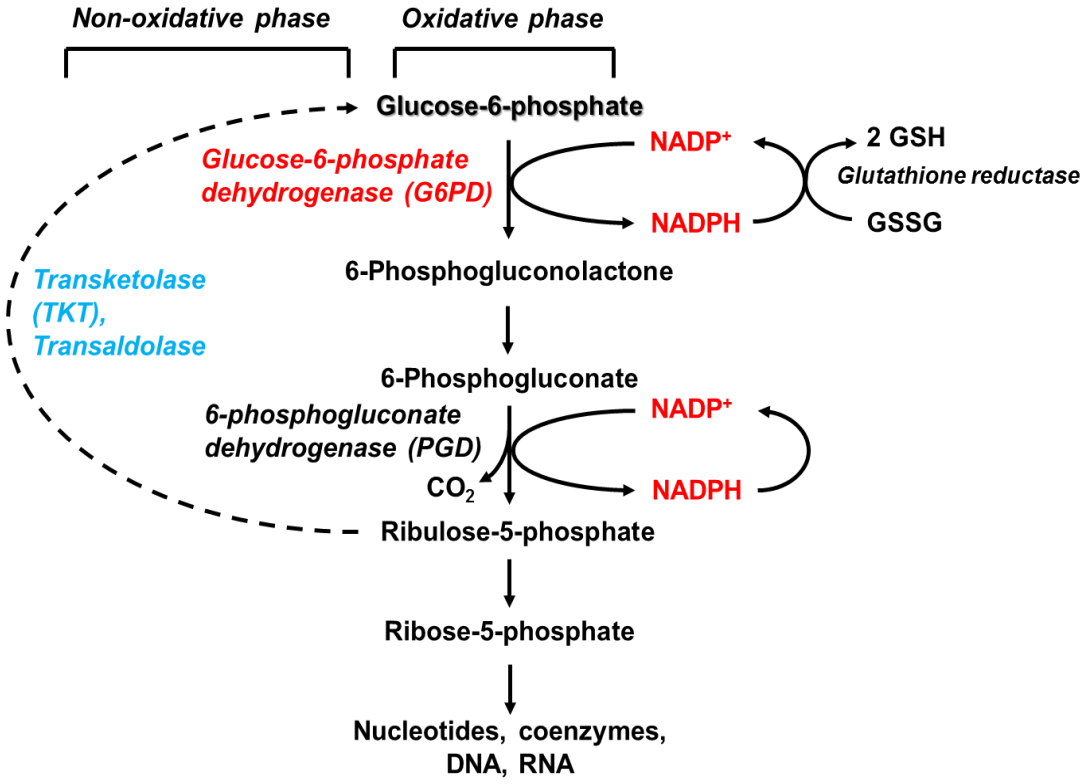

Figure 1.2.5

Fig.1.2.5 The pentose phosphate pathway. The PPP shunt includes both oxidative and non-oxidative branches. The glycolytic pathway and the PPP shunt are linked by transketolase and transaldolase (blue). Two major regulatory points are G6PD and NADPH/NAPD$^+$ (red) GSH: glutathione; GSSG: oxidized glutathione. Adapted from David L. Nelson (2008) Lehninger Principles of Biochemistry, Fifth Edition.

Glycogen synthesis and utilization

In astrocytes, Glc-6-p serves as a precursor for glycogen synthesis (Fig.1.2.6). Phosphoglucomutase catalyzes the conversion of Glc-6-p to glucose 1-phosphate (Glc-1-p), which together with uridine triphosphate, is used for the synthesis of uridine diphosphate glucose (UDP-glucose) in a reaction catalyzed by UDP-glucose pyrophosphorylase. Glycogen synthase (GYS), the key regulatory enzyme in glycogen synthesis, catalyzes the transfer of glucose from UDP-glucose to the C-4 hydroxyl group of a terminal residue in the growing glycogen molecule [258]. GYS exists in both active dephosphorylated (GYSa) and inactive phosphorylated (GYSb) forms, and the transformation of inactive GYSb to active GYSa is mediated by protein phosphatase 1 (PP1). On the contrary, GYSa can be phosphorylated at multiple sites by cAMP-dependent protein kinase A (PKA) or other kinases, leading to its inactivation. The breakdown of glycogen is catalyzed by glycogen phosphorylase (GP), during which Glc-1-p is released from glycogen through phosphorolysis [259]. In contrast to GYS, GP has the active phosphorylated form (GPa) and inactive dephosphorylated form (GPb) and the activation of phosphorylase kinase (PK) catalyzes the conversion of the b form into the a form. Like its substrate, the activity of PK can be modulated by phosphorylation of PK by PKA. PK contains Ca^{2+} binding sites and increased Ca^{2+} level can also activate PK [260]. In addition to covalent modification, GYS and GP are also regulated by noncovalent allosteric interactions depending on the energy state. For instance, GYSb can be activated by a high concentration of Glc-6-p. AMP may allosterically activate GPb by binding to its nucleotide-binding site and triggers a conformational change in GPb from a much less active tense (T) state into an active relaxed (R) state, which possesses similar

catalytic properties of the GPa phosphorylated form. By contrast, ATP may serve as a negative allosteric effector by competing with AMP and thus stabilizing the T confirmation [260]. Therefore, glycogen metabolism, which is reflected by the balance of glycogen synthesis and degradation, is tightly regulated by the activities of GYS and GP in response to changes in metabolic demand.

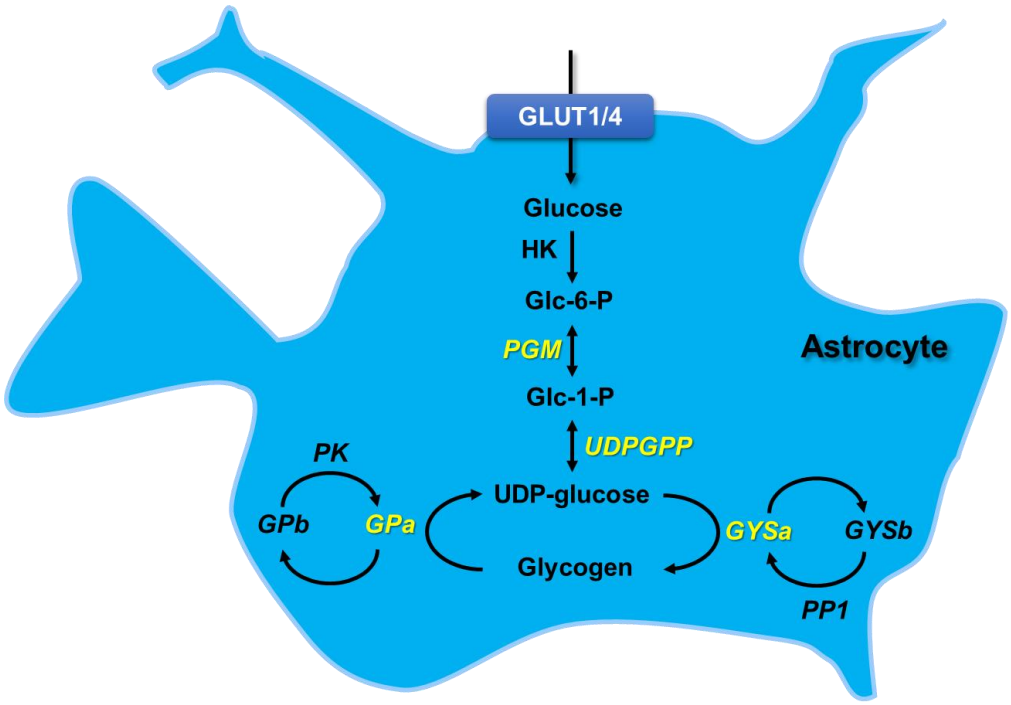

Figure 1.2.6

Fig.1.2.6 Glycogen synthesis and utilization. The uptake of glucose in astrocytes is likely mediated by both GLUT1 and GLUT4. Glucose-6-phosphate, which is converted from glucose by hexokinase, serves as a precursor for glycogen synthesis. Key enzymes and intermediates involved in glycogen synthesis and degradation were shown. HK: hexokinase; PGM: phosphoglucomutase; UDPGPP: UDP-glucose pyrophosphate; GYS: glycogen synthase; GYSa: active dephosphorylated form; GYSb: inactive phosphorylated form; PP1: protein phosphatase 1; GP: glycogen phosphorylase; GPa: active phosphorylated form; GPb: inactive dephosphorylated form; PK: phosphorylase kinase. Adapted from Falkowska, Anna et al. (2015) International Journal of Molecular Sciences 16(11): 25959–25981.

1.2.4.2 Ketone body uptake and metabolism in the brain

Brain monocarboxylate transporters

The brain uptake of ketone bodies is mediated by the monocarboxylate transporters (MCTs), which are a large transporter family containing 14 members. Only the first four members (MCT1 – MCT4) were identified as proton-linked transporters which facilitate the uptake of monocarboxylates such as lactate, pyruvate, and ketone bodies. Numerous studies have confirmed the expressions of MCT1, MCT2, and MCT4 in both rodent and human brains. A summary of major brain MCTs can be found in table 1.2.2. MCT1, the predominant form, is ubiquitously expressed throughout the brain. Immunohistochemical analyses of rat brain sections indicated that MCT1 was predominately expressed in both luminal and abluminal membranes of brain microvessel endothelial cells, suggesting MCT1 may play an important role in the brain uptake of ketone bodies and other monocarboxylates across the BBB [261, 262]. MCT1 immunoreactivity was also found in the astrocyte processes, particularly those of the glial limiting membrane [263-265]. The expression of MCT1 was also observed in a subset of neurons in several brain regions, particularly the hypothalamus, albeit at a much lower level [262, 266]. In contrast, MCT2 represents the major neuronal monocarboxylate transporter. The expression of MCT2 has been observed in the mouse brain regions including cortex, hippocampus, and cerebellum [265, 267]. At the subcellular level, MCT2 was found localized to postsynaptic densities and the expression of MCT2 appeared to correlate with synaptic development [265, 266, 268]. Specific populations of astrocytes in the white matter also exhibited MCT2 expression [266, 269]. Compared to MCT1 and MCT2, MCT4 has a more restricted cellular distribution. MCT4 has been found to be exclusively

expressed in the astrocytes in several brain regions including the cerebral cortex, hippocampus, cerebellum, and hypothalamus [266, 270, 271]. Given that astrocytes rely heavily on glycolytic metabolism, MCT4 may play a major role in the efflux of lactate.

Table 1.2.2 MCTs expressed in the central nervous system

Protein	Expression sites	Cell Types	Substrates	Comments
MCT1	Ubiquitous, blood brain barrier	Endothelial, astrocytes	Pyruvate, lactate, ketone bodies	Predominant isoform
MCT2	Hippocampus, cortex, cerebellum	Neurons, astrocytes	>>Lactate, pyruvate, ketones	Major neuronal isoform
MCT4	Cortex, hippocampus, cerebellum, hypothalamus	Astrocytes	Lactate	Restricted to astrocytes

Brain ketone body metabolism

Ketone bodies refer to three molecules: acetoacetate (AcAc), β-hydroxybutyrate (BHB) and acetone. Acetone is a minor product of spontaneous decarboxylation of AcAc. During glucose shortage, two predominant ketone bodies, AcAc and BHB, are generated in the liver, mainly from oxidation of fatty acids, serving as the alternative source of energy for the brain [272, 273]. It has been estimated that ketone bodies account for nearly two thirds of the brain's energy requirement during periods of prolonged fasting and starvation [273, 274]. As mentioned previously, MCT1 on the brain microvessels

mediates the transport of ketone bodies across the BBB and MCT2 regulates the neuronal uptake of ketone bodies. Within neurons, the metabolism of ketones occurs exclusively in the mitochondria and involves two steps, which is summarized in Fig.1.2.7. Briefly, β-hydroxybutyrate dehydrogenase (BDH) catalyzes the first reversible step of ketolysis by converting BHB to AcAc. The subsequent reconstitution of acetoacetyl coenzyme A (CoA) from AcAc is catalyzed by acetoacetyl succinyl-CoA transferase, which is also known as succinyl-CoA: 3-oxoacid CoA transferase (SCOT). The last step in ketolysis is the generation of 2 molecules of acetyl-CoA from acetoacetyl-CoA by the reversible enzyme acetoacetyl-CoA thiolase, also known as acetyl-CoA acetyltransferase (ACAT). Acetyl-CoA is then further metabolized to water and CO_2 via the TCA cycle and mitochondrial oxidative phosphorylation. SOCT has been found to be a critical regulatory point for ketone body metabolism [273]. It is inhibited in the presence of high concentration of AcAc.

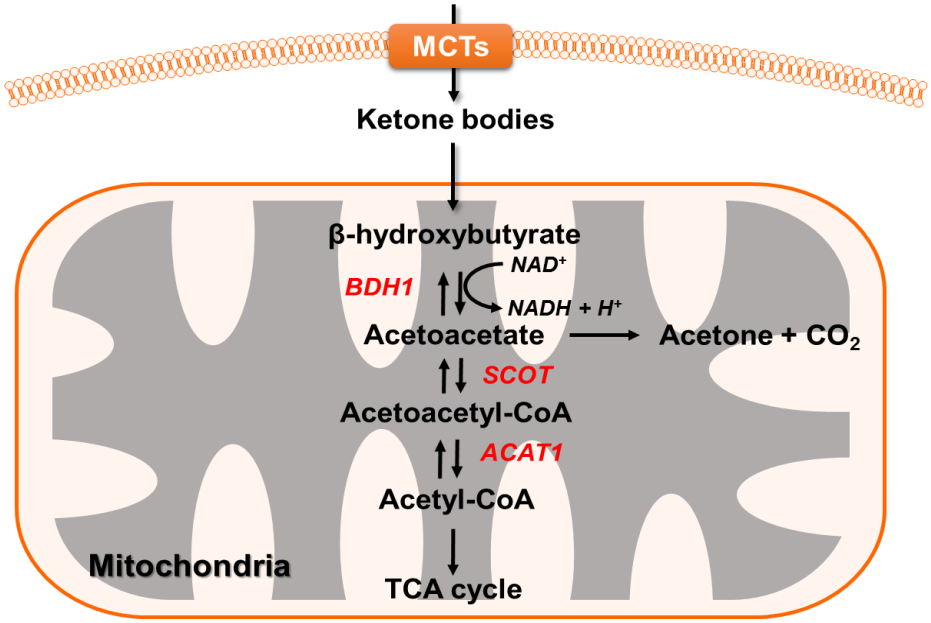

Figure 1.2.7

Fig.1.2.7 Ketone body uptake and metabolism. The uptake of ketone boides in the brain is mediated by MCT1 and MCT2. Ketone bodies can freely enter mitochondria where they are converted to acetyl-CoA through ketolysis. Key enzymes and intermediates involved in ketolysis are shown. BDH1: β-hydroxybutyrate dehydrogenase, mitochondrial; SCOT: succinyl CoA: 3-oxoacid CoA transferase; ACAT1: acetyl-CoA acetyltransferase, mitochondrial.

1.2.5 ApoE polymorphisms and perturbed brain energy metabolism

ApoE genetic status influences glucose metabolism and mitochondrial function

It has been shown that the preclinical development of AD begins 10-20 years prior to its clinical manifestation. One of the major changes that typically occur in the preclinical AD brain is the severe reduction of the cerebral glucose metabolic rate (CMRglc) as measured by FDG-PET scans [275]. Several longitudinal FDG-PET studies of non-demented elderly subjects indicate that reduction of CMRglc in AD-vulnerable regions during normal aging predicted cognitive decline years in advance of the clinical diagnosis [31, 276, 277]. In patients with MCI, which is considered a prodrome to AD, the extent of CMRglc reduction was in parallel to the severity of cognitive deficits [278, 279]. Additionally, CMRglc reductions were observed in individuals at genetic risk for AD. FDG-PET studies on cognitively normal middle- and late-middle-aged individuals bearing ApoE4 demonstrated similar region-specific patterns of glucose hypometabolism. The most significant deficit occured in the posterior cingulate cortex (PCC), the brain region which serves as a central node in the default mode network (DMN) and consistently shows early metabolic alterations in AD [280, 281]. Similar regional CMRglc reductions were also observed in cognitively normal young ApoE4 carriers, at an age several decades before the possible onset of dementia or clinical manifestations of AD [32]. Notably, in ApoE4 carriers, the gene dose of ApoE4 alleles was negatively correlated with values of CMRglc in the same brain regions as patients with probable AD [84]. Despite these observations, the cause and precise mechanisms underlying glucose hypometabolism in the preclinical AD brain remain largely unknown.

In the past decade, emerging evidence suggests ApoE isoforms differentially modulate mitochondrial respiration and cellular bioenergetics. A microarray analysis of hippocampal tissue from AD patients indicated that expression of ApoE4, in comparison to ApoE3, was associated with downregulation of gene transcripts involved in mitochondrial oxidative phosphorylation and energy metabolism [282]. Similarly, studies on the post-mortem cortical tissues from ApoE4 carriers showed abnormalities in the expressions of transcripts that regulate mitochondrial respiratory chain activity [283]. In young ApoE4 carriers, significantly lower mitochondrial cytochrome c oxidase activity was observed in PCC, a brain region later vulnerable to AD [284, 285]. A more detailed examination revealed extensive alterations in the uptake of brain energy substrates and their metabolism. It was found that young ApoE4 carriers exhibited enhanced protein expression of complexes I, II and IV of the mitochondrial electron transport chain compared to non-carriers [286]. Despite the increase in protein levels, the functional activities of these subunits may be decreased. Therefore, the upregulation of protein expression can be interpreted as a compensatory response to dysfunction.

Consistent with clinical findings, mice expressing ApoE4 also displayed mitochondrial structural alterations and functional abnormalities [287, 288]. While the precise mechanism by which ApoE4 induces mitochondrial dysfunction is not well understood, results obtained from *in vitro* studies suggest that a carboxyl-terminal-truncated form of ApoE4 (1-272), produced by proteolysis of ApoE via a chymotrypsin-like serine protease, may be responsible for the detrimental effects of ApoE4 on mitochondrial respiratory function [289]. Specifically, ApoE4(1-272) fragments were found to mislocalize to mitochondria [290] and bind to subunits of mitochondrial electron

transport chain complex III and complex IV, leading to impaired respiratory chain activity [291]. Recently, it was reported that ApoE4-containig lipoprotein particles significantly upregulate endoplasmic reticulum (ER)-mitochondrial communication and mitochondria-associated ER membranes (MAM) function in human fibroblasts [292]. Since the crosstalk between mitochondria and ER regulates mitochondrial homeostasis with MAM serving as the platform, the perturbations in ER-mitochondrial communication and MAM function may contribute to ApoE4-associated mitochondrial dysfunction. Collectively, these findings suggest ApoE genetic status influences mitochondrial bioenergetics, with ApoE4 adversely affecting mitochondrial functions.

While there is an abundance of research demonstrating the negative impact of ApoE4 on cerebral bioenergetics, few studies have explored the effects of ApoE2. To address this research gap, our laboratory has initiated a series of studies to identify the molecular differences in brain energy metabolism that separate ApoE2 brains from ApoE3 and ApoE4 brains. Our analyses demonstrated that human ApoE isoforms differentially modulate brain insulin-like growth factor 1 (Igf1) signaling and downstream glucose uptake and metabolism. Compared to ApoE3 and ApoE4 brains, ApoE2 brains exhibited the most bioenergetically robust profiles, providing a possible mechanism by which ApoE2 promotes neuroprotection [87]. Additionally, we have recently demonstrated for the first time that three ApoE isoforms differentially modulate a key component of the catalytic domain of the V-type H^+-ATPase, a proton pump that mediates the concentration of neurotransmitters into synaptic vesicles and thus plays a crucial role in synaptic transmission. Specifically, our data indicate that ApoE2 brains express significantly higher levels of the β subunit of V-type H^+-ATPase when compared to both ApoE3 and

ApoE4 brains, providing a mechanistic rationale for the positive impact on cognitive function conferred by ApoE2 [293]. Collectively, our data indicate that the three ApoE brains are significantly different in two major areas — bioenergetically and synaptically — and that a more efficient and robust status in both areas may underlie the neuroprotective and cognition-favoring properties associated with ApoE2.

ApoE4 genetic status modifies the efficacy of a ketogenic agent

The clinical application of a high-fat and low-carbohydrate ketogenic diet on patients with CNS disorders, starting with epilepsy, has been established almost a century ago [294, 295], whereas the mechanisms by which a ketogenic diet confers neuroprotection remain unknown. Preclinical studies indicate that enhanced mitochondrial respiration and ATP generation may underlie the neuroprotective effects of a ketogenic diet [296-299]. In patients with probable AD or mild cognitive impairment, treatment with a ketogenic agent, which is primarily composed of medium-chain triglycerides, resulted in a significant improvement in the cognitive function.The ketogenic agent induced a marked elevation in plasma ketone body (BHB) concentration and a positive correlation was found between BHB level and cognitive performance. Notably, the positive response was confined to ApoE4 non-carriers, whereas ApoE4 carriers showed no effect or even a minor deterioration [86]. The results obtained from this acute dosing study were replicated in a 90-day study of the same ketogenic compound, AC-1202 [85, 300]. In this randomized, double-blind, placebo-controlled study involving 152 probable AD subjects with mild to moderate cognitive impairment, the effects of AC-1202 on cognitive function were evaluated by the AD Assessment Scale-Cognitive subscale (ADAS-Cog).

Among participants who did not carry ApoE4, daily administration AC-1202 significantly improved scores of ADAS-Cog relative to placebo on day 45 and the effects were maintained throughout the study. In contrast, no difference was observed among subjects who were detected to be ApoE4 positive. Additional analyses revealed that some SNPs in genes of insulin degrading enzyme and a proinflammatory cytokine interleukin 1 beta may enhance the therapeutic efficacy of the ketogenic agent in ApoE4 non-carriers [301]. In contrast, such effects of SNP genotype were not detected on ApoE4 carriers. Despite these findings, it is unclear why ApoE4 carriers do not benefit from ketosis. While ApoE4-induced mitochondrial dysfunction may contribute to an impaired ability in metabolizing ketone bodies, abnormalities in the brain ketone body uptake and transport could also lead to a deficiency in ketone body utilization. Future studies are necessary to examine these possibilities.

The goals of the first chapter are to pinpoint the specific substrate and metabolic pathway that are differentially regulated by ApoE genetic status. We performed a custom gene expression profiling of the major metabolic pathways involved in brain energy substrate transport and cytosolic metabolism in human ApoE gene-targeted replacement mice. Utilizing Neuro2a cells expressing human ApoE isoforms, we validated our findings from the gene array analysis and further examined the mechanisms by which ApoE isoforms modulate glucose metabolism, particularly focused on hexokinase and glycolysis. Our data provide additional evidence that human ApoE isoforms exert differential impact on brain energy metabolism, which could serve as a potential mechanism underlying their discrete risk impact in AD.

1.3 Materials and Methods

1.3.1 Animals

All the animal work presented has been approved by the Institutional Animal Care and Use Committee (IACUC) of the University of Kansas and followed National Institutes of Health (NIH) guidelines for the care and use of laboratory animals. 6 month-old human ApoE2, ApoE3, and ApoE4 gene-targeted replacement (hApoE2-TR, hApoE3-TR, and hApoE4-TR) mice were obtained from Taconic Biosciences (Hudson, NY, USA). These mice express human ApoE at physiological levels in the same temporal and spatial patterns observed in humans [302], which allows the direct comparison of human ApoE isoform-specific effects *in vivo*.

1.3.2 Plasmids

Human ApoE2, ApoE3 and ApoE4 cDNA expressed in the mammalian vector pCMV6 with C-terminal Myc-DDK Tag were procured from OriGene Technologies (Rockville, MD, USA). ApoE3 cDNA clone (NM_000041) was directly purchased from OriGene. ApoE2 and ApoE4 cDNA clones were generated by genetic modification of the ApoE3 cDNA sequence. Specifically, an ApoE2 cDNA clone was obtained by mutating 388 T to C, resulting in a Cys to Arg substitution in codon 112. ApoE4 cDNA clone was obtained by mutating 526 C to T, which resulted in an Arg to Cys substitution in codon 158. Mouse PGC-1α cDNA clone (NM_008904) expressed in the vector pCMV6 was purchased from OriGene. For all the experiments, the empty pCMV6 vector was used as the control plasmid. 100 ng plasmid DNA was transformed into DH5α competent cells (Invitrogen) for amplification. The purification of plasmid DNA was performed using

Plasmid Midi Kit (Qiagen, Hilden, Germany) according to manufacturer's manual.

1.3.3 Cell Culture

Mouse neuroblastoma cell line Neuro-2a (N2a) was purchased from American Type Culture Collection (ATCC, Manassas, VA, USA). N2a cells were grown in Dulbecco's Modified Eagle Medium (DMEM, High Glucose) (Thermo Fisher Scientific, Waltham, MA, USA) supplemented with 10% Fetal Bovine Serum (FBS) (Thermo Fisher Scientific). Cells were sub-cultivated every 3-4 days and maintained at 37 °C in a humidified atmosphere with 5% CO_2. A new vial of frozen cell stock was recovered when the passage number exceeds 25.

1.3.4 Generation of Neuro-2a Cells Stably Expressing Human ApoE isoforms

N2a cells stably expressing human ApoE2, 3 and 4 were generated as described below. In brief, a kill curve assay was performed on N2a cells to determine the optimal concentration of Geneticin (G418, Thermo Fisher Scientific). Cells were then transfected with 2 μg hApoE2-pCMV6, hApoE3-pCMV6 or hApoE4-pCMV6 using Lipofectamine 3000 according to the manufacturer's instructions. 48 hours after transfection, the medium containing transfection complexes was replaced with N2a culture medium containing 600 μg/mL G418. Cells stably transfected were selected for 10 days, then dissociated from the plates and subjected to limited dilution on 96-well plates. Wells containing a single cell were marked and colonies formed in those wells were considered to be monoclonal. Cells were maintained in a humidified 37°C, 5% CO_2 environment and media containing 600 μg/mL G418 were changed every 3-4 days. An individual colony in

each well was transferred to one well in 24-well plates for further expansion. Cell lines stably expressing ApoE2 or ApoE4 at similar levels, as determined by qRT-PCR and Western blotting, were used in the study.

1.3.5 Transfection

Transient transfection of human ApoE isoforms in N2a cells N2a cells were transfected with 2 μg human ApoE2, ApoE3 and ApoE4 cDNA and empty vector using Lipofectamine 3000 transfection reagent (Thermo Fisher Scientific). Cells were incubated with plasmid DNA-transfection reagent complex for 48 hours prior to further experiments. The transfection efficiency was determined by measuring the protein and gene expression levels of ApoE.

PGC-1α overexpression in N2a cells stably expressing human ApoE4 Cells stably expressing human ApoE4 were plated at a density of 3×10^5 /well in a 6-well plate in DMEM without G418 the day before transfection. A reaction containing 500 ng of either PGC-1α-pCMV or empty pCMV vector and Lipofectamine 3000 reagent in Opti-MEM (Thermo Fisher Scientific) was prepared for each transfection. Cells were incubated with the prepared reaction mix for 24 hours at 37°C, 5% CO_2. Then DMEM containing transfection reagents were replaced with fresh culture medium and cells were grown for additional 24 hours before protein extraction, mitochondrial and glycolytic function assays.

The introduction of human ApoE2 to N2a cells expressing human ApoE4 2 μg human ApoE2 cDNA and empty vector were introduced into N2a cells stably expressing human ApoE4 using Lipofectamine 3000. 48 hours post transfection, mRNA level and protein

expression of ApoE were determined in the transfected cells to evaluate the transfection efficiency.

1.3.6 Immunoblotting Analysis

Cells were washed twice with cold Dulbecco's phosphate-buffered saline (dPBS) and lysed with Neuronal Protein Extraction Reagent (N-PER) (Thermo Fisher Scientific) supplemented with protease and phosphatase inhibitors (Thermo Fisher Scientific). Cortical tissue homogenates were prepared from 6-month-old hApoE-TR mice using Tissue Protein Extraction Reagent (T-PER) (Thermo Fisher Scientific) containing protease and phosphatase inhibitors. Protein concentrations of the cell extracts and tissue homogenates were determined by BCA protein assay kit (Thermo Fisher Scientific). Immunoblotting analyses were carried out as previously published [293]. The following primary antibodies were used: goat anti-Apolipoprotein E (1:5000, EMD Millipore), rabbit anti-hexokinase I (1:3000, Cell Signaling Technology, Danvers, MA), rabbit anti-hexokinase II (1:2000, Cell Signaling Technology), rabbit anti-PGC-1α (1:1000, Santa Cruz Biotechnology, Dallas, TX), mouse anti-PGC-1α (1:1000, EMD Millipore), rabbit anti-β-actin (1:5000, Thermo Fisher Scientific), mouse anti-β-tubulin (1:5000, Thermo Fisher Scientific). Secondary antibodies were species-specific horseradish peroxidase-conjugated immunoglobulins purchased from Thermo Fisher Scientific. Protein bands were visualized using chemiluminescence (BioRad) on C-Digit Blot Scanner (LI-COR). Band densities were quantified using the Image Studio Version 4.0 image digitizing software with signal normalized to loading control protein.

1.3.7 ATP Levels

Cells were plated at 1 x 10^4 / well in white opaque 96-well culture plate the day before experiments. ATP levels were measured using CellTiter-Glo Luminescent Cell Viability Assay (Promega, Madison, WI, USA) according to the manufacturer's instructions. The luminescence level was normalized to the protein content in each individual well.

1.3.8 RNA Extraction from Cells

Total RNA was extracted from stable N2a-hApoE4 cells transfected with human ApoE2-pCMV. In brief, 350 µL Trizol reagent (Thermo Fisher Scientific) was added to each well in a 6 well plate to lyse the cells. 100 µL chloroform was added to the cell lysates and samples were inverted vigorously several times to mix thoroughly. The samples were centrifuged for 15 minutes at 12,000 × g at 4°C. The upper aqueous phase containing RNA was carefully transferred to a new tube. Subsequent purification of RNA was performed using PureLink RNA Mini Kit (Thermo Fisher Scientific) following manufacturer's instructions. RNA concentration was measured by Qubit Assay Kit (Invitrogen). The quality of RNA was evaluated by 2200 TapeStation system (Agilent, Santa Clara, CA, USA).

1.3.9 Gene Expression Analysis

The gene expression of ApoE after transfection was measured by real-time PCR as previously described [303]. Genomic DNA was extracted from N2a cells transfected with human ApoE2, ApoE3, ApoE4 cDNA and mock vector using PureLink Genomic DNA Mini Kit (Thermo Fisher Scientific). For measurement of gene expression of human ApoE2 in N2a-hApoE4 cells transfected with hApoE2-pCMV, cDNA was synthesized

from RNA extracted from the transfected cells using High Capacity RNA-to-cDNA Master Mix (Applied Biosystem). The primers were synthesized and purchased from Integrated DNA Technologies (Coralville, IA, USA). The sequences of the primers were: 5'- CGGACATGGAGGACGTGT -3' (Forward) and 5'- CTGGTACACTGCCAGGCA -3' (Reverse) for ApoE2, 5'- CGGACATGGAGGACGTGT -3' (Forward) and 5'- CTGGTACACTGCCAGGCG -3' (Reverse) for ApoE3, 5'- CGGACATGGAGGACGTGC -3' (Forward) and 5'- CTGGTACACTGCCAGGCG -3' (Reverse) for ApoE4. DNA amplification was performed on 100 ng of genomic DNA or 20 ng cDNA mixed with 1× Power SYBR Green PCR Master Mix (Applied Biosystems) and 0.3 μM of each primer under the following protocol: stage 1: AmpErase UNG activation at 50°C for 2 min; stage 2: AmpliTaq Gold DNA Polymerase activation at 95 °C for 10 min; stage 3: denature at 95 °C for 15 s followed by annealing/extension at 60 °C for 1 min, for 40 cycles. Negative controls contained the same reaction mixture without DNA. Mouse GAPDH served as loading control. The fluorescence was detected on QuantStudio 7 Flex Real-Time PCR System (Applied Biosystems) and data were analyzed by the comparative Ct (ΔCt) method.

1.3.10 TaqMan Gene Expression Profiling

TaqMan gene expression array cards (96-well plate format, which enables analysis of 2 samples against 48 genes) were custom manufactured at Applied Biosystem. A list of 43 genes and 5 candidate control genes examined in the array can be found in Table 1.4.1. Total RNA was extracted from cortex tissues of 6-month-old hApoE-TR mice using PureLink RNA Mini Kit. RNA quantity was determined using Qubit Assay Kits and RNA

quality was analyzed using Agilent RNA 6000 Nano Kit on Agilent 2100 Bioanalyzer system (Agilent). The integrity of RNA samples was assessed by RNA integrity number (RIN). RNA samples with RIN greater than 8.0 proceeded to cDNA synthesis. The conversion of RNA to cDNA was performed using the High Capacity RNA-to-cDNA Master Mix on T100 thermocycler (Bio-Rad Laboratories, Hercules, CA, USA). Taqman qRT-PCR reaction was carried out on QuantStudio 7 Flex Real-Time PCR System under the following thermal cycling conditions: AmpErase UNG activation at 50°C for 2 min; AmpliTaq Gold DNA Polymerase activation at 95 °C for 10 min followed by 40 cycles of denaturation at 95 °C for 15 s and annealing/extension at 60 °C for 1 min. Each reaction mixture contained 10 ng cDNA samples mixed with 1× TaqMan Universal PCR Master Mix (Applied Biosystems).

Data were analyzed using the PCR Array Data Analysis Software (Qiagen, Hilden, Germany). Relative gene expression levels or fold change (FC) relative to the comparison group were calculated by the comparative Ct (ΔΔCt) method, with Ct denoting threshold cycle. Normalization factor calculation based on the geometric mean of multiple control genes was performed for selection of the endogenous control gene for normalization [304]. Samples collected from 4 animals per ApoE genotype group were included in the analysis. For each sample, ΔCt was calculated as the difference in average Ct of the target gene and the endogenous control gene. For each ApoE genotype, mean $2^{-\Delta Ct}$ was calculated as the arithmetic means of $2^{-\Delta Ct}$ of the 4 samples in the group. FC was then calculated as mean $2^{-\Delta Ct}$ (ApoE genotype group) divided by mean $2^{-\Delta Ct}$ (comparison group). The $2^{-\Delta Ct}$ values for each target gene between two ApoE genotype groups were statistically compared using Student's t-test; $p < 0.05$ was considered statistically

significant. The p-values were adjusted by Bonferroni correction.

The heat map graphically demonstrated the hierarchical clustering of gene expression data. Distances between samples and target genes were calculated based on ΔCt values using Pearson's correlations. The volcano plot displayed FC in the X-axis versus p-values in the Y-axis, which enabled the overview of gene fold regulation and identification of genes with fold change to the statistical significance level.

1.3.11 IPA Network Analysis

Data containing gene identifiers and corresponding FC relative to the comparison group (ApoE3) were uploaded to Ingenuity Pathway Analysis (IPA, Qiagen Bioinformatics). IPA upstream regulator analysis identified transcriptional regulators upstream of the genes in the dataset which potentially explained the observed gene expression changes. A prediction is made about the activation state of an upstream molecule when most of the target genes changed in the direction that is consistent with a particular activation state of the transcriptional regulator. Activation z-score was calculated to predict the state of the upstream regulator: activating (z-score ≥ 2) or inhibiting (z-score ≤ -2).

1.3.12 Hexokinase Activity Assay

Hexokinase activity assay was performed as previously described [305]. The assay is based on the reduction of nicotinamide adenine dinucleotide (NAD^+) through a coupled reaction with glucose-6-phosphate dehydrogenase. Briefly, 150 µL solution containing 13.3 mM $MgCl_2$, 0.112 M glucose, 0.55 mM adenosine 5' triphosphate, 0.227 mM NAD^+ and 1 IU/mL glucose-6-phosphate dehydrogenase in 0.05 M Tris-HCl buffer, pH 8.0 was

loaded in each well of 96-well microplate. The plate was incubated at room temperature for 6 - 8 minutes to achieve temperature equilibration. 20 µg whole cell lysates from transfected cells were added to start the reaction. Hexokinase solution prepared by dissolving hexokinase in 0.05 M Tris-HCl buffer, pH 8.0 served as positive control. Assay buffer without sample served as negative control. The increase in absorbance (A) at 340 nm was recorded every 1 min for 30 minutes at 30 °C. ΔA/min from an initial linear portion of the curve was used to calculate the enzyme activity.

1.3.13 Analysis of Mitochondrial respiration and Glycolysis

The XF96 Extracellular Flux Analyzer (Agilent Technologies), which measures oxygen consumption rate (OCR) and extracellular acidification rate (ECAR) was used to assess mitochondrial respiration and glycolytic function in N2a cells expressing human ApoE isoforms. Transfected cells were seeded at a density of 3.1×10^5 cells/cm^2 in the 96-well culture plate provided with the flux pack (Agilent Technologies) the day before the experiments. Both the Mito Stress Test and the Glycolysis Stress Test were performed according to manufacturer's instructions.

For the Mito Stress Test, cell growth media was replaced with pre-warmed assay medium (XF base medium supplemented with 5.5 mM glucose, 2 mM glutamine and 1 mM sodium pyruvate, pH 7.4) and incubated in 37°C incubator without CO_2 for 1 hour prior to the test. OCR was measured under basal condition followed by sequential injection of the compounds: ATP coupler oligomycin (2 µg/mL), ETC accelerator FCCP (1 µM), and a mix of mitochondrial electron transport chain (ETC) complex inhibitors rotenone (1 µM) and antimycin A (1 µM) to measure ATP-linked respiration, maximal respiration,

and non-mitochondrial respiration, respectively.

For the Glycolytic Stress Test, cell growth media was replaced with pre-warmed assay medium (XF base medium containing 2 mM glutamine, pH 7.4) and incubated at 37°C in the absence of CO_2 for 1 hour before the assay. ECAR was measured under basal condition followed by sequential addition of compounds. The initial injection was a saturating concentration of glucose (10 mM), which allows the measurement of glycolysis rate under basal conditions. The addition of oligomycin (2 μg/mL) results in the inhibition of mitochondrial ATP generation and thus shunting the energy production to glycolysis, with the subsequent increase in ECAR revealing the maximum glycolytic capacity of the cells. The final injection was 2-Deoxy-D-glucose (50 mM), a glucose analogue that competitively binds to hexokinase and inhibits the conversion of glucose to glucose-6-phosphate thereby terminating the glycolysis.

To examine the impact of human ApoE isoforms in cells' ability to metabolize ketone bodies, FCCP-induced maximal mitochondrial respiration rates were measured in ApoE-expressing cells sequentially injected with β-hydroxybutyrate (5 mM) and mitochondrial inhibitors oligomycin (5 μg/mL). OCR and ECAR values were normalized to the total protein content in each well. Data were analyzed using Seahorse XF Cell Mito\Glycolysis Stress Test Report Generator.

1.3.14 Statistical Analyses

Each experiment was performed independently at least three times. Data are presented as mean ± standard error of the mean (SEM). All statistical analyses were performed using GraphPad Prism 6 (GraphPad Software, La Jolla, CA, USA). All data were analyzed by

Student's t-test or one-way ANOVA. Post-hoc tests were performed using the Holm–Bonferroni method. A p-value < 0.05 was considered statistically significant and the degree of significance was represented by the number of asterisks and/or pound sign.

1.4 Results

1.4.1 Human ApoE isoforms differentially modulate brain energy substrate uptake and cytosolic metabolism

To probe the metabolic pathways that are differentially regulated by human ApoE isoforms, a TaqMan gene expression profiling was conducted on the cortical tissues collected from 6-month-old human ApoE gene-targeted replacement mice (hApoE-TR). A complete list of the 48 genes grouped according to functional class is provided in Table 1.4.1. We focused on the genes involved in the molecular processes from energy substrate uptake to cytosolic metabolic pathways leading to the generation of acetyl-CoA (Fig. 1.4.1A). The fold changes (FC) relative to gene expression levels in the comparison group (ApoE2 or ApoE3) with the corresponding p-value are indicated in Table 1.4.2. Both distinct and consistent patterns among the three ApoE brains were observed in the gene expression analysis. More specifically, the group heatmap demonstrated that the profile associated with ApoE4 appeared most distinct from those of ApoE2 and ApoE3 brains; in comparison, ApoE2 and ApoE3 brains shared some degree of similarity (Fig. 1.4.1B).

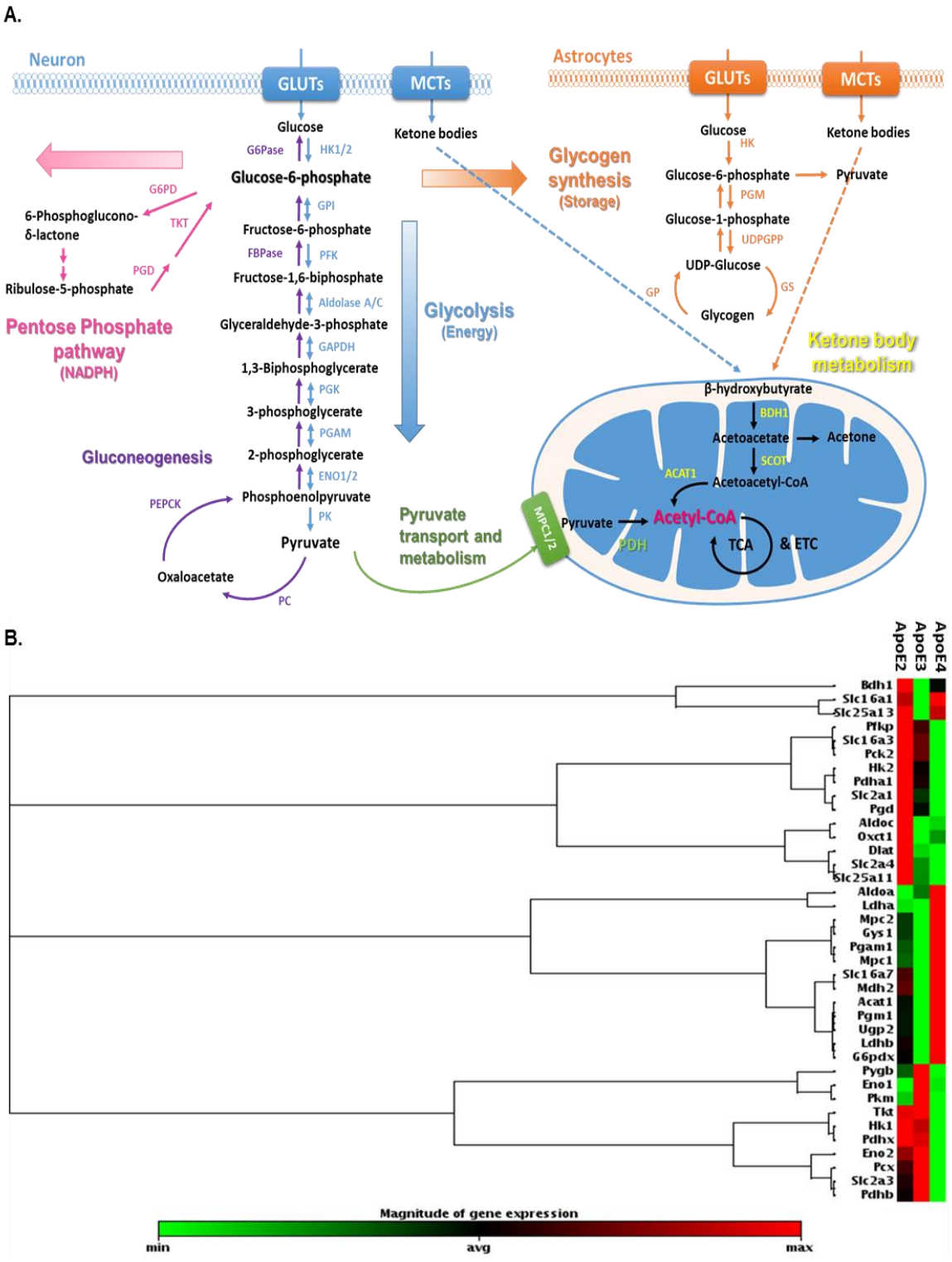
A.
Neuron
GLUTs
MCTs
Astrocytes
GLUTs
MCTs
Glucose
Ketone bodies
G6Pase
HK1/2
Glucose-6-phosphate
GPI
Fructose-6-phosphate
FBPase
PFK
Fructose-1,6-biphosphate
Aldolase A/C
Glyceraldehyde-3-phosphate
GAPDH
1,3-Biphosphoglycerate
PGK
3-phosphoglycerate
PGAM
2-phosphoglycerate
ENO1/2
Phosphoenolpyruvate
PK
Pyruvate
Oxaloacetate
PEPCK
PC
G6PD
TKT
PGD
6-Phosphoglucono-δ-lactone
Ribulose-5-phosphate
Pentose Phosphate pathway (NADPH)
Gluconeogenesis
Glycolysis (Energy)
Glycogen synthesis (Storage)
Glucose
HK
Glucose-6-phosphate
Pyruvate
PGM
Glucose-1-phosphate
UDPGPP
UDP-Glucose
GS
Glycogen
GP
Ketone body metabolism
β-hydroxybutyrate
BDH1
Acetoacetate
Acetone
SCOT
ACAT1
Acetoacetyl-CoA
Pyruvate
Acetyl-CoA
PDH
TCA
& ETC
MPC1/2
Pyruvate transport and metabolism
B.
ApoE2
ApoE3
ApoE4
Bdh1
Slc16a1
Slc25a13
Pfkp
Slc16a3
Pck2
Hk2
Pdha1
Slc2a1
Pgd
Aldoc
Oxct1
Dlat
Slc2a4
Slc25a11
Aldoa
Ldha
Mpc2
Gys1
Pgam1
Mpc1
Slc16a7
Mdh2
Acat1
Pgm1
Ugp2
Ldhb
G6pdx
Pygb
Eno1
Pkm
Tkt
Hk1
Pdhx
Eno2
Pcx
Slc2a3
Pdhb
Magnitude of gene expression
min
avg
max

Figure 1.4.1

Fig. 1.4.1 Human ApoE isoforms differentially modulate brain energy substrate uptake and cytosolic metabolism. A) Schematic illustration of brain energy substrate uptake and the generation of acetyl-CoA. Hexokinase 1/2 catalyze the conversion of glucose to glucose-6-phosphate, a "branch-point" metabolite that has alternative metabolic fates. Acetyl-CoA is a critical point of convergence of glucose and ketone body metabolism. Brain uptake of glucose and ketone body are strictly controlled by their respective transporters, glucose transporters (GLUTs) and monocarboxylate transporters (MCTs). Key enzymes involved in the glucose and ketones metabolic pathways are shown. B) Gene expression profiles on energy substrate uptake and cytosolic metabolism in the brains of 6-month-old hApoE-TR mice. n=4 per group.

1.4.2 ApoE2 brain exhibited the most robust whereas ApoE4 brain displayed the most deficient gene expression profile in glucose uptake and glycolytic pathway

We first examined the gene expression profiles on brain uptake and cytosolic metabolism of glucose, the primary brain fuel. The volcano plots illustrate the FC and p-values for significant differences in ApoE2 brains (Fig. 1.4.2B) and ApoE4 brains (Fig. 1.4.2C) compared to ApoE3 brains. Of the 12 genes analyzed, 2 genes exhibited significantly higher levels in ApoE2 brains versus ApoE3 brains, including solute carrier family 2, member 4 (Slc2a4, FC = 2.05, p = 0.039) and hexokinase 2 (Hk2, FC = 1.19, p = 0.022); In contrast, a comparison between ApoE4 and ApoE3 brains yielded 3 genes that were significantly downregulated in ApoE4 brains: solute carrier family 2, member 3 (Slc2a3, FC = 0.68, p = 0.037), hexokinase 1(Hk1, FC = 0.73, p = 0.042) and hexokinase 2 (Hk2, FC = 0.66, p = 0.004). The results of the gene array studies were further validated using independent mRNA quantitation and immunoblotting analysis. Among the 4 genes that significantly changed among three ApoE genotype groups, we were particularly interested in hexokinases for the following reasons: 1) the expression levels of hexokinase 1 and hexokinase 2 were significantly higher in the ApoE2 brain when

compared to the ApoE4 brain; 2) hexokinase acts as the "gateway" enzyme that catalyzes the first step in intracellular glucose metabolism; 3) hexokinase is the "pacemaker" of glycolysis. Consistent with the findings in the gene array study, significantly lower levels of mRNA (Fig. 1.4.2D) and protein (Fig. 1.4.2E) of hexokinase 1 were found in ApoE4 brains ($p < 0.05$) when compared to both ApoE2 and ApoE3 brains. Similarly, mRNA level (Fig. 1.4.2F) and protein expression (Fig. 1.4.2G) of hexokinase 2 were significantly reduced in ApoE3 brains ($p < 0.05$) and ApoE4 brains ($p < 0.01$) when compared to ApoE2 brains. These results suggest that ApoE2 brains possess the most robust expression profile in both glucose uptake and glycolysis, whereas ApoE4 brains display the most deficient profile in glucose uptake and glycolytic pathway.

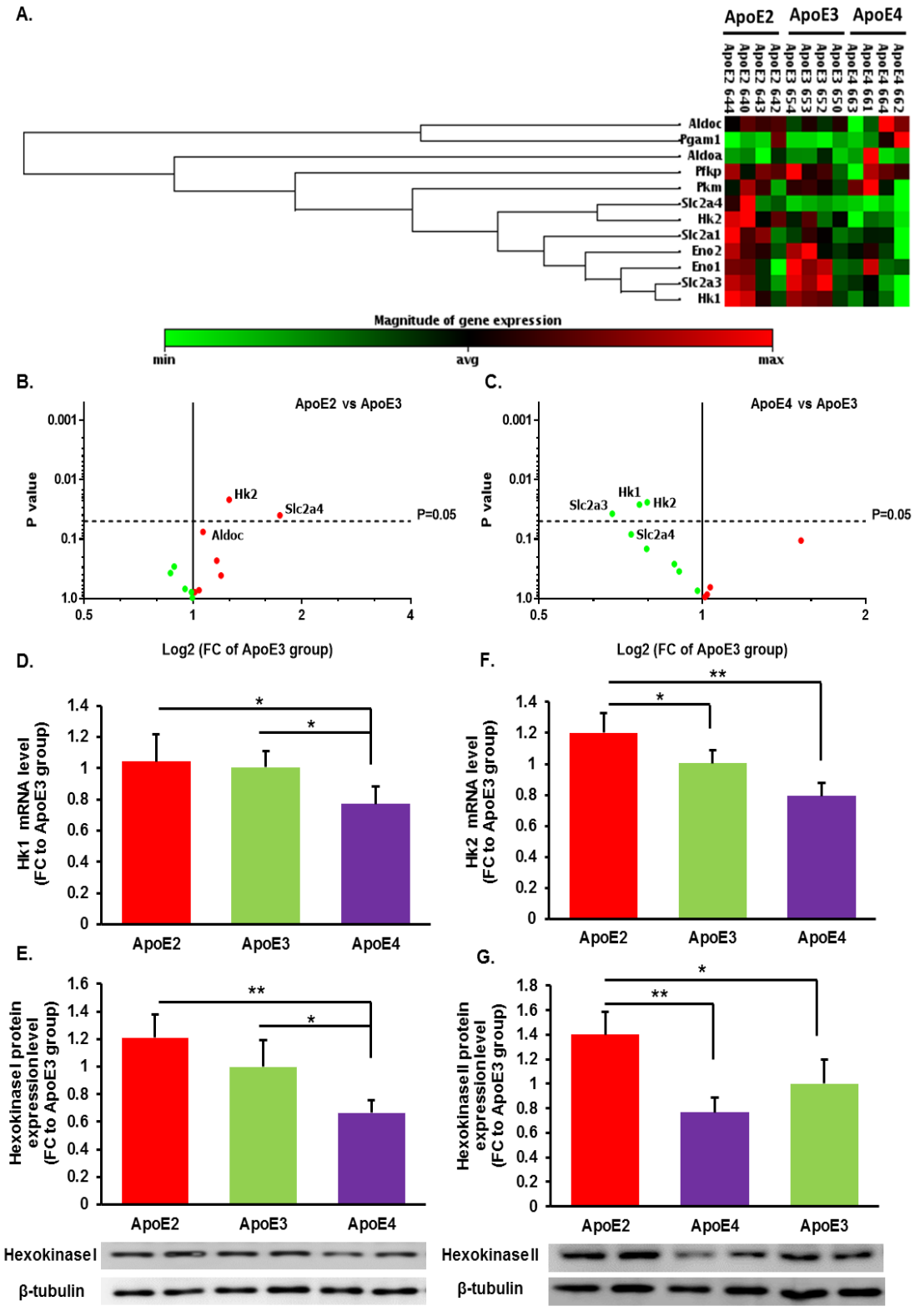
A.
ApoE2
ApoE3
ApoE4
ApoE2 644
ApoE2 640
ApoE2 643
ApoE2 642
ApoE3 654
ApoE3 653
ApoE3 652
ApoE3 650
ApoE4 663
ApoE4 661
ApoE4 664
ApoE4 662
Aldoc
Pgam1
Aldoa
Pfkp
Pkm
Slc2a4
Hk2
Slc2a1
Eno2
Eno1
Slc2a3
Hk1
Magnitude of gene expression
min
avg
max
B.
ApoE2 vs ApoE3
P value
0.001
0.01
0.1
1.0
0.5
1
2
4
Hk2
Slc2a4
Aldoc
P=0.05
C.
ApoE4 vs ApoE3
P value
0.001
0.01
0.1
1.0
0.5
1
2
Hk1
Hk2
Slc2a3
Slc2a4
P=0.05
D.
Log2 (FC of ApoE3 group)
Hk1 mRNA level (FC to ApoE3 group)
ApoE2
ApoE3
ApoE4
F.
Log2 (FC of ApoE3 group)
Hk2 mRNA level (FC to ApoE3 group)
ApoE2
ApoE3
ApoE4
E.
Hexokinase I protein expression level (FC to ApoE3 group)
ApoE2
ApoE3
ApoE4
Hexokinase I
β-tubulin
G.
Hexokinase II protein expression level (FC to ApoE3 group)
ApoE2
ApoE4
ApoE3
Hexokinase II
β-tubulin

Figure 1.4.2

Fig. 1.4.2 ApoE2 brains exhibited the most robust metabolic profiles in glucose uptake and glycolytic pathway. A) The heat map showed the expression of genes involved in glucose transport and glycolytic pathways for all three ApoE genotypes. B-C) The volcano plots illustrated fold changes (X-axis) and p-values (Y-axis) between (B) ApoE2 brains versus ApoE3 brains and (C) ApoE4 brains versus ApoE3 brains; Highlighted significantly altered expression – Hk1/2: hexokinase 1/2; Slc2a3: solute carrier family 2 facilitated glucose transporter 3 (Glut3) ; Slc2a4: solute carrier family 2 facilitated glucose transporter member 4 (Glut4). D-E) Gene and protein expression levels of hexokinase 1 were significantly lower in ApoE4 brains compared to ApoE2 and ApoE3 brains. F-G) ApoE2 brains exhibited significantly higher levels of mRNA and protein expression of hexokinase 2. Results were normalized to ApoE3 group. Statistical analysis was performed using One-way ANOVA with Bonferroni's post hoc method *$p<0.05$, **$p<0.01$. n=4-5 per group.

1.4.3 ApoE2 brain demonstrated a more robust expression profile in other glucose metabolic pathways

Next, we sought to examine the gene expression profile in other glucose metabolic pathways including pyruvate metabolism, pentose phosphate pathway (PPP), gluconeogenesis and glycogenesis. Unlike the one generated for glucose uptake and glycolytic pathway, no distinct pattern was observed in the heat map when comparing the three ApoE genotype groups (Fig. 1.4.3A). However, the volcano plots indicated trends in gene upregulation/downregulation. Out of 18 genes examined, 14 were upregulated in ApoE2 brains compared to ApoE3 brains (Fig. 1.4.3B). In comparison, 10 out of 18 genes were downregulated in ApoE4 brains compared to ApoE3 brains (Fig. 1.4.3C). Genes significantly changed include dihydrolipoamide S-acetyltransferase (Dlat, FC = 1.16, $p = 0.033$) and phosphogluconate dehydrogenase (Pgd, FC = 0.85, $p = 0.021$). Together, these data suggest that the ApoE2 brain exhibited the most metabolically robust profile in other glucose metabolic pathways. By contrast, the ApoE4 brain displayed some deficits in the PPP shunt and glycogen utilization.

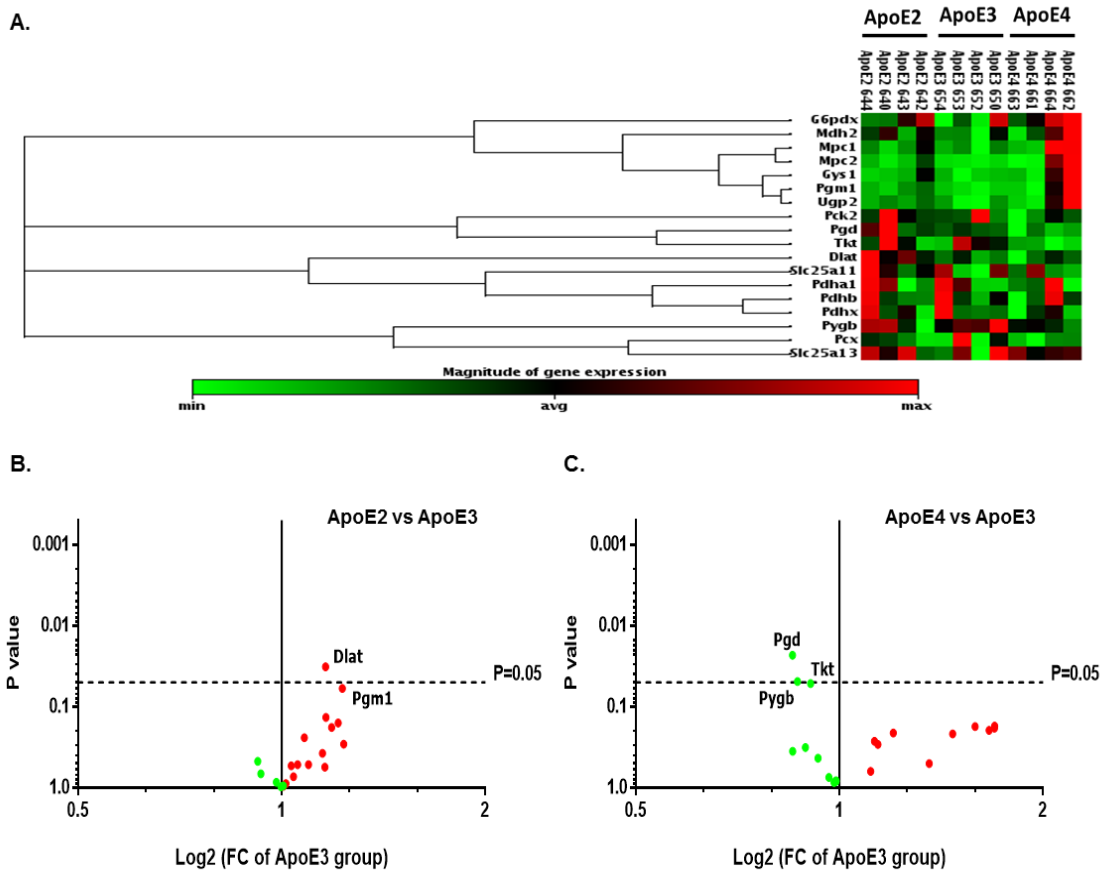

Figure 1.4.3

Fig. 1.4.3 ApoE2 brains displayed a more robust expression profile in other glucose metabolic pathways. A) The heat map showed the expression of key genes involved in the metabolic pathways including pyruvate metabolism, gluconeogenesis, glycogenesis and pentose phosphate pathways for all three ApoE genotypes. B-C) The volcano plots demonstrated fold changes (X-axis) and p-values (Y-axis) between (B) ApoE2 brains versus ApoE3 brains and (C) ApoE4 brains versus ApoE3 brains; Highlighted significantly altered expression – Dlat: Dihydrolipoamide S-Acetyltransferase; Pgd: 6-Phosphogluconate dehydrogenase.

1.4.4 ApoE2-expressing neurons had significantly higher protein levels and enzymatic activity of hexokinase

Based on our findings in the gene array analysis, we moved to a cell model to investigate how the three human ApoE isoforms modulate glucose and ketone body metabolism. Mouse N2a cells were transfected with empty vector or vectors encoding human ApoE2, ApoE3, and ApoE4. As shown in Fig. 1.4.4A and 1.4.4C, mRNA and protein levels of ApoE were comparable in cells transfected with human ApoE isoforms. The primers used for PCR amplification for each genotype were highly specific as the difference in threshold cycle (Ct) value between positive and negative was at least 11, which indicates that the specific amplifications are 2048-fold more efficient compared to the non-specific ones (Fig. 1.4.4B). We first validated the results from gene array study by measuring protein expression levels of hexokinase 1/2 in N2a cells expressing human ApoE isoforms (N2a-hApoE2, N2a-hApoE3, and N2a-hApoE4). Consistent with our findings in the brain of hApoE-TR mice, N2a cells transfected with ApoE2 exhibited a significantly higher level of hexokinase 2 compared with ApoE3 transfected group (FC = 1.20, p = 0.022) (Fig. 1.4.4E). The protein expression level of hexokinase 1 was also higher in ApoE2-transfected cells, however, it did not reach statistical significance (FC = 1.14, p = 0.205) (Fig. 1.4.4D). Cells transfected with ApoE4 showed a markedly lower levels of protein expression of both hexokinase 1 (FC = 0.71, p = 0.016) and hexokinase 2 (FC = 0.69, p = 0.002) as compared to those transfected with ApoE3 (Fig. 1.4.4D-E). Additionally, hexokinase enzyme activity was determined in whole cell lysates collected from transfected cells. In line with the protein expression data, N2a-hApoE2 cells demonstrated significantly higher (FC = 1.25, p = 0.0002) whereas N2a-hApoE4 cells

exhibited significantly lower (FC = 0.85, p = 0.026) hexokinase activity when compared to N2a-hApoE3 cells (Fig. 2.4.4F). These results suggest that human ApoE isoforms differentially modulate hexokinase expressions in N2a cells, with ApoE2-expressing cells exhibiting the highest expression of both hexokinase 1 and hexokinase 2 among the three ApoE genotypes.

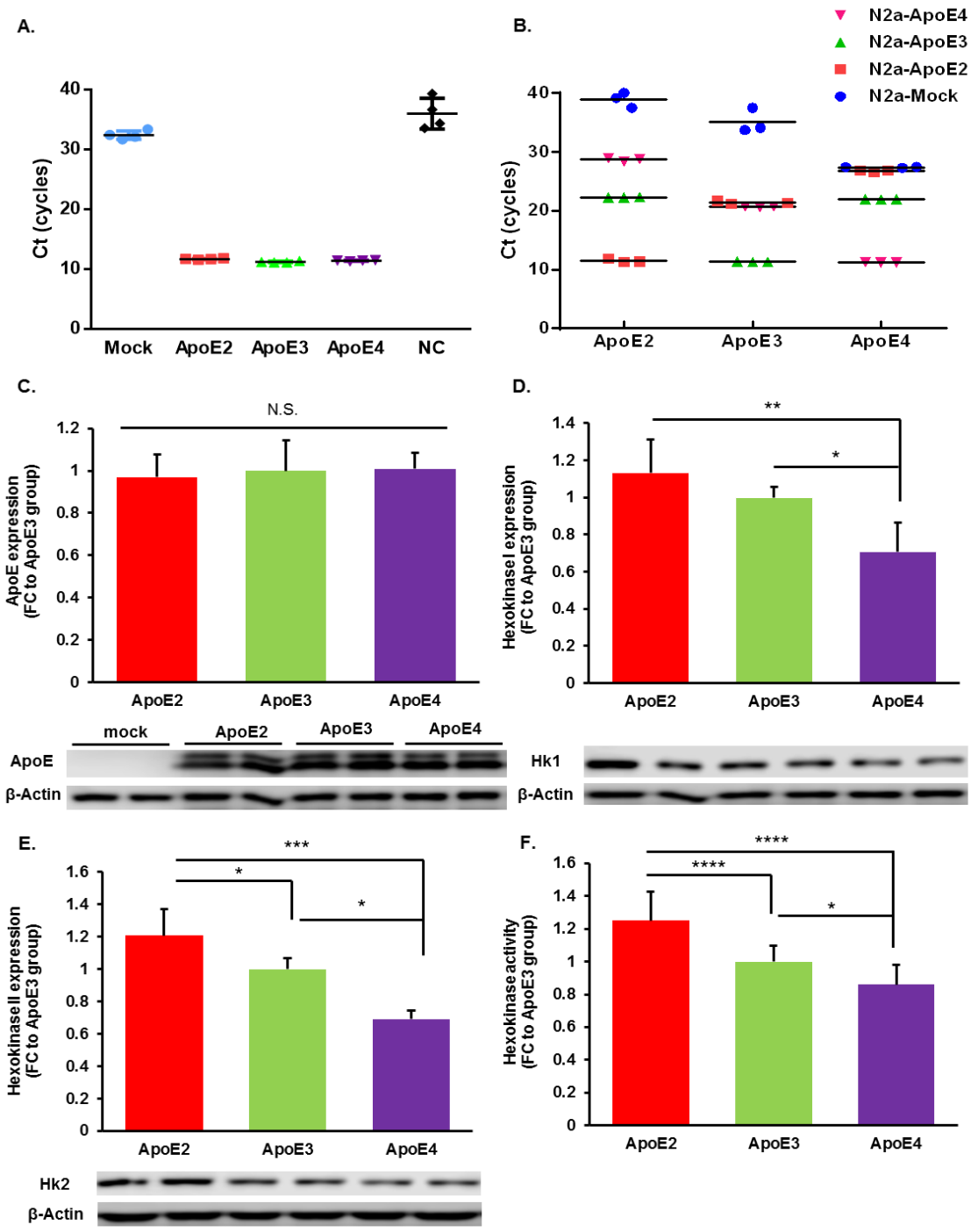
A.
Ct (cycles)
Mock
ApoE2
ApoE3
ApoE4
NC
B.
N2a-ApoE4
N2a-ApoE3
N2a-ApoE2
N2a-Mock
C.
N.S.
ApoE expression (FC to ApoE3 group)
mock
ApoE
β-Actin
D.
Hexokinase I expression (FC to ApoE3 group)
Hk1
E.
Hexokinase II expression (FC to ApoE3 group)
Hk2
F.
Hexokinase activity (FC to ApoE3 group)

Figure 1.4.4

Fig. 1.4.4 ApoE2-expressing neurons exhibited higher protein levels and enzymatic activity of hexokinase. A) Gene expression levels of ApoE were determined in N2a cells transfected with human ApoE cDNA by real time PCR. Amplification plots of 3 ApoE genotypes in transfected cells were shown. NC: negative control. Four replicates each group. B) Genomic DNA extracted from N2a cells transfected with human ApoE cDNA or empty vector were amplified with specific primers for ApoE2, ApoE3 and ApoE4 reactions. Three replicates per group. C) ApoE protein expression in the transfected cells were confirmed by immunoblotting analyses. ApoE levels were comparable among the three transfected groups. D-E) Protein expressions of hexokinase1/2 were assessed in N2a cells transfected with vectors encoding human ApoE isoforms. ApoE2-expressing cells displayed the highest whereas ApoE4-expressing cells exhibited the lowest protein expression levels of both hexokinase 1 and hexokinase 2. F) Hexokinase activity was determined in the cell lysates of N2a-hApoE cells. Results were normalized to ApoE3 group. *$p<0.05$, **$p<0.01$, ***$p<0.001$, ****$p<0.0001$ by ANOVA with Bonferroni's post hoc test. n=4-5 per group.

1.4.5 ApoE2-expressing neurons exhibited the most robust glycolysis and mitochondrial respiration

Given that the three human ApoE isoforms differentially modulate hexokinase expression and hexokinase is a critical regulator of glycolysis, we next performed the glycolytic stress test to assess ApoE isoform-specific effect on glycolytic function in N2a cells (Fig. 1.4.5A-B). Extracellular acidification rate (ECAR) is measured before and after glucose injection which provides the basal glycolytic rate. Subsequent addition of oligomycin inhibits ATP synthase which drives glycolysis to produce more ATP to compensate, allowing the measurement of maximal and reserve glycolytic capacity. Finally, 2-Deoxy-D-glucose (2-DG) shuts down glycolysis by binding to hexokinase which provides the measurement of non-glycolytic acidification. As shown in Fig. 1.4.5A, basal glycolysis was significantly lower in ApoE4-expressing cells compared to ApoE2- (FC = 0.65, $p < 0.0001$) and ApoE3- (FC = 0.76, $p = 0.017$) expressing cells. Oligomycin induced a

significantly larger ECAR increase, suggesting a significant higher cellular maximum glycolytic capacity, in ApoE2-expressing cells than that in ApoE3-expressing cells (FC = 1.17, p = 0.012). In comparison, the glycolytic capacity was significantly lower in ApoE4-expressing cells (FC = 0.74, p < 0.0001). Similarly, the glycolytic reserve was markedly higher in ApoE2- (FC = 1.19, p = 0.008) whereas lower in ApoE4- (FC = 0.95, p = 0.001) expressing cells when compared to ApoE3-expressing cells.

We also performed the mitochondrial stress test on N2a-hApoE cells to evaluate the impact of human ApoE isoforms on mitochondrial respiration (Fig. 1.4.5C-F). The basal respiration rate is established by measuring oxygen consumption rate (OCR) before the sequential injections of compounds. The difference in OCR before and after oligomycin injection provides a measure of ATP-linked respiration. FCCP induces the collapse of the proton gradient across the inner mitochondrial membrane resulting in the maximal mitochondrial respiration. The spare respiratory capacity is calculated by subtracting basal respiration from maximal respiration. The basal mitochondrial respiration was significantly higher in cells expressing ApoE2 than that in cells expressing ApoE3 (FC = 1.13, p = 0.004). ApoE4-expressing cells had significantly lower basal respiration when compared to ApoE2 cells (FC = 0.81, p < 0.0001). FCCP response was significantly higher in cells expressing ApoE2 compared to that in cells expressing ApoE3 (FC = 1.11, p = 0.021). ApoE4-expressing cells showed a significantly lower maximal respiratory capacity when compared to that of ApoE3- (FC = 0.85, p = 0.001) and ApoE2- (FC = 0.76, p < 0.0001) expressing cells. Additionally, N2a-hApoE4 cells exhibited a significantly lower spare respiratory capacity compared with both N2a-hApoE3 (FC = 0.77, p = 0.0001) and N2a-hApoE2 (FC = 0.71, p < 0.0001) cells. ATP generation was

determined in the cell lysates of N2a-hApoE to evaluate the level of cellular energy metabolism. In line with the results from mitochondrial and glycolytic stress tests, N2a-hApoE2 displayed significantly higher levels of ATP compared to N2a-hApoE3 cells (FC = 1.25, $p < 0.0001$). ATP levels were significantly lower in N2a-hApoE4 cells (FC = 0.81, $p < 0.0001$). These data indicate that ApoE2-expressing cells are the most robust whereas ApoE4-expressing cells are relatively deficient in both glycolytic metabolism and mitochondrial respiration.

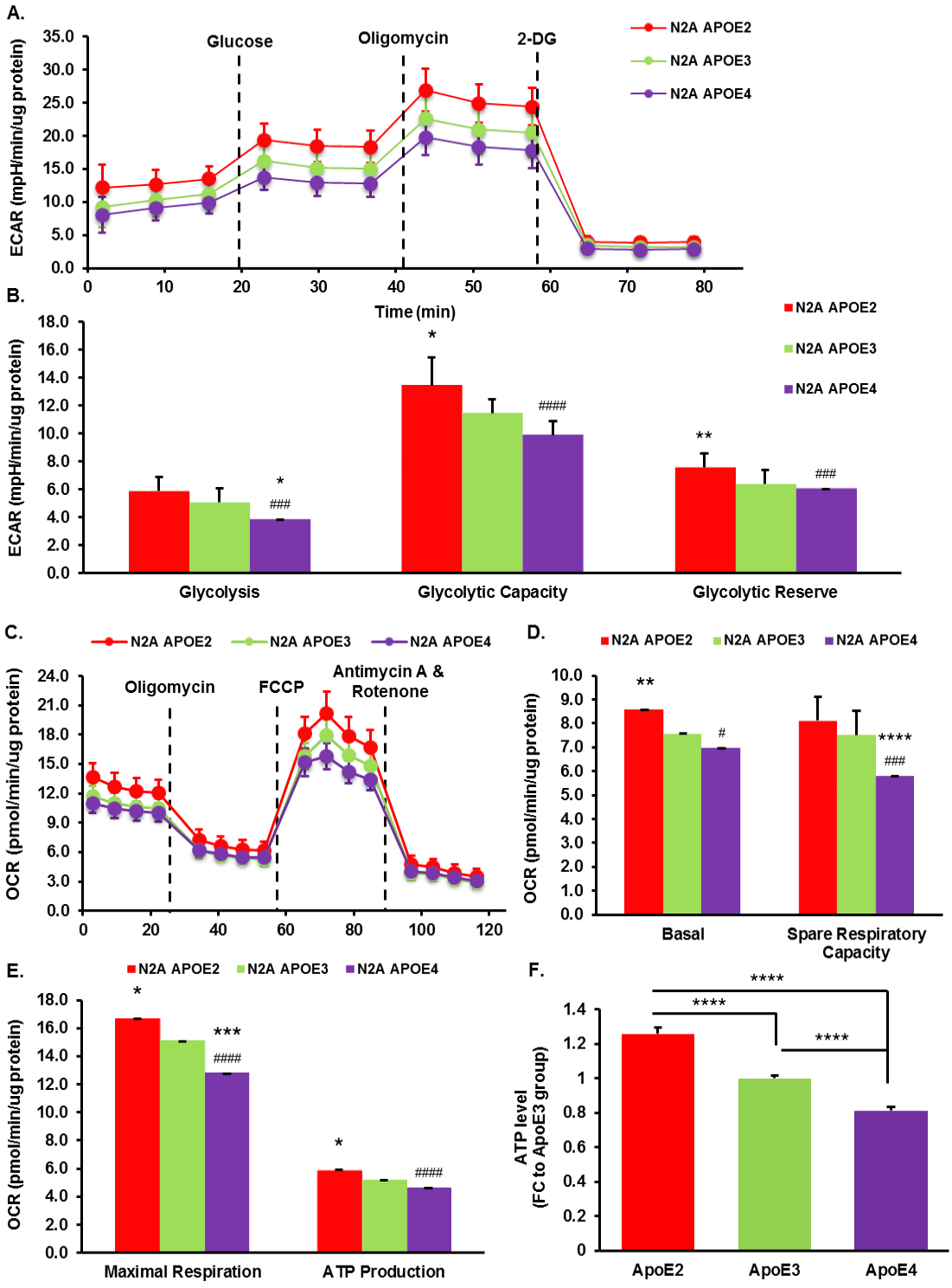
A.
ECAR (mpH/min/ug protein)
Glucose
Oligomycin
2-DG
N2A APOE2
N2A APOE3
N2A APOE4
Time (min)
B.
ECAR (mpH/min/ug protein)
Glycolysis
Glycolytic Capacity
Glycolytic Reserve
C.
OCR (pmol/min/ug protein)
Oligomycin
FCCP
Antimycin A & Rotenone
D.
OCR (pmol/min/ug protein)
Basal
Spare Respiratory Capacity
E.
OCR (pmol/min/ug protein)
Maximal Respiration
ATP Production
F.
ATP level (FC to ApoE3 group)
ApoE2
ApoE3
ApoE4

Figure 1.4.5

Fig. 1.4.5 ApoE2-expressing neurons displayed significantly enhanced glycolytic function and mitochondrial respiration. A-B) Glycolytic stress tests were performed using the Seahorse XF96 Extracellular Flux Analyzer to measure the basal glycolysis, glycolytic capacity and glycolytic reserve in N2a-hApoE cells. n= 18-20 per group. *p<0.05, **p<0.01 vs N2a-ApoE3 group. ### p<0.001, #### p< 0.0001 vs N2a-ApoE2 group. C-E) Mitochondrial stress tests were performed using the Seahorse XF96 Extracellular Flux Analyzer to measure mitochondrial basal respiration, maximal respiration capacity and ATP-linked respiration in N2a-hApoE cells. n= 18-20 per group. F) ATP level was determined in the cell lysates of N2a-hApoE cells. n=5 per group. Results were compared using one-way ANOVA with Bonferroni post hoc test. *p<0.05, ** p<0.01, ***p<0.001, ****p<0.0001 vs N2a-ApoE3 group. #p<0.05, ###, p<0.001, ####p<0.0001 vs N2a-ApoE2 group.

1.4.6 ApoE2 and ApoE4 brains displayed similar robustness in ketone body metabolism

In addition to glucose, we also examined gene expression profile on the uptake and metabolism of ketone bodies, the secondary brain energy source, on the brain tissues from the three ApoE genotypes. Previous clinical studies reported that ApoE4 carriers did not benefit from a ketogenic agent [85, 86], suggesting that individuals with ApoE4 might be deficient in the transporters which mediate the cellular uptake of ketone bodies or/and key enzymes which convert the ketone bodies to their metabolites. Surprisingly, both ApoE2 and ApoE4 brains demonstrated the similar extent of robustness in the gene expression profile of ketone body utilization (Fig. 1.4.6A). More specifically, all 5 genes examined were upregulated in ApoE2 and ApoE4 brains compared to ApoE3 brains (Fig. 1.4.6B-C). 2 genes exhibited significantly higher levels in ApoE2 brains versus ApoE3 brains, including 3-hydroxybutyrate dehydrogenase, type 1 (Bdh1, FC = 1.31, p = 0.0004) and solute carrier family 16, member 1 (Slc16a1, FC = 1.18, p = 0.019).

To validate the results from gene array study on cerebral ketone body utilization, we assessed the impact of human ApoE isoforms on the cells' capability of metabolizing β-hydroxybutyrate (BHB) in N2a cells. Specifically, N2a cells were transfected with vectors encoding three human ApoE isoforms. 48 hours post transfection, cells were treated with vehicle control or BHB and mitochondrial respiration was measured. Compared to vehicle-treated groups, the FCCP-induced response was markedly larger in BHB-treated groups, suggesting that N2a cells are capable of metabolizing ketone bodies for energy supply (Fig. 1.4.6D-F). For each genotype, when normalized to its corresponding vehicle-treated group, maximal mitochondrial respiration rate after FCCP injection was significantly higher in cells expressing ApoE2 and ApoE4 compared to cells expressing ApoE3 (Fig. 1.4.6D-F). The maximal respiration rates in BHB-treated cells divided by those in vehicle-treated cells in each ApoE genotype were compared using one-way ANOVA with Bonferroni correction (Fig. 1.4.6G). In line with the observations from the OCR data, statistical analysis revealed that both ApoE2- and ApoE4-expressing cells had significantly higher maximal mitochondrial OCR in response to FCCP upon BHB treatment as compared to ApoE3-expressing cells. Our data indicate that ApoE2 and ApoE4 brains possess a similar level of robustness whereas ApoE3 brain is associated with a relatively deficient capability in ketone body utilization.

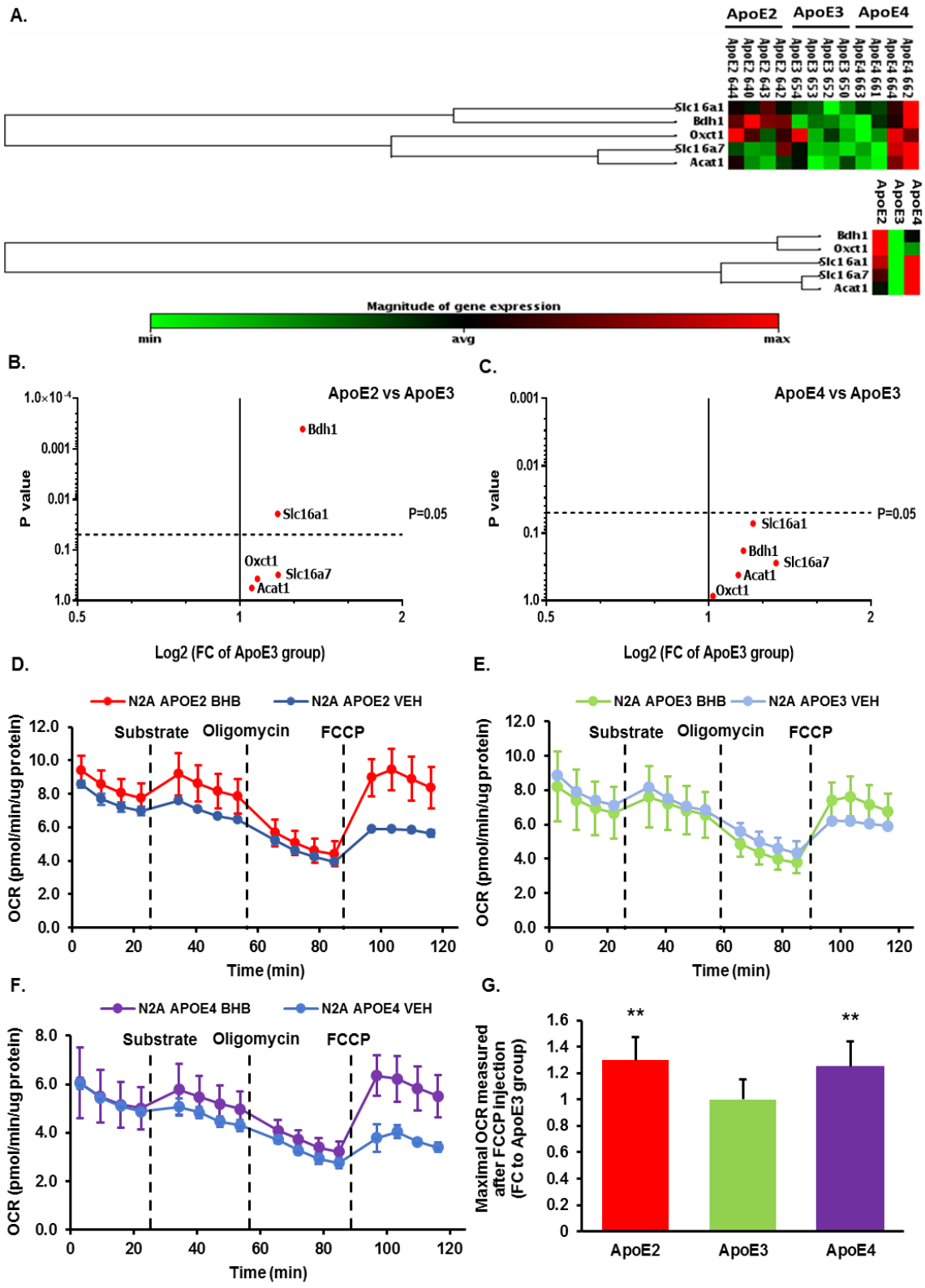
A.
ApoE2
ApoE3
ApoE4
ApoE2 644
ApoE2 640
ApoE2 643
ApoE2 642
ApoE3 654
ApoE3 653
ApoE3 652
ApoE3 650
ApoE4 663
ApoE4 661
ApoE4 664
ApoE4 662
Slc16a1
Bdh1
Oxct1
Slc16a7
Acat1
Magnitude of gene expression
min
avg
max
B.
ApoE2 vs ApoE3
P value
P=0.05
C.
ApoE4 vs ApoE3
Log2 (FC of ApoE3 group)
D.
N2A APOE2 BHB
N2A APOE2 VEH
Substrate
Oligomycin
FCCP
OCR (pmol/min/ug protein)
Time (min)
E.
N2A APOE3 BHB
N2A APOE3 VEH
F.
N2A APOE4 BHB
N2A APOE4 VEH
G.
Maximal OCR measured after FCCP injection (FC to ApoE3 group)
ApoE2
ApoE3
ApoE4

Figure 1.4.6

Fig. 1.4.6 ApoE2 and ApoE4 brains presented a similar level of robustness in ketone body utilization. A) The heat map showed the expression of genes implicated in brain ketone body uptake, transport and metabolism. B-C) The volcano plots illustrated fold changes and p-values between (B) ApoE2 brains versus ApoE3 brains and (C) ApoE4 brains versus ApoE3 brains; Highlighted significantly altered expression – Bdh1:β-hydroxybutyrate dehydrogenase, Slc16a1: monocarboxylate transporter 1; D-G) Mitochondrial oxygen consumption rate (OCR) was measured in in N2a-hApoE cells receiving sequential injection of substrate (BHB or vehicle), oligomycin and FCCP. The ketone body-metabolizing capacity of each ApoE genotype group was assessed by the maximum OCR measurements after FCCP injection. FCCP-induced OCR in BHB-treated cells was normalized to their vehicle-treated counterparts. n=8 per group. Results were compared using one-way ANOVA with Bonferroni post hoc test. **p<0.01 vs N2a-ApoE3 group. BHB: β-hydroxybutyrate.

1.4.7 Upstream regulator PGC-1α was upregulated in the ApoE2 brain

To further understand the biological relevance of the changes in gene expressions, we conducted a regulatory pathway and molecular network analysis using Ingenuity Pathway Analysis (IPA). IPA predicted that PPARGC1A, which encodes peroxisome proliferator-activated receptor gamma coactivator 1 alpha (PGC-1α), was activated in the ApoE2 brain when compared to the ApoE3 brain (Fig. 1.4.7A) (z-score = 2.507, p-value of overlap = 1.13E-12). Consistent with our previous findings, IPA predicted that peroxisome proliferator-activated receptor gamma (PPAR-γ) was inhibited in the ApoE4 brain compared to the ApoE2 brain (z-score = -2.146, p-value of overlap = 1.46E-09) [49]. To validate the results from bioinformatics analysis, mRNA and protein levels of PGC-1α were determined in the brains of hApoE-TR mice. In accordance with the prediction, ApoE2 brains exhibited significantly higher level of PGC-1α mRNA when compared to ApoE3 (FC = 1.13, p = 0.009) and ApoE4 brains (FC = 1.25, p = 0.0003) (Fig. 1.4.7B). Similarly, protein expression levels of PGC-1α was significantly lower in

ApoE4 brains compared to ApoE3 brains (FC = 0.70, p = 0.026) (Fig. 1.4.7C). PGC-1α protein expression was also significantly lower in ApoE4-expressing cells as compared to ApoE2-expressing cells (FC = 0.75, p =0.025) (Fig. 1.4.7D). These results suggest the activation of PGC-1α may underlie the bioenergetic robustness associated with ApoE2, whereas the lower protein levels of PGC-1α observed in ApoE4 brains and ApoE4-expressing cells may be responsible for the bioenergetic deficits.

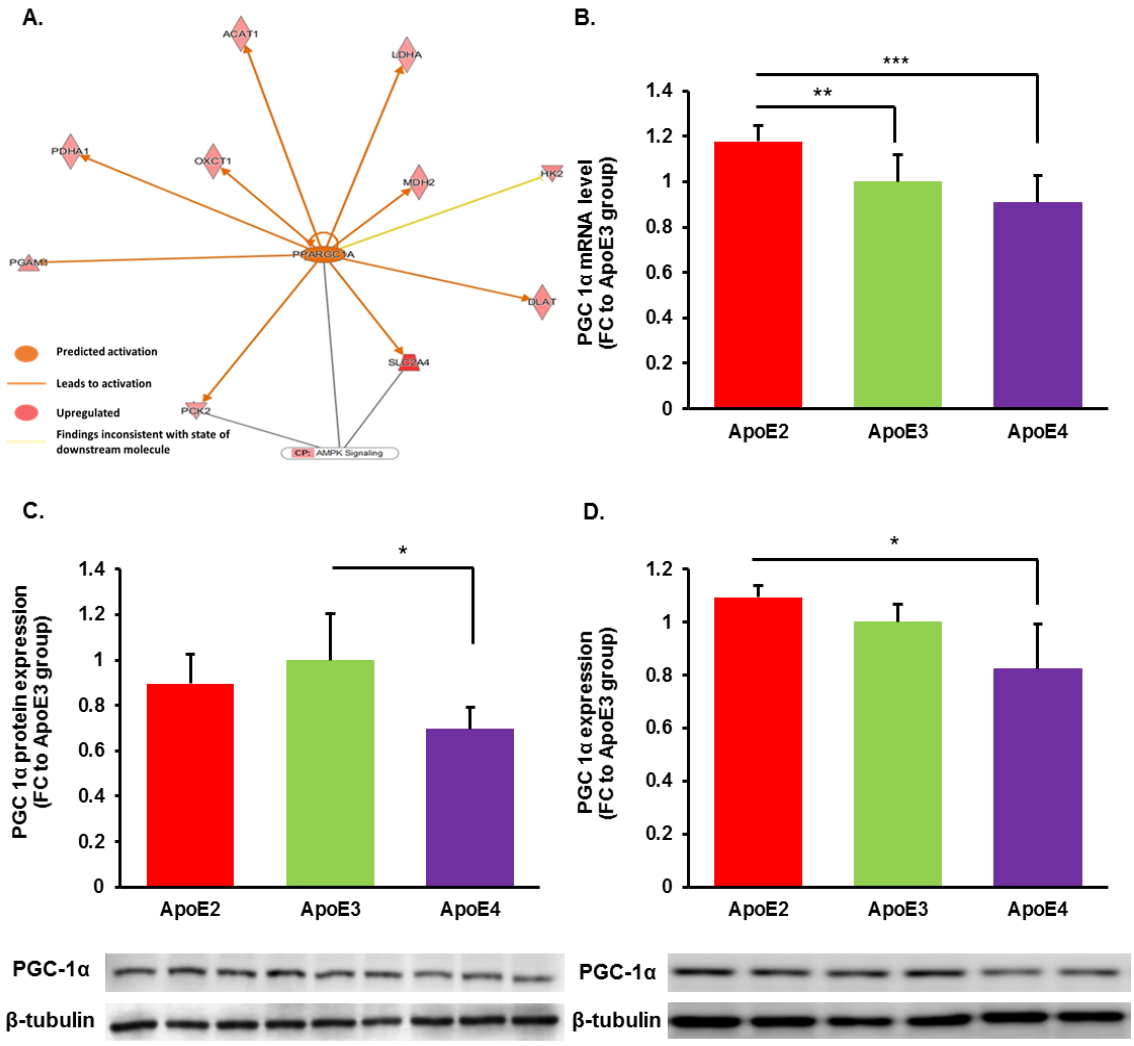

Figure 1.4.7

Fig. 1.4.7 PGC-1α as an upstream regulator in energy metabolism was activated in ApoE2 brains. A) IPA predicted the activation of PPARGC1A in the ApoE2 brain when compared to the ApoE3 brain. B) qRT-PCR was performed to examine the gene expression levels of PGC-1α in the brains of hApoE-TR mice. C-D) Protein expressions of PGC-1α were determined in cortex tissues of hApoE-TR mice (C) and N2a cells expressing human ApoE isoforms (D). Results were normalized to ApoE3 group. *p<0.05, **p<0.01, ***p<0.001 by ANOVA with Bonferroni post hoc test, n=4-5 per group.

1.4.8 PGC-1α overexpression ameliorated bioenergetic deficits in N2a cells stably expressing human ApoE4

To investigate the long-term effect of human ApoE expression in neurons, we transfected N2a cells with expression vectors encoding human ApoE isoforms and selected stable cell lines expressing matched levels of ApoE2, ApoE3, and ApoE4. Interestingly, N2a cells stably transfected with human ApoE isoforms exhibited similar metabolic features as those observed in the transient transfections. Specifically, neurons stably expressing ApoE2 demonstrated significantly higher protein expressions of hexokinase 1 and hexokinase 2 compared to neurons stably expressing ApoE3. By contrast, cells stably expressing ApoE4 exhibited the lowest expression of both hexokinase isoforms among the three ApoE genotype groups. In accordance with the protein expression levels, hexokinase activity was markedly higher in ApoE2-expressing neurons but was significantly lower in ApoE4-expressing neurons compared to ApoE3-expressing neurons. In fact, ApoE4 stably-transfected cells displayed altered cellular morphology (elongated, spindle-shaped with neurite outgrowth) at passage 10 and massive cell death after 13 passages whereas ApoE2 and ApoE3 stably-transfected cells were predominantly round shaped and remain healthy even after 20 passages. The aberrant morphological changes

and cell death observed in ApoE4-expressing cells were likely attributed to inherited defects in glucose metabolism and the resultant energy failure. Further characterization of the cell lines stably expressing ApoE isoforms will help to explain these observations. Data presented in this section and the following, unless specified otherwise, were generated on the stable cell lines.

Given that PGC-1α activation may underlie the bioenergetic robustness in ApoE2-expressing cells, we hypothesized that PGC-1α overexpression could ameliorate ApoE4-induced bioenergetic deficits. To test this hypothesis, ApoE4-expressing cells were transfected with empty vector or vectors encoding mouse PGC-1α for 48 hours, and hexokinase expressions, enzymatic activity, and ATP levels were assessed in the whole cell lysates. ApoE2-expressing cells served as positive control. Interestingly, we found that PGC-1α differentially modulated hexokinase expressions. Specifically, PGC-1α overexpression significantly increased hexokinase 1 expression (FC = 1.32, $p = 0.001$) but decreased hexokinase 2 expression (FC = 0.73, $p = 0.004$) in ApoE4-expressing cells (Fig. 1.4.8.1A-B). Additionally, the enzymatic activity of hexokinase was significantly improved by PGC-1α overexpression (FC = 1.23, $p < 0.0001$) (Fig.1.4.8.1C), which is likely attributed to enhanced hexokinase 1 expression.

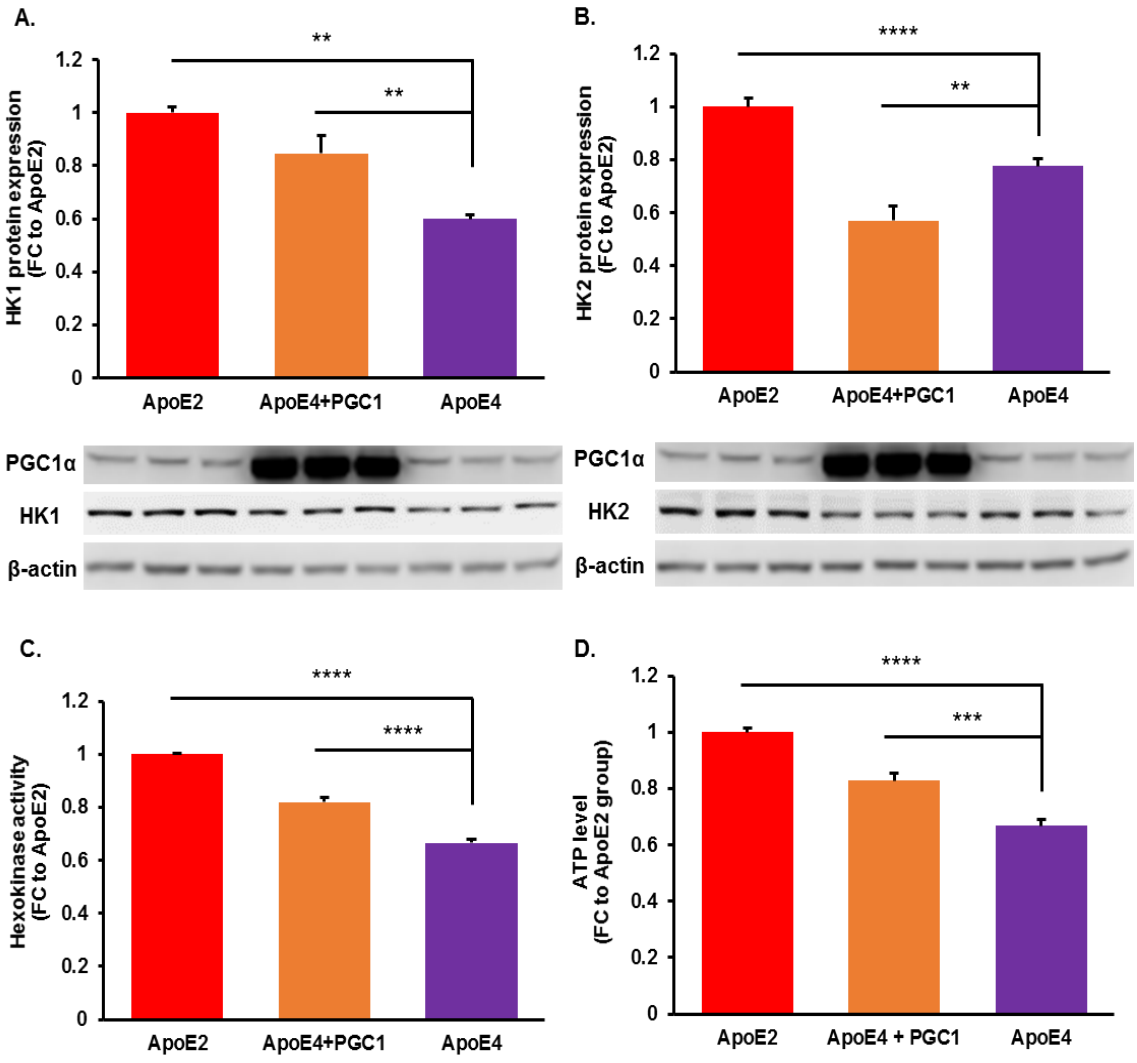

Figure 1.4.8.1

Fig. 1.4.8.1 PGC-1α overexpression differentially modulate hexokinase expression. A-B) Protein expressions of hexokinase 1 (A) and hexokinase 2 (B) were measured in ApoE4-expressing cells transfected with expression vectors encoding mouse PGC-1α or mock control. Hexokinase 1 and hexokinase 2 expressions were significantly lower in ApoE4-expressing cells compared to ApoE2-expressing cells. PGC-1α overexpression upregulated hexokinase 1 whereas downregulated hexokinase 2 in cells expressing ApoE4. C) Hexokinase activity was determined in the whole cell lysates for the indicated groups. PGC-1α overexpression improved hexokinase activity in ApoE4-expresssing cells. D) ATP levels were measured in ApoE4-expressing cells transfected with PGC-1α or empty vectors. Results were normalized to ApoE2 group. **p<0.01, ***p<0.001, ****p<0.0001 by ANOVA with Bonferroni post hoc test. n=6 per group.

Although both hexokinase isoforms are expressed in a variety of cell types, cells that are sensitive to insulin, such as adult muscle cells, express primarily hexokinase 2, whereas cells that rely heavily on glycolysis for energy production, such as neurons, express predominantly hexokinase 1. Additionally, it has been proposed that hexokinase 1 remains associated with mitochondria to promote glycolysis whereas hexokinase 2 dynamically translocates between cytosol and mitochondria where it directs the metabolic fate of glucose between anabolic (glycogen synthesis and pentose phosphate shunt) and catabolic (glycolysis) metabolism [246, 306]. To examine the functional consequence of the differential regulation of hexokinase expression by PGC-1α, the glycolytic stress test was performed in ApoE4-expressing cells transfected with PGC-1α. Sequential injections of glucose, oligomycin, and 2-DG measured basal glycolysis, glycolytic capacity, and non-glycolytic acidification. The glucose-induced increase in ECAR was significantly lower in ApoE4-expressing cells compared to ApoE2-expressing cells, suggesting ApoE4-expressing cells had a lower basal glycolytic rate (Fig.1.4.8.2A). Unexpectedly, PGC-1α overexpression did not increase basal glycolysis in ApoE4-expressing cells. However, defects in maximum glycolytic rate induced by ApoE4 was significantly ameliorated by PGC-1α overexpression (FC = 1.33, p = 0.003) (Fig.1.4.8.2B). Importantly, PGC-1α overexpression completely reversed ApoE4-induced defects in glycolytic reserve capacity (FC = 1.9, p <0.0001) (Fig.1.4.8.2B). These results suggest that hexokinase 1 is mainly responsible for promoting glycolysis in N2a cells and that improved glycolytic function by PGC-1α is primarily attributed to increased expression of hexokinase 1.

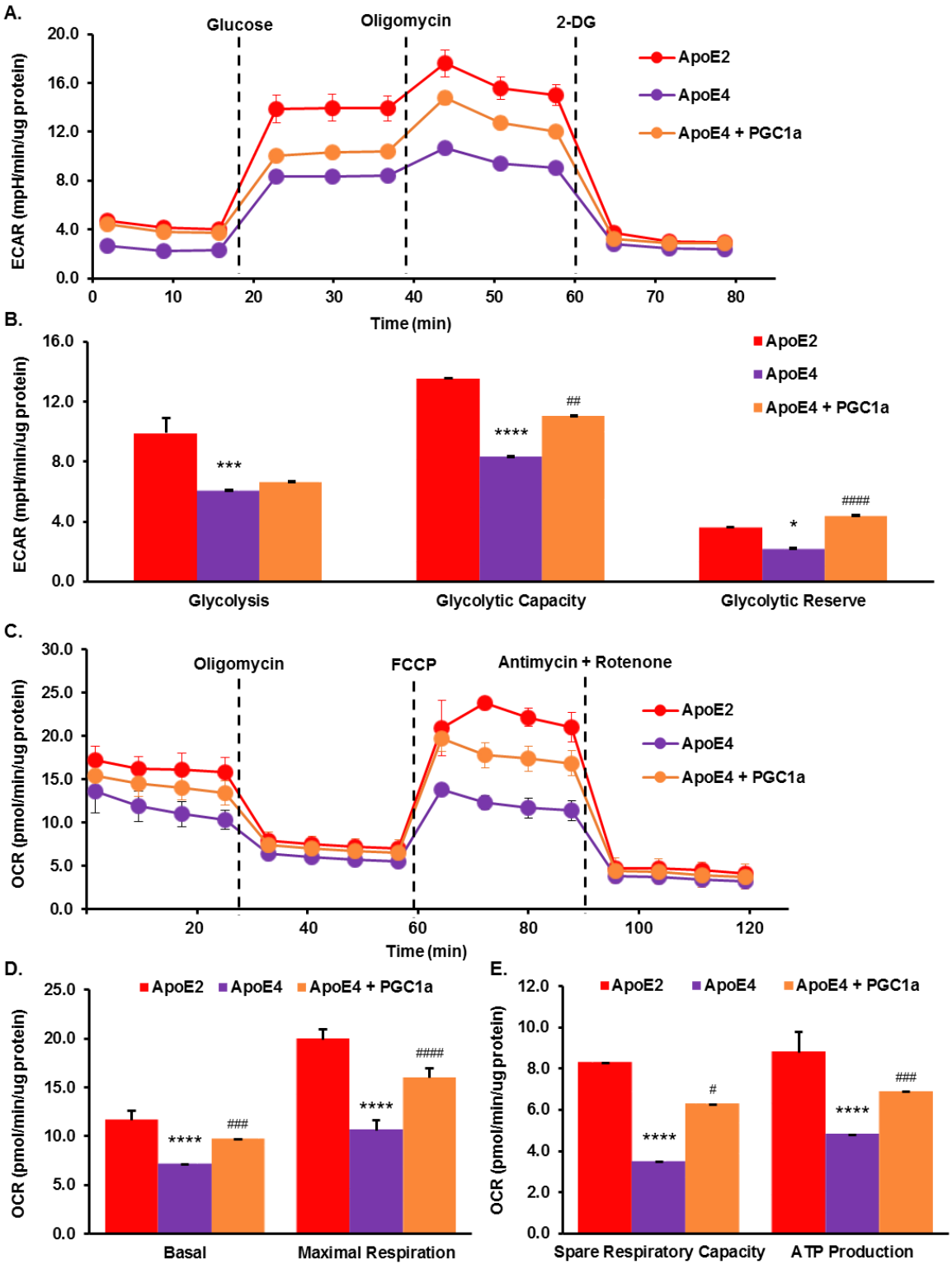
A.
Glucose
Oligomycin
2-DG
ECAR (mpH/min/ug protein)
Time (min)
ApoE2
ApoE4
ApoE4 + PGC1a
B.
ECAR (mpH/min/ug protein)
***
****
##
*
####
Glycolysis
Glycolytic Capacity
Glycolytic Reserve
C.
Oligomycin
FCCP
Antimycin + Rotenone
OCR (pmol/min/ug protein)
Time (min)
D.
OCR (pmol/min/ug protein)
****
###
####
Basal
Maximal Respiration
E.
OCR (pmol/min/ug protein)
****
#
###
Spare Respiratory Capacity
ATP Production

Figure 1.4.8.2

Fig. 1.4.8.2 PGC-1α overexpression ameliorated defects in glycolysis and mitochondrial respiration in ApoE4-expressing cells. A) ECAR was measured following sequential injections of glucose (10 mM), oligomycin (2 μM), and 2-deoxyglucose (2-DG) (50 mM) in ApoE4-expressing cells transfected with mouse PGC-1α. B) Individual parameters for glycolysis, glycolytic capacity and glycolytic reserve were calculated for the indicated groups. PGC-1α overexpression significantly enhanced glycolytic capacity and glycolytic reserve in ApoE4-expressing cells. C) Mitochondrial OCR was measured in ApoE4-expressing cells transfected with mouse PGC-1α after sequential additions of oligomycin (2 μM), FCCP (1 μM), as well as antimycin A & rotenone (1 μM), as indicated. D) Quantification of individual parameters for basal respiration, maximal respiration, spare respiratory capacity, and ATP-linked respiration. PGC-1α overexpression markedly improved mitochondrial respiratory function in ApoE4-expresssing cells. Results were compared using one-way ANOVA with Bonferroni post hoc test. *p<0.05, ***p<0.001, ****p<0.0001 vs ApoE2 group. #p<0.05, ##p<0.01, ###p<0.001, ####p<0.0001 vs ApoE4 group. Data were collected from 2 independent experiments. n=26-35 per group.

Because PGC-1α is well recognized as a mediator for mitochondrial biogenesis and oxidative phosphorylation, we examined the effect of PGC-1α overexpression on mitochondrial respiration in ApoE4-expressing cells (Fig. 1.4.8.2C-E). Higher levels of basal and maximal mitochondrial respiratory rates following FCCP injection were observed in ApoE4-expressing cells transfected with PGC-1α than those transfected with mock control (Fig 1.4.8.2C). Quantitative analysis confirmed that PGC-1α overexpression significantly improved basal (FC = 1.36, p = 0.0002) and maximal mitochondrial OCR (FC = 1.51, p < 0.0001) in ApoE4-expresssing cells. Similarly, PGC-1α overexpression resulted in a marked elevation in the spare respiratory capacity in ApoE4-expressing cells (FC = 1.80, p = 0.012). Consistent with results shown in Fig. 1.4.8.1, ATP-linked respiration was significantly improved by PGC-1α expression in N2a cells expressing ApoE4 (FC = 1.44, p = 0.0003). Further, PGC-1α overexpression markedly increased ATP levels (FC = 1.24, p = 0.0002) in ApoE4-expresing cells, which

may result from improvements in glycolysis and mitochondrial respiration (Fig.1.4.8.1D). Collectively, these results indicate that enhanced expression of PGC-1α is able to ameliorate mitochondrial respiratory deficits induced by ApoE4 in N2a cells.

1.4.9 *De novo* expression of ApoE2 reversed bioenergetic deficiencies in ApoE4-expressing cells

Given that ApoE2 is associated with a robust energy metabolic phenotype, we hypothesized that forced expression of ApoE2 could reverse bioenergetic defects induced by ApoE4. To test this hypothesis, ApoE4-expressing cells were transfected with mammalian expression vector encoding human ApoE2 or empty vector. 48 hours post transfection, gene expression, and protein levels were measured to determine the transfection efficiency. Then hexokinase protein expression, enzymatic activity, and ATP levels were measured in whole cell lysates collected from ApoE4-expressing cells transfected with ApoE2 or mock control. ApoE2-expressing cells served as a positive control. We first examined ApoE2 expression by real-time PCR and immunoblotting analysis. As shown in Fig. 1.4.9.1A, transfection of ApoE2 resulted in abundant gene expression of ApoE2 in ApoE4-expressing cells. The ApoE protein levels in ApoE4 + ApoE2 group were two-fold higher than non-transfected (ApoE2) or mock-transfected (ApoE4) groups (Fig.1.4.9.1B). The weak correlation between changes in the mRNA level (30-fold difference) and protein contents (2-fold difference) is likely due to regulatory processes at the transcriptional level, RNA processing, and RNA stability, as well as rapid protein turnover rate [307]. Intriguingly, introduction of ApoE2 resulted in a

marked increase in the expression of hexokinase 2 (FC = 1.42, p = 0.002) and hexokinase 1 (FC = 1.55, p = 0.015) (Fig. 1.4.9.1C-D). Hexokinase activity in ApoE4-expressing cells was also dramatically improved by ApoE2 expression (FC= 1.35, $p < 0.0001$) (Fig.1.4.9.1E).

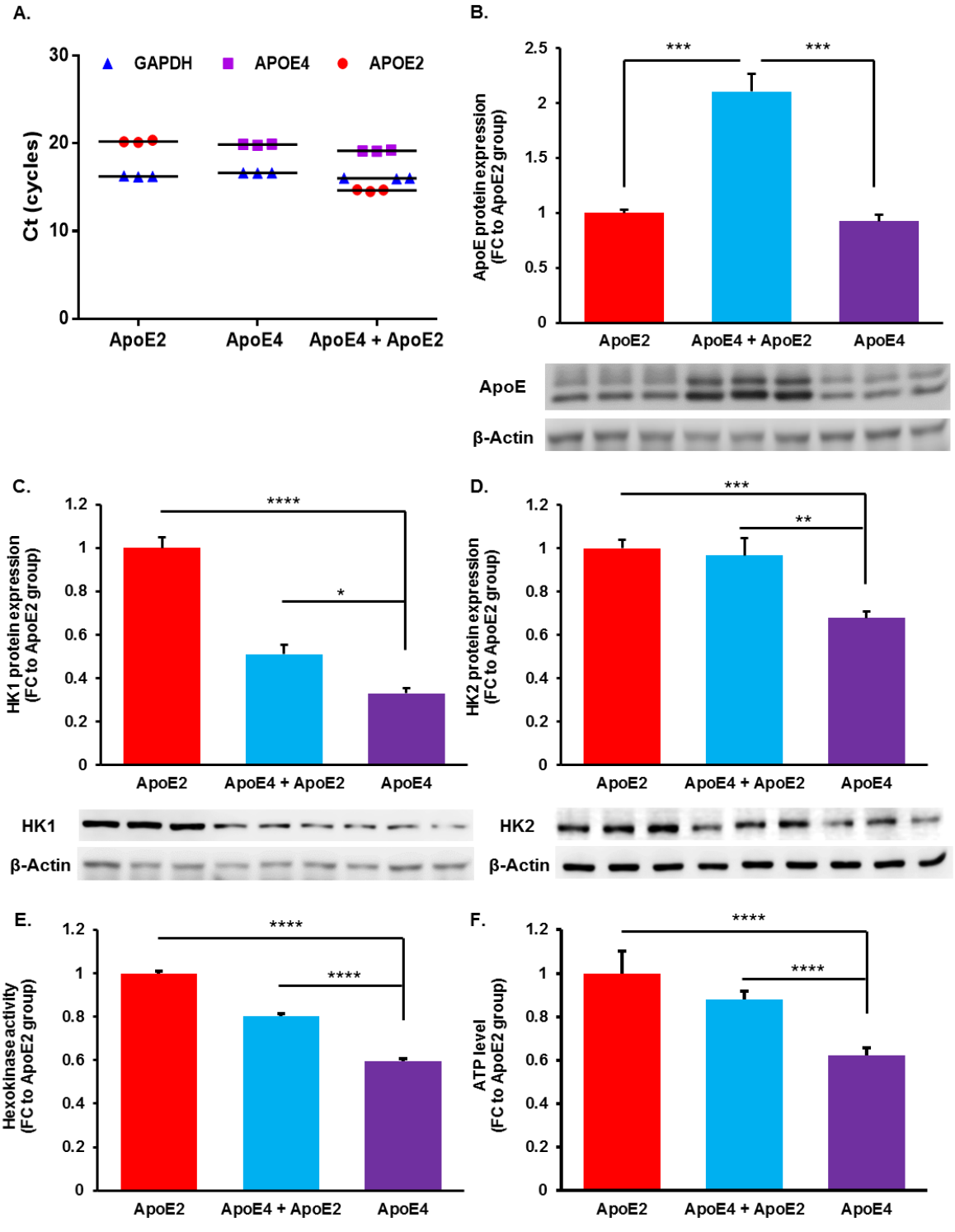
A.
GAPDH
APOE4
APOE2
Ct (cycles)
ApoE2
ApoE4
ApoE4 + ApoE2
B.
ApoE protein expression (FC to ApoE2 group)
ApoE2
ApoE4 + ApoE2
ApoE4
ApoE
β-Actin
C.
HK1 protein expression (FC to ApoE2 group)
HK1
β-Actin
D.
HK2 protein expression (FC to ApoE2 group)
HK2
β-Actin
E.
Hexokinase activity (FC to ApoE2 group)
F.
ATP level (FC to ApoE2 group)

Figure 1.4.9.1

Fig. 1.4.9.1 Forced expression of ApoE2 increased protein expression and enzymatic activity of hexokinase. A) ApoE2 mRNA level was determined in ApoE4-expressing cells transfected with empty vector or vectors encoding human ApoE2 by real time PCR. ApoE2-expressing cells served as positive control. Amplification plots for both ApoE2 and ApoE4 genotypes were shown. GAPDH was used as loading control. Three replicates each group. B) Protein expression of ApoE was confirmed with immunoblotting analysis. ApoE levels were comparable between ApoE2 and ApoE4 groups. C-D) Protein expressions of hexokinase1 (C) and hexokinase 2 (D) were assessed in ApoE2- or mock-transfected cells. Expression levels of both hexokinase isozymes were markedly elevated in ApoE4-expressing cells transfected with ApoE2 compared to those transfected with mock control E-F) Hexokinase activity (E) and ATP levels (F) were determined in the cell lysates of transfected cells. Results were normalized to ApoE2 group. *$p<0.05$, **$p<0.01$, ***$p<0.001$, ****$p<0.0001$ by ANOVA with Bonferroni's post hoc test. n=5-6 per group.

We next investigated whether the introduction of ApoE2 could counteract or rescue the detrimental effects of ApoE4 on glycolysis and mitochondrial respiratory function. 48 hours after transfection with ApoE2 or mock control, ApoE4-expressing cells were subjected to glycolytic and mitochondrial stress tests. Real-time glycolytic and mitochondrial respiratory rates were measured by a Seahorse extracellular flux analyzer. As shown in Fig. 1.4.9.2A, baseline glycolysis induced by high concentration of glucose was significantly lower in ApoE4-expressing cells compared to ApoE2-expressing cells (FC = 0.61, $p < 0.0001$), which is consistent with our previous findings. Intriguingly, introduction of ApoE2 increased basal glycolysis by 47% in ApoE4-expressing cells (FC = 1.47, $p <0.0001$) (Fig.1.4.9.2B). Similarly, the maximal glycolytic rate after oligomycin injection was markedly enhanced by ApoE2 expression. The quantitative analysis further confirmed that ECAR was significantly higher in ApoE4-expressing cells transfected with ApoE2 than those transfected with mock control (FC = 1.27, $p <0.0001$) (Fig. 1.4.9.2B). The introduction of ApoE2 also resulted in an increase in glycolytic reserve,

although the difference was not significant. Strikingly, forced expression of ApoE2 almost completely reversed mitochondrial bioenergetic defects induced by ApoE4. (Fig.1.4.9.2C-D). In addition to Basal OCR (FC = 1.58, p <0.0001), ATP-coupled respiration represented by oligomycin-sensitive OCR was significantly higher in ApoE4-expressing cells transfected with ApoE2 than those transfected with mock control (FC = 1.56, p <0.0001). Similarly, the introduction of ApoE2 resulted in a nearly 2-fold increase in the maximal mitochondrial respiration determined by FCCP-stimulated OCR in ApoE4-expressing cells (FC = 1.99, p <0.0001). Further, the spare respiratory capacity was also markedly improved by ApoE2 expression (FC = 8.22, p <0.0001). In line with the improvements in glycolysis and mitochondrial respiration, total ATP levels were significantly elevated by ApoE2 expression (FC = 1.41, p = 0.005) (Fig.1.4.9.1F). Collectively, our data indicate that *de novo* expression of ApoE2 could rescue the bioenergetic deficits induced by ApoE4.

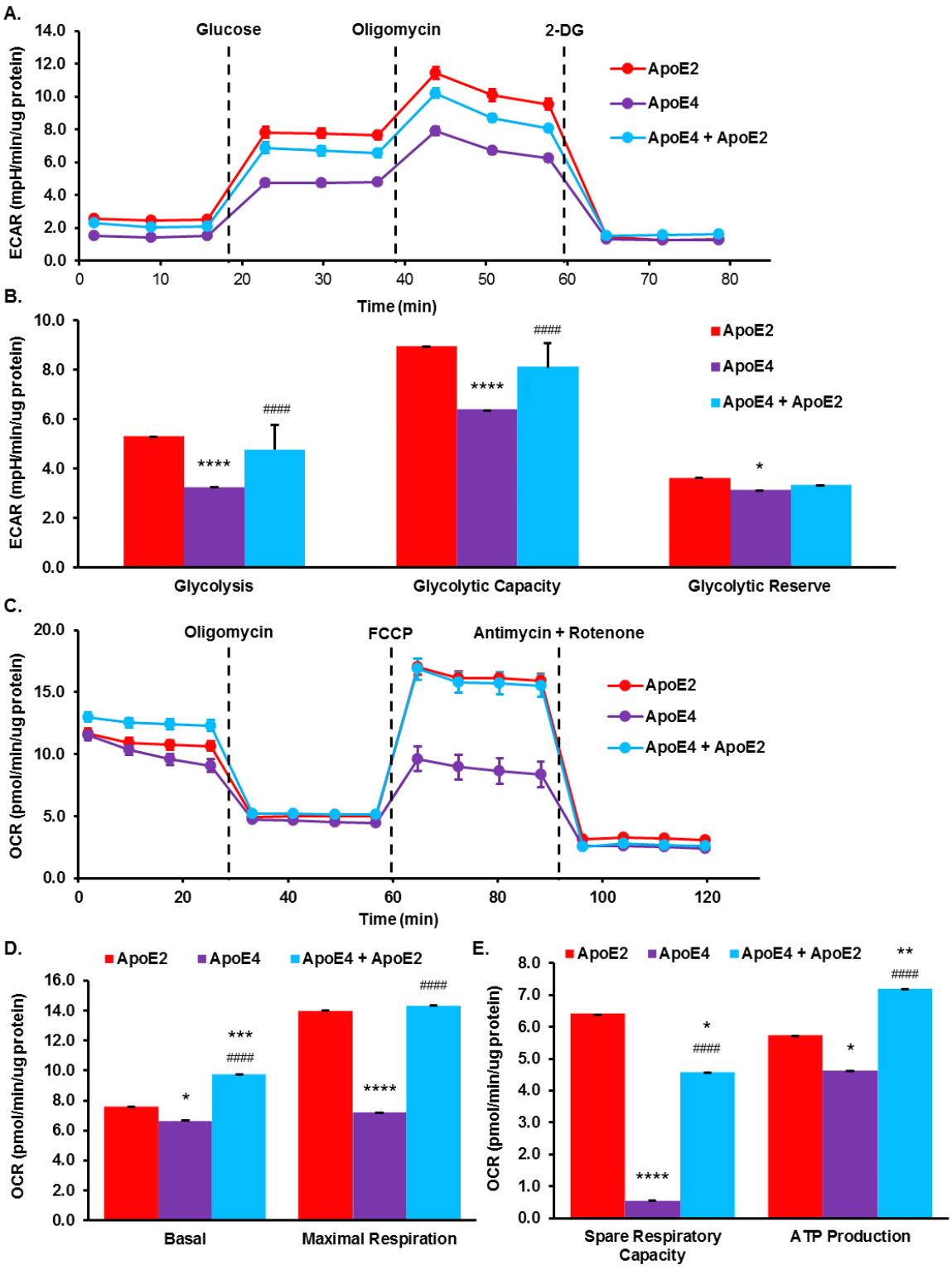
A.
Glucose
Oligomycin
2-DG
ECAR (mpH/min/ug protein)
Time (min)
ApoE2
ApoE4
ApoE4 + ApoE2
B.
ECAR (mpH/min/ug protein)
****
####
*
Glycolysis
Glycolytic Capacity
Glycolytic Reserve
C.
Oligomycin
FCCP
Antimycin + Rotenone
OCR (pmol/min/ug protein)
Time (min)
D.
OCR (pmol/min/ug protein)
*
***
####
****
Basal
Maximal Respiration
E.
OCR (pmol/min/ug protein)
****
*
**
Spare Respiratory Capacity
ATP Production

Figure 1.4.9.2

Fig. 1.4.9.2 Forced expression of ApoE2 improved glycolysis and mitochondrial respiration in ApoE4-expresssing cells. A) Kinetic ECAR responses of ApoE4-expressing cells transfected with ApoE2 to sequential injections of glucose (10 mM), oligomycin (2 μM), and 2-DG (50 mM) B) Quantitative analysis of basal glycolysis, glycolytic capacity and glycolytic reserve. ApoE2 expression significantly enhanced all the parameters for glycolysis in ApoE4-expressing cells. C) Kinetic OCR response of ApoE4-expressing cells transfected with ApoE2 to sequential additions of oligomycin (2 μM), FCCP (1 μM), as well as antimycin A & rotenone (1 μM). D) Calculated parameters including basal respiration, maximal respiration, spare respiratory capacity, and ATP production. Introduction of ApoE2 markedly improved mitochondrial respiratory function in ApoE4-expresssing cells. Results were compared using one-way ANOVA with Bonferroni post hoc test. *$p<0.05$, ***$p<0.001$, ****$p<0.0001$ vs ApoE2 group. ####$p<0.0001$ vs ApoE4 group. n=15-18 per group.

Table 1.4.1 List of genes examined in the TaqMan gene expression profiling

TaqMan Gene Expression Assay ID	Gene Symbol	Gene Name	Gene Aliases	Functional Category
Mm00441480_m1	Slc2a1	Solute carrier family 2, member 1	Glut1	Facilitative glucose transporter Class I members
Mm00446229_m1	Slc2a2*	Solute carrier family 2, member 2	Glut2	
Mm00441483_m1	Slc2a3	Solute carrier family 2, member 3	Glut3	
Mm00436615_m1	Slc2a4	Solute carrier family 2, member 4	Glut4	
Mm01306379_m1	slc16a1	Solute carrier family 16, member 1	Mct1	Monocarboxylate transporters
Mm00441442_m1	slc16a7	Solute carrier family 16, member 7	Mct2	
Mm00446102_m1	slc16a3*	Solute carrier family 16, member 3	Mct4	
Mm00439344_m1	Hk1	Hexokinase 1	Hk1	Glycolysis
Mm00443385_m1	Hk2	Hexokinase 2	Hk2	
Mm00444792_m1	Pfkp	Phosphofructokinase	Pfk-C	
Mm00833172_g1	Aldoa	Aldolase A, fructose-bisphosphate	Aldo1	
Mm01298116_g1	Aldoc	Aldolase C, fructose-bisphosphate	Aldo3	
Mm02526975_g1	Pgam1	Phosphoglycerate mutase 1	Pgama	
Mm01619597_g1	Eno1	Enolase 1 (Alpha, Non-neuron)	Mpb1	
Mm01185009_gH	Eno2	Enolase 2 (Gamma, Neuronal)	NSE	
Mm00834102_gH	Pkm	Pyruvate kinase	Pkm2	
Mm01316203_g1	Mpc1	Mitochondrial pyruvate carrier 1	Brp44l	Pyruvate uptake by mitochondria
Mm00770996_g1	Mpc2	Mitochondrial pyruvate carrier 2	Brp44	

Mm00468675_m1	Pdha1	Pyruvate dehydrogenase E1 alpha 1	Pdha	Pyruvate dehydrogenase complex
Mm00501060_s1	Pdha2*	Pyruvate dehydrogenase E1 alpha 2	Pdhal	
Mm00499323_m1	Pdhb	pyruvate dehydrogenase (lipoamide) beta	Pdhb	
Mm00455160_m1	Dlat	Dihydrolipoamide S-acetyltransferase	Dlat	
Mm00558275_m1	Pdhx	Pyruvate dehydrogenase complex, component X	Pdx1	
Mm01267402_m1	Ldhb	Lactate dehydrogenase B	Ldh2	Lactate shuttle
Mm01612132_g1	Ldha	Lactate dehydrogenase A	Ldh1	
Mm00500992_m1	Pcx	Pyruvate carboxylase	Pcb	Gluconeogenesis
Mm01247058_m1	Pck1*	Phosphoenolpyruvate carboxykinase 1, cytosolic	Pepck1	
Mm00551411_m1	Pck2	Phosphoenolpyruvate carboxykinase 2, mitochondrial	Pepck2	
Mm00490181_m1	Fbp1*	Fructose bisphosphatase 1	Fbp	
Mm00839363_m1	G6pc*	Glucose-6-phosphatase, catalytic subuit	G6Pase	
Mm00656735_g1	G6pdx	Glucose-6-phosphate dehydrogenase	G6pd	Pentose phosphate pathway
Mm00503037_m1	Pgd	Phosphogluconate dehydrogenase	6Pgd	
Mm00447559_m1	Tkt	Transketolase	Tkt	
Mm00804141_m1	Pgm1	Phosphoglucomutase 1	Pgm1	Glycogenesis
Mm00454826_m1	Ugp2	UDP-glucose pyrophosphorylase 2	Udpgp	
Mm01962575_s1	Gys1	Glycogen Synthase 1	Gys	
Mm00464080_m1	Pygb	Glycogen phosphorylase, brain form	Gpbb	
Mm00558330_m1	Bdh1	3-Hydroxybutyrate dehydrogenase, type 1	Bdh	Ketone body metabolism

Mm00499303_m1	Oxct1	3-Oxoacid CoA transferase 1	Scot	
Mm00507463_m1	Acat1	Acetyl-Coenzyme A acetyltransferase 1	Acat	
Mm00452509_m1	Slc25a11	Solute carrier family 25, member 11	Slc20a4	Malate-Aspartate shuttle
Mm00489442_m1	Slc25a13	Solute carrier family 25, member 13	Ctln2	
Mm00725890_s1	Mdh2	Malate dehydrogenase 2, NAD (mitochondrial)	Mdh	
Hs99999901_s1	18s	Eukaryotic 18S rRNA		Control genes
Mm02619580_g1	Actb	Actin, beta		
Mm03024075_m1	Hprt	Hypoxanthine guanine phosphoribosyl transferase		
Mm01197698_m1	Gusb	Glucuronidase, beta		
Mm99999915_g1	Gapdh	Glyceraldehyde-3-phosphate dehydrogenase		

*** Ct > 32 excluded from analysis**

Table 1.4.2 Changes in gene expression in ApoE2 and ApoE4 brains compared to ApoE3 brain

Gene Symbol	ApoE2 versus ApoE3		ApoE4 versus ApoE3		ApoE4 versus ApoE2	
	Fold Change	p-value	Fold Change	p-value	Fold Change	p-value
Slc2a1	1.1506	0.2308	0.8994	0.3482	0.7817	0.1056
Slc2a3	0.8606	0.3698	0.6804	**0.0368**	0.7906	0.1909
Slc2a4	2.0522	**0.0397**	0.7208	0.0838	0.3512	**0.0315**
Slc16a1	1.1775	**0.0190**	1.2048	0.0712	1.0231	0.7105
Slc16a7	1.1730	0.3090	1.2684	0.2767	1.0813	0.6108
Slc16a3	1.1189	0.5687	0.7135	0.1204	0.6377	0.1861
Hk1	1.0314	0.7218	0.7624	**0.0253**	0.7392	**0.0427**
Hk2	1.1937	**0.0216**	0.7898	**0.0236**	0.6616	**0.0042**
Pfkp	1.0122	0.7812	0.9786	0.7275	0.9668	0.5321
Aldoa	0.9892	0.7705	1.0289	0.6405	1.0401	0.5563
Aldoc	1.0661	0.0814	1.0047	0.8552	0.9424	0.6949
Pgam1	1.1497	0.4093	1.4578	0.1047	1.2679	0.3800
Eno1	0.8836	0.2865	0.8881	0.2577	1.0051	0.9912
Eno2	0.9553	0.6862	0.7854	0.1450	0.8221	0.1889
Pkm	0.9860	0.9651	0.9848	0.9371	0.9988	0.9249
Mpc1	1.1400	0.3765	1.4668	0.1750	1.2866	0.3090
Mpc2	1.1933	0.1590	1.5028	0.1821	1.2593	0.3516
Pdha1	1.0136	0.8878	0.9827	0.8538	0.9695	0.7474
Pdhb	0.9821	0.8506	0.9628	0.7382	0.9804	0.8712
Pdhx	1.0042	0.9582	0.9317	0.4225	0.9278	0.4042
Dlat	1.1588	**0.0325**	0.9867	0.8075	0.8514	**0.0383**
Ldha	1.0058	0.9447	1.1297	0.2866	1.1232	0.3066
Ldhb	1.0604	0.5225	1.1134	0.4997	1.0499	0.5640
Pcx	0.9539	0.6654	0.8751	0.3528	0.9175	0.2506
Pck2	1.0443	0.7285	0.8952	0.3134	0.8572	0.1393

G6pdx	1.1069	0.5211	1.2139	0.2114	1.0967	0.3996
Pgd	1.1676	0.1815	0.8488	**0.0214**	0.7269	**0.0421**
Tkt	0.9958	0.9590	0.9084	0.0534	0.9123	0.1051
Pgm1	1.2236	0.0588	1.4910	0.1942	1.2185	0.3818
Ugp2	1.1717	0.1357	1.3779	0.2149	1.1760	0.3903
Gys1	1.2053	0.2876	1.5342	0.1723	1.2729	0.3767
Pygb	0.9101	0.4675	0.8685	0.0506	0.9543	0.5852
Bdh1	1.3067	**0.0004**	1.1474	0.1802	0.8780	0.2238
Acat1	1.0539	0.5669	1.1160	0.4165	1.0589	0.6007
Oxct1	1.0812	0.3729	1.0163	0.8591	0.9400	0.5290
Slc25a11	1.0344	0.5373	0.9900	0.8239	0.9571	0.3137
Slc25a13	1.2203	0.5562	1.1956	0.6261	0.9798	0.7652
Mdh2	1.0804	0.2459	1.1183	0.2647	1.0350	0.6653

Genes that are significantly changed ($p<0.05$) were highlighted in bold

1.5 Discussion

Human ApoE isoforms (ApoE2, ApoE3, and ApoE4) have been shown to confer differential risk impact in late-onset AD, which comprises 95% of the total AD cases. While an immense amount of work has been done to examine the role of ApoE in AD pathogenesis, most studies have focused on identifying AD risk mechanisms conferred by ApoE4. In contrast, few studies have explored the role of ApoE2 in relation to AD, despite the fact that many of these studies suggest that ApoE2 is neuroprotective [308]. However, the underlying mechanisms by which ApoE2 confers neuroprotection remain largely unexplored.

Our previous gene array analysis on the hippocampal tissues from 6-month-old hApoE-TR mice revealed that the three human ApoE isoforms differentially regulate brain bioenergetics. Intriguingly, compared to ApoE3 and ApoE4 brains, the ApoE2 brain is associated with a more robust insulin/IGF1 signaling and downstream glucose utilization [87]. In the current study, we examined the potential differences in brain metabolic pathways involving glucose and ketone bodies as energy substrates. We focused primarily on substrate uptake metabolic pathways leading to the generation of acetyl-CoA among the three human ApoE genotypes using 6-month-old hApoE-TR mice. Our data demonstrated that three ApoE brains differentially express transporters that mediate the uptake of energy substrates and the enzymes that are involved in the cytosolic metabolism. These data provide potential mechanistic rationales for the protective effects associated with ApoE2 and the detrimental effects linked to ApoE4 in the aging and AD brain.

Under normal physiological conditions, glucose is the obligatory energy substrate for the

brain. As neurons have a high energy requirement, their function is heavily dependent on glucose availability and utilization [309].In this study, we initially examined the gene expression profile of glucose transporters and enzymes involved in glucose metabolism, in particular, glycolysis. The facilitative glucose transport proteins mediate the transport of glucose from the blood to the brain across the blood-brain barrier (BBB) and the uptake of glucose into the neuron and glial cells [310]. Here we focused on the main glucose transporters in the brain: glucose transporter 1 (GLUT1), which is abundantly detected in the BBB, glucose transporter 3 (GLUT3), the major isoform in neurons, and the insulin-sensitive glucose transporter 4 (GLUT4). Postmortem studies of the brains of AD patients demonstrated a marked decrease in protein levels of GLUT1 and GLUT3 in the AD-affected brain regions, particularly in the cerebral cortex, with a significant loss of GLUT3 [37, 311]. Reduced levels of GLUT1 and GLUT3 has been correlated with a decrease in O-GlcNAcylation and to the hyperphosphorylation of tau [39]. The underlying mechanisms implicated downregulation of the hexosamine biosynthesis pathway [47]. Therefore, abnormalities in glucose transport may lead to impaired brain glucose metabolism, contributing to the development of neuropathological hallmarks of AD. In the current study, we did not observe a significant difference in the mRNA level of GLUT1 among the three ApoE genotypes. However, studies on human AD brain tissues indicate markedly lower protein expression of GLUT1 with no change in mRNA level of GLUT1, suggesting post-transcriptional regulation [312]. Further, compared to hApoE2-TR and hApoE3-TR mice, hApoE4-TR mice showed reduced glucose transport across the BBB without altered levels of mRNA or protein of GLUT1, suggesting the function of GLUT1 may involve post-translational modification [313]. Therefore,

GLUT1 protein expression and/or function may be altered despite no detectable difference in mRNA levels. Future studies are necessary to clarify the role of GLUT1 in brain glucose uptake in the three ApoE brains. Additionally, we observed a significantly lower mRNA level of GLUT3 in ApoE4 brains than ApoE3 brains. The GLUT3 glucose transporter is the predominant isoform in the neurons [314, 315]. Compared to GLUT1 and GLUT4, GLUT3 has both a higher affinity for glucose and significantly greater transport capacity, making it uniquely suited to match the energy needs of the highly metabolic neurons [316]. In support of this notion, the protein expression of GLUT3 decreased in parallel with reduced cerebral glucose metabolism in AD-vulnerable brain regions [37]. Further, it has been shown that synaptic activity induced surface expression of GLUT3 following elevated rates of glucose import into neurons [317]. Therefore, the diminished GLUT3 expression could lead to insufficient energy supply during intense neuronal activity, resulting in deficits in neurotransmission in the ApoE4 brain. Of note, no changes in GLUT4 protein levels have been observed in the brains of AD patients [39]. Similarly, decreases in the expression levels of GLUT1 and GLUT3, but not GLUT4 were found in the brains of AD transgenic mice [318]. Here we reported that ApoE2 brains exhibited significantly higher levels of GLUT4 mRNA compared to both ApoE3 and ApoE4 brains, consistent with our previous findings [87]. The regional distribution of GLUT4 correspond to those of the insulin receptors, indicating that insulin may induce GLUT4 translocation and promote neuronal glucose transport, thus providing additional glucose to neurons under energy challenging conditions [319]. GLUT4 is also expressed in the synaptic terminals of some hippocampal neurons where it may play a critical role in memory processes [320]. While the mechanisms by which insulin

signaling regulates GLUT4 expression and neuronal glucose transport remain to be elucidated, upregulation of GLUT4 by insulin-like growth factor-1 (IGF1) could serve as a potential mechanism contributing to the neuroprotective properties conferred by ApoE2.

Intracellular glucose metabolism includes glycolysis in the cytosol, TCA cycle and oxidative phosphorylation in the mitochondria. Defects in the glycolytic pathway, particularly in the initial step, has been reported in the AD brain. For instance, markedly reduced glucose phosphorylation was found in the AD-affected brain regions, including parietal and temporal cortex [321]. Diminished activity of hexokinase, which catalyzes the phosphorylation of glucose, was observed in the brains of AD patients [41, 322]. In the current study, we reported that three ApoE isoforms differentially modulate hexokinase 1 (HK1) and hexokinase 2 (HK2). Specifically, ApoE2 brains exhibited higher expression of HK2 compared to ApoE3 brains. In contrast, ApoE4 brains displayed the lowest expressions of both HK1 and HK2 among the three ApoE phenotypes. In line with the *in vivo* data, compared to ApoE3-expressing cells, ApoE2-expressing cells showed higher whereas ApoE4-expressing cells demonstrated lower expression of both hexokinase isoforms and hexokinase activity. Accordingly, the glycolytic capacity was significantly higher in cells expressing ApoE2, but markedly lower in cells expressing ApoE4. Within the brain, ATP consumption primarily occurs at the synapses [323]. It has been shown that synaptic vesicle recycling requires considerable energy that could be met by ATP synthesis driven by neuronal activity [324]. In support of this notion, blockade of the activity-stimulated ATP synthesis results in severe impairment in synaptic functions [324]. While ATP generated by glycolysis only

accounts for a small percentage of total energy consumed by synaptic transmission [323], emerging evidence suggests that glycolysis plays a crucial role in the maintenance of synaptic function. Several glycolytic enzymes have been found in nerve terminals [325]. It has been shown that these enzymes interact with the subunits of vacuolar H^+-ATPase (V-ATPase), a proton pump that mediates the concentration of neurotransmitters into synaptic vesicles thereby regulating synaptic transmission [326, 327]. Additionally, it has been reported that V-ATPase activity at the steady state and glucose-dependent V-ATPase reassembly are controlled by glycolytic flux [328]. These findings suggest an intimate relationship between glycolysis and V-ATPase in regulating synaptic function and behavior. Previously, we have reported that three ApoE isoforms differentially modulate a key component of the catalytic domain of the V-ATPase. Specifically, our data demonstrated that ApoE2 brains express significantly higher levels of the β-subunit of V-ATPase when compared to ApoE3 and ApoE4 brains [293]. Here we showed that ApoE2 brains also possess the most robust glycolytic profile among the three ApoE brains. Therefore, the robustness in both glycolysis and V-ATPase expression may underlie the cognition-favoring properties associated with ApoE2.

In addition to defects in brain glucose transport and perturbed glycolysis, impaired mitochondrial function has been thought to contribute to the development of brain hypometabolism [329]. Results from both clinical and pre-clinical studies indicate a close link between mitochondrial dysfunction and AD pathophysiology [330, 331]. Additionally, it has been reported that ApoE4 carriers had reduced mitochondrial function in the hippocampus and posterior cingulate cortex [282, 285], brain regions that are most affected by AD. While the mechanisms of ApoE4-induced mitochondrial dysfunction

remain largely unknown, several *in vitro* studies suggest that a carboxyl-terminal-truncated form of ApoE4 mislocalizes to mitochondria and binds to subunits of mitochondrial respiratory chain complexes, leading to impaired electron transport chain activity and defects in mitochondrial oxidative phosphorylation [290, 291]. In line with these findings, we observed ApoE4-induced deficits in mitochondrial respiratory function in N2a cells. Specifically, the basal mitochondrial respiration, spare and maximal respiration capacities were all significantly lower in ApoE4-expressing cells compared to ApoE3-expressing cells. By contrast, ApoE2-expressing cells exhibited improved mitochondrial respiration. Apart from the mechanism mentioned above, reduced mitochondrial respiration may be secondary to impaired glycolysis. As less pyruvate is generated from glucose, lower levels of acetyl-CoA will enter the TCA cycle, resulting in decrease in mitochondrial oxidative phosphorylation. Similarly, the enhanced mitochondrial function associated with ApoE2 could be attributed to its increased rate of glycolysis. Additionally, compared to ApoE3 and ApoE4 brains, ApoE2 brains exhibited enhanced mRNA levels of dihydrolipoamide acetyltransferase (DLAT), a central component of pyruvate dehydrogenase complex (PDC), which mediates the conversation of pyruvate to acetyl-CoA. Therefore, increased expression of DLAT could also contribute to the elevated mitochondrial respiration in ApoE2-expressing cells by providing more acetyl-CoA for feeding into the TCA cycle.

In addition to glucose, we also examined the metabolic profile of ketone bodies, the main alternative fuel for the brain under glucose limiting conditions. Brain uptake and transport of ketone bodies are mediated by monocarboxylate transporters (MCTs), which are proton-linked membrane carriers that transport a range of monocarboxylate

metabolites such as lactate, pyruvate, and ketone bodies [332]. Although clinical studies have shown that a ketogenic agent improved cognitive performance in AD patients, the therapeutic benefits appear to be confined to ApoE4 non-carriers [85, 86, 333]. This led us to hypothesize that ketone body transport is defective or/and key enzymes that metabolize ketone bodies are impaired in the ApoE4 brain. We examined the gene expression of several brain MCTs, including MCT1, which is widely expressed in the endothelial cells of brain BBB, MCT4, whose expression appears to be restricted to astrocytes, and MCT2, the predominant neuronal monocarboxylate transporter [332] as well as the enzymes involved in ketolysis. Surprisingly, we found that ApoE2 and ApoE4 brains displayed a similar expression profile of ketone body uptake and metabolism. Compared to ApoE3 brains, MCTs and metabolic enzymes were upregulated in both ApoE2 and ApoE4 brains. Of note, mRNA levels of MCT1 and β-hydroxybutyrate dehydrogenase were significantly higher in the brains or hApoE2-TR mice than those of hApoE3-TR mice. These results suggest that ApoE2 and ApoE4 brains are capable of taking up and metabolizing ketone bodies more efficiently than ApoE3 brains. In support of this notion, maximal mitochondrial respiration rates upon BHB treatment were significantly higher in ApoE2- and ApoE4-expressing neurons compared to ApoE3-expressing neurons. Intriguingly, our data indicate a relatively robust, rather than defective, metabolic profile for ketone body utilization in the ApoE4 brain relative to the ApoE3 brain, which could explain, in part, the clinical observation that a ketogenic agent provides a more meaningful benefit in ApoE3 than in ApoE4 carriers. In the AD context, as the ApoE4 brain is associated with glucose hypometabolism, increased ketone body metabolism could serve as an adaptive response to compensate for the bioenergetic

defects. We hypothesized that there is an upper limit of ketone body transport and metabolism in the ApoE4 brain and that the maximal capacity of ketone utilization has been reached as a result of this compensatory response. Hence, when supplied with exogenous ketone bodies, the ApoE4 brain would be unable to further metabolize ketones for energy production, therefore do not show amelioration in cognitive function. Additionally, enhanced ketone body metabolism may be another important contributor to the intact cognition associated with ApoE2.

To further understand the biological implications of gene changes, we utilized Ingenuity Pathway Analysis (IPA) to conduct a regulatory pathway and molecular network analysis. The results generated from IPA suggest that an upstream regulator, peroxisome proliferator-activated receptor gamma coactivator 1-alpha (PGC-1α), is activated in the ApoE2 brain. Studies on adipose tissue, liver, and skeletal muscle have pointed out a central role of PGC-1α in modulating mitochondrial biogenesis and oxidative phosphorylation [334]. Comparatively fewer studies have examined its function in the brain. A marked decrease in the expression of PGC-1α has been observed in the brains of patients with neurodegenerative diseases [335-338]. PGC-1α downregulation has been associated with extensive alterations in several metabolic pathways, particularly in oxidative phosphorylation and the mitochondrial electron transport chain [337, 338]. Additionally, gene expression analysis of PGC-1α null mouse brain indicated significant downregulation of genes associated with neuronal functions [339, 340]. These findings suggest a pivotal role of PGC-1α in maintaining neuronal functions by controlling mitochondrial oxidative metabolism and energy homeostasis. In this study, we found significantly higher mRNA levels of PGC-1α in ApoE2 brains compared to ApoE3 and

ApoE4 brains. Protein levels of PGC-1α were significantly lower in ApoE4 brains compared to both ApoE2 and ApoE3 brains. It has been reported that forced expression of ApoE4 reduced mRNA and protein levels of sirtuin 1 (Sirt1) [341], an enzyme which mediates NAD^+-dependent deacetylation of PGC-1α [342]. As the deacetylation of PGC-1α results in enhanced PGC-1α transcriptional activity, the lower expression of Sirt1 may lead to reduced PGC-1α transcriptional activity. Therefore, lower protein expression and activation of PGC-1α may contribute to the bioenergetic deficits associated with the ApoE4. To date, there is no report on Sirt1 expression and transcriptional regulation in the ApoE2 genotype. However, ApoE2 may modulate PGC-1α activity through a similar mechanism. Given that PGC-1α is a master regulator of mitochondrial oxidative metabolism, the elevated expression and/or activity of PGC-1α may underlie the bioenergetic robustness associated with ApoE2.

The role of PGC-1α in glycolysis has been examined in the liver, heart, muscle and several types of cancer cells. In cultured hepatocytes, PGC-1α overexpression suppressed glycolysis by downregulating glucokinase and pyruvate kinase [343]. Reduced expression of PGC-1α has been postulated to promote aerobic glycolysis in some most aggressive types of cancer, such as breast cancer [344] and colon cancer [345]. In the neonatal cardiac myocytes, PGC-1α expression was strongly induced, which directed the metabolic switch from glycolysis to mitochondrial oxidative metabolism [346, 347]. In skeletal muscles, conflicting findings exist. Muscle-specific overexpression of PGC-1α significantly increased expression of glucose transporters and hexokinase, which contribute to elevated glucose uptake and utilization [348]. In line with this finding, activation of AMP-activated protein kinase (AMPK), which has been shown to promote

PGC-1α expression and enhance PGC-1α activity by phosphorylation, significantly increased the expression of HK2 and GLUT4, the major hexokinase isoform and glucose transporter in the skeletal muscle [349]. However, a recent study indicates that HK2 may be regulated independently of PGC-1α upon AMPK activation [350]. To date, no study has explored the role of PGC-1α in the glycolytic pathway in the brain. Here we show, for the first time, that PGC-1α differentially modulates hexokinase isozymes in neurons. Specifically, overexpression of PGC-1α increased the protein expression of HK1, decreased HK2 expression. While both hexokinase isozymes catalyze the conversion of glucose into glucose-6-phosphate (Glc-6-p), they appear to direct glucose to different metabolic fates depending on their subcellular locations. The idea that HK1 functions primarily in a catabolic role derived from the findings that the inhibition of HK1 by Glc-6-p can be overcome by increased cellular phosphate (Pi) [351, 352], which is a signal for increased energy demand. In contrast, Pi does not antagonize but enhances the inhibitory effect of glucose-6-phosphate on HK2 [353, 354]. Both hexokinase isozymes were found to bind to mitochondria. HK1 binds to mitochondrial via the interaction with voltage-dependent anion channel (VDAC), which controls metabolite exchange across the mitochondrial outer membrane [355, 356]. Additionally, it has been demonstrated that HK1 preferentially utilized ATP generated by oxidative phosphorylation within the mitochondria for phosphorylating glucose [357, 358]. Therefore, a picture has emerged that HK1 is mainly catabolic by shuttling Glc-6-p to glycolysis with the terminal stage of glucose oxidative metabolism occurring in the mitochondria. In contrast to HK1, HK2 has been suggested to dynamically translocate between cytoplasm and mitochondria. When bound to mitochondria, HK2 fulfills a similar function as HK1; when localized to

cytosol, HK2 channels Glc-6-p into glycogen synthesis and other anabolic pathways such as the pentose phosphate shunt to provide NADPH for lipid synthesis [246, 306, 359, 360]. Taken together, these findings suggest HK1 is primarily responsible for glycolysis whereas HK2 may play multiple roles in response to different metabolic conditions. Therefore, increased HK1 may facilitate glycolysis whereas decreased HK2 may lead to inhibition of glucose anabolic metabolism, thus promoting the overall glucose catabolism. Indeed, PGC-1α overexpression resulted in a significant improvement in glycolytic capacity, which is likely attributed to the enhanced HK1 expression.

In the present study we found that three ApoE isoforms differentially modulate brain energy metabolism, however, the underlying mechanism remains to be elucidated. A recent study cast the lipid-binding ApoE in an entirely new light by showing that ApoE could act as a transcription factor [362]. Human recombinant ApoE, specifically ApoE3 and ApoE4, were found to translocate to the nucleus and bind to double-stranded DNA with high affinity. Chromatin immunoprecipitation and high-throughput DNA sequencing (ChIP-seq) analyses revealed ApoE4 targeted the promoter regions of over 1700 genes, of which 76 have been implicated in AD pathogenesis [362]. These genes can be broadly grouped into several functional classes including neuronal signaling, glucose metabolism and energy homeostasis, inflammation, and neuronal cell death. Both ApoE3 and ApoE4 were found to bind to the promoter region of Sirt1, but only ApoE4 suppressed its transcriptional activity [362]. Importantly, ApoE-Sirt1 interaction was also observed in fibroblasts from AD patients that possess ApoE ε3/ε4, suggesting ApoE may regulate Sirt1 activity *in vivo* [362]. As mentioned previously, Sirt1 directly affects PGC-1α activity through deacetylation. Therefore, suppression of Sirt1 activity by ApoE4 may

result in increased acetylation of PGC-1α and a decrease in its transcriptional activity, which could ultimately lead to downregulation of the genes involved in glucose metabolism and mitochondrial function. In contrast to ApoE4, which functions as a transcriptional repressor, ApoE2 may serve as a positive transcriptional regulator. Thus, ApoE2 may increase Sirt1 activity transcriptionally, leading to the deacetylation of PGC-1α and the upregulation of genes involved in glucose metabolism and mitochondrial bioenergetics. Further, ApoE may also target other metabolic pathways known to regulate glucose oxidative metabolisms, such as AMPK [342] and hypoxia-inducible factor -1 (HIF-1) [363]. Further investigations are warranted to delineate the mechanisms by which different ApoE isoforms achieve their diverse impacts on multiple energy metabolic processes, particularly glycolysis.

In summary, our data indicate that the ApoE2 brain exhibits the most robust while the ApoE4 brain displays the most deficient profile for the uptake and metabolism of glucose. In particular, these two ApoE genotypes differ significantly in the expression of facilitated glucose transporters and hexokinases. While the uptake and metabolism of ketone bodies was similar between ApoE2 and ApoE4 brains, ApoE3 brain display a more deficient profile. These findings are supported by both molecular and functional studies. Importantly, we discovered that the glycolytic pathway is differentially modulated by the three ApoE genotypes. The significantly higher hexokinase protein expression and activity could contribute to the overall bioenergetic robustness associated with ApoE2. In contrast, the remarkably lower expression and activity of hexokinase may be responsible for the bioenergetic deficits associated with ApoE4. Therefore, a therapeutic approach that could circumvent the defects in the cytosolic metabolism of

glucose by providing glucose metabolizing intermediates, e. g. pyruvate may hold benefits for ApoE4 carriers. Importantly, we also provide preliminary evidence that introduction of ApoE2 could elicit protective effects in ApoE4 and AD brains. The numerous failures in AD clinical trials suggest a loss in translation from pre-clinical research to humans and the possibility that we are aiming at the wrong targets. Thus it has been proposed that instead of focusing on reducing Aβ, treatment should target processes preceding plaque formation or appearance of AD pathology. In this context, strategies that target the neuroprotective mechanism could hold promise for preventing, reducing risk or delaying the onset of AD by increasing the brain's internal defense against aging and AD-related insults. Therefore, the introduction of ApoE2 may represent a promising approach via enhancing bioenergetic mechanism contributing to brain resilience against AD.

1.6 Future Directions

There are a couple of opportunities for the future studies. We have shown that PGC-1α overexpression ameliorated ApoE4-induced deficits in glycolysis and mitochondrial respiration. To further validate the role of PGC-1α in the bioenergetic robustness associated with ApoE2, we will evaluate the effects of shRNA-mediated PGC-1α knockdown on hexokinase protein expressions, glycolytic function and mitochondrial respiration in the cell line stably expressing human ApoE2. Additionally, a further in-depth investigation is necessary to elucidate the molecular mechanisms by which PGC-1α modulates hexokinase expression. As PGC-1α overexpression improved glycolysis, mitochondrial respiration may be improved due to increased availability of substrates and reducing equivalents. However, given that PGC-1α is the master regulator of mitochondrial oxidative metabolism, the amelioration in mitochondrial respiratory dysfunction may be also attributed to enhanced mitochondrial biogenesis and improved respiratory capacity. Examination of mitochondrial mass and the expression levels of several transcription factors that regulate the expression of mitochondrial genes, such as nuclear respiratory factor 1 (NRF1), transcription factor A, mitochondrial (TFAM) and estrogen-related receptors (ERRs), could provide insights into the mechanisms underlying PGC-1α-mediated protective effects against ApoE4-induced defects in mitochondrial function.

In the present study, PGC-1α overexpression decreased HK2 expression, whereas the introduction of ApoE2 significantly increased HK2 expression, suggesting other upstream regulators also modulate HK2 expression in the ApoE2 brain. A gene expression profiling of the major upstream and downstream signaling pathways with

HK2 serving as the node will help to delineate the molecular mechanisms by which ApoE2 regulates HK2 expression.

Another opportunity worth exploring is the potential benefit of pyruvate supplementation in ApoE4 carriers. It has been reported that oxidative stress-induced activation of poly (ADP-ribose) polymerase-1 (PARP-1) resulted in the depletion of cytosolic NAD^+ followed by inhibition of glycolysis, leading to sustained energy failure and ultimately cell death [364]. As a direct substrate for mitochondrial metabolism, pyruvate can be oxidized in the absence of cytosolic NAD^+, therefore, it can bypass the restrictions imposed by PARP-1 and thus restore energy efficiency [365]. Consistent with this concept, administration of pyruvate significantly improved neuron survival in the brains of rats subjected to insulin-induced hypoglycemia [364]. These findings and results from our study indicate that pyruvate may benefit ApoE4 brain by circumventing a sustained impairment in neuronal glucose utilization due to defects in glycolysis. More work is necessary to examine the potential therapeutic effects of pyruvate in the pre-clinical AD brain, particularly in those bearing ApoE4.

Further, results obtained from our *in vitro* studies suggest that forced expression of ApoE2 reversed bioenergetic deficits induced by ApoE4. In future studies, the neuroprotective effects of ApoE2 will be evaluated in *in vivo* studies using hApoE4-TR mice. Specifically, the E-cadherin peptides will be used to disrupt the BBB and facilitate the delivery of ApoE2 into the ApoE4 brain. Then the effects of ApoE2 introduction on ApoE4-induced bioenergetic deficits and other AD-related neuropathological features such as synaptic dysfunction, neuronal loss, and cognitive impairment, will be evaluated via behavioral tests and biochemical analyses.

1.7 Conclusion

In the current study, we explored the potential differences in the brain energy metabolic pathways involving glucose and ketones as substrates, among the three human ApoE genotypes. Our data demonstrated that compared to the ApoE3 brain, the ApoE2 brain was associated with a more metabolically robust profile, whereas the ApoE4 brain demonstrated a relatively deficient profile in the transport and metabolism of glucose, the primary brain energy source (Fig. 1.7.1). Importantly, our data indicated that human ApoE isoforms differentially modulate the expression and activity of hexokinase, the "gateway" enzyme in glucose metabolism and the "pacemaker" for glycolysis. Enhanced glucose metabolism associated with ApoE2 sets a foundation for an increased defense against aging and AD-risk-related stress, which may underlie its cognition-favoring properties. By contrast, the deficit in glucose metabolism associated with ApoE4 renders the brain vulnerable to aging and neurodegeneration, which could contribute to its increased susceptibility to AD. Pertaining to the capability of utilizing ketones, the secondary fuel for the brain, surprisingly, ApoE2 and ApoE4 brains showed a similar level of robustness (Fig. 1.7.1). The vigorous metabolic utilization of ketone bodies in the ApoE4 brain could be an adaptive response to compensate for energy deficiency resulting from impaired glucose metabolism. Additionally, it may provide a mechanistic rationale for the clinical observations that ApoE4 carriers do not benefit from ketogenic therapy. Moreover, a bioinformatic analysis suggests the potentiation of an upstream regulator, PGC-1α, may be responsible for the bioenergetic robustness associated with ApoE2. In support of this prediction, PGC-1α overexpression significantly improved glycolytic function and mitochondrial respiration in the cell line stably expressing ApoE4. More

importantly, we provide preliminary evidence that *de novo* expression of ApoE2 could counteract the detrimental effects in glycolysis and mitochondrial respiratory function induced by ApoE4 (Fig. 1.7.1). While *in vivo* studies and in-depth mechanistic investigations are warranted, the introduction of ApoE2 could hold promise for preventing or delaying the onset of AD by enhancing the overall bioenergetic robustness in the brain, particularly in the high-risk ApoE4 carriers.

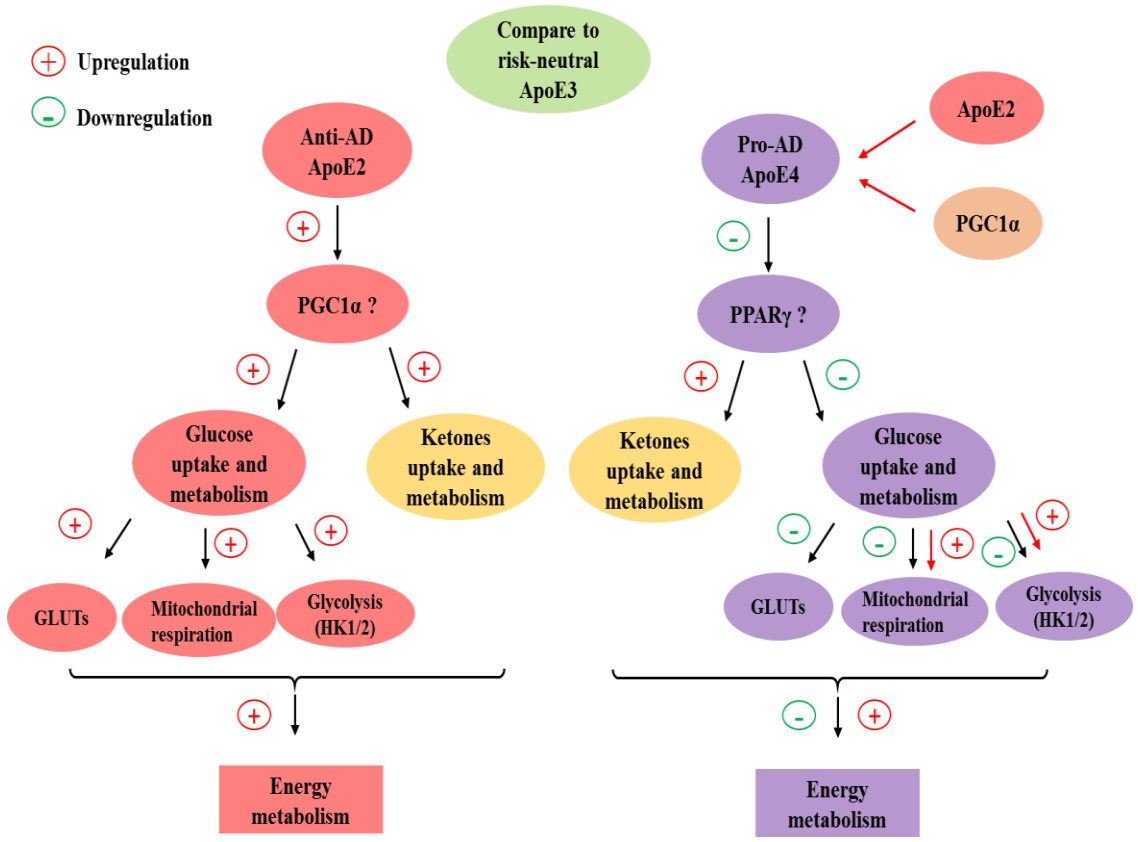

Figure 1.7.1

Fig.1.7.1 Conclusion: human ApoE isoforms differentially modulate brain energy metabolism. ApoE2 brain exhibits the most metabolically robust while ApoE4 brain associates with the most deficient profile on both the uptake and metabolism of glucose. In particular, these two ApoE genotypes differs significantly in the expression of GLUTs and hexokinases. On the uptake and metabolism of ketones, ApoE2 and ApoE4 brains present similar levels of robustness, while ApoE3 brain displays a most deficient profile. The activation of PGC-1α may be responsible for the bioenergetic robustness associated with ApoE2 as PGC-1α overexpression and forced expression of ApoE2 reversed the bioenergetic defects induced by ApoE4.

Chapter 2 Cyclophilin D-Mediated Mitochondrial Perturbation Underlies Diabetes-Associated Cognitive Dysfunction

2.1 Abstract

Diabetes mellitus is a heterogeneous metabolic disorder associated with an increased risk of synaptic injury and cognitive dysfunction. Diabetic patients have a greater prevalence of dementia including Alzheimer's Disease (AD). However, the underlying mechanisms of diabetes-associated cognitive deficits remain to be elucidated. Emerging evidence indicates mitochondrial dysfunction is a common pathological feature in diabetes-affected brains, however, the precise underlying mechanisms are not clear. Brain mitochondria isolated from streptozotocin (STZ)-injected mice, a mouse model of type 1 diabetes, demonstrated reduced calcium buffering capacity and increased reactive oxygen species (ROS) generation, suggesting an increased susceptibility to the induction of mitochondrial permeability of transition (mPT) and mitochondrial dysfunction. Here, we show that Cyclophilin D (CypD), a critical regulator of mPT, plays a major role in diabetes-induced mitochondrial abnormalities and related cognitive dysfunction in a type 1 diabetic mouse model. Compared with vehicle-treated mice, STZ treatment resulted in a significant increase in CypD expression and marked decrease in mitochondrial respiratory function in the brain, as well as impaired spatial learning and memory abilities. Intriguingly, genetic deletion of CypD significantly attenuated diabetes-induced cognitive deficits. Compared with STZ-treated non-transgenic mice, CypD null mice injected with STZ exhibited substantial improvement in the cognitive function assessed by the Morris Water Maze task. In contrast, diabetes-associated upregulation in CypD and defects in mitochondrial respiration were greatly exacerbated in the brains of AD

transgenic mice made diabetic, suggesting a synergistic effect of diabetes and AD on the regulation of CypD expression and mitochondrial dysfunction. In accordance with the aggravated mitochondrial perturbation, the diabetes-related cognitive decline was greatly accelerated. Therefore, our results provide new insights into the role of CypD-mediated mPT in brain mitochondrial malfunction and cognitive impairment related to diabetes. Inhibition of the induction of mPT by blocking CypD may represent a promising therapeutic strategy for diabetes-associated cognitive dysfunction and dementia including AD.

2.2 Introduction

2.2.1 Diabetic encephalopathy

Diabetes mellitus is a metabolic disorder that affects 422 million people worldwide, including 29.1 million in the US [366]. The vast majority of cases of diabetes fall into two broad classifications. Type 1 diabetes, comprises only 5-10% of diabetic cases and primarily results from autoimmune destruction of the β-cells in the pancreas. Type 2 diabetes accounts for 90-95% of total cases and is associated with insulin resistance and relative insulin deficiency. Diabetes is a chronic illness associated with a number of complications including cardiovascular disease, nephropathy, retinopathy, and neuropathy. In addition to these peripheral complications, diabetes may also cause pathological alterations in the brain. The relationship between diabetes and cognitive impairment was noted as early as 1922 [367]. Later in 1950, the term diabetic encephalopathy was introduced to describe cognitive impairment as a central nervous system (CNS) complication of diabetes [368]. While the clear definition and diagnostic criteria of diabetic encephalopathy remains to be established, increasing interest has been drawn to investigate the cognitive impairment in relation to diabetes in recent years. A number of epidemiological studies indicate that the presence of diabetes significantly increases the risk of dementia including the Alzheimer's type [5, 369-372]. Additionally, longitudinal analyses from population-based studies reveal that diabetes is associated with an accelerated cognitive decline in aging [373, 374]. In line with these findings, compared to age-matched healthy control subjects, diabetic patients exhibited worse performance in the cognitive screening tests involving multiple brain regions [2, 375, 376]. In accordance with clinical evidence, synaptic injury and cognitive dysfunction

were observed in animal models of type 1 and type 2 diabetes [90, 91, 377-381]. For instance, rats injected with streptozotocin (STZ), a toxin which causes the destruction of pancreatic β cells and insulin deficiency, exhibited poor performance in the Morris water maze task, suggesting deficits in spatial learning and memory [377, 379]. Consistent with these observations, hippocampal long-term potentiation (LTP), which is believed to be linked to the cellular mechanisms of learning and memory, was severely impaired in the diabetic rats [377, 379, 382]. Similar defects in synaptic plasticity and memory formation were also detected in leptin receptor-deficient rodents, the Zucker rats and db/db mice, which are characterized by insulin resistance [88, 379]. Collectively, these findings point out an intimate association between cognitive impairment and diabetes.

In contrast to the well-characterized vascular complications, the mechanisms underlying diabetic encephalopathy remain largely unexplored. Several animal studies suggest the molecular mechanisms of diabetic encephalopathy differ between type 1 and type 2 diabetes [383]. In type 2 diabetic encephalopathy, insulin resistance and an increased level of cholesterol appear to play significant roles in facilitating amyloidogenesis, tau hyperphosphorylation, oxidative stress and neuronal degeneration [384, 385]. In type 1 diabetic encephalopathy, however, insulin deficiency and hyperglycemia play major roles in contributing to neuronal loss and cognitive dysfunction [386, 387]. Therefore, further mechanistic studies should be conducted separately on animal models of type 1 and type 2 diabetes to advance our understandings on the etiology of diabetes-associated CNS complication.

Diabetic encephalopathy has been estimated to occur in 40% of the total diabetic cases, primarily in patients with a long diabetic history and/or poorly controlled hyperglycemia

[388]. The cognitive deficits are generally mild to moderate, however, they could lead to poor self-management, worse glycemic control and lower quality of life [389]. Moreover, conventional therapeutic strategies were found to be less effective for diabetic CNS complications [390]. With the significantly increasing prevalence of both type 1 and type 2 diabetes, more research should be directed to uncover the pathophysiological basis of diabetic encephalopathy and to find a novel therapeutic approach to prevent or slow down the progression of cognitive impairment.

2.2.2 Mitochondrial dysfunction in diabetes

Mitochondrial dysfunction has long been implicated in the pathogenesis, progression, and complications of diabetes [391]. A genetic mutation in mitochondrial DNA (A3243G) results in mitochondrial diabetes, a rare form of diabetes characterized by decreased glucose-induced insulin release but not insulin resistance [392]. It was proposed that mitochondrial dysfunction in the pancreatic β cells, hyperglycemia-induced ROS generation, and subsequent oxidative damage play significant roles in the progression of the disease [393]. The pathophysiological impacts of mitochondrial dysfunction in type 1 and type 2 diabetes involve both insulin sensitivity and insulin secretion. While a cause-effect relationship between perturbed mitochondrial function and insulin resistance remains to be established, it is without doubt that alterations in mitochondrial morphology [394-396], dynamics (fission/fusion) [397, 398], reduced mitochondrial biogenesis [399, 400] and oxidative phosphorylation [396, 400, 401] are all associated with impaired insulin actions in the target organs. Additionally, mitochondrial dysfunction leads to decreased insulin secretion due to insufficient ATP production and

consequently diminished ratio of ATP/ADP [402, 403]. High glucose and fatty acid flux into mitochondria elicit ROS generation, presumably from the mitochondrial respiratory chain [404, 405]. Mounting evidence suggests mitochondrial oxygen radicals cause damage to a number of cell types and tissues, such as vascular endothelial cells [406], retinal endothelial cells [404, 407] and renal mesangial cells [408, 409], which may underlie the development of diabetes-related complications. Comparatively, few studies have explored the role of mitochondrial dysfunction in diabetic encephalopathy.

Mitochondrial dysfunction in diabetic CNS complication

Given that brain has high energy requirements and mitochondria are the main source of ATP production, it is not surprising that mitochondrial dysfunction is implicated in diabetes-associated defects in the brain. Functional impairments of mitochondria, as evidenced by a significant reduction in mitochondrial respiration, membrane potential, and energy levels, have been observed in the brains of type 2 diabetic mice [410]. Additionally, levels of transcription factors involved in mitochondrial biogenesis were markedly decreased [410]. Importantly, mitochondrial dysfunction is accompanied by a loss of synaptic integrity [410, 411], which may contribute to the cognitive deficits. Interestingly, it has been shown that aging facilitated diabetes-related mitochondrial dysfunction. Moreira et al. reported a reduction in mitochondrial respiratory chain activity and an uncoupling of oxidative phosphorylation in the brain mitochondria isolated from Goto-Kakizaki diabetic rats [74]. These defects in mitochondrial bioenergetics were greatly exacerbated by aging. The accelerated mitochondrial dysfunction could partially explain the increased prevalence of diabetic encephalopathy in the elderly [412].

Apart from the defects in mitochondrial respiratory function, several studies suggest that oxidative stress plays a major role in the pathology of diabetic encephalopathy. Previously, it has been shown that acute hyperglycemia-induced oxidative damage in the rat brain [413], with mitochondria being the major target [414]. Indeed, ROS levels, nitric oxide production, and mitochondrial nitric oxide synthase expression were found to be increased in the brain mitochondria isolated from diabetic rats [73, 415]. Alongside elevated oxidative stress, deficits in antioxidant defense such as diminished activity of glutathione peroxidase and manganese superoxide dismutase (MnSOD), a lower content of coenzyme Q, as well as a reduced ratio of glutathione to glutathione disulfide (GSH/GSSG) were also noted [72, 73, 415]. Consequently, nitrosative and oxidative stress-induced damage to mitochondrial proteins and DNA may contribute to the pathological alterations in mitochondrial structure and function.

In addition to impairments in mitochondrial function, altered mitochondrial morphology resulting from perturbed mitochondrial dynamics has been implicated in type 2 diabetes and its complications [416]. Previous studies have shown that hyperglycemia facilitates mitochondrial fragmentation by promoting mitochondrial fission or suppressing mitochondrial fusion in a variety of cell types, including pancreatic β cells [417, 418], skeletal muscle cells [419], cardiomyocytes [420], endothelial cells [421, 422], and dorsal root ganglia (DRG) neurons [423-425]. However, the role of mitochondrial dynamics in diabetes-induced brain mitochondrial dysfunction and cognitive impairment remains unexplored. To address this research gap, mitochondrial dynamics was evaluated in the brain of a mouse model of type 2 diabetes (db/db) [75]. A significant decrease in mitochondrial density and increased mitochondrial fragmentation were observed in the

hippocampus of diabetic mice compared with age-matched nondiabetic littermates [75]. The perturbation in mitochondrial dynamics was accompanied by defects in the mitochondrial respiratory chain and reduced ATP levels. Consistent with the findings from the *in vivo* studies, a human neuronal SK cell line treated with high concentrations of glucose also showed mitochondrial fragmentation and respiratory dysfunction [75]. Intriguingly, restoration of mitochondrial fission/fusion balance markedly ameliorated diabetes-induced defects in respiratory function and impairment in synaptic plasticity [75]. Taken together, these findings indicate that alterations in mitochondrial morphology and function due to perturbation in mitochondrial dynamics contribute to diabetes-associated deficits in synaptic plasticity and cognitive function.

2.2.3 Mitochondrial permeability transition pore (mPTP)

mPTP in physiological and pathological conditions

Previous studies have demonstrated a decrease in the capacity of mitochondria to accumulate Ca^{2+} in the brain of diabetic rats, suggesting an increased susceptibility to induction of the mitochondrial permeability transition (mPT) [72, 74]. In physiological conditions, mitochondria are impermeable and the mitochondrial permeability transition pore (mPTP) exists in a low-conductance state, which only allows for the exchange of small metabolites between the cytosol and mitochondrial matrix [426]. In the presence of some inducers, such as excessive ROS or Ca^{2+} overload, the formation and opening of the mPTP results in a sudden increase in the permeability of mitochondrial inner membrane (IMM) to solutes with molecular weight up to 1,500 Da [427]. The high-conductance pore allows the entry of small solutes into the mitochondrial matrix, leading to osmotic

swelling of the mitochondrial matrix, eventually resulting in the rupture of outer mitochondrial membrane (OMM). The subsequent release of cytotoxic proteins, such as cytochrome c or apoptosis-inducing factor (AIF), could trigger cellular apoptosis in both caspase-dependent and independent pathways. Additionally, the dissipation of mitochondrial membrane potential due to the disruption of proton gradient in the IMM will lead to uncoupling of oxidative phosphorylation, resulting in ATP depletion and ROS generation (Fig.2.2.1). Multiple studies have demonstrated that mPT is involved in tissue injuries under certain pathological conditions such as traumatic brain injury [428, 429], ischemia-reperfusion injury [430-432], as well as stroke [433]. mPT has also been associated with tissue damage in diabetic complications. A number of studies have shown that diabetic mitochondria exhibit greater sensitivity to mPTP opening and augmented susceptibility to cell dysfunction in heart [434, 435], liver [436] and kidney [437, 438] than non-diabetic counterparts. However, it remains unknown whether the mPT contributes to diabetes-related brain mitochondrial abnormalities and cognitive dysfunction.

The molecular composition of mPTP

Despite the considerable efforts to delineate the molecular composition of mPTP, its exact structure remains elusive. The old model [439] proposed that mPTP consists of three major proteins: the voltage-dependent anion channel (VDAC) in the OMM, the adenine nucleotide translocator (ANT) in the IMM, and cyclophilin D (CypD) as a regulatory component in the mitochondrial matrix. It was suggested that CypD binds to VDAC/ANT complex, forming a tunnel-like structure at the junction between the inner and outer mitochondrial membranes [439]. The crucial role of CypD in mPTP and cell death have

been confirmed in a number of *in vivo* and *in vitro* studies (discussed in details in section 2.2.4). However, several genetic knockout experiments raise the question as to whether other major components of mPTP are dispensable. For instance, Ca^{2+}- and oxidative stress-induced mPT and apoptosis were unaltered or even exacerbated in mitochondria lacking all three VDAC isoforms [440, 441], suggesting VDAC may not be an essential component for mPTP. Liver mitochondria lacking the two most abundant ANT isoforms (Ant1 and Ant2) were still able to undergo mPT, albeit more Ca^{2+} than usual was required [442]. However, it cannot be ruled out that other isoforms, such as Ant4, may compensate for the loss of Ant1 and Ant2. Thus, more work is needed to determine whether ANT is an essential component of mPTP and the potential role of ANT in the induction of mPT.

Recent studies suggest the involvement of other molecules in the modulation of mPTP activity, including mitochondrial phosphate carrier (PiC) in the IMM. Overexpression of PiC has been shown to induce apoptosis [443]. Additionally, PiC was found to associate with ANT and binds to CypD [444]. Although the reduction in protein level of PiC did not prevent mPTP opening, genetic deletion of PiC in cardiomyocytes blunted mPTP opening in response to Ca^{2+} challenge [445]. Collectively, these findings suggest PiC may not be a requisite component of mPTP, but it could regulate its activity.

In addition to PiC, Bcl-2 family member proteins Bax and Bak, which are central players in apoptotic cell death, have also been implicated in mPT regulation by enhancing the permeability of the OMM [446]. Indeed, loss of Bax and Bak reduced OMM permeability, resulting in resistance to Ca^{2+} overload-induced mPTP opening and necrotic cell death [447, 448]. Further, reconstitution of Bax/Bak-deficient mitochondria with Bax mutants not capable of oligomerization or forming apoptotic pores enhanced OMM

permeability, restored mPTP opening [447, 448]. These findings suggest Bax/Bak facilitate mPT induction and the resulting mitochondrial swelling and organelle rupture.

Evidence for mitochondrial F_1F_0 ATP synthase as a core component of mPTP is just beginning to emerge. Previously, CypD was found to modulate the catalytic activity of F_1F_0 ATP synthase via binding to the oligomycin sensitivity-conferring protein (OSCP) subunits of the lateral stalk [449]. Later, the same group reported that dimers of the F_1F_0 ATP synthase incorporated into lipid bilayers formed Ca^{2+}-activated channels with the key features of the mPTP [450]. It was found that the c subunit in the F_0 domain played a critical role in the opening of mPTP induced by cytosolic Ca^{2+} overload [451]. In line with these findings, purified subunit c, when reconstituted to artificial bilayer lipid membranes, formed a high-conductance voltage-sensitive channel [452]. Importantly, siRNA-mediated downregulation of the c subunit inhibited Ca^{2+}-mediated mPT, abolished mitochondrial fragmentation and prevented mPT driven cell death [451]. More recently, it was proposed that the c subunit associated with inorganic polyphosphate (polyP) and polyhydroxybutyrate (PHB) to form ion channels with properties recapitulating those of the native mPTP [453]. Taken together, these findings indicated that F_1F_0 ATP synthase is required for the assembly and function of mPTP, however, further investigations are warranted to elucidate the precise role of F_1F_0 ATP synthase in mPTP formation.

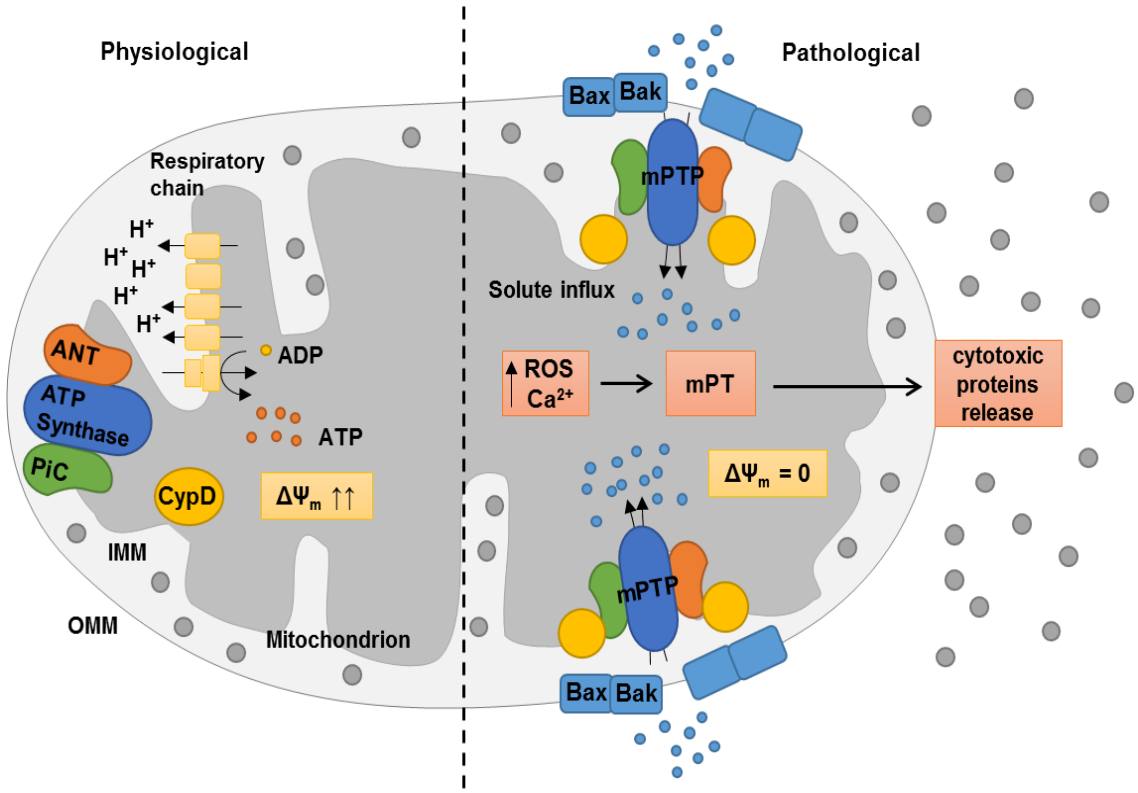

Figure 2.2.1

Fig. 2.2.1 mPTP in physiological and pathological conditions. Key components of the mPTP include mitochondrial phosphate carrier (PiC), adenine nucleotide translocator (ANT) and F_1F_0 ATP synthase in the inner mitochondrial membrane (IMM), and cyclophilin D (CypD) in the mitochondrial matrix. In physiological conditions, mitochondria exhibit high mitochondrial transmembrane potential ($\Delta\psi m$), which is generated by proton extrusion from the respiratory chain, and is used to drive ATP generation. In response to some cellular stress, such as excessive ROS generation and Ca^{2+} overload, mPTP opens, resulting in the influx of small solutes into the mitochondrial matrix driven by the electrochemical forces. Pro-apoptotic proteins Bax and Bak aid in the mPT process by enhancing the permeability of outer mitochondrial membrane (OMM). The opening of mPTP results in the loss of the $\Delta\psi m$, ATP depletion, mitochondrial swelling, and eventually the rupture of OMM. Subsequent release of cytotoxic proteins such as cytochrome c and apoptosis-inducing factor could lead to cell death via both caspase-dependent and independent pathways. Adapted from Fulda et al. (2010) Nature Reviews Drug Discovery 9, 447-464.

2.2.4 CypD and CypD-mediated mPT

CypD: history, domain, and structure

Cyclophilin D is the most characterized and undisputed molecular component in the mPTP. Preliminary evidence leading to the discovery of CypD as an important regulator in mPTP came from studies examining the effect of the immunosuppressive drug cyclosporine A (CsA) on mitochondrial functions. Fournier et al. observed that CsA inhibited mitochondrial respiration and caused a large amount of Ca^{2+} accumulation in the mitochondrial matrix [454]. Later, it was found that CsA was able to bind to and inhibit Ca^{2+}-induced pore formation and mPT induction [455, 456]. Subsequent studies identified mitochondrial peptidyl-prolyl cis-trans isomerase (PPIase) as the target of CsA, and a model where CypD interacts with ANT in the presence of Ca^{2+} to cause pore opening was proposed [457]. Genetic studies further demonstrated CypD as an essential component of the mPTP. In 2005, two laboratories simultaneously reported that mice lacking CypD are protected from ischemia/reperfusion-induced cell death. Additionally, CypD-deficient mitochondrial are resistance to mPT and mitochondrial swelling induced by oxidative stress and Ca^{2+} overload [432, 458]. Since then, numerous loss-of-function studies have corroborated previous findings, supporting the notion that CypD is of critical importance in mPT regulation under both normal and pathological conditions [459, 460].

CypD is a mitochondrial matrix protein encoded by the peptidyl-prolyl cis-trans isomerase F gene (PPIF). Human PPIF gene is located on chromosome 10 and is composed of 6 exons and 5 introns (National Center for Biotechnology Information, Gene ID: 10105). More than 17 cyclophilins have been identified in the human genome. They all have protein-folding and protein chaperone-like functions and have high binding

affinity to CsA [461]. The full-length CypD protein consists of 207 amino acids including a 109-amino acid cyclophilin-like domain (CLD) conserved among members of the cyclophilin family [462]. The inherent peptidyl-prolyl cis-trans isomerase (PPIase) activity, imparted by the CLD, is essential for the immunosuppressive effects of CsA and CypD-dependent mPTP-induced necrotic cell death [432, 462]. It has been shown that 1-29 residues in the N-terminal of CypD formed the mitochondrial targeting sequence [463, 464]. Immunoblotting analyses of cellular subfractions using a CypD-specific antibody detected two isoforms: a full-length CypD with a molecular mass of 22 kDa in the cytosol and a protein of 18 kDa in the mitochondria [465]. Using [^{35}S]-labeled CypD, Johnson et al. reported that the 22-kDa CypD was imported into mitochondria and localized to mitochondrial matrix [463, 464]. Thus it has been proposed that the truncated form of CypD (18 kDa) results from post-translational processing and cleavage of the N-terminal targeting sequence of the cytosolic form (22 kDa) [463]. More recently, the crystal structure of human CypD in complex with CsA was defined. It was found that human CypD consists of eight β-strands, two α-helices, and one 3_{10} helix. Intriguingly, the binding sites for CsA are well conserved in all human cyclophilins [466].

Physiological functions of CypD and CypD-mediated mPT

Studies using CypD null (Ppif $^{-/-}$) mice provide solid evidence for a central role of CypD in necrotic cell death [431, 432, 458]. It has been shown that CypD-deficient cells are highly resistant to cell death induced by hydrogen peroxide-mediated oxidative stress and Ca^{2+} overload, whereas the deficient cells display similar susceptibility as wild-type cells to cell death induced by classical apoptotic stimuli such as staurosporine and tumor necrosis factor-alpha (TNF-α). These findings suggest that CypD is essential for some

forms of necrotic cell death, but are not required for apoptotic cell death.

Apart from regulating necrotic cell death, CypD and CypD-mediated mPT have been implicated in the modulation of energy homeostasis. Metabolic changes have been observed in mice lacking CypD. For instance, CypD null mice showed elevated levels of mitochondrial matrix Ca^{2+} and enhanced activities of pyruvate dehydrogenase and α-ketoglutarate dehydrogenase, suggesting altered capacity of tricarboxylic acid (TCA) cycle [467]. Similarly, a proteomics study in the heart of CypD null mice indicates changes in branched chain amino acid metabolism, pyruvate metabolism and the TCA cycle [468]. Moreover, metabolic profiling of the CypD-deficient mouse embryonic fibroblasts revealed enhanced glycolysis with transcriptional upregulation of genes involved in glucose metabolism [469]. Further, primary hepatocytes isolated from mice lacking CypD exhibited heightened glucose consumption and ATP production [469]. It was suggested that the metabolic reprogramming and improved glucose tolerance due to CypD deficiency protect mice against high-fat-diet-induced liver damage [469]. Taken together, these findings strongly support a crucial role of CypD in cellular metabolism. However, questions like how CypD-mediated mPT modulates energy homeostasis and whether the mPT-independent mechanism is involved remain to be addressed.

In addition to energy production, mitochondria also play a major role in regulating cellular Ca^{2+} homeostasis. It has been hypothesized that the transient opening of the Ca^{2+}-dependent mPTP may provide mitochondria with a fast Ca^{2+} release channel, therefore preventing Ca^{2+} overload [470]. In support of this hypothesis, Altschuld et al. observed that CsA, which desensitized the mPTP, inhibited mitochondrial Ca^{2+} efflux in isolated adult rat cardiomyocytes [471]. The hypothesis was refined by a model stating that Ca^{2+}

fluxes generated by mitochondria during Ca^{2+} -induced release of Ca^{2+} was dependent on the transitory opening of the mPTP operating in a low-conductance mode [472-474]. Consistent with the proposed homeostatic function of the mPTP as a Ca^{2+} release channel, genetic ablation of CypD resulted in the accumulation of Ca^{2+} in the mitochondrial matrix and CsA-treated cardiomyocytes showed a significantly greater mitochondrial Ca^{2+} transient and prolonged time of decay after pacing [467]. Additionally, it was found that asynchronous transient mPTP openings allow membrane depolarization to extrude Ca^{2+} and then rapidly repolarization after pore closure [475]. In addition to cardiomyocytes, a similar role of CypD-mediated mPT in maintaining Ca^{2+} homeostasis was observed in cortical neurons from adult mice [476]. Collectively, these findings suggest CypD-mediated mPT is implicated in the physiological regulation of Ca^{2+} homeostasis by a transient Ca^{2+} release mechanism.

CypD and CypD-mediated mPT in AD

Given that oxidative stress, mitochondrial dysfunction and neuronal loss are common features of neurodegenerative disorders, it is not surprising that mPTP opening is implicated in the pathogenesis and progression of a vast variety of neurodegenerative disorders such as multiple sclerosis (MS) [477], amyotrophic lateral sclerosis (ALS) [459, 478], Parkinson's disease (PD) [479, 480], Huntington's disease (HD) [481], and AD [58].

Amyloid beta (Aβ), a major component of amyloid plaques, has been shown to directly perturb mPTP function in brain mitochondria. Aβ treatment significantly decreased mitochondrial membrane potential, reduced Ca^{2+} accumulation, induced mitochondrial swelling, the subsequent release of cytochrome c and apoptosis [58, 482, 483]. The

indirect effects of Aβ on mPTP function include dysregulated Ca^{2+} homeostasis and oxidative stress. Numerous studies have shown that Aβ peptides increase intracellular Ca^{2+} levels [484-486] and the production of oxygen free radicals [483, 487, 488] in cultured primary neurons. Since both conditions favor the opening of mPTP, Aβ-induced Ca^{2+} overload and ROS generation may contribute to mPTP formation, mitochondrial dysfunction and neuronal loss. The target of Aβ in the mPTP was later identified as CypD. Co-immunoprecipitation analyses demonstrated that CypD-Aβ complexes exist in the cortical mitochondria from AD patients and transgenic mice overexpressing a mutant form of the human amyloid precursor protein (mAPP), as well as isolated brain mitochondria treated with Aβ [58]. The interaction of CypD with Aβ was also confirmed using surface plasmon resonance (SPR) spectroscopy. Recombinant human CypD protein was found to bind to different species of Aβ in a dose-dependent manner [58]. Given that CypD expression is enhanced in the AD brain [58], and mPTP is implicated in mitochondrial dysfunction and neuronal degeneration, CypD-mediated mPT may represent a potential therapeutic target for AD. Indeed, blockage of mPTP by genetic ablation or pharmacological inhibition of CypD protected neurons against Aβ-induced damage. Cortical mitochondria lacking CypD were resistant to mitochondrial swelling induced by Aβ [58]. CypD-deficient neurons were protected from Aβ-induced oxidative stress and synaptic loss [58, 489]. Similarly, CsA treatment prevented mitochondrial swelling, attenuated ROS production and inhibited apoptosis induced by Aβ. In line with the *in vitro* findings, mice lacking CypD showed preserved inner mitochondrial membrane potential, reduced ROS generation, attenuated mitochondrial respiratory dysfunction and neuronal death in the presence of mAPP. These data suggest that the

absence of CypD may confer neuroprotection by abolishing Aβ-induced mPTP opening [58]. Intriguingly, genetic deletion of CypD resulted in markedly improved synaptic function and spatial learning memory in mAPP mice, likely due to the attenuated oxidative stress and amelioration in mitochondrial dysfunction [58]. Further, the above-mentioned neuroprotective effects associated with CypD deficiency were preserved in old mAPP mice, suggesting that the absence of CypD confers a persistent protection against Aβ toxicity during aging [490]. In addition to the perturbation on mitochondrial function, Aβ also induces defects in mitochondrial motility [70, 491]. Wild-type hippocampal neurons exposed to oligomeric Aβ showed decreased mitochondrial density and reduced number and velocity of mitochondrial movement in the axons. Since proper mitochondrial distribution and efficient mitochondrial transport are essential for maintenance of synaptic functions, perturbations in axonal mitochondrial trafficking may result in a loss of synaptic integrity [70]. Importantly, Aβ-induced defects in axonal mitochondrial movement and synaptic dysfunction were greatly attenuated in neurons lacking CypD [491]. Together, these results provide compelling evidence that interventions of CypD-mediated mPT could counteract mitochondrial dysfunction, synaptic impairment and cognitive deficits induced by Aβ.

CypD and CypD-mediated mPT in diabetes

Emerging evidence implicates CypD-mediated mPT in the pathogenesis and complications of diabetes. Fujimoto et al. reported that blocking mPTP opening with CypD inhibitor CsA or genetic deletion of CypD restored IMM electrochemical gradient and reduced β-cell death in a diabetic mouse model induced by pancreatic duodenal homeobox gene-1(Pdx1) deficiency [492]. Notably, in Pdx1-deficient mice maintained on

a high-fat diet, genetic ablation of CypD resulted in a lower fasting blood glucose and markedly increased insulin levels at baseline and in response to glucose challenge, suggesting that CypD deficiency rescues the characteristic diabetic phenotype of Pdx1 insufficiency [492]. In adipose tissue, CypD-mediated mPTP opening was found to contribute to high-fat-diet-induced cell death [493]. More recently, studies on diabetic skeletal muscles suggest that CypD-mediated mPTP opening may serve as a link between mitochondrial dysfunction and insulin resistance [494]. Specifically, CypD-deficient mice were protected from high-fat-diet-induced glucose intolerance likely due to the elevated glucose uptake by skeletal muscles. Mitochondria isolated from CypD null muscle were resistant to diet-induced swelling and had improved Ca^{2+} retention capacity [494]. Importantly, in cell culture models of insulin resistance, treatment with CsA prevented insulin resistance, as evidenced by enhanced insulin-stimulated translocation of GLUT4. It was suggested that improved insulin sensitivity was attributed to the increase in mitochondrial Ca^{2+} retention and not alterations in insulin signaling or mitochondrial bioenergetics [494]. Together, these findings indicate CypD-mediated mPT is implicated in diabetes, particularly in impaired insulin secretion and insulin resistance. Whether CypD-mediated mPTP opening contributes to diabetes-associated mitochondrial dysfunction in the brain, synaptic impairment and cognitive dysfunction remain to be determined.

2.2.5 CypD inhibitors

In preclinical studies, CsA is the most commonly used pharmacological inhibitor for CypD-mediated mPT. Studies have shown that administration of CsA protects against mPTP-induced mitochondrial perturbations in several animal models of neurodegenerative diseases [495-498]. CsA was initially discovered as an agent for immunosuppression following organ transplants. It acts by inhibiting calcineurin, a calcium/calmodulin-dependent protein phosphatase, thereby preventing the dephosphorylation of nuclear factors of activated T-lymphocytes, resulting in the suppression of T-cell activation and overall immune response [499]. In addition to its immunosuppressive effect, CsA is associated with severe toxic effects in liver and kidney, which significantly limits its clinical applications. Several non-immunosuppressive CsA derivatives such as N-Me-Val-4-cyclosporin A and N-Me-Ala-6-cyclosporin A, retain high potency in inhibiting PPIase activity of CypD, thus protect cells against mPTP opening and apoptosis [430, 500]. However, the efficacy and potential cytotoxic effects of these CsA analogs have not been evaluated *in vivo*. Sanglifehrin A (SfA), a novel immunophilin-binding agent was found to bind to CypD but at a different site from CsA [501]. SfA showed protection against ischemia-reperfusion-induced necrotic damage in isolated rat hearts, presumably through inhibition of PPIase activity of CypD, the conformational change of ANT, and subsequent mPTP formation [501]. Although SfA does not inhibit calcineurin, it exerts its immunosuppressive action through a distinct mechanism which is not well elucidated [502]. Another novel derivative of CsA, FR901459 exhibits greater potency than CsA in suppressing Ca^{2+}-induced mitochondrial swelling and protecting against transient cerebral ischemia-induced neuronal cell death

[503]. Interestingly, it was thought that the immunosuppressive properties of FR901459, rather than its inhibitory effect on mPTP opening, plays a more important role in attenuating brain damage. More recently, antamanide (AA), a monocyclic decapeptide isolated from the poisonous mushroom *Amanita phalloides*, was found to prevent mPTP opening by targeting the PPIase of CypD, thus protecting cells against apoptosis caused by mPT inducers [504]. Although *in vitro* studies demonstrated the great potency of these inhibitors in the blockage of CypD-mediated mPT, the potential neuroprotective effects of these CypD inhibitors have not been evaluated *in vivo*. Additionally, these CypD inhibitors are large molecules which may significantly limit their brain uptake across the blood-brain barrier. Further, the immunosuppressive properties of some inhibitors may cause a number of side effects and tissue injuries. Therefore, a non-immunosuppressive agent which targets CypD in the brain may be an ideal drug candidate to combat mitochondrial dysfunction and cognitive impairment associated with diabetes.

The goals of the second chapter of my dissertation were to investigate the potential role of CypD in diabetes-related mitochondrial dysfunction and cognitive impairment. Using a mouse model of type 1 diabetes, we evaluated the consequence of changes in CypD expression in brain mitochondrial function and cognitive abilities. Results from the current study provide new insights into the mechanisms underlying mitochondrial malfunction relevant to the pathogenesis of diabetes-associated cognitive deficits.

2.3 Materials and Methods

2.3.1 Animals

Animal studies have been approved by the Institutional Animal Care and Use Committee (IACUC) of the University of Kansas and followed National Institutes of Health guidelines for the care and use of laboratory animals. Cyclophilin D homozygous null mice ($Ppif^{-/-}$) were generous gifts from Dr. Jeffery Molkentin [432]. These mice were backcrossed to C57BL6/J mice at least 10 times before the experiments to eliminate the potential effects of genetic background. For the second study, we used transgenic mice overexpressing a mutant form of the human amyloid precursor protein (mAPP) bearing both the Swedish (K670N/M671L) and the Indiana (V717F) mutations driven by the PDGF-β promoter (J-20 line). Only male mice were used in the current studies as female mice are relatively unresponsive to streptozotocin.

2.3.2 Induction of Type 1 Diabetes

Type 1 diabetes was induced by intraperitoneal administration of streptozotocin (STZ, Sigma, St. Louis, MO, USA). Specifically, 3-month-old male mice were treated with STZ (freshly prepared in 100 mM sterile citric acid, pH 4.5) at a dosage of 50 mg/kg for 5 consecutive days. Control animals received injections of citrate buffer. Diabetes was monitored by measurements of blood glucose at 2 weeks, 1 month and 2 months after STZ injection. Blood glucose levels were determined using a glucose meter and blood samples obtained by tail snipping. Hyperglycemia was defined as fasting glucose concentration above 250 mg/dL. 2 months after diabetes induction, Morris water maze behavior task was performed for 7 days and then the mice were euthanized and processed

for brain mitochondria isolation, mitochondrial respiratory chain activity and immunoblot analysis as described below.

2.3.3 Morris Water Maze task

Mice were tested in the Morris Water Maze task to assess spatial learning and memory as described previously [505]. The apparatus is composed of a pool, which is 150 cm in diameter and 50 cm in height, a platform is placed in one of the fixed quadrants for mice to escape, and a camera above the center of the pool captures images of the swimming mice. The tank is filled with water kept at 23 ± 2 °C during the trials. The platform is hidden 0.5-1 cm below the water surface and the white paint was added to the water to make the platform less visible. In spatial acquisition session, mice were trained for 6 consecutive days with 4 trials for each mouse per day. A trial started with releasing one mouse facing the pool wall and the mouse allowed to swim freely and search for the escape platform. If the mouse cannot reach the platform within 60 seconds, it was guided to the platform and allowed to stay on for 15 seconds before the next trial. After all trials, mice were dried with paper towels and returned to their cages. The escape latency was analyzed by the behavior software system (HVS water 2020). On the 7th day, a probe trial was performed to assess the reference memory of mice. The platform was removed from the pool and the mice were allowed to swim freely for 60 seconds. The location of mice were recorded and data were analyzed by HVS water 2020.

2.3.4 Mitochondrial Isolation

Mitochondrial fractions prepared from brain tissues of mice as described previously [58].

Briefly, cerebral cortex or hippocampus was dissected and homogenized in cold mitochondrial isolation buffer (225 mM D-mannitol, 75 mM sucrose, 2 mM K_2HPO_4, pH 7.2). Brain homogenates were centrifuged at 1,300 g for 5 min at 4 °C. The supernatant was centrifuged at 34,000g for 10 min after layering on 15% Percoll. The pellet was resuspended in 20 ml mitochondrial isolation buffer containing 0.01% digitonin, incubated on ice for 5 min, and centrifuged at 8,000 g for 10 min. After two washes with mitochondrial isolation buffer (1.5 mL each), final mitochondrial pellets were collected.

2.3.5 Mitochondrial Electron Transport Chain Complex Activities

NADH dehydrogenase (Complex I) Enzyme activity of NADH dehydrogenase was measured by the decrease of absorbance at 340 nm following the oxidation of NADH. Mitochondrial fractions containing 30 μg of protein were added to the reaction solution containing 50 mM KCl, 30 mM Tris-HCl pH 7.4, 6 mM EDTA, 5 mM $MgCl_2$, 2 mM KCN, 0.13 mM NADH, 2 μg/mL antimycin A. The reaction was initiated by addition of CoQ1 and the enzyme activity was measured by the changes in absorbance at 340 nm for a total of 360 seconds with 20 seconds interval on Shimadzu (Kyoto, Japan) UV1200 spectrophotometer. To exclude the rotenone nonspecific activity, 2 μg/mL rotenone was added at 180 seconds and NADH dehydrogenase activity was calculated by subtracting the reaction rate in the presence of rotenone from that in the absence of rotenone. An extinction coefficient of 6.2 mM^{-1} cm^{-1} for NADH was used for the calculation. Complex I specific activity was expressed as micromoles of NADH oxidized per min per mg protein.

Succinate dehydrogenase (Complex II) Enzyme activity of succinate dehydrogenase was

measured by the decrease in absorbance at 600 nm due to the reduction of dichlorophenol indophenols (DCPIP). Briefly, 40 μg of cortical mitochondria were incubated 1 mL reaction buffer (50 mM KCl, 30 mM Tris-HCl pH 7.4, 6 mM EDTA, 5 mM $MgCl_2$, 20 mM sodium succinate) and equilibrated in a water bath at 37°C for 10 minutes. The reaction was started by adding (2 mM KCN, 2 μg/mL rotenone, 2 μg/mL antimycin A) containing 50 μM DCPIP. Absorbance at 600 nm was recorded for 180 seconds with 20 seconds interval on UV1200 spectrophotometer. Then CoQ2 was added to the reaction mixture and changes in absorbance at 600 nm was measured for an additional 180s with 20 seconds interval. Succinate dehydrogenase activity was calculated by the difference in the reaction rate before and after the addition of CoQ2. Complex II specific activity was expressed as micromoles of DCPIP oxidized per min per mg protein using an extinction coefficient of 19.1 mM^{-1} cm^{-1}.

Ubiquinol-cytochrome c reductase (Complex III) Enzyme activity of ubiquinol-cytochrome c reductase was measured by the increase in absorbance at 550 nm due to the reduction of cytochrome c. In brief, CoQ2 was added into the reaction solution containing 50 mM KCl, 30 mM Tris-HCl pH 7.4, 6 mM EDTA, 5 mM $MgCl_2$, 2mM KCN, 15 μM oxidized cytochrome c, 2 μg/mL rotenone and 0.6 mM n-Dodecyl-β-d-maltoside, to a final concentration of 32.5 μM. Baseline was measured for 1 min with 20 seconds interval on Shimadzu UV1200 spectrophotometer. 80 μg of protein was added to the reaction mixture and enzyme-catalyzed reduction of cytochrome c was measured for 180 seconds. Cytochrome c reductase activity was calculated by subtracting the baseline rate from the reaction rate after CoQ2 addition. Complex III specific activity was expressed as micromoles of cytochrome c reduced per min per mg protein using an

extinction coefficient of 18.7 mM^{-1} cm^{-1}.

Cytochrome c oxidase (Complex IV) Enzymatic activity of cytochrome c oxidase was measured in cortical mitochondria as previously described [58, 506]. The mitochondrial fraction containing 30 μg of protein and enzyme dilution buffer (10 mM Tris-HCl, pH 7.0) were added into 950 μL of assay buffer (10 mM Tris-HCl and 120 mM KCl). The reaction was initiated by the addition of 50 μL ferrocytochrome c into the cuvette. The changes in absorbance at 550 nm was recorded for 60 seconds using a kinetic program with 3 seconds delay and 10 seconds interval on UV1200 spectrophotometer. Complex IV activity was expressed as micromoles of cytochrome c oxidized per min per mg protein using an extinction coefficient of 21.2 mM^{-1} cm^{-1}.

2.3.6 Immunoblotting Analysis

Brain tissues from transgenic mice were homogenized in cell lysis buffer (Cell signaling, Danvers, MA, USA) supplemented with protease inhibitor cocktail (Calbiochem, San Diego, CA, USA). Protein samples were then separated on 10% SDS-PAGE gels and transferred to 0.45 μm nitrocellulose membranes (Amersham, Pittsburgh, PA, USA), followed by blocking with 5% nonfat dry milk (Santa Cruz Biotechnology, Dallas, TX, USA) in TBST buffer (20 mm Tris-HCl, 150 mm sodium chloride, 0.1% Tween-20) for 1 hour at room temperature. Membranes were then incubated and gently shaken overnight at 4°C with primary antibodies. The following primary antibodies were used: mouse anti-CypD (1:4000, Abcam, Cambridge, UK), rabbit anti-Hsp60 (1:6000, Enzo Life Sciences, Farmingdale, NY, USA), mouse anti-β-actin (1:8000, Sigma, St. Louis, MO, USA), rabbit anti-tubulin (1:10000, Sigma, St. Louis, MO, USA). The binding sites of primary

antibody were visualized with horseradish peroxidase-conjugated anti-rabbit IgG antibody (1:5000, Life Technology) or anti-mouse IgG antibody (1:5000, Life Technology) followed by addition of super signal west pico chemiluminescent substrate (Thermo Scientific) and a FluorChem HD2 image system (ProteinSimple, San Jose, CA, USA). The densitometry of the immunoblotting bands was quantified using NIH Image J software (National Institutes of Health, Bethesda, MD, USA).

2.3.7 Statistical Analysis

Data are expressed as mean ± standard error of the mean (SEM). All statistical analyses were performed using StatView (SAS Institute). Student's t-test and one-way ANOVA with Fisher's protected least significant difference post hoc test were used for comparisons of mean values of the experimental groups. $p<0.05$ was considered significant and the degree of significance was represented by the number of asterisks.

2.4 Results

2.4.1 Cyclophilin D deficiency ameliorated diabetes-associated mitochondrial dysfunction and cognitive impairment

2.4.1.1 Increased expression of cyclophilin D in STZ-induced diabetic mice

To explore the potential role of cyclophilin D (CypD) in diabetes-related brain dysfunction, we first examined the expression of CypD in the brains of STZ-injected mice. Interestingly, CypD protein expression was significantly elevated in both hippocampus and cortex of STZ-treated mice compared with vehicle-treated mice (Fig 2.4.1.1A). Because CypD is localized to the mitochondrial matrix, we also evaluated CypD expression in cortical mitochondria isolated from the diabetic mice. Immunoblot analysis indicated that CypD expression was increased by 1.6 fold in brain mitochondria from diabetic mice compared to non-diabetic mice (Fig.2.4.1.1B). The expression of Hsp60, serving as a loading control and was comparable between the two groups.

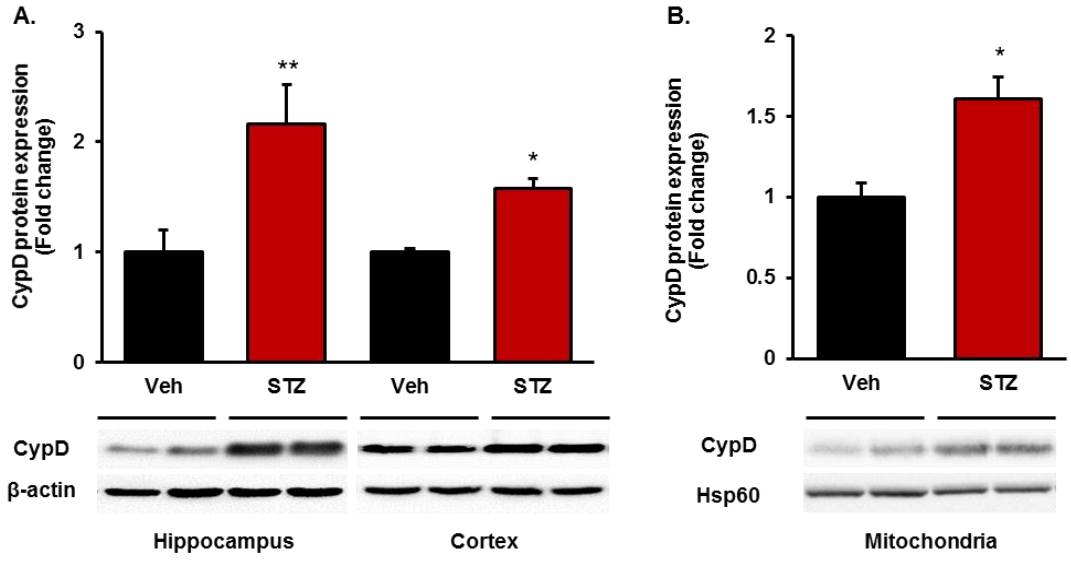

Figure 2.4.1.1

Fig. 2.4.1.1 Enhanced CypD expression levels in the brains of STZ-induced diabetic mice. A) Densitometric analysis of CypD immunoreactive bands in tissue homogenates of hippocampus and cortex from vehicle- and STZ-treated mice. Data were normalized to β-actin. B) CypD expression level in cortical mitochondria isolated from vehicle- and STZ-treated mice. Hsp60 was used as a mitochondrial marker. n= 3-5 mice per group, *p<0.05, **p<0.01 vs Veh group.

2.4.1.2 Experimental induction of type 1 diabetes in transgenic cyclophilin D null mice

Given that CypD expression was elevated in diabetic brain and CypD-mediated mPT has been implicated in diabetes-induced mitochondrial dysfunction, we sought to determine whether CypD deficiency could ameliorate diabetes-associated deficits in the brain. 3-month-old nontransgenic mice (nonTg) and cyclophilin D null mice ($Ppif^{-/-}$) were subjected to intraperitoneal injection of streptozotocin (STZ) for five consecutive days. Blood glucose concentration was determined to validate the establishment of diabetes. Compared with vehicle-injected groups, STZ injection resulted in significantly enhanced blood glucose levels in both nonTg and $Ppif^{-/-}$ mice 2 weeks after initiation of STZ injection (387.7 ± 17.8 mg/dL in nonTg STZ and 451.9 ± 15.6 mg/dL in $Ppif^{-/-}$ STZ mice, Fig. 2.4.1.2A). Blood glucose levels remained significantly high in the diabetic mice two months post injection (503.9 ± 38.0 mg/dL in nonTg STZ and 565.9 ± 15.4 mg/dL in $Ppif^{-/-}$ STZ mice, Fig.2.4.1.2A). Progressive body weight loss is a typical feature of type 1 diabetes. Indeed, mice injected with vehicle displayed positive changes in body weight (4.2 ± 0.6 g in nonTg Veh and 2.9 ± 0.5 g in $Ppif^{-/-}$ Veh, Fig2.4.1.2B). In contrast, significant body weight loss was observed in nonTg mice injected with STZ (-3.7 ± 0.5 g). STZ also induced body weight loss in CypD-deficient mice, albeit at a lower

magnitude (-0.2 ± 0.3 g). Together, these results indicate that both nonTg and CypD-null mice developed type 1 diabetes as early as two weeks after STZ treatment and was sustained for more than 2 months after induction.

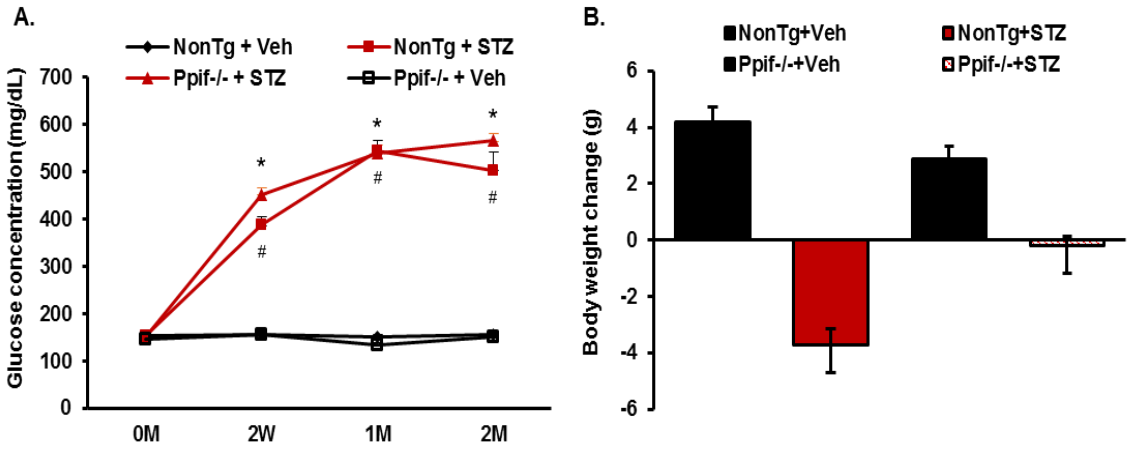

Figure 2.4.1.2

Fig. 2.4.1.2 Induction of type 1 diabetes in nonTg and CypD null mice. A) Fasting blood glucose levels measured before STZ injection, 2 weeks, 1 month and 2 months after STZ treatment were shown for the indicated groups. B) Mean body weight change were assessed before and 2 months after STZ treatment. n=7-12 per group. *p<0.05 vs nonTg Veh group. #p<0.05 vs mAPP Veh group.

2.4.1.3 Cyclophilin D deficiency attenuated diabetes-induced mitochondrial dysfunction

Given that CypD is a key regulatory component of mitochondrial permeability transition pore (mPTP) and the opening of mPTP results in mitochondrial dysfunction, we investigated whether genetic deletion of CypD could rescue diabetes-induced mitochondrial dysfunction. We evaluated mitochondrial function by measuring mitochondrial electron transport chain (ETC) complexes activities in both vehicle- and STZ- treated mice. No significant difference was detected in the enzymatic activity of NADH dehydrogenase (complex I), ubiquinol-cytochrome c reductase (complex III), and cytochrome c oxidase (complex IV) between nonTg mice treated with vehicle and those with STZ (Fig. 2.4.1.3B-D). Succinate dehydrogenase (complex II) activity was significantly decreased in the brain mitochondria from STZ-treated nonTg mice compared to vehicle-treated nonTg mice (FC = 0.78, p = 0.041) (Fig.2.4.1.3A). Notably, complex II activity was markedly improved in the CypD null mice injected with STZ (FC = 1.27, p = 0.038), suggesting that CypD deficiency attenuated mitochondrial respiratory dysfunction induced by diabetes.

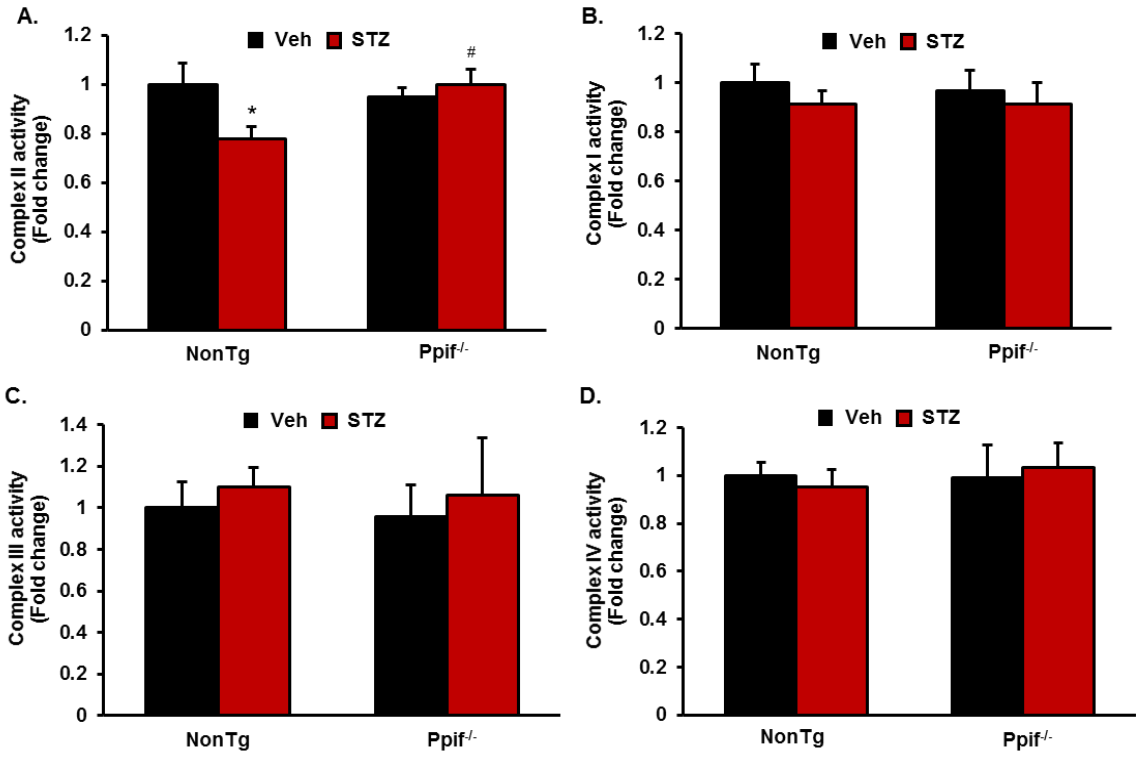

Figure 2.4.1.3

Fig. 2.4.1.3 CypD deficiency rescued STZ-induced defects in mitochondrial respiratory function. A-D) Enzymatic activities of complex I-IV were determined in the mitochondrial fractions prepared from cortex of vehicle- and STZ- treated mice. Diabetic nonTg mice were not different from their non-diabetic littermates in complex I (B), complex III (C) or complex IV (D). Complex II activity (A) was reduced in nonTg STZ group; CypD deficiency restored complex II activity. Results were compared using one-way ANOVA with Fisher's Least Significant Difference post hoc test. n= 6-9 per group. *p<0.05 vs nonTg Veh group. #p<0.05 vs nonTg STZ group.

2.4.1.4 Cyclophilin D deficiency ameliorated diabetes-induced cognitive impairment

As mitochondrial function is closely associated with synaptic plasticity and cognitive function, we next examined the effect of CypD deficiency on diabetes-associated cognitive dysfunction. Morris Water Maze task (MWM) was performed to assess spatial learning and memory in nonTg and Ppif$^{-/-}$ mice treated with vehicle or STZ. During the

acquisition phase, vehicle-treated nonTg mice showed intact learning abilities as demonstrated by a day-to-day decrease in escape latency. STZ treatment resulted in an impairment in spatial learning as nonTg mice injected with STZ spent significantly longer time searching for the platform (nonTg Veh = 21.8 ± 2.7s, nonTg STZ = ± 2.6s on day 6) (Fig. 2.4.1.4A). For the probe trials, STZ-treated nonTg mice spent significantly less time in the target quadrant and achieved fewer times of platform crossings, suggesting diabetes-induced deficits in reference memory (Fig. 2.4.1.4C-D). Importantly, STZ-induced defects in learning and memory were greatly attenuated by genetic deletion of CypD, as evidenced by the reduction in escape latency ($Ppif^{-/-}$ STZ = 28.5 ± 2.9 s, nonTg STZ = 44.8 ± 2.6 s), increased target quadrant occupation ($Ppif^{-/-}$ STZ = 41.1 ±1.1%, nonTg STZ = 23.1 ± 3.3%), and enhanced number of platform crossings ($Ppif^{-/-}$ STZ = 4 ± 0.7, nonTg STZ = 1.2 ± 0.3) (Fig. 2.4.1.4A, C-D). In vehicle-treated groups, CypD null mice did not differ from their nonTg littermates in the MWM performance (Fig. 2.4.1.3A, C-D), suggesting CypD deficiency has no effect on hippocampus-dependent spatial learning and memory. The average swimming speed was comparable among the four groups of mice, suggesting that the differences observed in MWM task were independent of locomotor activity (Fig 2.4.1.4B).

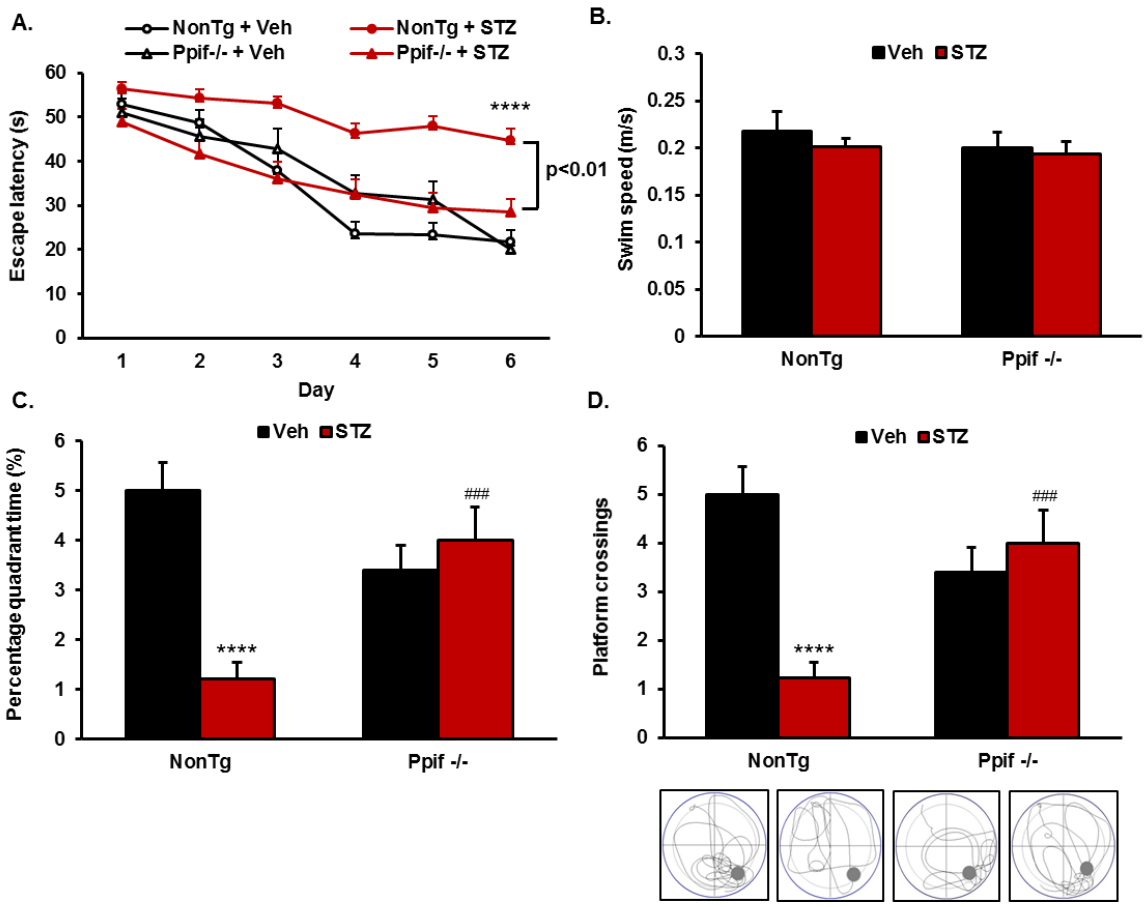

Figure 2.4.1.4

Fig. 2.4.1.4 CypD deficiency ameliorated STZ-induced deficits in spatial learning and memory. A) Mean latency to escape to the hidden platform during each day of acquisition session. B) Average swimming speed were shown for the indicated groups. C) Percentage of time spent in the quadrant where the hidden platform locates. D) The mean number of mice crossing the target zone in probe trials. Representative images of swimming paths for groups indicated were shown in the bottom. Results were compared using one-way ANOVA with Fisher's Least Significant Difference test. n= 5-9 per group. ****p<0.0001 vs nonTg Veh group. ###p<0.001 vs nonTg STZ group.

2.4.2 Synergistic exacerbation of mitochondrial dysfunction and cognitive impairment in an AD mouse model with diabetes

2.4.2.1 Experimental induction of type 1 diabetes in mAPP mice

nonTg and mAPP mice were injected with STZ for 5 successive days to induce type 1 diabetes. Hyperglycemia was confirmed in STZ-treated groups two weeks after STZ injection and sustained more than 2 months (Fig. 2.4.2.1A). Significant body weight loss was observed in STZ-induced diabetic mice but not in vehicle-treated mice (Fig.2.4.2.1B). Collectively, these results indicate the successful induction of type 1 diabetes in both mAPP and nonTg mice.

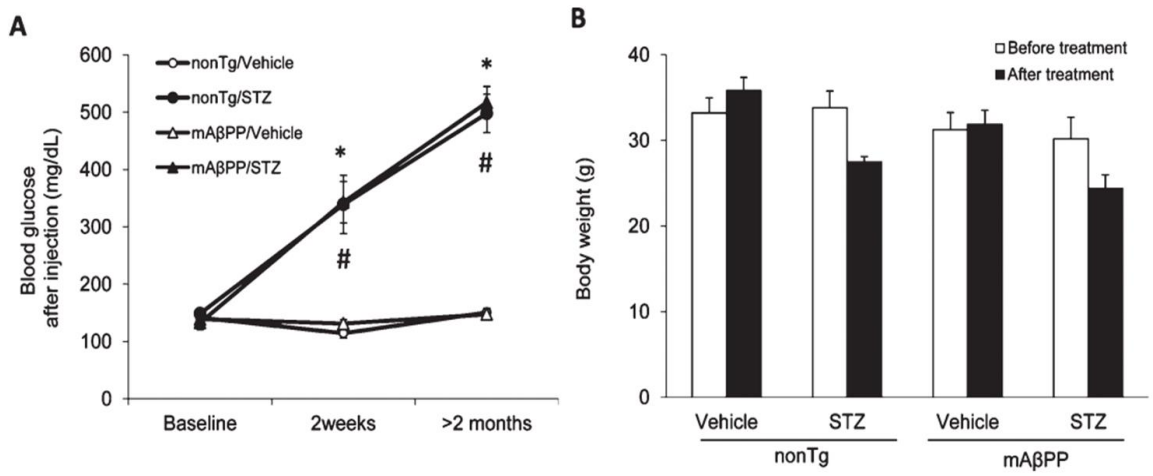

Figure 2.4.2.1

Fig. 2.4.2.1 Induction of type 1 diabetes in nonTg and mAPP mice. A) Fasting blood glucose levels were measured before STZ injection (baseline), 2 weeks and 2 months after STZ treatment for the indicated groups. B) Mean body weight changes were assessed before and 2 months after STZ treatment. n=5-10 per group. *p <0.01 nonTg/Vehicle vs nonTg/STZ, # p <0.01 mAβPP/Vehicle vs mAβPP/STZ. Adapted from Wang, Yongfu et al. (2015) *JAD* 43.2

2.4.2.2 Further enhancement of Cyclophilin D expression in diabetic mAPP mice

Previous studies indicate that CypD expression is markedly elevated in the brains of mAPP mice at 6-12 months compared to age-matched nonTg mice. The diabetic brains also show increased CypD expression when compared to non-diabetic brains (Fig.2.4.1.1). To determine the effects of diabetes and AD on CypD expression, we examined CypD protein levels in the brains of diabetic mAPP mice. Consistent with previous findings, CypD expression was significantly higher in the hippocampus of vehicle-treated mAPP mice and STZ-treated nonTg mice when compared to vehicle-treated nonTg mice. Intriguingly, CypD expression was further enhanced in diabetic mAPP mice, suggesting that diabetes and AD may have synergistic effects on the regulation of CypD expression (Fig. 2.4.2.2).

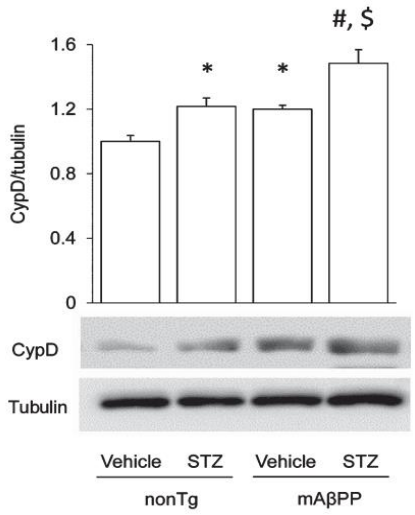

Fig. 2.4.2.2 Expression of CypD was further enhanced in the brains of diabetic mAPP mice. CypD protein expression levels were determined in the hippocampal homogenates from mice in the indicated groups. Densitometry of CypD immunoreactive bands were shown on the upper panel. Tubulin was used as loading control. Representative immunoblots were shown on the bottom. n= 5 per group. *p<0.05 vs nonTg Vehicle group, #p<0.05 vs nonTg STZ group, $p<0.01 vs mAPP Vehicle group. Adapted from Wang, Yongfu et al. (2015) *JAD* 43.2

2.4.2.3 Exacerbation of mitochondrial dysfunction in diabetic mAPP mice

Impaired mitochondrial function has been implicated in the pathogenesis and progression of AD and diabetes. To determine the effects of AD and diabetes on mitochondrial function, we measured mitochondrial ETC complexes activities in brain mitochondria of mice in the designated groups. Consistent with our previous findings, STZ-treated nonTg mice exhibited significantly lower complex II activity than vehicle-treated nonTg mice (FC = 0.62, p = 0.005). However, the diabetic mice did not differ from their vehicle-treated counterparts in complex I and IV activity (Fig. 2.4.2.3). However, the activity of both complexes were significantly decreased in STZ-treated mAPP mice when compared to STZ-treated nonTg mice (FC = 0.42, p = 0.042 for complex I; FC = 0.79, p = 0.026 for complex IV). These results suggest that diabetes-induced deficits in mitochondrial respiration function were exacerbated in the presence of Aβ.

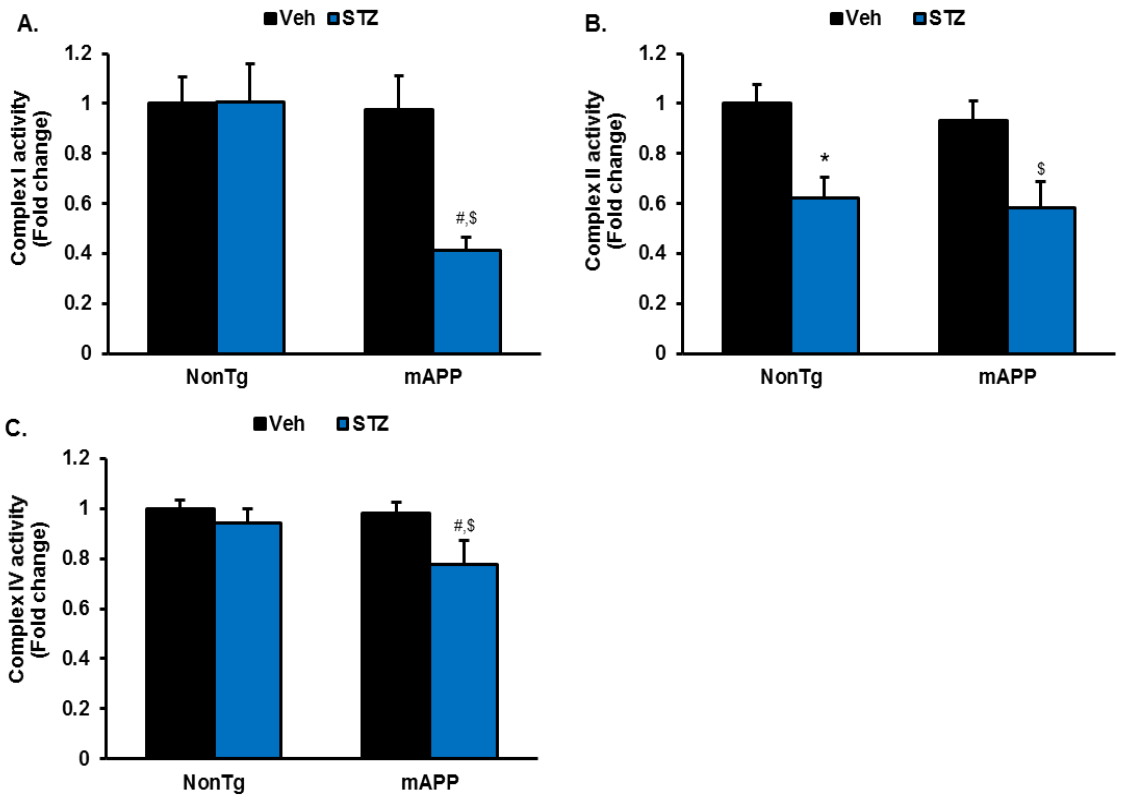

Figure 2.4.2.3

Fig. 2.4.2.3 Diabetes-induced defects in mitochondrial respiratory function were exacerbated in diabetic mAPP mice. A-C) Complex I, II and IV activities were determined in the cortical mitochondria for the indicated groups. STZ-treated nonTg mice were not different from their vehicle-treated counterparts in complex I (A) or complex IV (C). Activities of both complexes were markedly reduced in the STZ-treated mAPP mice. Results were compared using one-way ANOVA with Fisher's Least Significant Difference test. n= 4-7 per group. *$p<0.05$ vs nonTg Veh group. #$p<0.05$ vs nonTg STZ group. \$$p<0.05$ vs mAPP Veh group.

2.4.2.4 Accelerated cognitive decline in diabetic mAPP mice

Hippocampus-dependent cognitive deficits were observed in STZ-induced diabetic mice (Fig. 2.4.1.4) and mAPP mice as early as 6 months old. To evaluate the synergistic effects of type 1 diabetes and AD on spatial learning and memory function, we performed MWM on mAPP mice after 2 months of diabetes induction. Vehicle-treated nonTg mice had gradually decreased escape latency over the training period, suggesting they showed some spatial learning. In comparison, STZ-treated nonTg and vehicle-treated mAPP mice displayed a significantly prolonged escape latency (nonTg STZ = 41.5 ± 3.5s, mAPP Veh = 43.9 ± 5.2s vs nonTg Veh = 19.9 ± 3.3s), indicating deficits in spatial learning. STZ-treated mAPP mice showed the worst performance as they failed to find the platform within the maximum testing time (Fig.2.4.2.4A). For the memory retention test, both diabetic nonTg mice and non-diabetic mAPP mice exhibited impaired performance compared to vehicle-treated nonTg mice, since they spent significantly less time searching in the target quadrant (nonTg STZ = 31.5 ± 1.8%, mAPP Veh = 38.0 ± 4.0% vs nonTg Veh = 57.2 ± 4.4%), and achieved fewer times of platform crossings (nonTg STZ = 2 ± 0.3, mAPP Veh = 2 ± 0.6 vs nonTg Veh = 5.4 ± 0.5) (Fig.2.4.2.4C-D). Notably, defects in reference memory were greatly exacerbated in diabetic mAPP mice. Shown in Fig 2.4.1.4 C-D, STZ-treated mAPP mice had the least percentage quadrant time (16.3 ± 1.8%) and the lowest number of target zone crossings (0.6 ± 0.2). No significant difference in the average swimming speed was observed among the groups (Fig. 2.4.2.4B). Taken together, these results indicate that diabetes-induced cognitive impairment was greatly accelerated in diabetic mAPP mice.

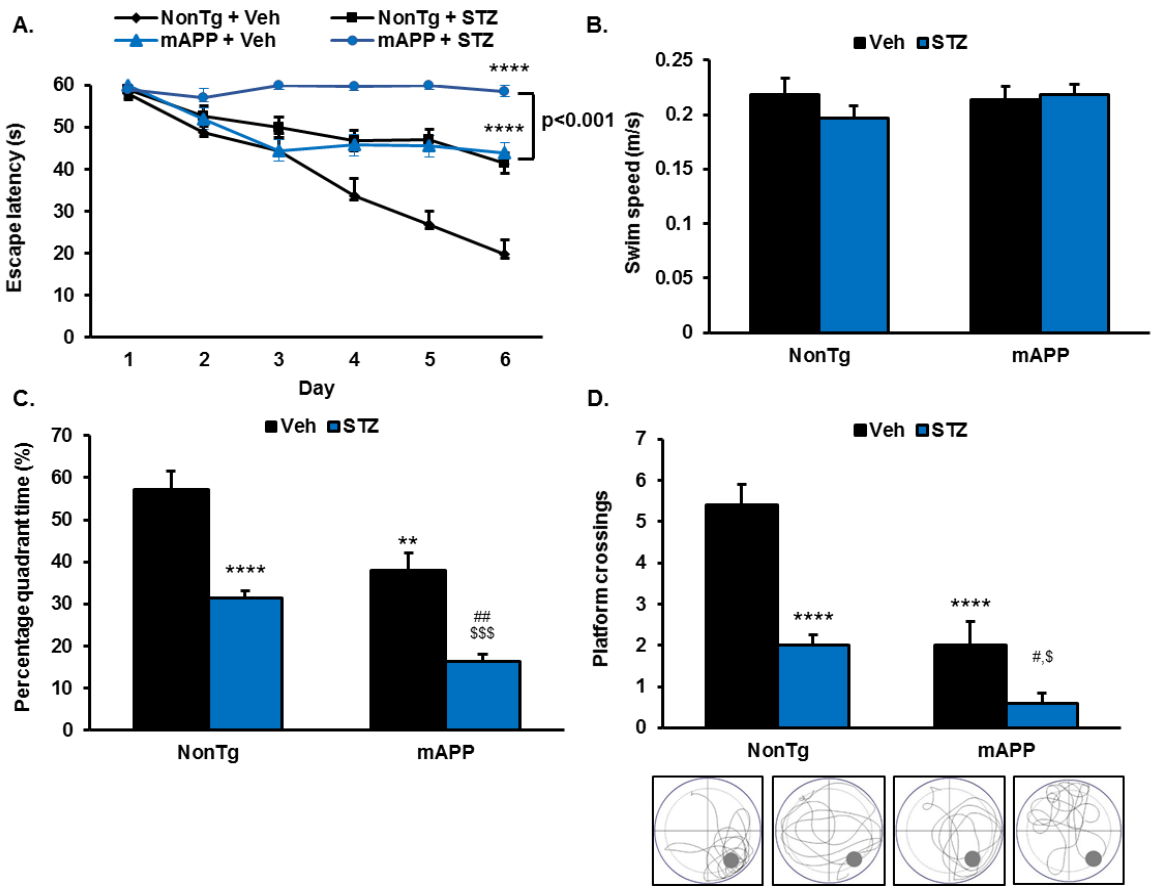

Figure 2.4.2.4

Fig. 2.4.2.4 Diabetes-associated cognitive decline was accelerated in diabetic mAPP mice. Mean escape latency to the hidden platform during 6 days of acquisition session (A), average swimming speed (B), percentage of time spent in the target quadrant (C), and the number of platform crossings (D) were shown for the indicated groups. Representative images of swimming paths for groups indicated were shown in the bottom. Results were compared using one-way ANOVA with Fisher's Least Significant Difference test. n= 4-7 per group. ****p<0.0001, **p<0.01 vs nonTg Veh group. #p<0.05, ##p<0.01 vs nonTg STZ group. $p<0.5, $$$p<0.001 vs mAPP Veh group.

2.5 Discussion

Mitochondrial dysfunction has been implicated in diabetes-associated brain damage. Compared with other cell types, neurons rely heavily on mitochondria for their functions and survival, primarily due to their exceptional cellular morphology. Proper mitochondrial distribution, efficient mitochondrial transport, normal mitochondrial dynamics and intact mitochondrial respiratory capacity are all critically important for the maintenance of synaptic function. Previously, we have shown that hyperglycemia-induced ROS generation disrupted mitochondrial dynamics, resulting in alterations in mitochondrial morphology and defects in mitochondrial respiratory function [75]. Impaired mitochondrial function was accompanied by injured synaptic plasticity [75]. Notably, restoration of mitochondrial fission/fusion balance ameliorated hyperglycemia-induced defects in mitochondrial respiratory function and synaptic plasticity, suggesting an intrinsic link between mitochondrial dysfunction and diabetes-induced cognitive impairment. In the current study, we demonstrated that CypD, a critical regulator of the mPT, plays a major role in diabetes-induced brain mitochondrial malfunction and cognitive impairment using a mouse model of type 1 diabetes.

In the present study, we observed increased CypD protein expressions in both hippocampus and cerebellar cortex of diabetic mice (Fig.2.4.1.1). Additionally, STZ-induced diabetic mice also showed deficits in synaptic plasticity [507], as reflected by the suppression of long-term potentiation (LTP), loss of synaptic integrity [507], as evidenced by reduced expression levels of postsynaptic proteins, as well as impairments in hippocampus-dependent learning and memory (Fig.2.4.1.4). It has been shown that the expression level of CypD is correlated with the susceptibility of mPTP opening.

Specifically, mitochondria with low CypD expression displayed higher calcium threshold toward mPT induction, therefore more resistance to mPTP opening [508]. In contrast, mitochondria with high CypD expression exhibited elevated sensitivity to mPTP opening [508, 509]. Therefore, diabetes-induced upregulation of CypD may enhance the probability of mPTP opening, leading to mitochondrial dysfunction, and subsequent synaptic injury and cognitive impairment. In support of this notion, genetic deletion of CypD significantly improved mitochondrial function (Fig. 2.4.1.3), attenuated synaptic injury [507], restored synaptic function, and ameliorated learning and memory deficits in STZ-induced diabetic mice (Fig. 2.4.1.4). On the contrary, when the diabetes-induced increase in CypD was further enhanced in the presence of Aβ (Fig.2.4.2.2), diabetes-related defects in mitochondrial function (Fig.2.4.2.3), synaptic plasticity[510] and learning and memory function (Fig.2.4.2.4) were significantly exacerbated. In addition to animal models of diabetes, enhanced protein levels of CypD were also observed in the brains of diabetic patients when compared to age-matched healthy subjects [507]. Intriguingly, postmortem studies of diabetic brains demonstrate a negative correlation between CypD expression and score on the Mini-Mental State Examination (MMSE) [507]. Given that elevated brain CypD expression and cognitive decline were observed in both diabetic patients and STZ-induced diabetic mice, our data indicate the clinical relevance of CypD-mediated brain mitochondrial abnormalities in diabetes-associated cognitive dysfunction and dementia.

CypD is a crucial regulatory component in the formation of mPTP in the presence of inducers such as ROS generation and Ca^{2+} overload. Genetic ablation or pharmacological inhibition of CypD by CsA prevents CypD-mediated mPTP opening, thus preserving

mitochondrial membrane potential, mitochondrial structure, and function, and preventing cell death. Its role in physiological regulation of Ca^{2+} homeostasis by transient Ca^{2+} release suggests CypD may function as a switch, which controls transient or prolonged opening of the mPTP [473]. Therefore, changes in CypD expressions may have a profound impact on the susceptibility and status of mPTP opening. In support of this assumption, single-channel patch clamp studies indicate that brain mitochondria isolated from STZ-induced diabetic mice displayed increased opening probability in CsA-sensitive high-conductance channel when compared to non-diabetic mice [507]. In line with these findings, mitochondria isolated from diabetic brains also exhibited aggravated mitochondrial swelling and cytochrome c release induced by Ca^{2+} overload, which were attenuated by CsA treatment [507]. These results suggest that enhanced CypD expression contributes to the hypersensitivity of CypD-mediated mPTP opening, which may underlie diabetes-induced mitochondrial dysfunction and cognitive impairment.

Despite being recognized as an essential component of mPTP, the precise mechanism by which CypD regulates mPTP formation is not clear. In addition to CypD, the molecular identity of mPTP remains controversial. Recent studies, however, suggest that F_1F_0 ATP synthase is the central core component of mPTP and CypD binds the lateral stalk of F_1F_0 ATP synthase and modulates its hydrolytic activity [511-513]. Thus a question is raised as to whether CypD-F_1F_0 ATP synthase interaction is implicated in CypD-mediated mPTP in the diabetic brain? Co-immunoprecipitation analysis in brain mitochondrial lysates confirmed the interaction between F_1F_0 ATP synthase and CypD [507]. Interestingly, increased amount of CypD was found in the F_1F_0 ATP synthase immunoprecipitates in the brain mitochondria isolated from diabetic mice, suggesting an augmented CypD-F_1F_0

ATP synthase interaction in the diabetic brain [507], which may serve as a potential mechanism underlying CypD-mediated mitochondrial malfunction. Chronic hyperglycemia and consequent ROS production can trigger the translocation of CypD from the mitochondrial matrix to the IMM where it interacts with F_1F_0 ATP synthase to facilitate conformational change and pore formation. mPTP opening leads to the collapse of the mitochondrial membrane potential, depletion of ATP, mitochondrial swelling, mitochondrial respiratory dysfunction, which will further exacerbate oxidative stress, forming a vicious feedback loop. In support of this hypothesis, blocking the interaction between CypD and F_1F_0 ATP synthase by genetic deletion of CypD ameliorated mitochondrial ROS generation and defects in the mitochondrial respiratory chain (Fig.2.4.1.3)[507]. Further, other presumed components of mPTP, such as ANT, PiC, and BH3 pro-apoptotic proteins, BAX and BAK, may also be implicated in the regulation of mPTP in the diabetic brain. Further investigations are needed to uncover the molecular basis of CypD-F_1F_0 ATP synthase interaction, its role in mPTP formation and how it is regulated under both physiological and diabetic conditions.

Another potential mechanism underlying diabetes-induced mitochondrial dysfunction and cognitive impairment may implicate the interaction between CypD and Aβ. Both *in vitro* and *in vivo* studies have demonstrated that hyperglycemia facilitates the production and processing of amyloid precursor protein, thus promoting Aβ generation [514-517]. In the current study, we did not observe significant difference in Aβ40 and Aβ42 levels between STZ-treated and vehicle-treated non-transgenic mice nor between STZ-treated and vehicle-treated AD transgenic mice (data not shown), which are consistent with previous findings that STZ-induced diabetes exacerbated Alzheimer-like cognitive dysfunction

without increasing brain Aβ load in presymptomatic AD transgenic mice [518]. However, recent studies suggest that induction of chronic diabetes facilitates cerebral Aβ accumulation. For instance, experimental induction of type 2 diabetes by high-fat diet treatment increased brain Aβ levels in the senescence-accelerated mouse model (SAMP8), which displays early pathological features of AD [519]. Obese mice overexpressing mutant human APP (mAPP) showed aggravated Aβ accumulation in the brain microvascular vessels when compared to non-diabetic mAPP mice [520]. In line with these findings, an increase in cerebellar Aβ42 level was observed in a mouse model of type 2 diabetes (db/db) (data not shown). It has been shown that Aβ can bind to CypD, promote CypD translocation to inner mitochondrial membrane and subsequent formation of mPTP [58]. Enhanced CypD and Aβ expression may synergistically contribute to an increased probability of mPTP opening, that exacerbates mitochondrial dysfunction, synaptic injury and cognitive impairment as observed in the brains of diabetic mAPP mice.

In summary, we report CypD is a major player in brain mitochondrial perturbation and cognitive impairment related to diabetes. Enhanced CypD expression increases the brain's susceptibility to hyperglycemia-induced oxidative damage, whereas CypD deficiency protects against hyperglycemic insults. While future mechanistic studies are necessary to elucidate the precise role of CypD in mPTP formation in the diabetic brain, this study provides evidence for a causal link between oxidative stress-induced mitochondrial dysfunction and cognitive impairment, thus providing further insights into the mechanisms underlying diabetes-associated CNS complications.

2.6 Future Directions

In the present study, we provide evidence for the involvement of CypD-mediated mPTP in diabetes-associated mitochondrial dysfunction and cognitive impairment. However, several questions remain to be addressed. The first question is how diabetes regulates gene and protein expression of CypD. In contrast to its well-characterized role in mPTP formation, much less is known about how CypD expression is regulated. A recent study suggests hematopoietic-substrate-1 associated protein X-1 (HAX-1) inhibited oxidative stress induced-mPTP opening through downregulation of CypD levels in the cardiac mitochondria [521]. Mechanistic studies reveal that HAX-1 recruited heat shock protein-90 (Hsp90) from CypD, rendering CypD susceptible to ubiquitin-proteasomal degradation [521]. Therefore, such Hsp90/HAX-1 interaction may also underlie the altered CypD protein levels in the brain mitochondria. Examination of the expression levels of HAX-1, Hsp90, and their interaction may help to validate this assumption. Additionally, CypD expression may also be regulated at the transcriptional and post-transcriptional levels. Further investigations are warranted to elucidate the molecular mechanisms underlying the regulation of CypD in brain mitochondria under both physiological and pathological conditions, particularly in diabetes and AD.

Another question that remains to be addressed is which signaling pathway is responsible for the hyperglycemia-induced oxidative damage in diabetic brain. Previous studies have shown that oxidative stress activates several mitogen-activated protein kinase signaling pathways (MAPK) including p38 and ERK, as well as other signaling pathways such as cAMP-dependent protein kinase (PKA)/cAMP response element binding (CREB) signal transduction pathway. Additionally, the activation of glycogen synthase kinase-3

(GSK3β) has been implicated in hyperglycemia-induced perturbation in mitochondrial and synaptic function. Examination of the pathways mentioned above may help to elucidate the cellular processes that occur in brain mitochondrial dysfunction and synaptic deficit, thus providing insights into diabetes-associated cognitive dysfunction.

Further, studies on rodent models of diabetes suggest the molecular mechanisms of diabetes-associated CNS disorder differ in type 1 and type 2 diabetes. The observations made in the present study were based on a mouse model of type 1 diabetes. We have previously reported hyperglycemia-induced oxidative stress, mitochondrial respiratory dysfunction and synaptic injury in the brains of mice with spontaneous type 2 diabetes (db/db). Since CypD-mediated mPTP induction represents a causal link between oxidative stress-induced mitochondrial perturbation and cognitive impairment, future studies are needed to examine the implication of CypD in cognitive dysfunction induced by type 2 diabetes, a much more common form of diabetes.

2.7 Conclusion

In summary, the results of the present study clearly demonstrate that CypD is a major player in diabetes-associated brain damage (Fig. 2.7.1). The absence of CypD markedly improved brain mitochondrial respiration and cognitive function in mice with diabetes induced by STZ, whereas enhanced CypD expression exacerbated brain mitochondrial dysfunction and accelerated cognitive deficits in mice overexpressing mAPP and made diabetic. The Cypd-mediated opening of mPTP may serve as one of the mechanisms underlying diabetes-induced defects in mitochondrial respiration, dynamics and motility, which contribute to synaptic injury and ultimately cognitive impairment. Therefore, inhibition of CypD-mediated mPTP opening by blocking the interaction of CypD and other components in the mPTP may represent a promising therapeutic strategy for the intervention of diabetes-related cognitive dysfunction.

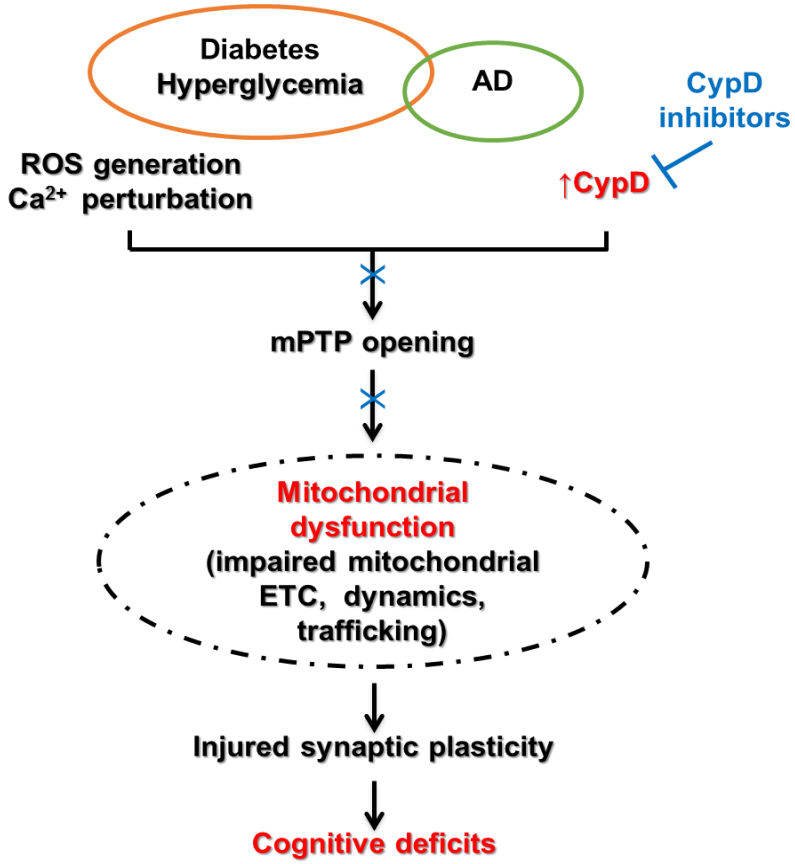

Figure 2.7.1

Fig. 2.7.1 CypD-mediated mPTP is implicated in diabetes-induced cognitive impairment including AD. Diabetes is typically accompanied by increased production of ROS and perturbed calcium homeostasis invoked by chronic hyperglycemia. In the context of AD, Aβ also elevates intracellular calcium and ROS generation. Increased CypD expressions have been observed in both diabetic and AD brains. These conditions favor the opening of mPTP, resulting in mitochondrial dysfunction including reduced mitochondrial electron transport chain (ETC) complex activities, impaired axonal mitochondrial trafficking and mitochondrial fragmentation. Severe mitochondrial perturbations lead to synaptic injury and ultimately deficits in learning and memory function. Blocking mPTP opening by pharmacological inhibition of CypD may represent a promising therapeutic strategy for treatment of diabetes-associated cognitive dysfunction including AD.

Final Conclusion

In summary, the data presented in this dissertation indicate that perturbation in brain energy metabolism and resulting energy deficits may form the pathophysiological basis for brain disorders including AD and diabetes. However, in different diseases, distinct metabolic processes, and discrete mechanisms are affected. Results obtained from the first study suggest that three human ApoE isoforms differentially modulate glucose transport and glycolysis, with ApoE2-expressing brain exhibiting the most robust profile whereas ApoE4-expressing brain demonstrating a most deficient profile. The bioenergetic robustness associated with ApoE2 may underlie its protective properties against AD. By contrast, the defects in glucose metabolism associated with ApoE4 may lead to energy failure, rendering the brain vulnerable to aging and AD-related insults, which may underlie its increased susceptibility to AD. Notably, the introduction of ApoE2 completely reversed the bioenergetic deficits induced by ApoE4, suggesting that brain delivery of ApoE2 may represent a promising therapeutic approach for AD prevention or early intervention, particularly in the high-risk ApoE4 carriers.

Results obtained from the second study reveal a pivotal role of CypD in brain mitochondrial perturbation and cognitive dysfunction related to diabetes. Intriguingly, CypD deficiency attenuated whereas enhanced CypD expression exacerbated diabetes-induced defects in brain mitochondrial respiration and cognitive function. Given that CypD is a key regulatory component of mPTP, CypD-mediated opening of mPTP may be one of the mechanisms underlying diabetes-induced mitochondrial dysfunction and subsequent synaptic injury and cognitive impairment. Therefore, a therapeutic strategy

that could inhibit mPTP opening by blocking the interaction of CypD and other components in mPTP may hold benefits for diabetes-associated cognitive dysfunction.

References

1. Mathers, C.D. and D. Loncar, *Projections of Global Mortality and Burden of Disease from 2002 to 2030.* PLOS Medicine, 2006. **3**(11): p. e442.
2. Messier, C., *Impact of impaired glucose tolerance and type 2 diabetes on cognitive aging.* Neurobiol Aging, 2005. **26 Suppl 1**: p. 26-30.
3. Perlmuter, L.C., M.K. Hakami, C. Hodgson-Harrington, J. Ginsberg, J. Katz, D.E. Singer, and D.M. Nathan, *Decreased cognitive function in aging non-insulin-dependent diabetic patients.* The American Journal of Medicine. **77**(6): p. 1043-1048.
4. Brands, A.M., G.J. Biessels, E.H. de Haan, L.J. Kappelle, and R.P. Kessels, *The effects of type 1 diabetes on cognitive performance: a meta-analysis.* Diabetes Care, 2005. **28**(3): p. 726-35.
5. Ott, A., R.P. Stolk, F. van Harskamp, H.A. Pols, A. Hofman, and M.M. Breteler, *Diabetes mellitus and the risk of dementia: The Rotterdam Study.* Neurology, 1999. **53**(9): p. 1937-42.
6. Stolk, R.P., M.M. Breteler, A. Ott, H.A. Pols, S.W. Lamberts, D.E. Grobbee, and A. Hofman, *Insulin and cognitive function in an elderly population. The Rotterdam Study.* Diabetes Care, 1997. **20**(5): p. 792-5.
7. Kilander, L., H. Nyman, M. Boberg, L. Hansson, and H. Lithell, *Hypertension is related to cognitive impairment: a 20-year follow-up of 999 men.* Hypertension, 1998. **31**(3): p. 780-6.
8. Luchsinger, J.A., C. Reitz, B. Patel, M.X. Tang, J.J. Manly, and R. Mayeux, *Relation of diabetes to mild cognitive impairment.* Arch Neurol, 2007. **64**(4): p. 570-5.
9. Irie, F., A.L. Fitzpatrick, O.L. Lopez, L.H. Kuller, R. Peila, A.B. Newman, and L.J. Launer, *Enhanced risk for Alzheimer disease in persons with type 2 diabetes and APOE epsilon4: the Cardiovascular Health Study Cognition Study.* Arch Neurol, 2008. **65**(1): p. 89-93.
10. Janson, J., T. Laedtke, J.E. Parisi, P. O'Brien, R.C. Petersen, and P.C. Butler, *Increased risk of type 2 diabetes in Alzheimer disease.* Diabetes, 2004. **53**(2): p. 474-81.
11. Kreis, R. and B.D. Ross, *Cerebral metabolic disturbances in patients with subacute and chronic diabetes mellitus: detection with proton MR spectroscopy.* Radiology, 1992. **184**(1): p. 123-30.
12. Criego, A.B., I. Tkac, A. Kumar, W. Thomas, R. Gruetter, and E.R. Seaquist, *Brain glucose concentrations in patients with type 1 diabetes and hypoglycemia unawareness.* J Neurosci Res, 2005. **79**(1-2): p. 42-7.
13. Baker, L.D., D.J. Cross, S. Minoshima, D. Belongia, G.S. Watson, and S. Craft, *Insulin resistance and Alzheimer-like reductions in regional cerebral glucose metabolism for cognitively normal adults with prediabetes or early type 2 diabetes.* Arch Neurol, 2011. **68**(1): p. 51-7.
14. Duelli, R., M.H. Maurer, R. Staudt, S. Heiland, L. Duembgen, and W. Kuschinsky, *Increased cerebral glucose utilization and decreased glucose transporter Glut1 during chronic hyperglycemia in rat brain.* Brain Res, 2000. **858**(2): p. 338-47.

15. Jacob, R.J., X. Fan, M.L. Evans, J. Dziura, and R.S. Sherwin, *Brain glucose levels are elevated in chronically hyperglycemic diabetic rats: no evidence for protective adaptation by the blood brain barrier.* Metabolism, 2002. **51**(12): p. 1522-4.
16. Mans, A.M., M.R. DeJoseph, D.W. Davis, and R.A. Hawkins, *Brain energy metabolism in streptozotocin-diabetes.* Biochemical Journal, 1988. **249**(1): p. 57-62.
17. Jakobsen, J., M. Nedergaard, M. Aarslew-Jensen, and N.H. Diemer, *Regional brain glucose metabolism and blood flow in streptozocin-induced diabetic rats.* Diabetes, 1990. **39**(4): p. 437-40.
18. Lakhman, S.S., P. Sharma, G. Kaur, and G. Kaur, *Changes in glucose metabolism from discrete regions of rat brain and its relationship to reproductive failure during experimental diabetes.* Molecular and Cellular Biochemistry, 1994. **141**(2): p. 97-102.
19. Warren, R.E. and B.M. Frier, *Hypoglycaemia and cognitive function.* Diabetes Obes Metab, 2005. **7**(5): p. 493-503.
20. Cox, D.J., B.P. Kovatchev, L.A. Gonder-Frederick, K.H. Summers, A. McCall, K.J. Grimm, and W.L. Clarke, *Relationships between hyperglycemia and cognitive performance among adults with type 1 and type 2 diabetes.* Diabetes Care, 2005. **28**(1): p. 71-7.
21. Cukierman-Yaffe, T., H.C. Gerstein, J.D. Williamson, R.M. Lazar, L. Lovato, M.E. Miller, L.H. Coker, A. Murray, M.D. Sullivan, S.M. Marcovina, and L.J. Launer, *Relationship Between Baseline Glycemic Control and Cognitive Function in Individuals With Type 2 Diabetes and Other Cardiovascular Risk Factors: The Action to Control Cardiovascular Risk in Diabetes-Memory in Diabetes (ACCORD-MIND) trial.* Diabetes Care, 2009. **32**(2): p. 221-6.
22. Gonder-Frederick, L.A., J.F. Zrebiec, A.U. Bauchowitz, L.M. Ritterband, J.C. Magee, D.J. Cox, and W.L. Clarke, *Cognitive function is disrupted by both hypo- and hyperglycemia in school-aged children with type 1 diabetes: a field study.* Diabetes Care, 2009. **32**(6): p. 1001-6.
23. McNay, E.C. and R.S. Sherwin, *Effect of recurrent hypoglycemia on spatial cognition and cognitive metabolism in normal and diabetic rats.* Diabetes, 2004. **53**(2): p. 418-25.
24. McNay, E.C., A. Williamson, R.J. McCrimmon, and R.S. Sherwin, *Cognitive and Neural Hippocampal Effects of Long-Term Moderate Recurrent Hypoglycemia.* Diabetes, 2006. **55**(4): p. 1088-1095.
25. Moreira, T., E. Malec, C.G. Ostenson, S. Efendic, and S. Liljequist, *Diabetic type II Goto-Kakizaki rats show progressively decreasing exploratory activity and learning impairments in fixed and progressive ratios of a lever-press task.* Behav Brain Res, 2007. **180**(1): p. 28-41.
26. Li, Z.-g., W. Zhang, and A.A.F. Sima, *Alzheimer-Like Changes in Rat Models of Spontaneous Diabetes.* Diabetes, 2007. **56**(7): p. 1817-1824.
27. Foster, N.L., T.N. Chase, L. Mansi, R. Brooks, P. Fedio, N.J. Patronas, and G. Di Chiro, *Cortical abnormalities in Alzheimer's disease.* Ann Neurol, 1984. **16**(6): p. 649-54.

28. Friedland, R.P., T.F. Budinger, E. Koss, and B.A. Ober, *Alzheimer's disease: anterior-posterior and lateral hemispheric alterations in cortical glucose utilization.* Neurosci Lett, 1985. **53**(3): p. 235-40.
29. Koss, E., R.P. Friedland, B.A. Ober, and W.J. Jagust, *Differences in lateral hemispheric asymmetries of glucose utilization between early- and late-onset Alzheimer-type dementia.* Am J Psychiatry, 1985. **142**(5): p. 638-40.
30. Mosconi, L., W.H. Tsui, K. Herholz, A. Pupi, A. Drzezga, G. Lucignani, E.M. Reiman, V. Holthoff, E. Kalbe, S. Sorbi, J. Diehl-Schmid, R. Perneczky, F. Clerici, R. Caselli, B. Beuthien-Baumann, A. Kurz, S. Minoshima, and M.J. de Leon, *Multicenter standardized 18F-FDG PET diagnosis of mild cognitive impairment, Alzheimer's disease, and other dementias.* J Nucl Med, 2008. **49**(3): p. 390-8.
31. Mosconi, L., S. De Santi, J. Li, W.H. Tsui, Y. Li, M. Boppana, E. Laska, H. Rusinek, and M.J. de Leon, *Hippocampal hypometabolism predicts cognitive decline from normal aging.* Neurobiol Aging, 2008. **29**(5): p. 676-92.
32. Reiman, E.M., K. Chen, G.E. Alexander, R.J. Caselli, D. Bandy, D. Osborne, A.M. Saunders, and J. Hardy, *Functional brain abnormalities in young adults at genetic risk for late-onset Alzheimer's dementia.* Proc Natl Acad Sci U S A, 2004. **101**(1): p. 284-9.
33. Reiman, E.M., R.J. Caselli, L.S. Yun, K. Chen, D. Bandy, S. Minoshima, S.N. Thibodeau, and D. Osborne, *Preclinical evidence of Alzheimer's disease in persons homozygous for the epsilon 4 allele for apolipoprotein E.* N Engl J Med, 1996. **334**(12): p. 752-8.
34. Reiman, E.M., R.J. Caselli, K. Chen, G.E. Alexander, D. Bandy, and J. Frost, *Declining brain activity in cognitively normal apolipoprotein E epsilon 4 heterozygotes: A foundation for using positron emission tomography to efficiently test treatments to prevent Alzheimer's disease.* Proc Natl Acad Sci U S A, 2001. **98**(6): p. 3334-9.
35. Kennedy, A.M., R.S. Frackowiak, S.K. Newman, P.M. Bloomfield, J. Seaward, P. Roques, G. Lewington, V.J. Cunningham, and M.N. Rossor, *Deficits in cerebral glucose metabolism demonstrated by positron emission tomography in individuals at risk of familial Alzheimer's disease.* Neurosci Lett, 1995. **186**(1): p. 17-20.
36. Small, G.W., L.M. Ercoli, D.H. Silverman, S.C. Huang, S. Komo, S.Y. Bookheimer, H. Lavretsky, K. Miller, P. Siddarth, N.L. Rasgon, J.C. Mazziotta, S. Saxena, H.M. Wu, M.S. Mega, J.L. Cummings, A.M. Saunders, M.A. Pericak-Vance, A.D. Roses, J.R. Barrio, and M.E. Phelps, *Cerebral metabolic and cognitive decline in persons at genetic risk for Alzheimer's disease.* Proc Natl Acad Sci U S A, 2000. **97**(11): p. 6037-42.
37. Simpson, I.A., K.R. Chundu, T. Davies-Hill, W.G. Honer, and P. Davies, *Decreased concentrations of GLUT1 and GLUT3 glucose transporters in the brains of patients with Alzheimer's disease.* Ann Neurol, 1994. **35**(5): p. 546-51.
38. Harr, S.D., N.A. Simonian, and B.T. Hyman, *Functional alterations in Alzheimer's disease: decreased glucose transporter 3 immunoreactivity in the perforant pathway terminal zone.* J Neuropathol Exp Neurol, 1995. **54**(1): p. 38-41.

39. Liu, Y., F. Liu, K. Iqbal, I. Grundke-Iqbal, and C.X. Gong, *Decreased glucose transporters correlate to abnormal hyperphosphorylation of tau in Alzheimer disease.* FEBS Lett, 2008. **582**(2): p. 359-64.
40. Bigl, M., M.K. Brückner, T. Arendt, V. Bigl, and K. Eschrich, *Activities of key glycolytic enzymes in the brains of patients with Alzheimer's disease.* Journal of Neural Transmission, 1999. **106**(5): p. 499-511.
41. Mortilla, M. and S. Sorbi, *[Hexokinase in Alzheimer's disease]*. Medicina (Firenze), 1990. **10**(2): p. 168-9.
42. Sorbi, S., E.D. Bird, and J.P. Blass, *Decreased pyruvate dehydrogenase complex activity in Huntington and Alzheimer brain.* Ann Neurol, 1983. **13**(1): p. 72-8.
43. Bubber, P., V. Haroutunian, G. Fisch, J.P. Blass, and G.E. Gibson, *Mitochondrial abnormalities in Alzheimer brain: mechanistic implications.* Ann Neurol, 2005. **57**(5): p. 695-703.
44. Valla, J., F. Gonzalez-Lima, and E.M. Reiman, *FDG autoradiography reveals developmental and pathological effects of mutant amyloid in PDAPP transgenic mice.* Int J Dev Neurosci, 2008. **26**(3-4): p. 253-8.
45. Bigl, M., J. Apelt, K. Eschrich, and R. Schliebs, *Cortical glucose metabolism is altered in aged transgenic Tg2576 mice that demonstrate Alzheimer plaque pathology*. Journal of Neural Transmission, 2003. **110**(1): p. 77-94.
46. Hooijmans, C.R., C. Graven, P.J. Dederen, H. Tanila, T. van Groen, and A.J. Kiliaan, *Amyloid beta deposition is related to decreased glucose transporter-1 levels and hippocampal atrophy in brains of aged APP/PS1 mice.* Brain Res, 2007. **1181**: p. 93-103.
47. Liu, F., J. Shi, H. Tanimukai, J. Gu, J. Gu, I. Grundke-Iqbal, K. Iqbal, and C.X. Gong, *Reduced O-GlcNAcylation links lower brain glucose metabolism and tau pathology in Alzheimer's disease.* Brain, 2009. **132**(Pt 7): p. 1820-32.
48. Bosetti, F., F. Brizzi, S. Barogi, M. Mancuso, G. Siciliano, E.A. Tendi, L. Murri, S.I. Rapoport, and G. Solaini, *Cytochrome c oxidase and mitochondrial F1F0-ATPase (ATP synthase) activities in platelets and brain from patients with Alzheimer's disease.* Neurobiol Aging, 2002. **23**(3): p. 371-6.
49. Kish, S.J., C. Bergeron, A. Rajput, S. Dozic, F. Mastrogiacomo, L.J. Chang, J.M. Wilson, L.M. DiStefano, and J.N. Nobrega, *Brain cytochrome oxidase in Alzheimer's disease.* J Neurochem, 1992. **59**(2): p. 776-9.
50. Maurer, I., S. Zierz, and H.J. Möller, *A selective defect of cytochrome c oxidase is present in brain of Alzheimer disease patients.* Neurobiology of Aging, 2000. **21**(3): p. 455-462.
51. Mutisya, E.M., A.C. Bowling, and M.F. Beal, *Cortical cytochrome oxidase activity is reduced in Alzheimer's disease*. J Neurochem, 1994. **63**(6): p. 2179-84.
52. Castellani, R.J., P.L. Harris, L.M. Sayre, J. Fujii, N. Taniguchi, M.P. Vitek, H. Founds, C.S. Atwood, G. Perry, and M.A. Smith, *Active glycation in neurofibrillary pathology of Alzheimer disease: N(epsilon)-(carboxymethyl) lysine and hexitol-lysine.* Free Radic Biol Med, 2001. **31**(2): p. 175-80.
53. Nunomura, A., G. Perry, M.A. Pappolla, R. Wade, K. Hirai, S. Chiba, and M.A. Smith, *RNA oxidation is a prominent feature of vulnerable neurons in Alzheimer's disease.* J Neurosci, 1999. **19**(6): p. 1959-64.

54. Nunomura, A., G. Perry, G. Aliev, K. Hirai, A. Takeda, E.K. Balraj, P.K. Jones, H. Ghanbari, T. Wataya, S. Shimohama, S. Chiba, C.S. Atwood, R.B. Petersen, and M.A. Smith, *Oxidative damage is the earliest event in Alzheimer disease.* J Neuropathol Exp Neurol, 2001. **60**(8): p. 759-67.
55. Butterfield, D.A. and C.M. Lauderback, *Lipid peroxidation and protein oxidation in Alzheimer's disease brain: potential causes and consequences involving amyloid β-peptide-associated free radical oxidative stress1,2.* Free Radical Biology and Medicine, 2002. **32**(11): p. 1050-1060.
56. Hansson Petersen, C.A., N. Alikhani, H. Behbahani, B. Wiehager, P.F. Pavlov, I. Alafuzoff, V. Leinonen, A. Ito, B. Winblad, E. Glaser, and M. Ankarcrona, *The amyloid beta-peptide is imported into mitochondria via the TOM import machinery and localized to mitochondrial cristae.* Proc Natl Acad Sci U S A, 2008. **105**(35): p. 13145-50.
57. Lustbader, J.W., M. Cirilli, C. Lin, H.W. Xu, K. Takuma, N. Wang, C. Caspersen, X. Chen, S. Pollak, M. Chaney, F. Trinchese, S. Liu, F. Gunn-Moore, L.F. Lue, D.G. Walker, P. Kuppusamy, Z.L. Zewier, O. Arancio, D. Stern, S.S. Yan, and H. Wu, *ABAD directly links Abeta to mitochondrial toxicity in Alzheimer's disease.* Science, 2004. **304**(5669): p. 448-52.
58. Du, H., L. Guo, F. Fang, D. Chen, A.A. Sosunov, G.M. McKhann, Y. Yan, C. Wang, H. Zhang, J.D. Molkentin, F.J. Gunn-Moore, J.P. Vonsattel, O. Arancio, J.X. Chen, and S.D. Yan, *Cyclophilin D deficiency attenuates mitochondrial and neuronal perturbation and ameliorates learning and memory in Alzheimer's disease.* Nat Med, 2008. **14**(10): p. 1097-105.
59. Crompton, M., *Mitochondria and aging: a role for the permeability transition?* Aging Cell, 2004. **3**(1): p. 3-6.
60. Zamzami, N., N. Larochette, and G. Kroemer, *Mitochondrial permeability transition in apoptosis and necrosis.* Cell Death Differ, 2005. **12 Suppl 2**: p. 1478-80.
61. Sanz-Blasco, S., R.A. Valero, I. Rodriguez-Crespo, C. Villalobos, and L. Nunez, *Mitochondrial Ca2+ overload underlies Abeta oligomers neurotoxicity providing an unexpected mechanism of neuroprotection by NSAIDs.* PLoS One, 2008. **3**(7): p. e2718.
62. Hirai, K., G. Aliev, A. Nunomura, H. Fujioka, R.L. Russell, C.S. Atwood, A.B. Johnson, Y. Kress, H.V. Vinters, M. Tabaton, S. Shimohama, A.D. Cash, S.L. Siedlak, P.L. Harris, P.K. Jones, R.B. Petersen, G. Perry, and M.A. Smith, *Mitochondrial abnormalities in Alzheimer's disease.* J Neurosci, 2001. **21**(9): p. 3017-23.
63. Wang, X., B. Su, S.L. Siedlak, P.I. Moreira, H. Fujioka, Y. Wang, G. Casadesus, and X. Zhu, *Amyloid-beta overproduction causes abnormal mitochondrial dynamics via differential modulation of mitochondrial fission/fusion proteins.* Proc Natl Acad Sci U S A, 2008. **105**(49): p. 19318-23.
64. Cho, D.H., T. Nakamura, J. Fang, P. Cieplak, A. Godzik, Z. Gu, and S.A. Lipton, *S-nitrosylation of Drp1 mediates beta-amyloid-related mitochondrial fission and neuronal injury.* Science, 2009. **324**(5923): p. 102-5.
65. Stokin, G.B., C. Lillo, T.L. Falzone, R.G. Brusch, E. Rockenstein, S.L. Mount, R. Raman, P. Davies, E. Masliah, D.S. Williams, and L.S. Goldstein, *Axonopathy*

and transport deficits early in the pathogenesis of Alzheimer's disease. Science, 2005. **307**(5713): p. 1282-8.
66. Wang, X., G. Perry, M.A. Smith, and X. Zhu, *Amyloid-beta-derived diffusible ligands cause impaired axonal transport of mitochondria in neurons.* Neurodegener Dis, 2010. **7**(1-3): p. 56-9.
67. Rui, Y., P. Tiwari, Z. Xie, and J.Q. Zheng, *Acute impairment of mitochondrial trafficking by beta-amyloid peptides in hippocampal neurons.* J Neurosci, 2006. **26**(41): p. 10480-7.
68. Guo, L., H. Du, S. Yan, X. Wu, G.M. McKhann, J.X. Chen, and S.S. Yan, *Cyclophilin D deficiency rescues axonal mitochondrial transport in Alzheimer's neurons.* PLoS One, 2013. **8**(1): p. e54914.
69. Wang, X., B. Su, H. Lee, X. Li, G. Perry, M.A. Smith, and X. Zhu, *Impaired Balance of Mitochondria Fission and Fusion in Alzheimer Disease.* J Neurosci, 2009. **29**(28): p. 9090-103.
70. Du, H., L. Guo, S. Yan, A.A. Sosunov, G.M. McKhann, and S. ShiDu Yan, *Early deficits in synaptic mitochondria in an Alzheimer's disease mouse model.* Proc Natl Acad Sci U S A, 2010. **107**(43): p. 18670-5.
71. Moreira, P.I., A.P. Rolo, C. Sena, R. Seica, C.R. Oliveira, and M.S. Santos, *Insulin attenuates diabetes-related mitochondrial alterations: a comparative study.* Med Chem, 2006. **2**(3): p. 299-308.
72. Moreira, P.I., M.S. Santos, C. Sena, R. Seica, and C.R. Oliveira, *Insulin protects against amyloid beta-peptide toxicity in brain mitochondria of diabetic rats.* Neurobiol Dis, 2005. **18**(3): p. 628-37.
73. Mastrocola, R., F. Restivo, I. Vercellinatto, O. Danni, E. Brignardello, M. Aragno, and G. Boccuzzi, *Oxidative and nitrosative stress in brain mitochondria of diabetic rats.* J Endocrinol, 2005. **187**(1): p. 37-44.
74. Moreira, P.I., M.S. Santos, A.M. Moreno, R. Seica, and C.R. Oliveira, *Increased vulnerability of brain mitochondria in diabetic (Goto-Kakizaki) rats with aging and amyloid-beta exposure.* Diabetes, 2003. **52**(6): p. 1449-56.
75. Huang, S., Y. Wang, X. Gan, D. Fang, C. Zhong, L. Wu, G. Hu, A.A. Sosunov, G.M. McKhann, H. Yu, and S.S.D. Yan, *Drp1-Mediated Mitochondrial Abnormalities Link to Synaptic Injury in Diabetes Model.* Diabetes, 2015. **64**(5): p. 1728-42.
76. Cardoso, S., M.S. Santos, R. Seica, and P.I. Moreira, *Cortical and hippocampal mitochondria bioenergetics and oxidative status during hyperglycemia and/or insulin-induced hypoglycemia.* Biochim Biophys Acta, 2010. **1802**(11): p. 942-51.
77. Cardoso, S., C. Carvalho, R. Santos, S. Correia, M.S. Santos, R. Seica, C.R. Oliveira, and P.I. Moreira, *Impact of STZ-induced hyperglycemia and insulin-induced hypoglycemia in plasma amino acids and cortical synaptosomal neurotransmitters.* Synapse, 2011. **65**(6): p. 457-66.
78. Akomolafe, A., A. Beiser, J.B. Meigs, R. Au, R.C. Green, L.A. Farrer, P.A. Wolf, and S. Seshadri, *Diabetes mellitus and risk of developing Alzheimer disease: results from the Framingham Study.* Arch Neurol, 2006. **63**(11): p. 1551-5.
79. Kukull, W.A., R. Higdon, J.D. Bowen, W.C. McCormick, L. Teri, G.D. Schellenberg, G. van Belle, L. Jolley, and E.B. Larson, *Dementia and Alzheimer*

disease incidence: a prospective cohort study. Arch Neurol, 2002. **59**(11): p. 1737-46.
80. Watson, G.S. and S. Craft, *The role of insulin resistance in the pathogenesis of Alzheimer's disease: implications for treatment.* CNS Drugs, 2003. **17**(1): p. 27-45.
81. De Felice, F.G., M.V. Lourenco, and S.T. Ferreira, *How does brain insulin resistance develop in Alzheimer's disease?* Alzheimers Dement, 2014. **10**(1 Suppl): p. S26-32.
82. Hoyer, S., *The aging brain. Changes in the neuronal insulin/insulin receptor signal transduction cascade trigger late-onset sporadic Alzheimer disease (SAD). A mini-review.* Journal of Neural Transmission, 2002. **109**(7): p. 991-1002.
83. Gasparini, L., W.J. Netzer, P. Greengard, and H. Xu, *Does insulin dysfunction play a role in Alzheimer's disease?* Trends Pharmacol Sci, 2002. **23**(6): p. 288-93.
84. Reiman, E.M., K. Chen, G.E. Alexander, R.J. Caselli, D. Bandy, D. Osborne, A.M. Saunders, and J. Hardy, *Correlations between apolipoprotein E epsilon4 gene dose and brain-imaging measurements of regional hypometabolism.* Proc Natl Acad Sci U S A, 2005. **102**(23): p. 8299-302.
85. Henderson, S.T., J.L. Vogel, L.J. Barr, F. Garvin, J.J. Jones, and L.C. Costantini, *Study of the ketogenic agent AC-1202 in mild to moderate Alzheimer's disease: a randomized, double-blind, placebo-controlled, multicenter trial.* Nutr Metab (Lond), 2009. **6**: p. 31.
86. Reger, M.A., S.T. Henderson, C. Hale, B. Cholerton, L.D. Baker, G.S. Watson, K. Hyde, D. Chapman, and S. Craft, *Effects of beta-hydroxybutyrate on cognition in memory-impaired adults.* Neurobiol Aging, 2004. **25**(3): p. 311-4.
87. Keeney, J.T., S. Ibrahimi, and L. Zhao, *Human ApoE Isoforms Differentially Modulate Glucose and Amyloid Metabolic Pathways in Female Brain: Evidence of the Mechanism of Neuroprotection by ApoE2 and Implications for Alzheimer's Disease Prevention and Early Intervention.* J Alzheimers Dis, 2015. **48**(2): p. 411-24.
88. Li, X.L., S. Aou, Y. Oomura, N. Hori, K. Fukunaga, and T. Hori, *Impairment of long-term potentiation and spatial memory in leptin receptor-deficient rodents.* Neuroscience, 2002. **113**(3): p. 607-15.
89. Biessels, G.J., A. Kamal, G.M. Ramakers, I.J. Urban, B.M. Spruijt, D.W. Erkelens, and W.H. Gispen, *Place learning and hippocampal synaptic plasticity in streptozotocin-induced diabetic rats.* Diabetes, 1996. **45**(9): p. 1259-66.
90. Abbas, T., E. Faivre, and C. Holscher, *Impairment of synaptic plasticity and memory formation in GLP-1 receptor KO mice: Interaction between type 2 diabetes and Alzheimer's disease.* Behav Brain Res, 2009. **205**(1): p. 265-71.
91. Nistico, R., V. Cavallucci, S. Piccinin, S. Macri, M. Pignatelli, B. Mehdawy, F. Blandini, G. Laviola, D. Lauro, N.B. Mercuri, and M. D'Amelio, *Insulin receptor beta-subunit haploinsufficiency impairs hippocampal late-phase LTP and recognition memory.* Neuromolecular Med, 2012. **14**(4): p. 262-9.
92. Alzheimer's, A., *2015 Alzheimer's disease facts and figures.* Alzheimers Dement, 2015. **11**(3): p. 332-84.

93. Cummings, J.L., T. Morstorf, and K. Zhong, *Alzheimer's disease drug-development pipeline: few candidates, frequent failures.* Alzheimers Res Ther, 2014. **6**(4): p. 37.
94. Sloane, P.D., S. Zimmerman, C. Suchindran, P. Reed, L. Wang, M. Boustani, and S. Sudha, *The public health impact of Alzheimer's disease, 2000-2050: potential implication of treatment advances.* Annu Rev Public Health, 2002. **23**: p. 213-31.
95. Shore, V.G. and B. Shore, *Heterogeneity of human plasma very low density lipoproteins. Separation of species differing in protein components.* Biochemistry, 1973. **12**(3): p. 502-507.
96. Utermann, G., M. Jaeschke, and J. Menzel, *Familial hyperlipoproteinemia type III: deficiency of a specific apolipoprotein (apo E-III) in the very-low-density lipoproteins.* FEBS Lett, 1975. **56**(2): p. 352-5.
97. Havel, R.J. and J.P. Kane, *Primary dysbetalipoproteinemia: predominance of a specific apoprotein species in triglyceride-rich lipoproteins.* Proc Natl Acad Sci U S A, 1973. **70**(7): p. 2015-9.
98. Paik, Y.K., D.J. Chang, C.A. Reardon, G.E. Davies, R.W. Mahley, and J.M. Taylor, *Nucleotide sequence and structure of the human apolipoprotein E gene.* Proceedings of the National Academy of Sciences of the United States of America, 1985. **82**(10): p. 3445-3449.
99. Das, H.K., J. McPherson, G.A. Bruns, S.K. Karathanasis, and J.L. Breslow, *Isolation, characterization, and mapping to chromosome 19 of the human apolipoprotein E gene.* J Biol Chem, 1985. **260**(10): p. 6240-7.
100. Zannis, V.I., J. McPherson, G. Goldberger, S.K. Karathanasis, and J.L. Breslow, *Synthesis, intracellular processing, and signal peptide of human apolipoprotein E.* J Biol Chem, 1984. **259**(9): p. 5495-9.
101. McLean, J.W., N.A. Elshourbagy, D.J. Chang, R.W. Mahley, and J.M. Taylor, *Human apolipoprotein E mRNA. cDNA cloning and nucleotide sequencing of a new variant.* J Biol Chem, 1984. **259**(10): p. 6498-504.
102. Mahley, R.W., T.L. Innerarity, R.E. Pitas, K.H. Weisgraber, J.H. Brown, and E. Gross, *Inhibition of lipoprotein binding to cell surface receptors of fibroblasts following selective modification of arginyl residues in arginine-rich and B apoproteins.* J Biol Chem, 1977. **252**(20): p. 7279-87.
103. Weisgraber, K.H., T.L. Innerarity, and R.W. Mahley, *Role of lysine residues of plasma lipoproteins in high affinity binding to cell surface receptors on human fibroblasts.* J Biol Chem, 1978. **253**(24): p. 9053-62.
104. Zhong, N., *Understanding the Association of Apolipoprotein E4 with Alzheimer.* 2009. **284**(10): p. 6027-31.
105. Dong, L.M., C. Wilson, M.R. Wardell, T. Simmons, R.W. Mahley, K.H. Weisgraber, and D.A. Agard, *Human apolipoprotein E. Role of arginine 61 in mediating the lipoprotein preferences of the E3 and E4 isoforms.* J Biol Chem, 1994. **269**(35): p. 22358-65.
106. Dong, L.M. and K.H. Weisgraber, *Human apolipoprotein E4 domain interaction. Arginine 61 and glutamic acid 255 interact to direct the preference for very low density lipoproteins.* J Biol Chem, 1996. **271**(32): p. 19053-7.

107. Hatters, D.M., M.S. Budamagunta, J.C. Voss, and K.H. Weisgraber, *Modulation of apolipoprotein E structure by domain interaction: differences in lipid-bound and lipid-free forms.* J Biol Chem, 2005. **280**(40): p. 34288-95.
108. Xu, Q., W.J. Brecht, K.H. Weisgraber, R.W. Mahley, and Y. Huang, *Apolipoprotein E4 domain interaction occurs in living neuronal cells as determined by fluorescence resonance energy transfer.* J Biol Chem, 2004. **279**(24): p. 25511-6.
109. Raffaï, R.L., *Introduction of human apolipoprotein E4 "domain.* 2001. **98**(20): p. 11587-91.
110. Weisgraber, K.H., *Apolipoprotein E: structure-function relationships.* Adv Protein Chem, 1994. **45**: p. 249-302.
111. Morrow, J.A., D.M. Hatters, B. Lu, P. Hochtl, K.A. Oberg, B. Rupp, and K.H. Weisgraber, *Apolipoprotein E4 forms a molten globule. A potential basis for its association with disease.* J Biol Chem, 2002. **277**(52): p. 50380-5.
112. Morrow, J.A., M.L. Segall, S. Lund-Katz, M.C. Phillips, M. Knapp, B. Rupp, and K.H. Weisgraber, *Differences in stability among the human apolipoprotein E isoforms determined by the amino-terminal domain.* Biochemistry, 2000. **39**(38): p. 11657-66.
113. Ye, S., Y. Huang, K. Müllendorff, L. Dong, G. Giedt, E.C. Meng, F.E. Cohen, I.D. Kuntz, K.H. Weisgraber, and R.W. Mahley, *Apolipoprotein (apo) E4 enhances amyloid β peptide production in cultured neuronal cells: ApoE structure as a potential therapeutic target.* Proc Natl Acad Sci U S A, 2005. **102**(51): p. 18700-5.
114. Ji, Z.S., R.D. Miranda, Y.M. Newhouse, K.H. Weisgraber, Y. Huang, and R.W. Mahley, *Apolipoprotein E4 potentiates amyloid beta peptide-induced lysosomal leakage and apoptosis in neuronal cells.* J Biol Chem, 2002. **277**(24): p. 21821-8.
115. Brecht, W.J., F.M. Harris, S. Chang, I. Tesseur, G.Q. Yu, Q. Xu, J. Dee Fish, T. Wyss-Coray, M. Buttini, L. Mucke, R.W. Mahley, and Y. Huang, *Neuron-specific apolipoprotein e4 proteolysis is associated with increased tau phosphorylation in brains of transgenic mice.* J Neurosci, 2004. **24**(10): p. 2527-34.
116. Harris, F.M., W.J. Brecht, Q. Xu, I. Tesseur, L. Kekonius, T. Wyss-Coray, J.D. Fish, E. Masliah, P.C. Hopkins, K. Scearce-Levie, K.H. Weisgraber, L. Mucke, R.W. Mahley, and Y. Huang, *Carboxyl-terminal-truncated apolipoprotein E4 causes Alzheimer's disease-like neurodegeneration and behavioral deficits in transgenic mice.* Proc Natl Acad Sci U S A, 2003. **100**(19): p. 10966-71.
117. Newman, T.C., P.A. Dawson, L.L. Rudel, and D.L. Williams, *Quantitation of apolipoprotein E mRNA in the liver and peripheral tissues of nonhuman primates.* J Biol Chem, 1985. **260**(4): p. 2452-7.
118. Driscoll, D.M. and G.S. Getz, *Extrahepatic synthesis of apolipoprotein E.* J Lipid Res, 1984. **25**(12): p. 1368-79.
119. Zannis, V.I., F.S. Cole, C.L. Jackson, D.M. Kurnit, and S.K. Karathanasis, *Distribution of apolipoprotein A-I, C-II, C-III, and E mRNA in fetal human tissues. Time-dependent induction of apolipoprotein E mRNA by cultures of human monocyte-macrophages.* Biochemistry, 1985. **24**(16): p. 4450-5.
120. Elshourbagy, N.A., W.S. Liao, R.W. Mahley, and J.M. Taylor, *Apolipoprotein E mRNA is abundant in the brain and adrenals, as well as in the liver, and is*

present in other peripheral tissues of rats and marmosets. Proc Natl Acad Sci U S A, 1985. **82**(1): p. 203-7.
121. Wallis, S.C., S. Rogne, L. Gill, A. Markham, M. Edge, D. Woods, R. Williamson, and S. Humphries, *The isolation of cDNA clones for human apolipoprotein E and the detection of apoE RNA in hepatic and extra-hepatic tissues.* The EMBO Journal, 1983. **2**(12): p. 2369-2373.
122. Boyles, J.K., R.E. Pitas, E. Wilson, R.W. Mahley, and J.M. Taylor, *Apolipoprotein E associated with astrocytic glia of the central nervous system and with nonmyelinating glia of the peripheral nervous system.* J Clin Invest, 1985. **76**(4): p. 1501-13.
123. Han, S.H., G. Einstein, K.H. Weisgraber, W.J. Strittmatter, A.M. Saunders, M. Pericak-Vance, A.D. Roses, and D.E. Schmechel, *Apolipoprotein E is localized to the cytoplasm of human cortical neurons: a light and electron microscopic study.* J Neuropathol Exp Neurol, 1994. **53**(5): p. 535-44.
124. Metzger, R.E., M.J. LaDu, J.B. Pan, G.S. Getz, D.E. Frail, and M.T. Falduto, *Neurons of the human frontal cortex display apolipoprotein E immunoreactivity: implications for Alzheimer's disease.* J Neuropathol Exp Neurol, 1996. **55**(3): p. 372-80.
125. Xu, P.T., J.R. Gilbert, H.L. Qiu, J. Ervin, T.R. Rothrock-Christian, C. Hulette, and D.E. Schmechel, *Specific regional transcription of apolipoprotein E in human brain neurons.* Am J Pathol, 1999. **154**(2): p. 601-11.
126. Xu, Q., A. Bernardo, D. Walker, T. Kanegawa, R.W. Mahley, and Y. Huang, *Profile and regulation of apolipoprotein E (ApoE) expression in the CNS in mice with targeting of green fluorescent protein gene to the ApoE locus.* J Neurosci, 2006. **26**(19): p. 4985-94.
127. Pitas, R.E., J.K. Boyles, S.H. Lee, D. Hui, and K.H. Weisgraber, *Lipoproteins and their receptors in the central nervous system. Characterization of the lipoproteins in cerebrospinal fluid and identification of apolipoprotein B,E(LDL) receptors in the brain.* Journal of Biological Chemistry, 1987. **262**(29): p. 14352-14360.
128. Roheim, P.S., M. Carey, T. Forte, and G.L. Vega, *Apolipoproteins in human cerebrospinal fluid.* Proceedings of the National Academy of Sciences, 1979. **76**(9): p. 4646-4649.
129. Demeester, N., G. Castro, C. Desrumaux, C. De Geitere, J.C. Fruchart, P. Santens, E. Mulleners, S. Engelborghs, P.P. De Deyn, J. Vandekerckhove, M. Rosseneu, and C. Labeur, *Characterization and functional studies of lipoproteins, lipid transfer proteins, and lecithin:cholesterol acyltransferase in CSF of normal individuals and patients with Alzheimer's disease.* J Lipid Res, 2000. **41**(6): p. 963-74.
130. Carlsson, J., V.W. Armstrong, H. Reiber, K. Felgenhauer, and D. Seidel, *Clinical relevance of the quantification of apolipoprotein E in cerebrospinal fluid.* Clin Chim Acta, 1991. **196**(2-3): p. 167-76.
131. Song, H., K. Saito, M. Seishima, A. Noma, K. Urakami, and K. Nakashima, *Cerebrospinal fluid apo E and apo A-I concentrations in early- and late-onset Alzheimer's disease.* Neurosci Lett, 1997. **231**(3): p. 175-8.
132. Lindh, M., M. Blomberg, M. Jensen, H. Basun, L. Lannfelt, B. Engvall, H. Scharnagel, W. Marz, L.O. Wahlund, and R.F. Cowburn, *Cerebrospinal fluid*

apolipoprotein E (apoE) levels in Alzheimer's disease patients are increased at follow up and show a correlation with levels of tau protein. Neurosci Lett, 1997. **229**(2): p. 85-8.
133. Skoog, I., C. Hesse, P. Fredman, L.A. Andreasson, B. Palmertz, and K. Blennow, *Apolipoprotein E in cerebrospinal fluid in 85-year-old subjects. Relation to dementia, apolipoprotein E polymorphism, cerebral atrophy, and white matter lesions.* Arch Neurol, 1997. **54**(3): p. 267-72.
134. Fukuyama, R., T. Mizuno, S. Mori, K. Yanagisawa, K. Nakajima, and S. Fushiki, *Age-Dependent Decline in the Apolipoprotein E Level in Cerebrospinal Fluid from Control Subjects and Its Increase in Cerebrospinal Fluid from Patients with Alzheimer's Disease.* European Neurology, 2000. **43**(3): p. 161-169.
135. Toledo, J.B., X. Da, M.W. Weiner, D.A. Wolk, S.X. Xie, S.E. Arnold, C. Davatzikos, L.M. Shaw, and J.Q. Trojanowski, *CSF Apo-E levels associate with cognitive decline and MRI changes.* Acta Neuropathol, 2014. **127**(5): p. 621-32.
136. Shafaati, M., A. Solomon, M. Kivipelto, I. Bjorkhem, and V. Leoni, *Levels of ApoE in cerebrospinal fluid are correlated with Tau and 24S-hydroxycholesterol in patients with cognitive disorders.* Neurosci Lett, 2007. **425**(2): p. 78-82.
137. Lefranc, D., P. Vermersch, J. Dallongeville, C. Daems-Monpeurt, H. Petit, and A. Delacourte, *Relevance of the quantification of apolipoprotein E in the cerebrospinal fluid in Alzheimer's disease.* Neurosci Lett, 1996. **212**(2): p. 91-4.
138. Hahne, S., C. Nordstedt, A. Ahlin, and H. Nyback, *Levels of cerebrospinal fluid apolipoprotein E in patients with Alzheimer's disease and healthy controls.* Neurosci Lett, 1997. **224**(2): p. 99-102.
139. Wahrle, S.E., A.R. Shah, A.M. Fagan, S. Smemo, J.S. Kauwe, A. Grupe, A. Hinrichs, K. Mayo, H. Jiang, L.J. Thal, A.M. Goate, and D.M. Holtzman, *Apolipoprotein E levels in cerebrospinal fluid and the effects of ABCA1 polymorphisms.* Mol Neurodegener, 2007. **2**: p. 7.
140. Kandimalla, R.J., W.Y. Wani, R. Anand, A. Kaushal, S. Prabhakar, V.K. Grover, N. Bharadwaj, K. Jain, and K.D. Gill, *Apolipoprotein E levels in the cerebrospinal fluid of north Indian patients with Alzheimer's disease.* Am J Alzheimers Dis Other Demen, 2013. **28**(3): p. 258-62.
141. Martinez-Morillo, E., O. Hansson, Y. Atagi, G. Bu, L. Minthon, E.P. Diamandis, and H.M. Nielsen, *Total apolipoprotein E levels and specific isoform composition in cerebrospinal fluid and plasma from Alzheimer's disease patients and controls.* Acta Neuropathol, 2014. **127**(5): p. 633-43.
142. Talwar, P., J. Sinha, S. Grover, R. Agarwal, S. Kushwaha, M.V. Srivastava, and R. Kukreti, *Meta-analysis of apolipoprotein E levels in the cerebrospinal fluid of patients with Alzheimer's disease.* J Neurol Sci, 2016. **360**: p. 179-87.
143. Pfrieger, F.W., *Cholesterol homeostasis and function in neurons of the central nervous system.* Cell Mol Life Sci, 2003. **60**(6): p. 1158-71.
144. Poirier, J., *Apolipoprotein E in the brain and its role in Alzheimer's disease.* J Psychiatry Neurosci, 1996. **21**(2): p. 128-34.
145. Poirier, J., A. Baccichet, D. Dea, and S. Gauthier, *Cholesterol synthesis and lipoprotein reuptake during synaptic remodelling in hippocampus in adult rats.* Neuroscience, 1993. **55**(1): p. 81-90.

146. Poirier, J., M. Hess, P.C. May, and C.E. Finch, *Astrocytic apolipoprotein E mRNA and GFAP mRNA in hippocampus after entorhinal cortex lesioning.* Brain Res Mol Brain Res, 1991. **11**(2): p. 97-106.
147. Guillaume, D., P. Bertrand, D. Dea, J. Davignon, and J. Poirier, *Apolipoprotein E and low-density lipoprotein binding and internalization in primary cultures of rat astrocytes: isoform-specific alterations.* J Neurochem, 1996. **66**(6): p. 2410-8.
148. Han, X., H. Cheng, J.D. Fryer, A.M. Fagan, and D.M. Holtzman, *Novel role for apolipoprotein E in the central nervous system. Modulation of sulfatide content.* J Biol Chem, 2003. **278**(10): p. 8043-51.
149. Nathan, B.P., S. Bellosta, D.A. Sanan, K.H. Weisgraber, R.W. Mahley, and R.E. Pitas, *Differential effects of apolipoproteins E3 and E4 on neuronal growth in vitro.* Science, 1994. **264**(5160): p. 850-2.
150. Bellosta, S., B.P. Nathan, M. Orth, L.M. Dong, R.W. Mahley, and R.E. Pitas, *Stable expression and secretion of apolipoproteins E3 and E4 in mouse neuroblastoma cells produces differential effects on neurite outgrowth.* J Biol Chem, 1995. **270**(45): p. 27063-71.
151. Holtzman, D.M., R.E. Pitas, J. Kilbridge, B. Nathan, R.W. Mahley, G. Bu, and A.L. Schwartz, *Low density lipoprotein receptor-related protein mediates apolipoprotein E-dependent neurite outgrowth in a central nervous system-derived neuronal cell line.* Proc Natl Acad Sci U S A, 1995. **92**(21): p. 9480-4.
152. Pitas, R.E., Z.S. Ji, K.H. Weisgraber, and R.W. Mahley, *Role of apolipoprotein E in modulating neurite outgrowth: potential effect of intracellular apolipoprotein E.* Biochem Soc Trans, 1998. **26**(2): p. 257-62.
153. Masliah, E., M. Mallory, N. Ge, M. Alford, I. Veinbergs, and A.D. Roses, *Neurodegeneration in the central nervous system of apoE-deficient mice.* Exp Neurol, 1995. **136**(2): p. 107-22.
154. Oitzl, M.S., M. Mulder, P.J. Lucassen, L.M. Havekes, J. Grootendorst, and E.R. de Kloet, *Severe learning deficits in apolipoprotein E-knockout mice in a water maze task.* Brain Res, 1997. **752**(1-2): p. 189-96.
155. Gordon, I., E. Grauer, I. Genis, E. Sehayek, and D.M. Michaelson, *Memory deficits and cholinergic impairments in apolipoprotein E-deficient mice.* Neurosci Lett, 1995. **199**(1): p. 1-4.
156. Fisher, A., R. Brandeis, S. Chapman, Z. Pittel, and D.M. Michaelson, *M1 Muscarinic Agonist Treatment Reverses Cognitive and Cholinergic Impairments of Apolipoprotein E-Deficient Mice.* Journal of Neurochemistry, 1998. **70**(5): p. 1991-1997.
157. Masliah, E., W. Samuel, I. Veinbergs, M. Mallory, M. Mante, and T. Saitoh, *Neurodegeneration and cognitive impairment in apoE-deficient mice is ameliorated by infusion of recombinant apoE.* Brain Res, 1997. **751**(2): p. 307-14.
158. Fagan, A.M., B.A. Murphy, S.N. Patel, J.F. Kilbridge, W.C. Mobley, G. Bu, and D.M. Holtzman, *Evidence for normal aging of the septo-hippocampal cholinergic system in apoE (-/-) mice but impaired clearance of axonal degeneration products following injury.* Exp Neurol, 1998. **151**(2): p. 314-25.
159. Bronfman, F.C., I. Tesseur, M.H. Hofker, L.M. Havekens, and F. Van Leuven, *No evidence for cholinergic problems in apolipoprotein E knockout and apolipoprotein E4 transgenic mice.* Neuroscience, 2000. **97**(3): p. 411-8.

160. Anderson, R. and A.G. Higgins, *Absence of central cholinergic deficits in ApoE knockout mice.* Psychopharmacology, 1997. **132**(2): p. 135-144.
161. Hartman, R.E., D.F. Wozniak, A. Nardi, J.W. Olney, L. Sartorius, and D.M. Holtzman, *Behavioral phenotyping of GFAP-apoE3 and -apoE4 transgenic mice: apoE4 mice show profound working memory impairments in the absence of Alzheimer's-like neuropathology.* Exp Neurol, 2001. **170**(2): p. 326-44.
162. Champagne, D., J.B. Dupuy, J. Rochford, and J. Poirier, *Apolipoprotein E knockout mice display procedural deficits in the Morris water maze: analysis of learning strategies in three versions of the task.* Neuroscience, 2002. **114**(3): p. 641-54.
163. Anderson, R., J.C. Barnes, T.V. Bliss, D.P. Cain, K. Cambon, H.A. Davies, M.L. Errington, L.A. Fellows, R.A. Gray, T. Hoh, M. Stewart, C.H. Large, and G.A. Higgins, *Behavioural, physiological and morphological analysis of a line of apolipoprotein E knockout mouse.* Neuroscience, 1998. **85**(1): p. 93-110.
164. Valastro, B., O. Ghribi, J. Poirier, P. Krzywkowski, and G. Massicotte, *AMPA receptor regulation and LTP in the hippocampus of young and aged apolipoprotein E-deficient mice.* Neurobiol Aging, 2001. **22**(1): p. 9-15.
165. Cambon, K., H.A. Davies, and M.G. Stewart, *Synaptic loss is accompanied by an increase in synaptic area in the dentate gyrus of aged human apolipoprotein E4 transgenic mice.* Neuroscience, 2000. **97**(4): p. 685-92.
166. White, F., J.A. Nicoll, and K. Horsburgh, *Alterations in ApoE and ApoJ in relation to degeneration and regeneration in a mouse model of entorhinal cortex lesion.* Exp Neurol, 2001. **169**(2): p. 307-18.
167. Huang, Z., C. Cheng, L. Jiang, Z. Yu, F. Cao, J. Zhong, Z. Guo, and X. Sun, *Intraventricular apolipoprotein ApoJ infusion acts protectively in Traumatic Brain Injury.* J Neurochem, 2016. **136**(5): p. 1017-25.
168. Iwata, A., K.D. Browne, X.H. Chen, T. Yuguchi, and D.H. Smith, *Traumatic brain injury induces biphasic upregulation of ApoE and ApoJ protein in rats.* J Neurosci Res, 2005. **82**(1): p. 103-14.
169. Utermann, G., M. Hees, and A. Steinmetz, *Polymorphism of apolipoprotein E and occurrence of dysbetalipoproteinaemia in man.* Nature, 1977. **269**(5629): p. 604-607.
170. Farrer, L.A., L.A. Cupples, J.L. Haines, B. Hyman, W.A. Kukull, R. Mayeux, R.H. Myers, M.A. Pericak-Vance, N. Risch, and C.M. van Duijn, *Effects of age, sex, and ethnicity on the association between apolipoprotein E genotype and Alzheimer disease. A meta-analysis. APOE and Alzheimer Disease Meta Analysis Consortium.* Jama, 1997. **278**(16): p. 1349-56.
171. Corder, E.H., A.M. Saunders, W.J. Strittmatter, D.E. Schmechel, P.C. Gaskell, G.W. Small, A.D. Roses, J.L. Haines, and M.A. Pericak-Vance, *Gene dose of apolipoprotein E type 4 allele and the risk of Alzheimer's disease in late onset families.* Science, 1993. **261**(5123): p. 921-3.
172. Caselli, R.J., E.M. Reiman, D.E. Locke, M.L. Hutton, J.G. Hentz, C. Hoffman-Snyder, B.K. Woodruff, G.E. Alexander, and D. Osborne, *Cognitive domain decline in healthy apolipoprotein E epsilon4 homozygotes before the diagnosis of mild cognitive impairment.* Arch Neurol, 2007. **64**(9): p. 1306-11.

173. Caselli, R.J., E.M. Reiman, D. Osborne, J.G. Hentz, L.C. Baxter, J.L. Hernandez, and G.G. Alexander, *Longitudinal changes in cognition and behavior in asymptomatic carriers of the APOE e4 allele.* Neurology, 2004. **62**(11): p. 1990-5.
174. Caselli, R.J., A.C. Dueck, D. Osborne, M.N. Sabbagh, D.J. Connor, G.L. Ahern, L.C. Baxter, S.Z. Rapcsak, J. Shi, B.K. Woodruff, D.E. Locke, C.H. Snyder, G.E. Alexander, R. Rademakers, and E.M. Reiman, *Longitudinal modeling of age-related memory decline and the APOE epsilon4 effect.* N Engl J Med, 2009. **361**(3): p. 255-63.
175. Caselli, R.J., A.C. Dueck, D.E. Locke, C.R. Hoffman-Snyder, B.K. Woodruff, S.Z. Rapcsak, and E.M. Reiman, *Longitudinal modeling of frontal cognition in APOE epsilon4 homozygotes, heterozygotes, and noncarriers.* Neurology, 2011. **76**(16): p. 1383-8.
176. Schiepers, O.J.G., S.E. Harris, A.J. Gow, A. Pattie, C.E. Brett, J.M. Starr, and I.J. Deary, *APOE E4 status predicts age-related cognitive decline in the ninth decade: longitudinal follow-up of the Lothian Birth Cohort 1921.* Mol Psychiatry, 2012. **17**(3): p. 315-324.
177. Lim, Y.Y., V.L. Villemagne, S.M. Laws, R.H. Pietrzak, P.J. Snyder, D. Ames, K.A. Ellis, K. Harrington, A. Rembach, R.N. Martins, C.C. Rowe, C.L. Masters, and P. Maruff, *APOE and BDNF polymorphisms moderate amyloid [beta]-related cognitive decline in preclinical Alzheimer/'s disease.* Mol Psychiatry, 2015. **20**(11): p. 1322-1328.
178. Lim, Y.Y., V.L. Villemagne, R.H. Pietrzak, D. Ames, K.A. Ellis, K. Harrington, P.J. Snyder, R.N. Martins, C.L. Masters, C.C. Rowe, and P. Maruff, *APOE epsilon4 moderates amyloid-related memory decline in preclinical Alzheimer's disease.* Neurobiol Aging, 2015. **36**(3): p. 1239-44.
179. Ramakers, I.H., P.J. Visser, P. Aalten, O. Bekers, K. Sleegers, C.L. van Broeckhoven, J. Jolles, and F.R. Verhey, *The association between APOE genotype and memory dysfunction in subjects with mild cognitive impairment is related to age and Alzheimer pathology.* Dement Geriatr Cogn Disord, 2008. **26**(2): p. 101-8.
180. Dik, M.G., C. Jonker, L.M. Bouter, M.I. Geerlings, G.J. van Kamp, and D.J.H. Deeg, *APOE-ε4 is associated with memory decline in cognitively impaired elderly.* Neurology, 2000. **54**(7): p. 1492-1497.
181. Whitehair, D.C., A. Sherzai, J. Emond, R. Raman, P.S. Aisen, R.C. Petersen, and A.S. Fleisher, *Influence of Apolipoprotein E ε4 on rates of cognitive and functional decline in mild cognitive impairment.* Alzheimer's & dementia : the journal of the Alzheimer's Association, 2010. **6**(5): p. 412-419.
182. Cosentino, S., N. Scarmeas, E. Helzner, M.M. Glymour, J. Brandt, M. Albert, D. Blacker, and Y. Stern, *APOE epsilon 4 allele predicts faster cognitive decline in mild Alzheimer disease.* Neurology, 2008. **70**(19 Pt 2): p. 1842-9.
183. Martins, C.A., A. Oulhaj, C.A. de Jager, and J.H. Williams, *APOE alleles predict the rate of cognitive decline in Alzheimer disease: a nonlinear model.* Neurology, 2005. **65**(12): p. 1888-93.
184. Craft, S., L. Teri, S.D. Edland, W.A. Kukull, G. Schellenberg, W.C. McCormick, J.D. Bowen, and E.B. Larson, *Accelerated decline in apolipoprotein E-epsilon4 homozygotes with Alzheimer's disease.* Neurology, 1998. **51**(1): p. 149-53.

185. Carrasquillo, M.M., J.E. Crook, O. Pedraza, C.S. Thomas, V.S. Pankratz, M. Allen, T. Nguyen, K.G. Malphrus, L. Ma, G.D. Bisceglio, R.O. Roberts, J.A. Lucas, G.E. Smith, R.J. Ivnik, M.M. Machulda, N.R. Graff-Radford, R.C. Petersen, S.G. Younkin, and N. Ertekin-Taner, *Late-onset Alzheimer's risk variants in memory decline, incident mild cognitive impairment, and Alzheimer's disease.* Neurobiol Aging, 2015. **36**(1): p. 60-7.
186. Hirono, N., M. Hashimoto, M. Yasuda, H. Kazui, and E. Mori, *Accelerated memory decline in Alzheimer's disease with apolipoprotein epsilon4 allele.* J Neuropsychiatry Clin Neurosci, 2003. **15**(3): p. 354-8.
187. Murphy, G.M., Jr., J. Taylor, H.C. Kraemer, J. Yesavage, and J.R. Tinklenberg, *No association between apolipoprotein E epsilon 4 allele and rate of decline in Alzheimer's disease.* Am J Psychiatry, 1997. **154**(5): p. 603-8.
188. Gomez-Isla, T., H.L. West, G.W. Rebeck, S.D. Harr, J.H. Growdon, J.J. Locascio, T.T. Perls, L.A. Lipsitz, and B.T. Hyman, *Clinical and pathological correlates of apolipoprotein E epsilon 4 in Alzheimer's disease.* Ann Neurol, 1996. **39**(1): p. 62-70.
189. Kleiman, T., K. Zdanys, B. Black, T. Rightmer, M. Grey, K. Garman, M. Macavoy, J. Gelernter, and C. van Dyck, *Apolipoprotein E epsilon4 allele is unrelated to cognitive or functional decline in Alzheimer's disease: retrospective and prospective analysis.* Dement Geriatr Cogn Disord, 2006. **22**(1): p. 73-82.
190. Shinohara, M., T. Kanekiyo, L. Yang, D. Linthicum, M. Shinohara, Y. Fu, L. Price, J.L. Frisch-Daiello, X. Han, J.D. Fryer, and G. Bu, *APOE2 eases cognitive decline during Aging: Clinical and preclinical evaluations.* Ann Neurol, 2016.
191. Chen, J., H. Shu, Z. Wang, D. Liu, Y. Shi, L. Xu, and Z. Zhang, *Protective effect of APOE epsilon 2 on intrinsic functional connectivity of the entorhinal cortex is associated with better episodic memory in elderly individuals with risk factors for Alzheimer's disease.* Oncotarget, 2016.
192. Wilson, R., J. Bienias, E. Berry-Kravis, D. Evans, and D. Bennett, *The apolipoprotein E ε2 allele and decline in episodic memory.* J Neurol Neurosurg Psychiatry, 2002. **73**(6): p. 672-7.
193. Kerchner, G.A., D. Berdnik, J.C. Shen, J.D. Bernstein, M.C. Fenesy, G.K. Deutsch, T. Wyss-Coray, and B.K. Rutt, *APOE epsilon4 worsens hippocampal CA1 apical neuropil atrophy and episodic memory.* Neurology, 2014. **82**(8): p. 691-7.
194. Manning, E.N., J. Barnes, D.M. Cash, J.W. Bartlett, K.K. Leung, S. Ourselin, and N.C. Fox, *APOE epsilon4 is associated with disproportionate progressive hippocampal atrophy in AD.* PLoS One, 2014. **9**(5): p. e97608.
195. Liu, Y., T. Paajanen, E. Westman, L.O. Wahlund, A. Simmons, C. Tunnard, T. Sobow, P. Proitsi, J. Powell, P. Mecocci, M. Tsolaki, B. Vellas, S. Muehlboeck, A. Evans, C. Spenger, S. Lovestone, and H. Soininen, *Effect of APOE epsilon4 allele on cortical thicknesses and volumes: the AddNeuroMed study.* J Alzheimers Dis, 2010. **21**(3): p. 947-66.
196. Gispert, J.D., L. Rami, G. Sanchez-Benavides, C. Falcon, A. Tucholka, S. Rojas, and J.L. Molinuevo, *Nonlinear cerebral atrophy patterns across the Alzheimer's disease continuum: impact of APOE4 genotype.* Neurobiol Aging, 2015. **36**(10): p. 2687-701.

197. Espeseth, T., L.T. Westlye, A.M. Fjell, K.B. Walhovd, H. Rootwelt, and I. Reinvang, *Accelerated age-related cortical thinning in healthy carriers of apolipoprotein E epsilon 4.* Neurobiol Aging, 2008. **29**(3): p. 329-40.
198. Fennema-Notestine, C., M.S. Panizzon, W.R. Thompson, C.H. Chen, L.T. Eyler, B. Fischl, C.E. Franz, M.D. Grant, A.J. Jak, T.L. Jernigan, M.J. Lyons, M.C. Neale, L.J. Seidman, M.T. Tsuang, H. Xian, A.M. Dale, and W.S. Kremen, *Presence of ApoE epsilon4 allele associated with thinner frontal cortex in middle age.* J Alzheimers Dis, 2011. **26 Suppl 3**: p. 49-60.
199. Burggren, A.C., M.M. Zeineh, A.D. Ekstrom, M.N. Braskie, P.M. Thompson, G.W. Small, and S.Y. Bookheimer, *Reduced cortical thickness in hippocampal subregions among cognitively normal apolipoprotein E e4 carriers.* Neuroimage, 2008. **41**(4): p. 1177-83.
200. Dean, D.C., 3rd, B.A. Jerskey, K. Chen, H. Protas, P. Thiyyagura, A. Roontiva, J. O'Muircheartaigh, H. Dirks, N. Waskiewicz, K. Lehman, A.L. Siniard, M.N. Turk, X. Hua, S.K. Madsen, P.M. Thompson, A.S. Fleisher, M.J. Huentelman, S.C. Deoni, and E.M. Reiman, *Brain differences in infants at differential genetic risk for late-onset Alzheimer disease: a cross-sectional imaging study.* JAMA Neurol, 2014. **71**(1): p. 11-22.
201. Bartzokis, G., P.H. Lu, D.H. Geschwind, N. Edwards, J. Mintz, and J.L. Cummings, *Apolipoprotein E genotype and age-related myelin breakdown in healthy individuals: implications for cognitive decline and dementia.* Arch Gen Psychiatry, 2006. **63**(1): p. 63-72.
202. Shaw, P., J.P. Lerch, J.C. Pruessner, K.N. Taylor, A.B. Rose, D. Greenstein, L. Clasen, A. Evans, J.L. Rapoport, and J.N. Giedd, *Cortical morphology in children and adolescents with different apolipoprotein E gene polymorphisms: an observational study.* Lancet Neurol, 2007. **6**(6): p. 494-500.
203. Chiang, G.C., P.S. Insel, D. Tosun, N. Schuff, D. Truran-Sacrey, S.T. Raptentsetsang, C.R. Jack, Jr., P.S. Aisen, R.C. Petersen, and M.W. Weiner, *Hippocampal atrophy rates and CSF biomarkers in elderly APOE2 normal subjects.* Neurology, 2010. **75**(22): p. 1976-81.
204. Attwell, D. and S.B. Laughlin, *An energy budget for signaling in the grey matter of the brain.* J Cereb Blood Flow Metab, 2001. **21**(10): p. 1133-45.
205. Alle, H., A. Roth, and J.R. Geiger, *Energy-efficient action potentials in hippocampal mossy fibers.* Science, 2009. **325**(5946): p. 1405-8.
206. Hyder, F., D.L. Rothman, and M.R. Bennett, *Cortical energy demands of signaling and nonsignaling components in brain are conserved across mammalian species and activity levels.* Proc Natl Acad Sci U S A, 2013. **110**(9): p. 3549-54.
207. Dick, A.P., S.I. Harik, A. Klip, and D.M. Walker, *Identification and characterization of the glucose transporter of the blood-brain barrier by cytochalasin B binding and immunological reactivity.* Proc Natl Acad Sci U S A, 1984. **81**(22): p. 7233-7.
208. Virgintino, D., D. Robertson, P. Monaghan, M. Errede, M. Bertossi, G. Ambrosi, and L. Roncali, *Glucose transporter GLUT1 in human brain microvessels revealed by ultrastructural immunocytochemistry.* J Submicrosc Cytol Pathol, 1997. **29**(3): p. 365-70.

209. Farrell, C.L., J. Yang, and W.M. Pardridge, *GLUT-1 glucose transporter is present within apical and basolateral membranes of brain epithelial interfaces and in microvascular endothelia with and without tight junctions.* J Histochem Cytochem, 1992. **40**(2): p. 193-9.
210. Maher, F., S.J. Vannucci, and I.A. Simpson, *Glucose transporter proteins in brain.* Faseb j, 1994. **8**(13): p. 1003-11.
211. Leino, R.L., D.Z. Gerhart, A.M. van Bueren, A.L. McCall, and L.R. Drewes, *Ultrastructural localization of GLUT 1 and GLUT 3 glucose transporters in rat brain.* J Neurosci Res, 1997. **49**(5): p. 617-26.
212. Morgello, S., R.R. Uson, E.J. Schwartz, and R.S. Haber, *The human blood-brain barrier glucose transporter (GLUT1) is a glucose transporter of gray matter astrocytes.* Glia, 1995. **14**(1): p. 43-54.
213. Zeller, K., S. Rahner-Welsch, and W. Kuschinsky, *Distribution of Glut1 glucose transporters in different brain structures compared to glucose utilization and capillary density of adult rat brains.* J Cereb Blood Flow Metab, 1997. **17**(2): p. 204-9.
214. Young, J.K. and J.C. McKenzie, *GLUT2 Immunoreactivity in Gomori-positive Astrocytes of the Hypothalamus.* J Histochem Cytochem, 2004. **52**(11): p. 1519-24.
215. Leloup, C., M. Arluison, N. Lepetit, N. Cartier, P. Marfaing-Jallat, P. Ferre, and L. Penicaud, *Glucose transporter 2 (GLUT 2): expression in specific brain nuclei.* Brain Res, 1994. **638**(1-2): p. 221-6.
216. Li, B., X. Xi, D.S. Roane, D.H. Ryan, and R.J. Martin, *Distribution of glucokinase, glucose transporter GLUT2, sulfonylurea receptor-1, glucagon-like peptide-1 receptor and neuropeptide Y messenger RNAs in rat brain by quantitative real time RT-PCR.* Brain Res Mol Brain Res, 2003. **113**(1-2): p. 139-42.
217. Arluison, M., M. Quignon, P. Nguyen, B. Thorens, C. Leloup, and L. Penicaud, *Distribution and anatomical localization of the glucose transporter 2 (GLUT2) in the adult rat brain--an immunohistochemical study.* J Chem Neuroanat, 2004. **28**(3): p. 117-36.
218. Arluison, M., M. Quignon, B. Thorens, C. Leloup, and L. Penicaud, *Immunocytochemical localization of the glucose transporter 2 (GLUT2) in the adult rat brain. II. Electron microscopic study.* J Chem Neuroanat, 2004. **28**(3): p. 137-46.
219. Brant, A.M., T.J. Jess, G. Milligan, C.M. Brown, and G.W. Gould, *Immunological analysis of glucose transporters expressed in different regions of the rat brain and central nervous system.* Biochem Biophys Res Commun, 1993. **192**(3): p. 1297-302.
220. Nagamatsu, S., H. Sawa, K. Kamada, Y. Nakamichi, K. Yoshimoto, and T. Hoshino, *Neuron-specific glucose transporter (NSGT): CNS distribution of GLUT3 rat glucose transporter (RGT3) in rat central neurons.* FEBS Lett, 1993. **334**(3): p. 289-95.
221. Gerhart, D.Z., R.L. Leino, N.D. Borson, W.E. Taylor, K.M. Gronlund, A.L. McCall, and L.R. Drewes, *Localization of glucose transporter GLUT 3 in brain:*

comparison of rodent and dog using species-specific carboxyl-terminal antisera. Neuroscience, 1995. **66**(1): p. 237-46.
222. McCall, A.L., A.M. Van Bueren, M. Moholt-Siebert, N.J. Cherry, and W.R. Woodward, *Immunohistochemical localization of the neuron-specific glucose transporter (GLUT3) to neuropil in adult rat brain.* Brain Research, 1994. **659**(1–2): p. 292-297.
223. Uemura, E. and H.W. Greenlee, *Insulin regulates neuronal glucose uptake by promoting translocation of glucose transporter GLUT3.* Experimental Neurology, 2006. **198**(1): p. 48-53.
224. Leloup, C., M. Arluison, N. Kassis, N. Lepetit, N. Cartier, P. Ferre, and L. Penicaud, *Discrete brain areas express the insulin-responsive glucose transporter GLUT4.* Brain Res Mol Brain Res, 1996. **38**(1): p. 45-53.
225. Vannucci, S.J., E.M. Koehler-Stec, K. Li, T.H. Reynolds, R. Clark, and I.A. Simpson, *GLUT4 glucose transporter expression in rodent brain: effect of diabetes.* Brain Res, 1998. **797**(1): p. 1-11.
226. Kobayashi, M., H. Nikami, M. Morimatsu, and M. Saito, *Expression and localization of insulin-regulatable glucose transporter (GLUT4) in rat brain.* Neuroscience Letters, 1996. **213**(2): p. 103-106.
227. El Messari, S., C. Leloup, M. Quignon, M.J. Brisorgueil, L. Penicaud, and M. Arluison, *Immunocytochemical localization of the insulin-responsive glucose transporter 4 (Glut4) in the rat central nervous system.* J Comp Neurol, 1998. **399**(4): p. 492-512.
228. Marks, J.L., D. Porte, Jr., W.L. Stahl, and D.G. Baskin, *Localization of insulin receptor mRNA in rat brain by in situ hybridization.* Endocrinology, 1990. **127**(6): p. 3234-6.
229. Campbell, I.W., A.F. Dominiczak, C. Livingstone, and G.W. Gould, *Analysis of the glucose transporter compliment of metabolically important tissues from the Milan hypertensive rat.* Biochem Biophys Res Commun, 1995. **211**(3): p. 780-91.
230. Komori, T., Y. Morikawa, S. Tamura, A. Doi, K. Nanjo, and E. Senba, *Subcellular localization of glucose transporter 4 in the hypothalamic arcuate nucleus of ob/ob mice under basal conditions.* Brain Res, 2005. **1049**(1): p. 34-42.
231. Benomar, Y., N. Naour, A. Aubourg, V. Bailleux, A. Gertler, J. Djiane, M. Guerre-Millo, and M. Taouis, *Insulin and leptin induce Glut4 plasma membrane translocation and glucose uptake in a human neuronal cell line by a phosphatidylinositol 3-kinase- dependent mechanism.* Endocrinology, 2006. **147**(5): p. 2550-6.
232. Vissing, J., M. Andersen, and N.H. Diemer, *Exercise-induced changes in local cerebral glucose utilization in the rat.* J Cereb Blood Flow Metab, 1996. **16**(4): p. 729-36.
233. Burant, C.F., J. Takeda, E. Brot-Laroche, G.I. Bell, and N.O. Davidson, *Fructose transporter in human spermatozoa and small intestine is GLUT5.* J Biol Chem, 1992. **267**(21): p. 14523-6.
234. Mantych, G.J., D.E. James, and S.U. Devaskar, *Jejunal/kidney glucose transporter isoform (Glut-5) is expressed in the human blood-brain barrier.* Endocrinology, 1993. **132**(1): p. 35-40.

235. Funari, V.A., V.L.M. Herrera, D. Freeman, and D.R. Tolan, *Genes required for fructose metabolism are expressed in Purkinje cells in the cerebellum.* Molecular Brain Research, 2005. **142**(2): p. 115-122.
236. Shu, H.J., K. Isenberg, R.J. Cormier, A. Benz, and C.F. Zorumski, *Expression of fructose sensitive glucose transporter in the brains of fructose-fed rats.* Neuroscience, 2006. **140**(3): p. 889-95.
237. Hassel, B., A. Elsais, A.S. Froland, E. Tauboll, L. Gjerstad, Y. Quan, R. Dingledine, and F. Rise, *Uptake and metabolism of fructose by rat neocortical cells in vivo and by isolated nerve terminals in vitro.* J Neurochem, 2015. **133**(4): p. 572-81.
238. Reagan, L.P., D.R. Rosell, S.E. Alves, E.K. Hoskin, A.L. McCall, M.J. Charron, and B.S. McEwen, *GLUT8 glucose transporter is localized to excitatory and inhibitory neurons in the rat hippocampus.* Brain Res, 2002. **932**(1-2): p. 129-34.
239. Ibberson, M., B.M. Riederer, M. Uldry, B. Guhl, J. Roth, and B. Thorens, *Immunolocalization of GLUTX1 in the testis and to specific brain areas and vasopressin-containing neurons.* Endocrinology, 2002. **143**(1): p. 276-84.
240. Reagan, L.P., N. Gorovits, E.K. Hoskin, S.E. Alves, E.B. Katz, C.A. Grillo, G.G. Piroli, B.S. McEwen, and M.J. Charron, *Localization and regulation of GLUTx1 glucose transporter in the hippocampus of streptozotocin diabetic rats.* Proc Natl Acad Sci U S A, 2001. **98**(5): p. 2820-5.
241. Sankar, R., S. Thamotharan, D. Shin, K.H. Moley, and S.U. Devaskar, *Insulin-responsive glucose transporters-GLUT8 and GLUT4 are expressed in the developing mammalian brain.* Brain Res Mol Brain Res, 2002. **107**(2): p. 157-65.
242. Piroli, G.G., C.A. Grillo, E.K. Hoskin, V. Znamensky, E.B. Katz, T.A. Milner, B.S. McEwen, M.J. Charron, and L.P. Reagan, *Peripheral glucose administration stimulates the translocation of GLUT8 glucose transporter to the endoplasmic reticulum in the rat hippocampus.* J Comp Neurol, 2002. **452**(2): p. 103-14.
243. Piroli, G.G., C.A. Grillo, M.J. Charron, B.S. McEwen, and L.P. Reagan, *Biphasic effects of stress upon GLUT8 glucose transporter expression and trafficking in the diabetic rat hippocampus.* Brain Res, 2004. **1006**(1): p. 28-35.
244. Shin, B.C., R.A. McKnight, and S.U. Devaskar, *Glucose transporter GLUT8 translocation in neurons is not insulin responsive.* J Neurosci Res, 2004. **75**(6): p. 835-44.
245. Widmer, M., M. Uldry, and B. Thorens, *GLUT8 subcellular localization and absence of translocation to the plasma membrane in PC12 cells and hippocampal neurons.* Endocrinology, 2005. **146**(11): p. 4727-36.
246. Wilson, J.E., *Isozymes of mammalian hexokinase: structure, subcellular localization and metabolic function.* J Exp Biol, 2003. **206**(Pt 12): p. 2049-57.
247. Roberts, D.J. and S. Miyamoto, *Hexokinase II integrates energy metabolism and cellular protection: Akting on mitochondria and TORCing to autophagy.* Cell Death Differ, 2015. **22**(2): p. 248-57.
248. Berg JM, T.J., Stryer, *The Glycolytic Pathway Is Tightly Controlled*, in *Biochemistry. 5th edition*. 2002.
249. Vaishnavi, S.N., A.G. Vlassenko, M.M. Rundle, A.Z. Snyder, M.A. Mintun, and M.E. Raichle, *Regional aerobic glycolysis in the human brain.* Proceedings of the National Academy of Sciences, 2010. **107**(41): p. 17757-17762.

250. Goyal, Manu S., M. Hawrylycz, Jeremy A. Miller, Abraham Z. Snyder, and Marcus E. Raichle, *Aerobic Glycolysis in the Human Brain Is Associated with Development and Neotenous Gene Expression.* Cell Metabolism. **19**(1): p. 49-57.
251. Shannon, B.J., S.N. Vaishnavi, A.G. Vlassenko, J.S. Shimony, J. Rutlin, and M.E. Raichle, *Brain aerobic glycolysis and motor adaptation learning.* Proceedings of the National Academy of Sciences, 2016. **113**(26): p. E3782-E3791.
252. Berg JM, T.J., Stryer L., *The Metabolism of Glucose 6-Phosphate by the Pentose Phosphate Pathway Is Coordinated with Glycolysis.*, in *Biochemistry. 5th edition*. 2002.
253. Kletzien, R.F., P.K. Harris, and L.A. Foellmi, *Glucose-6-phosphate dehydrogenase: a "housekeeping" enzyme subject to tissue-specific regulation by hormones, nutrients, and oxidant stress.* Faseb j, 1994. **8**(2): p. 174-81.
254. Ben-Yoseph, O., P.A. Boxer, and B.D. Ross, *Assessment of the role of the glutathione and pentose phosphate pathways in the protection of primary cerebrocortical cultures from oxidative stress.* J Neurochem, 1996. **66**(6): p. 2329-37.
255. Kussmaul, L., B. Hamprecht, and R. Dringen, *The detoxification of cumene hydroperoxide by the glutathione system of cultured astroglial cells hinges on hexose availability for the regeneration of NADPH.* J Neurochem, 1999. **73**(3): p. 1246-53.
256. Garcia-Nogales, P., A. Almeida, and J.P. Bolanos, *Peroxynitrite protects neurons against nitric oxide-mediated apoptosis. A key role for glucose-6-phosphate dehydrogenase activity in neuroprotection.* J Biol Chem, 2003. **278**(2): p. 864-74.
257. Delgado-Esteban, M., A. Almeida, and J.P. Bolanos, *D-Glucose prevents glutathione oxidation and mitochondrial damage after glutamate receptor stimulation in rat cortical primary neurons.* J Neurochem, 2000. **75**(4): p. 1618-24.
258. Berg JM, T.J., Stryer L., *Glycogen Is Synthesized and Degraded by Different Pathways*, in *Biochemistry. 5th edition*. 2002, New York: W H Freeman.
259. Berg JM, T.J., Stryer L., *Glycogen Breakdown Requires the Interplay of Several Enzymes*, in *Biochemistry. 5th edition*. 2002, New York: W H Freeman.
260. Berg JM, T.J., Stryer L., *Phosphorylase Is Regulated by Allosteric Interactions and Reversible Phosphorylation*, in *Biochemistry. 5th edition*. 2002, New York: W H Freeman.
261. Gerhart, D.Z., B.E. Enerson, O.Y. Zhdankina, R.L. Leino, and L.R. Drewes, *Expression of monocarboxylate transporter MCT1 by brain endothelium and glia in adult and suckling rats.* Am J Physiol, 1997. **273**(1 Pt 1): p. E207-13.
262. Leino, R.L., D.Z. Gerhart, and L.R. Drewes, *Monocarboxylate transporter (MCT1) abundance in brains of suckling and adult rats: a quantitative electron microscopic immunogold study.* Brain Res Dev Brain Res, 1999. **113**(1-2): p. 47-54.
263. Pierre, K., L. Pellerin, R. Debernardi, B.M. Riederer, and P.J. Magistretti, *Cell-specific localization of monocarboxylate transporters, MCT1 and MCT2, in the adult mouse brain revealed by double immunohistochemical labeling and confocal microscopy.* Neuroscience, 2000. **100**(3): p. 617-27.

264. Hanu, R., M. McKenna, A. O'Neill, W.G. Resneck, and R.J. Bloch, *Monocarboxylic acid transporters, MCT1 and MCT2, in cortical astrocytes in vitro and in vivo.* Am J Physiol Cell Physiol, 2000. **278**(5): p. C921-30.
265. Debernardi, R., K. Pierre, S. Lengacher, P.J. Magistretti, and L. Pellerin, *Cell-specific expression pattern of monocarboxylate transporters in astrocytes and neurons observed in different mouse brain cortical cell cultures.* J Neurosci Res, 2003. **73**(2): p. 141-55.
266. Pellerin, L., L.H. Bergersen, A.P. Halestrap, and K. Pierre, *Cellular and subcellular distribution of monocarboxylate transporters in cultured brain cells and in the adult brain.* J Neurosci Res, 2005. **79**(1-2): p. 55-64.
267. Pellerin, L., G. Pellegri, J.L. Martin, and P.J. Magistretti, *Expression of monocarboxylate transporter mRNAs in mouse brain: Support for a distinct role of lactate as an energy substrate for the neonatal vs. adult brain.* Proc Natl Acad Sci U S A, 1998. **95**(7): p. 3990-5.
268. Pierre, K., P.J. Magistretti, and L. Pellerin, *MCT2 is a major neuronal monocarboxylate transporter in the adult mouse brain.* J Cereb Blood Flow Metab, 2002. **22**(5): p. 586-95.
269. Gerhart, D.Z., B.E. Enerson, O.Y. Zhdankina, R.L. Leino, and L.R. Drewes, *Expression of the monocarboxylate transporter MCT2 by rat brain glia.* Glia, 1998. **22**(3): p. 272-81.
270. Rafiki, A., J.L. Boulland, A.P. Halestrap, O.P. Ottersen, and L. Bergersen, *Highly differential expression of the monocarboxylate transporters MCT2 and MCT4 in the developing rat brain.* Neuroscience, 2003. **122**(3): p. 677-88.
271. Bergersen, L., A. Rafiki, and O.P. Ottersen, *Immunogold cytochemistry identifies specialized membrane domains for monocarboxylate transport in the central nervous system.* Neurochem Res, 2002. **27**(1-2): p. 89-96.
272. McGarry, J.D. and D.W. Foster, *Regulation of hepatic fatty acid oxidation and ketone body production.* Annu Rev Biochem, 1980. **49**: p. 395-420.
273. Laffel, L., *Ketone bodies: a review of physiology, pathophysiology and application of monitoring to diabetes.* Diabetes Metab Res Rev, 1999. **15**(6): p. 412-26.
274. Owen, O.E., A.P. Morgan, H.G. Kemp, J.M. Sullivan, M.G. Herrera, and G.F. Cahill, *Brain Metabolism during Fasting.* J Clin Invest, 1967. **46**(10): p. 1589-95.
275. Mosconi, L., S. Sorbi, M.J. de Leon, Y. Li, B. Nacmias, P.S. Myoung, W. Tsui, A. Ginestroni, V. Bessi, M. Fayyazz, P. Caffarra, and A. Pupi, *Hypometabolism exceeds atrophy in presymptomatic early-onset familial Alzheimer's disease.* J Nucl Med, 2006. **47**(11): p. 1778-86.
276. Jagust, W., A. Gitcho, F. Sun, B. Kuczynski, D. Mungas, and M. Haan, *Brain imaging evidence of preclinical Alzheimer's disease in normal aging.* Ann Neurol, 2006. **59**(4): p. 673-81.
277. de Leon, M.J., A. Convit, O.T. Wolf, C.Y. Tarshish, S. DeSanti, H. Rusinek, W. Tsui, E. Kandil, A.J. Scherer, A. Roche, A. Imossi, E. Thorn, M. Bobinski, C. Caraos, P. Lesbre, D. Schlyer, J. Poirier, B. Reisberg, and J. Fowler, *Prediction of cognitive decline in normal elderly subjects with 2-[(18)F]fluoro-2-deoxy-d-glucose/positron-emission tomography (FDG/PET).* Proceedings of the National

Academy of Sciences of the United States of America, 2001. **98**(19): p. 10966-10971.
278. Mosconi, L., *Brain glucose metabolism in the early and specific diagnosis of Alzheimer's disease. FDG-PET studies in MCI and AD.* Eur J Nucl Med Mol Imaging, 2005. **32**(4): p. 486-510.
279. Mosconi, L., *Brain glucose metabolism in the early and specific diagnosis of Alzheimer's disease.* European Journal of Nuclear Medicine and Molecular Imaging, 2005. **32**(4): p. 486-510.
280. Reiman, E.M., *Declining brain activity in cognitively normal apolipoprotein E.* 2001. **98**(6): p. 3334-9.
281. Reiman, E.M., K. Chen, G.E. Alexander, R.J. Caselli, D. Bandy, D. Osborne, A.M. Saunders, and J. Hardy, *Correlations between apolipoprotein E ε4 gene dose and brain-imaging measurements of regional hypometabolism.* Proc Natl Acad Sci U S A, 2005. **102**(23): p. 8299-302.
282. Xu, P.T., Y.J. Li, X.J. Qin, C.R. Scherzer, H. Xu, D.E. Schmechel, C.M. Hulette, J. Ervin, S.R. Gullans, J. Haines, M.A. Pericak-Vance, and J.R. Gilbert, *Differences in apolipoprotein E3/3 and E4/4 allele-specific gene expression in hippocampus in Alzheimer disease.* Neurobiol Dis, 2006. **21**(2): p. 256-75.
283. Conejero-Goldberg, C., T.M. Hyde, S. Chen, U. Dreses-Werringloer, M.M. Herman, J.E. Kleinman, P. Davies, and T.E. Goldberg, *Molecular signatures in post-mortem brain tissue of younger individuals at high risk for Alzheimer's disease as based on APOE genotype.* Mol Psychiatry, 2011. **16**(8): p. 836-47.
284. Liang, W.S., E.M. Reiman, J. Valla, T. Dunckley, T.G. Beach, A. Grover, T.L. Niedzielko, L.E. Schneider, D. Mastroeni, R. Caselli, W. Kukull, J.C. Morris, C.M. Hulette, D. Schmechel, J. Rogers, and D.A. Stephan, *Alzheimer's disease is associated with reduced expression of energy metabolism genes in posterior cingulate neurons.* Proc Natl Acad Sci U S A, 2008. **105**(11): p. 4441-6.
285. Valla, J., R. Yaari, A.B. Wolf, Y. Kusne, T.G. Beach, A.E. Roher, J.J. Corneveaux, M.J. Huentelman, R.J. Caselli, and E.M. Reiman, *Reduced posterior cingulate mitochondrial activity in expired young adult carriers of the APOE epsilon4 allele, the major late-onset Alzheimer's susceptibility gene.* J Alzheimers Dis, 2010. **22**(1): p. 307-13.
286. Perkins, M., A.B. Wolf, B. Chavira, D. Shonebarger, J.P. Meckel, L. Leung, L. Ballina, S. Ly, A. Saini, T.B. Jones, J. Vallejo, G. Jentarra, and J. Valla, *Altered Energy Metabolism Pathways in the Posterior Cingulate in Young Adult Apolipoprotein E varepsilon4 Carriers.* J Alzheimers Dis, 2016. **53**(1): p. 95-106.
287. Shenk, J.C., J. Liu, K. Fischbach, K. Xu, M. Puchowicz, M.E. Obrenovich, E. Gasimov, L.M. Alvarez, B.N. Ames, J.C. Lamanna, and G. Aliev, *The effect of acetyl-L-carnitine and R-alpha-lipoic acid treatment in ApoE4 mouse as a model of human Alzheimer's disease.* J Neurol Sci, 2009. **283**(1-2): p. 199-206.
288. Chen, H.K., Z.S. Ji, S.E. Dodson, R.D. Miranda, C.I. Rosenblum, I.J. Reynolds, S.B. Freedman, K.H. Weisgraber, Y. Huang, and R.W. Mahley, *Apolipoprotein E4 domain interaction mediates detrimental effects on mitochondria and is a potential therapeutic target for Alzheimer disease.* J Biol Chem, 2011. **286**(7): p. 5215-21.

289. Harris, F.M., W.J. Brecht, Q. Xu, I. Tesseur, L. Kekonius, T. Wyss-Coray, J.D. Fish, E. Masliah, P.C. Hopkins, K. Scearce-Levie, K.H. Weisgraber, L. Mucke, R.W. Mahley, and Y. Huang, *Carboxyl-terminal-truncated apolipoprotein E4 causes Alzheimer's disease-like neurodegeneration and behavioral deficits in transgenic mice.* Proceedings of the National Academy of Sciences, 2003. **100**(19): p. 10966-10971.
290. Chang, S., T.r. Ma, R.D. Miranda, M.E. Balestra, R.W. Mahley, and Y. Huang, *Lipid- and receptor-binding regions of apolipoprotein E4 fragments act in concert to cause mitochondrial dysfunction and neurotoxicity.* Proceedings of the National Academy of Sciences of the United States of America, 2005. **102**(51): p. 18694-18699.
291. Nakamura, T., A. Watanabe, T. Fujino, T. Hosono, and M. Michikawa, *Apolipoprotein E4 (1-272) fragment is associated with mitochondrial proteins and affects mitochondrial function in neuronal cells.* Mol Neurodegener, 2009. **4**: p. 35.
292. Tambini, M.D., M. Pera, E. Kanter, H. Yang, C. Guardia-Laguarta, D. Holtzman, D. Sulzer, E. Area-Gomez, and E.A. Schon, *ApoE4 upregulates the activity of mitochondria-associated ER membranes.* EMBO Rep, 2016. **17**(1): p. 27-36.
293. Woody, S.K., H. Zhou, S. Ibrahimi, Y. Dong, and L. Zhao, *Human ApoE varepsilon2 Promotes Regulatory Mechanisms of Bioenergetic and Synaptic Function in Female Brain: A Focus on V-type H+-ATPase.* J Alzheimers Dis, 2016. **53**(3): p. 1015-31.
294. Gasior, M., M.A. Rogawski, and A.L. Hartman, *Neuroprotective and disease-modifying effects of the ketogenic diet.* Behav Pharmacol, 2006. **17**(5-6): p. 431-9.
295. McNally, M.A. and A.L. Hartman, *Ketone Bodies in Epilepsy.* J Neurochem, 2012. **121**(1): p. 28-35.
296. Tieu, K., C. Perier, C. Caspersen, P. Teismann, D.C. Wu, S.D. Yan, A. Naini, M. Vila, V. Jackson-Lewis, R. Ramasamy, and S. Przedborski, *D-beta-hydroxybutyrate rescues mitochondrial respiration and mitigates features of Parkinson disease.* J Clin Invest, 2003. **112**(6): p. 892-901.
297. Kashiwaya, Y., T. Takeshima, N. Mori, K. Nakashima, K. Clarke, and R.L. Veech, *D-beta-hydroxybutyrate protects neurons in models of Alzheimer's and Parkinson's disease.* Proc Natl Acad Sci U S A, 2000. **97**(10): p. 5440-4.
298. Bough, K.J., J. Wetherington, B. Hassel, J.F. Pare, J.W. Gawryluk, J.G. Greene, R. Shaw, Y. Smith, J.D. Geiger, and R.J. Dingledine, *Mitochondrial biogenesis in the anticonvulsant mechanism of the ketogenic diet.* Ann Neurol, 2006. **60**(2): p. 223-35.
299. Kim, D.Y., J. Vallejo, and J.M. Rho, *Ketones prevent synaptic dysfunction induced by mitochondrial respiratory complex inhibitors.* J Neurochem, 2010. **114**(1): p. 130-41.
300. Costantini, L.C., L.J. Barr, J.L. Vogel, and S.T. Henderson, *Hypometabolism as a therapeutic target in Alzheimer's disease.* BMC Neurosci, 2008. **9 Suppl 2**: p. S16.
301. Henderson, S.T. and J. Poirier, *Pharmacogenetic analysis of the effects of polymorphisms in APOE, IDE and IL1B on a ketone body based therapeutic on cognition in mild to moderate Alzheimer's disease; a randomized, double-blind, placebo-controlled study.* BMC Med Genet, 2011. **12**: p. 137.

302. Sullivan, P.M., H. Mezdour, Y. Aratani, C. Knouff, J. Najib, R.L. Reddick, S.H. Quarfordt, and N. Maeda, *Targeted replacement of the mouse apolipoprotein E gene with the common human APOE3 allele enhances diet-induced hypercholesterolemia and atherosclerosis.* J Biol Chem, 1997. **272**(29): p. 17972-80.
303. Calero, O., R. Hortigüela, M.J. Bullido, and M. Calero, *Apolipoprotein E genotyping method by Real Time PCR, a fast and cost-effective alternative to the TaqMan® and FRET assays.* Journal of Neuroscience Methods, 2009. **183**(2): p. 238-240.
304. Vandesompele, J., K. De Preter, F. Pattyn, B. Poppe, N. Van Roy, A. De Paepe, and F. Speleman, *Accurate normalization of real-time quantitative RT-PCR data by geometric averaging of multiple internal control genes.* Genome Biol, 2002. **3**(7): p. RESEARCH0034.
305. Ding, F., J. Yao, J.R. Rettberg, S. Chen, and R.D. Brinton, *Early decline in glucose transport and metabolism precedes shift to ketogenic system in female aging and Alzheimer's mouse brain: implication for bioenergetic intervention.* PLoS One, 2013. **8**(11): p. e79977.
306. John, S., J.N. Weiss, and B. Ribalet, *Subcellular localization of hexokinases I and II directs the metabolic fate of glucose.* PLoS One, 2011. **6**(3): p. e17674.
307. Vogel, C. and E.M. Marcotte, *Insights into the regulation of protein abundance from proteomic and transcriptomic analyses.* Nat Rev Genet, 2012. **13**(4): p. 227-32.
308. Wu, L. and L. Zhao, *ApoE2 and Alzheimer's disease: time to take a closer look.* Neural Regen Res, 2016. **11**(3): p. 412-3.
309. Mosconi, L., *Glucose metabolism in normal aging and Alzheimer's disease: Methodological and physiological considerations for PET studies.* Clin Transl Imaging, 2013. **1**(4).
310. Vannucci, S.J., F. Maher, and I.A. Simpson, *Glucose transporter proteins in brain: delivery of glucose to neurons and glia.* Glia, 1997. **21**(1): p. 2-21.
311. Kalaria, R.N. and S.I. Harik, *Reduced glucose transporter at the blood-brain barrier and in cerebral cortex in Alzheimer disease.* J Neurochem, 1989. **53**(4): p. 1083-8.
312. Mooradian, A.D., H.C. Chung, and G.N. Shah, *GLUT-1 expression in the cerebra of patients with Alzheimer's disease.* Neurobiol Aging, 1997. **18**(5): p. 469-74.
313. Alata, W., *Human apolipoprotein E ε4 expression impairs cerebral.* 2015. **35**(1): p. 86-94.
314. Shepherd, P.R., G.W. Gould, C.A. Colville, S.C. McCoid, E.M. Gibbs, and B.B. Kahn, *Distribution of GLUT3 glucose transporter protein in human tissues.* Biochem Biophys Res Commun, 1992. **188**(1): p. 149-54.
315. Nagamatsu, S., J.M. Kornhauser, C.F. Burant, S. Seino, K.E. Mayo, and G.I. Bell, *Glucose transporter expression in brain. cDNA sequence of mouse GLUT3, the brain facilitative glucose transporter isoform, and identification of sites of expression by in situ hybridization.* J Biol Chem, 1992. **267**(1): p. 467-72.
316. Simpson, I.A., D. Dwyer, D. Malide, K.H. Moley, A. Travis, and S.J. Vannucci, *The facilitative glucose transporter GLUT3: 20 years of distinction.* Am J Physiol Endocrinol Metab, 2008. **295**(2): p. E242-53.

317. Ferreira, J.M., A.L. Burnett, and G.A. Rameau, *Activity-dependent regulation of surface glucose transporter-3.* J Neurosci, 2011. **31**(6): p. 1991-9.
318. Lee, Y.J., J.E. Kim, I.S. Hwang, M.H. Kwak, J.H. Lee, Y.J. Jung, B.S. An, H.S. Kwon, B.C. Kim, S.J. Kim, J.M. Kim, and D.Y. Hwang, *Alzheimer's phenotypes induced by overexpression of human presenilin 2 mutant proteins stimulate significant changes in key factors of glucose metabolism.* Mol Med Rep, 2013. **7**(5): p. 1571-8.
319. Alquier, T., C. Leloup, A. Lorsignol, and L. Pénicaud, *Translocable Glucose Transporters in the Brain.* Where Are We in 2006?, 2006. **55**(Supplement 2): p. S131-S138.
320. Pearson-Leary, J. and E.C. McNay, *Novel Roles for the Insulin-Regulated Glucose Transporter-4 in Hippocampally Dependent Memory.* J Neurosci, 2016. **36**(47): p. 11851-11864.
321. Piert, M., R.A. Koeppe, B. Giordani, S. Berent, and D.E. Kuhl, *Diminished glucose transport and phosphorylation in Alzheimer's disease determined by dynamic FDG-PET.* J Nucl Med, 1996. **37**(2): p. 201-8.
322. Sorbi, S., M. Mortilla, S. Piacentini, S. Tonini, and L. Amaducci, *Altered hexokinase activity in skin cultured fibroblasts and leukocytes from Alzheimer's disease patients.* Neurosci Lett, 1990. **117**(1-2): p. 165-8.
323. Harris, Julia J., R. Jolivet, and D. Attwell, *Synaptic Energy Use and Supply.* Neuron. **75**(5): p. 762-777.
324. Rangaraju, V., N. Calloway, and Timothy A. Ryan, *Activity-Driven Local ATP Synthesis Is Required for Synaptic Function.* Cell. **156**(4): p. 825-835.
325. Knull, H.R., *Association of glycolytic enzymes with particulate fractions from nerve endings.* Biochim Biophys Acta, 1978. **522**(1): p. 1-9.
326. Lu, M., Y.Y. Sautin, L.S. Holliday, and S.L. Gluck, *The Glycolytic Enzyme Aldolase Mediates Assembly, Expression, and Activity of Vacuolar H+-ATPase.* Journal of Biological Chemistry, 2004. **279**(10): p. 8732-8739.
327. Lu, M., D. Ammar, H. Ives, F. Albrecht, and S.L. Gluck, *Physical interaction between aldolase and vacuolar H+-ATPase is essential for the assembly and activity of the proton pump.* J Biol Chem, 2007. **282**(34): p. 24495-503.
328. Chan, C.Y., D. Dominguez, and K.J. Parra, *Regulation of Vacuolar H+-ATPase (V-ATPase) Reassembly by Glycolysis Flow in 6-Phosphofructo-1-kinase (PFK-1)-deficient Yeast Cells.* J Biol Chem, 2016. **291**(30): p. 15820-9.
329. Yao, J., R.W. Irwin, L. Zhao, J. Nilsen, R.T. Hamilton, and R.D. Brinton, *Mitochondrial bioenergetic deficit precedes Alzheimer's pathology in female mouse model of Alzheimer's disease.* Proceedings of the National Academy of Sciences, 2009. **106**(34): p. 14670-14675.
330. Moreira, P.I., C. Carvalho, X. Zhu, M.A. Smith, and G. Perry, *Mitochondrial dysfunction is a trigger of Alzheimer's disease pathophysiology.* Biochimica et Biophysica Acta (BBA) - Molecular Basis of Disease, 2010. **1802**(1): p. 2-10.
331. Swerdlow, R.H., J.M. Burns, and S.M. Khan, *The Alzheimer's disease mitochondrial cascade hypothesis.* J Alzheimers Dis, 2010. **20 Suppl 2**: p. S265-79.
332. Pierre, K. and L. Pellerin, *Monocarboxylate transporters in the central nervous system: distribution, regulation and function.* J Neurochem, 2005. **94**(1): p. 1-14.

333. Costantini, L.C., L.J. Barr, J.L. Vogel, and S.T. Henderson, *Hypometabolism as a therapeutic target in Alzheimer's disease.* BMC Neurosci, 2008. **9**(Suppl 2): p. S16.
334. Puigserver, P., *Tissue-specific regulation of metabolic pathways through the transcriptional coactivator PGC1-[alpha].* Int J Obes Relat Metab Disord, 2005. **29**(S1): p. S5-S9.
335. Katsouri, L., C. Parr, N. Bogdanovic, M. Willem, and M. Sastre, *PPARgamma co-activator-1alpha (PGC-1alpha) reduces amyloid-beta generation through a PPARgamma-dependent mechanism.* J Alzheimers Dis, 2011. **25**(1): p. 151-62.
336. Qin, W., V. Haroutunian, P. Katsel, C.P. Cardozo, L. Ho, J.D. Buxbaum, and G.M. Pasinetti, *PGC-1alpha expression decreases in the Alzheimer disease brain as a function of dementia.* Arch Neurol, 2009. **66**(3): p. 352-61.
337. Cui, L., H. Jeong, F. Borovecki, C.N. Parkhurst, N. Tanese, and D. Krainc, *Transcriptional repression of PGC-1alpha by mutant huntingtin leads to mitochondrial dysfunction and neurodegeneration.* Cell, 2006. **127**(1): p. 59-69.
338. Taherzadeh-Fard, E., C. Saft, J. Andrich, S. Wieczorek, and L. Arning, *PGC-1alpha as modifier of onset age in Huntington disease.* Mol Neurodegener, 2009. **4**: p. 10.
339. Ma, D., S. Li, E.K. Lucas, R.M. Cowell, and J.D. Lin, *Neuronal inactivation of peroxisome proliferator-activated receptor gamma coactivator 1alpha (PGC-1alpha) protects mice from diet-induced obesity and leads to degenerative lesions.* J Biol Chem, 2010. **285**(50): p. 39087-95.
340. Lin, J., P.H. Wu, P.T. Tarr, K.S. Lindenberg, J. St-Pierre, C.Y. Zhang, V.K. Mootha, S. Jager, C.R. Vianna, R.M. Reznick, L. Cui, M. Manieri, M.X. Donovan, Z. Wu, M.P. Cooper, M.C. Fan, L.M. Rohas, A.M. Zavacki, S. Cinti, G.I. Shulman, B.B. Lowell, D. Krainc, and B.M. Spiegelman, *Defects in adaptive energy metabolism with CNS-linked hyperactivity in PGC-1alpha null mice.* Cell, 2004. **119**(1): p. 121-35.
341. Theendakara, V., A. Patent, C.A. Peters Libeu, B. Philpot, S. Flores, O. Descamps, K.S. Poksay, Q. Zhang, G. Cailing, M. Hart, V. John, R.V. Rao, and D.E. Bredesen, *Neuroprotective Sirtuin ratio reversed by ApoE4.* Proc Natl Acad Sci U S A, 2013. **110**(45): p. 18303-8.
342. Cantó, C. and J. Auwerx, *PGC-1alpha, SIRT1 and AMPK, an energy sensing network that controls energy expenditure.* Curr Opin Lipidol, 2009. **20**(2): p. 98-105.
343. Rodgers, J.T., C. Lerin, W. Haas, S.P. Gygi, B.M. Spiegelman, and P. Puigserver, *Nutrient control of glucose homeostasis through a complex of PGC-1alpha and SIRT1.* Nature, 2005. **434**(7029): p. 113-8.
344. Watkins, G., A. Douglas-Jones, R.E. Mansel, and W.G. Jiang, *The localisation and reduction of nuclear staining of PPARgamma and PGC-1 in human breast cancer.* Oncol Rep, 2004. **12**(2): p. 483-8.
345. Feilchenfeldt, J., M.A. Brundler, C. Soravia, M. Totsch, and C.A. Meier, *Peroxisome proliferator-activated receptors (PPARs) and associated transcription factors in colon cancer: reduced expression of PPARgamma-coactivator 1 (PGC-1).* Cancer Lett, 2004. **203**(1): p. 25-33.

346. Lehman, J.J., P.M. Barger, A. Kovacs, J.E. Saffitz, D.M. Medeiros, and D.P. Kelly, *Peroxisome proliferator-activated receptor gamma coactivator-1 promotes cardiac mitochondrial biogenesis.* J Clin Invest, 2000. **106**(7): p. 847-56.
347. Lai, L., T.C. Leone, C. Zechner, P.J. Schaeffer, S.M. Kelly, D.P. Flanagan, D.M. Medeiros, A. Kovacs, and D.P. Kelly, *Transcriptional coactivators PGC-1α and PGC-lβ control overlapping programs required for perinatal maturation of the heart.* Genes Dev, 2008. **22**(14): p. 1948-61.
348. Wende, A.R., P.J. Schaeffer, G.J. Parker, C. Zechner, D.H. Han, M.M. Chen, C.R. Hancock, J.J. Lehman, J.M. Huss, D.A. McClain, J.O. Holloszy, and D.P. Kelly, *A role for the transcriptional coactivator PGC-1alpha in muscle refueling.* J Biol Chem, 2007. **282**(50): p. 36642-51.
349. Jorgensen, S.B., J.T. Treebak, B. Viollet, P. Schjerling, S. Vaulont, J.F. Wojtaszewski, and E.A. Richter, *Role of AMPKalpha2 in basal, training-, and AICAR-induced GLUT4, hexokinase II, and mitochondrial protein expression in mouse muscle.* Am J Physiol Endocrinol Metab, 2007. **292**(1): p. E331-9.
350. Leick, L., J. Fentz, R.S. Bienso, J.G. Knudsen, J. Jeppesen, B. Kiens, J.F. Wojtaszewski, and H. Pilegaard, *PGC-1{alpha} is required for AICAR-induced expression of GLUT4 and mitochondrial proteins in mouse skeletal muscle.* Am J Physiol Endocrinol Metab, 2010. **299**(3): p. E456-65.
351. Ellison, W.R., J.D. Lueck, and H.J. Fromm, *Studies on the mechanism of orthophosphate regulation of bovine brain hexokinase.* J Biol Chem, 1975. **250**(5): p. 1864-71.
352. Fang, T.Y., O. Alechina, A.E. Aleshin, H.J. Fromm, and R.B. Honzatko, *Identification of a phosphate regulatory site and a low affinity binding site for glucose 6-phosphate in the N-terminal half of human brain hexokinase.* J Biol Chem, 1998. **273**(31): p. 19548-53.
353. Tsai, H.J. and J.E. Wilson, *Functional organization of mammalian hexokinases: characterization of chimeric hexokinases constructed from the N- and C-terminal domains of the rat type I and type II isozymes.* Arch Biochem Biophys, 1995. **316**(1): p. 206-14.
354. Tsai, H.J. and J.E. Wilson, *Functional organization of mammalian hexokinases: both N- and C-terminal halves of the rat type II isozyme possess catalytic sites.* Arch Biochem Biophys, 1996. **329**(1): p. 17-23.
355. Felgner, P.L., J.L. Messer, and J.E. Wilson, *Purification of a hexokinase-binding protein from the outer mitochondrial membrane.* Journal of Biological Chemistry, 1979. **254**(12): p. 4946-9.
356. Linden, M., P. Gellerfors, and B.D. Nelson, *Pore protein and the hexokinase-binding protein from the outer membrane of rat liver mitochondria are identical.* FEBS Lett, 1982. **141**(2): p. 189-92.
357. de Cerqueira Cesar, M. and J.E. Wilson, *Application of a double isotopic labeling method to a study of the interaction of mitochondrially bound rat brain hexokinase with intramitochondrial compartments of ATP generated by oxidative phosphorylation.* Arch Biochem Biophys, 1995. **324**(1): p. 9-14.
358. Cesar Mde, C. and J.E. Wilson, *Further studies on the coupling of mitochondrially bound hexokinase to intramitochondrially compartmented ATP,*

generated by oxidative phosphorylation. Arch Biochem Biophys, 1998. **350**(1): p. 109-17.
359. Calmettes, G., S.A. John, J.N. Weiss, and B. Ribalet, *Hexokinase–mitochondrial interactions regulate glucose metabolism differentially in adult and neonatal cardiac myocytes.* The Journal of General Physiology, 2013. **142**(4): p. 425-436.
360. Rose, I.A. and J.V.B. Warms, *Mitochondrial Hexokinase: RELEASE, REBINDING, AND LOCATION.* Journal of Biological Chemistry, 1967. **242**(7): p. 1635-1645.
361. Jurczak, M.J., A.M. Danos, V.R. Rehrmann, and M.J. Brady, *The role of protein translocation in the regulation of glycogen metabolism.* J Cell Biochem, 2008. **104**(2): p. 435-43.
362. Theendakara, V., C.A. Peters-Libeu, P. Spilman, K.S. Poksay, D.E. Bredesen, and R.V. Rao, *Direct Transcriptional Effects of Apolipoprotein E.* J Neurosci, 2016. **36**(3): p. 685-700.
363. Shoag, J. and Z. Arany, *Regulation of hypoxia-inducible genes by PGC-1 alpha.* Arterioscler Thromb Vasc Biol, 2010. **30**(4): p. 662-6.
364. Suh, S.W., K. Aoyama, Y. Matsumori, J. Liu, and R.A. Swanson, *Pyruvate Administered After Severe Hypoglycemia Reduces Neuronal Death and Cognitive Impairment.* Diabetes, 2005. **54**(5): p. 1452-1458.
365. Zilberter, Y., O. Gubkina, and A.I. Ivanov, *A unique array of neuroprotective effects of pyruvate in neuropathology.* Frontiers in Neuroscience, 2015. **9**(17).
366. Collaboration, N.C.D.R.F., *Worldwide trends in diabetes since 1980: a pooled analysis of 751 population-based studies with 4.4 million participants.* Lancet, 2016. **387**(10027): p. 1513-30.
367. Miles, W. and H. Root, *Psychologic tests applied to diabetic patients.* Archives of Internal Medicine, 1922. **30**(6): p. 767-777.
368. Dejong, R.N., *THE NERVOUS SYSTEM COMPLICATIONS OF DIABETES MELLITUS, WITH SPECIAL REFERENCE TO CEREBROVASCULAR CHANGES.* The Journal of Nervous and Mental Disease, 1950. **111**(3): p. 181-206.
369. Talbot, K., H.Y. Wang, H. Kazi, L.Y. Han, K.P. Bakshi, A. Stucky, R.L. Fuino, K.R. Kawaguchi, A.J. Samoyedny, R.S. Wilson, Z. Arvanitakis, J.A. Schneider, B.A. Wolf, D.A. Bennett, J.Q. Trojanowski, and S.E. Arnold, *Demonstrated brain insulin resistance in Alzheimer's disease patients is associated with IGF-1 resistance, IRS-1 dysregulation, and cognitive decline.* J Clin Invest, 2012. **122**(4): p. 1316-38.
370. Huang, C.C., C.M. Chung, H.B. Leu, L.Y. Lin, C.C. Chiu, C.Y. Hsu, C.H. Chiang, P.H. Huang, T.J. Chen, S.J. Lin, J.W. Chen, and W.L. Chan, *Diabetes mellitus and the risk of Alzheimer's disease: a nationwide population-based study.* PLoS One, 2014. **9**(1): p. e87095.
371. Arvanitakis, Z., R.S. Wilson, J.L. Bienias, D.A. Evans, and D.A. Bennett, *Diabetes mellitus and risk of Alzheimer disease and decline in cognitive function.* Arch Neurol, 2004. **61**(5): p. 661-6.
372. Xu, W.L., C.X. Qiu, A. Wahlin, B. Winblad, and L. Fratiglioni, *Diabetes mellitus and risk of dementia in the Kungsholmen project: a 6-year follow-up study.* Neurology, 2004. **63**(7): p. 1181-6.

373. Wu, J.H., M.N. Haan, J. Liang, D. Ghosh, H.M. Gonzalez, and W.H. Herman, *Impact of diabetes on cognitive function among older Latinos: a population-based cohort study*. Journal of clinical epidemiology, 2003. **56**(7): p. 686-693.
374. Hassing, L.B., M.D. Grant, S.M. Hofer, N.L. Pedersen, S.E. Nilsson, S. Berg, G. McClearn, and B. Johansson, *Type 2 diabetes mellitus contributes to cognitive decline in old age: a longitudinal population-based study*. Journal of the International Neuropsychological Society, 2004. **10**(04): p. 599-607.
375. Nguyen, H.T., S.A. Black, L.A. Ray, D.V. Espino, and K.S. Markides, *Predictors of decline in MMSE scores among older Mexican Americans.* The Journals of Gerontology Series A: Biological Sciences and Medical Sciences, 2002. **57**(3): p. M181-M185.
376. Van Harten, B., J. Oosterman, D. Muslimovic, B.-J.P. Van Loon, P. Scheltens, and H.C. Weinstein, *Cognitive impairment and MRI correlates in the elderly patients with type 2 diabetes mellitus.* Age and ageing, 2007. **36**(2): p. 164-170.
377. Biessels, G.-J., A. Kamal, G.M. Ramakers, I.J. Urban, B.M. Spruijt, D.W. Erkelens, and W.H. Gispen, *Place learning and hippocampal synaptic plasticity in streptozotocin-induced diabetic rats.* Diabetes, 1996. **45**(9): p. 1259-1266.
378. Li, X.-L., S. Aou, Y. Oomura, N. Hori, K. Fukunaga, and T. Hori, *Impairment of long-term potentiation and spatial memory in leptin receptor-deficient rodents.* Neuroscience, 2002. **113**(3): p. 607-615.
379. Stranahan, A.M., T.V. Arumugam, R.G. Cutler, K. Lee, J.M. Egan, and M.P. Mattson, *Diabetes impairs hippocampal function through glucocorticoid-mediated effects on new and mature neurons.* Nat Neurosci, 2008. **11**(3): p. 309-17.
380. Stranahan, A.M., T.V. Arumugam, K. Lee, and M.P. Mattson, *Mineralocorticoid receptor activation restores medial perforant path LTP in diabetic rats.* Synapse, 2010. **64**(7): p. 528-32.
381. Artola, A., A. Kamal, G.M. Ramakers, G.J. Biessels, and W.H. Gispen, *Diabetes mellitus concomitantly facilitates the induction of long-term depression and inhibits that of long-term potentiation in hippocampus.* Eur J Neurosci, 2005. **22**(1): p. 169-78.
382. Shonesy, B.C., K. Thiruchelvam, K. Parameshwaran, E.A. Rahman, S.S. Karuppagounder, K.W. Huggins, C.A. Pinkert, R. Amin, M. Dhanasekaran, and V. Suppiramaniam, *Central insulin resistance and synaptic dysfunction in intracerebroventricular-streptozotocin injected rodents.* Neurobiol Aging, 2012. **33**(2): p. 430.e5-18.
383. Sima, A.A.F., *Encephalopathies: the emerging diabetic complications.* Acta Diabetologica, 2010. **47**(4): p. 279-293.
384. Li, Z.-g., W. Zhang, and A.A. Sima, *Alzheimer-like changes in rat models of spontaneous diabetes.* Diabetes, 2007. **56**(7): p. 1817-1824.
385. Sima, A.A.F., *Pathobiology of Diabetic Encephalopathy in Animal Models*, in *Diabetes and the Brain*, G.J. Biessels and J.A. Luchsinger, Editors. 2010, Humana Press: Totowa, NJ. p. 409-431.
386. Sima, A.A. and Z.-g. Li, *The effect of C-peptide on cognitive dysfunction and hippocampal apoptosis in type 1 diabetic rats.* Diabetes, 2005. **54**(5): p. 1497-1505.

387. Sima, A.A., W. Zhang, C.W. Kreipke, J.A. Rafols, and W.H. Hoffman, *Inflammation in Diabetic Encephalopathy is Prevented by C-Peptide.* Rev Diabet Stud, 2009. **6**(1): p. 37-42.
388. Dejgaard, A., A. Gade, H. Larsson, V. Balle, A. Parving, and H.H. Parving, *Evidence for diabetic encephalopathy.* Diabetic Medicine, 1991. **8**(2): p. 162-167.
389. Cuevas, H. and A. Stuifbergen, *Perceived cognitive deficits are associated with diabetes self-management in a multiethnic sample.* J Diabetes Metab Disord, 2017. **16**.
390. Strachan, M.W., R.M. Reynolds, R.E. Marioni, and J.F. Price, *Cognitive function, dementia and type 2 diabetes mellitus in the elderly.* Nat Rev Endocrinol, 2011. **7**(2): p. 108-14.
391. Sivitz, W.I. and M.A. Yorek, *Mitochondrial Dysfunction in Diabetes: From Molecular Mechanisms to Functional Significance and Therapeutic Opportunities.* Antioxid Redox Signal, 2010. **12**(4): p. 537-77.
392. Maassen, J.A., T.H. LM, E. Van Essen, R.J. Heine, G. Nijpels, R.S. Jahangir Tafrechi, A.K. Raap, G.M. Janssen, and H.H. Lemkes, *Mitochondrial diabetes: molecular mechanisms and clinical presentation.* Diabetes, 2004. **53 Suppl 1**: p. S103-9.
393. Green, K., M.D. Brand, and M.P. Murphy, *Prevention of mitochondrial oxidative damage as a therapeutic strategy in diabetes.* Diabetes, 2004. **53 Suppl 1**: p. S110-8.
394. Ritov, V.B., E.V. Menshikova, J. He, R.E. Ferrell, B.H. Goodpaster, and D.E. Kelley, *Deficiency of subsarcolemmal mitochondria in obesity and type 2 diabetes.* Diabetes, 2005. **54**(1): p. 8-14.
395. Chao, T.T., C.D. Ianuzzo, R.B. Armstrong, J.T. Albright, and S.E. Anapolle, *Ultrastructural alterations in skeletal muscle fibers of streptozotocin-diabetic rats.* Cell Tissue Res, 1976. **168**(2): p. 239-46.
396. Kelley, D.E., J. He, E.V. Menshikova, and V.B. Ritov, *Dysfunction of mitochondria in human skeletal muscle in type 2 diabetes.* Diabetes, 2002. **51**(10): p. 2944-50.
397. Bach, D., S. Pich, F.X. Soriano, N. Vega, B. Baumgartner, J. Oriola, J.R. Daugaard, J. Lloberas, M. Camps, J.R. Zierath, R. Rabasa-Lhoret, H. Wallberg-Henriksson, M. Laville, M. Palacin, H. Vidal, F. Rivera, M. Brand, and A. Zorzano, *Mitofusin-2 determines mitochondrial network architecture and mitochondrial metabolism. A novel regulatory mechanism altered in obesity.* J Biol Chem, 2003. **278**(19): p. 17190-7.
398. Fealy, C.E., A. Mulya, N. Lai, and J.P. Kirwan, *Exercise training decreases activation of the mitochondrial fission protein dynamin-related protein-1 in insulin-resistant human skeletal muscle.* J Appl Physiol (1985), 2014. **117**(3): p. 239-45.
399. Mensink, M., M.K. Hesselink, A.P. Russell, G. Schaart, J.P. Sels, and P. Schrauwen, *Improved skeletal muscle oxidative enzyme activity and restoration of PGC-1 alpha and PPAR beta/delta gene expression upon rosiglitazone treatment in obese patients with type 2 diabetes mellitus.* Int J Obes (Lond), 2007. **31**(8): p. 1302-10.

400. Mootha, V.K., C.M. Lindgren, K.F. Eriksson, A. Subramanian, S. Sihag, J. Lehar, P. Puigserver, E. Carlsson, M. Ridderstrale, E. Laurila, N. Houstis, M.J. Daly, N. Patterson, J.P. Mesirov, T.R. Golub, P. Tamayo, B. Spiegelman, E.S. Lander, J.N. Hirschhorn, D. Altshuler, and L.C. Groop, *PGC-1alpha-responsive genes involved in oxidative phosphorylation are coordinately downregulated in human diabetes.* Nat Genet, 2003. **34**(3): p. 267-73.
401. Patti, M.E., A.J. Butte, S. Crunkhorn, K. Cusi, R. Berria, S. Kashyap, Y. Miyazaki, I. Kohane, M. Costello, R. Saccone, E.J. Landaker, A.B. Goldfine, E. Mun, R. DeFronzo, J. Finlayson, C.R. Kahn, and L.J. Mandarino, *Coordinated reduction of genes of oxidative metabolism in humans with insulin resistance and diabetes: Potential role of PGC1 and NRF1.* Proc Natl Acad Sci U S A, 2003. **100**(14): p. 8466-71.
402. Ashcroft, F.M., P. Proks, P.A. Smith, C. Ammala, K. Bokvist, and P. Rorsman, *Stimulus-secretion coupling in pancreatic beta cells.* J Cell Biochem, 1994. **55 Suppl**: p. 54-65.
403. Maechler, P. and C.B. Wollheim, *Mitochondrial function in normal and diabetic beta-cells.* Nature, 2001. **414**(6865): p. 807-12.
404. Du, Y., C.M. Miller, and T.S. Kern, *Hyperglycemia increases mitochondrial superoxide in retina and retinal cells.* Free Radic Biol Med, 2003. **35**(11): p. 1491-9.
405. Nishikawa, T., D. Edelstein, and M. Brownlee, *The missing link: a single unifying mechanism for diabetic complications.* Kidney Int Suppl, 2000. **77**: p. S26-30.
406. Nishikawa, T., D. Edelstein, X.L. Du, S. Yamagishi, T. Matsumura, Y. Kaneda, M.A. Yorek, D. Beebe, P.J. Oates, H.P. Hammes, I. Giardino, and M. Brownlee, *Normalizing mitochondrial superoxide production blocks three pathways of hyperglycaemic damage.* Nature, 2000. **404**(6779): p. 787-90.
407. Busik, J.V., S. Mohr, and M.B. Grant, *Hyperglycemia-induced reactive oxygen species toxicity to endothelial cells is dependent on paracrine mediators.* Diabetes, 2008. **57**(7): p. 1952-65.
408. Manabe, E., O. Handa, Y. Naito, K. Mizushima, S. Akagiri, S. Adachi, T. Takagi, S. Kokura, T. Maoka, and T. Yoshikawa, *Astaxanthin protects mesangial cells from hyperglycemia-induced oxidative signaling.* J Cell Biochem, 2008. **103**(6): p. 1925-37.
409. Kiritoshi, S., T. Nishikawa, K. Sonoda, D. Kukidome, T. Senokuchi, T. Matsuo, T. Matsumura, H. Tokunaga, M. Brownlee, and E. Araki, *Reactive oxygen species from mitochondria induce cyclooxygenase-2 gene expression in human mesangial cells: potential role in diabetic nephropathy.* Diabetes, 2003. **52**(10): p. 2570-7.
410. Carvalho, C., M.S. Santos, C.R. Oliveira, and P.I. Moreira, *Alzheimer's disease and type 2 diabetes-related alterations in brain mitochondria, autophagy and synaptic markers.* Biochim Biophys Acta, 2015. **1852**(8): p. 1665-75.
411. Cardoso, S., R.X. Santos, S.C. Correia, C. Carvalho, M.S. Santos, I. Baldeiras, C.R. Oliveira, and P.I. Moreira, *Insulin-induced recurrent hypoglycemia exacerbates diabetic brain mitochondrial dysfunction and oxidative imbalance.* Neurobiol Dis, 2013. **49**: p. 1-12.

412. Kirkman, M.S., V.J. Briscoe, N. Clark, H. Florez, L.B. Haas, J.B. Halter, E.S. Huang, M.T. Korytkowski, M.N. Munshi, P.S. Odegard, R.E. Pratley, and C.S. Swift, *Diabetes in Older Adults.* Diabetes Care, 2012. **35**(12): p. 2650-64.
413. Aragno, M., E. Brignardello, E. Tamagno, V. Gatto, O. Danni, and G. Boccuzzi, *Dehydroepiandrosterone administration prevents the oxidative damage induced by acute hyperglycemia in rats.* J Endocrinol, 1997. **155**(2): p. 233-40.
414. Schmeichel, A.M., J.D. Schmelzer, and P.A. Low, *Oxidative injury and apoptosis of dorsal root ganglion neurons in chronic experimental diabetic neuropathy.* Diabetes, 2003. **52**(1): p. 165-71.
415. Raza, H., A. John, and F.C. Howarth, *Increased oxidative stress and mitochondrial dysfunction in zucker diabetic rat liver and brain.* Cell Physiol Biochem, 2015. **35**(3): p. 1241-51.
416. Rovira-Llopis, S., C. Bañuls, N. Diaz-Morales, A. Hernandez-Mijares, M. Rocha, and V.M. Victor, *Mitochondrial dynamics in type 2 diabetes: Pathophysiological implications.* Redox Biol, 2017. **11**: p. 637-45.
417. Men, X., H. Wang, M. Li, H. Cai, S. Xu, W. Zhang, Y. Xu, L. Ye, W. Yang, C.B. Wollheim, and J. Lou, *Dynamin-related protein 1 mediates high glucose induced pancreatic beta cell apoptosis.* Int J Biochem Cell Biol, 2009. **41**(4): p. 879-90.
418. Molina, A.J., J.D. Wikstrom, L. Stiles, G. Las, H. Mohamed, A. Elorza, G. Walzer, G. Twig, S. Katz, and B.E. Corkey, *Mitochondrial networking protects β-cells from nutrient-induced apoptosis.* Diabetes, 2009. **58**(10): p. 2303-2315.
419. Bach, D., S. Pich, F.X. Soriano, N. Vega, B. Baumgartner, J. Oriola, J.R. Daugaard, J. Lloberas, M. Camps, and J.R. Zierath, *Mitofusin-2 determines mitochondrial network architecture and mitochondrial metabolism A novel regulatory mechanism altered in obesity.* Journal of Biological Chemistry, 2003. **278**(19): p. 17190-17197.
420. Yu, T., S.S. Sheu, J.L. Robotham, and Y. Yoon, *Mitochondrial fission mediates high glucose-induced cell death through elevated production of reactive oxygen species.* Cardiovasc Res, 2008. **79**(2): p. 341-51.
421. Makino, A., B.T. Scott, and W.H. Dillmann, *Mitochondrial fragmentation and superoxide anion production in coronary endothelial cells from a mouse model of type 1 diabetes.* Diabetologia, 2010. **53**(8): p. 1783-94.
422. Paltauf-Doburzynska, J., R. Malli, and W.F. Graier, *Hyperglycemic conditions affect shape and Ca2+ homeostasis of mitochondria in endothelial cells.* J Cardiovasc Pharmacol, 2004. **44**(4): p. 423-36.
423. Edwards, J., *Diabetes regulates mitochondrial biogenesis and fission in.* 2010. **53**(1): p. 160-9.
424. Vincent, A.M., J.L. Edwards, L.L. McLean, Y. Hong, F. Cerri, I. Lopez, A. Quattrini, and E.L. Feldman, *Mitochondrial biogenesis and fission in axons in cell culture and animal models of diabetic neuropathy.* Acta Neuropathol, 2010. **120**(4): p. 477-89.
425. Leinninger, G.M., C. Backus, A.M. Sastry, Y.B. Yi, C.W. Wang, and E.L. Feldman, *Mitochondria in DRG neurons undergo hyperglycemic mediated injury through Bim, Bax and the fission protein Drp1.* Neurobiol Dis, 2006. **23**(1): p. 11-22.

426. Elrod, J.W. and J.D. Molkentin, *Physiologic functions of cyclophilin D and the mitochondrial permeability transition pore.* Circ J, 2013. **77**(5): p. 1111-22.
427. Halestrap, A.P., *What is the mitochondrial permeability transition pore?* J Mol Cell Cardiol, 2009. **46**(6): p. 821-31.
428. Mbye, L., I. Singh, P. Sullivan, J. Springer, and E. Hall, *Attenuation of acute mitochondrial dysfunction after traumatic brain injury in mice by NIM811, a non-immunosuppressive cyclosporin A analog.* Experimental neurology, 2008. **209**(1): p. 243-253.
429. Hånell, A., J.E. Greer, M.J. McGinn, and J.T. Povlishock, *Traumatic brain injury-induced axonal phenotypes react differently to treatment.* Acta neuropathologica, 2015. **129**(2): p. 317-332.
430. Griffiths, E.J. and A.P. Halestrap, *Mitochondrial non-specific pores remain closed during cardiac ischaemia, but open upon reperfusion.* Biochem J, 1995. **307**(Pt 1): p. 93-8.
431. Schinzel, A.C., O. Takeuchi, Z. Huang, J.K. Fisher, Z. Zhou, J. Rubens, C. Hetz, N.N. Danial, M.A. Moskowitz, and S.J. Korsmeyer, *Cyclophilin D is a component of mitochondrial permeability transition and mediates neuronal cell death after focal cerebral ischemia.* Proc Natl Acad Sci U S A, 2005. **102**(34): p. 12005-10.
432. Baines, C.P., R.A. Kaiser, N.H. Purcell, N.S. Blair, H. Osinska, M.A. Hambleton, E.W. Brunskill, M.R. Sayen, R.A. Gottlieb, G.W. Dorn, J. Robbins, and J.D. Molkentin, *Loss of cyclophilin D reveals a critical role for mitochondrial permeability transition in cell death.* Nature, 2005. **434**(7033): p. 658-62.
433. Vaseva, A.V., N.D. Marchenko, K. Ji, S.E. Tsirka, S. Holzmann, and U.M. Moll, *p53 opens the mitochondrial permeability transition pore to trigger necrosis.* Cell, 2012. **149**(7): p. 1536-48.
434. Sloan, R.C., F. Moukdar, C.R. Frasier, H.D. Patel, P.A. Bostian, R.M. Lust, and D.A. Brown, *Mitochondrial permeability transition in the diabetic heart: contributions of thiol redox state and mitochondrial calcium to augmented reperfusion injury*. J Mol Cell Cardiol, 2012. **52**(5): p. 1009-18.
435. Najafi, M., S. Farajnia, M. Mohammadi, R. Badalzadeh, N. Ahmadi Asl, B. Baradaran, and M. Amani, *Inhibition of mitochondrial permeability transition pore restores the cardioprotection by postconditioning in diabetic hearts.* J Diabetes Metab Disord, 2014. **13**(1): p. 106.
436. Grishina, E.V., M.H. Galimova, R.H. Djafarov, A.I. Sergeev, N.I. Fedotcheva, and V.V. Dynnik, *Induction of cyclosporine-sensitive mitochondrial permeability transition pore by substrates forming acetyl-CoA under normal conditions and in type 2 diabetes.* Biochemistry (Moscow) Supplement Series A: Membrane and Cell Biology, 2016. **10**(1): p. 11-18.
437. Oliveira, P.J., T.C. Esteves, R. Seica, A.J. Moreno, and M.S. Santos, *Calcium-dependent mitochondrial permeability transition is augmented in the kidney of Goto-Kakizaki diabetic rat.* Diabetes Metab Res Rev, 2004. **20**(2): p. 131-6.
438. Kundu, S., S. Pushpakumar, and U. Sen, *Hydrogen Sulfide Inhibits Ca2+-induced Mitochondrial Permeability Transition PoreOpening in Type-1 Diabetes.* The FASEB Journal, 2015. **29**(1 Supplement).
439. Crompton, M., S. Virji, and J.M. Ward, *Cyclophilin-D binds strongly to complexes of the voltage-dependent anion channel and the adenine nucleotide*

translocase to form the permeability transition pore. Eur J Biochem, 1998. **258**(2): p. 729-35.
440. Baines, C.P., R.A. Kaiser, T. Sheiko, W.J. Craigen, and J.D. Molkentin, *Voltage-dependent anion channels are dispensable for mitochondrial-dependent cell death.* Nat Cell Biol, 2007. **9**(5): p. 550-5.
441. Cheng, E.H., T.V. Sheiko, J.K. Fisher, W.J. Craigen, and S.J. Korsmeyer, *VDAC2 inhibits BAK activation and mitochondrial apoptosis.* Science, 2003. **301**(5632): p. 513-7.
442. Kokoszka, J.E., K.G. Waymire, S.E. Levy, J.E. Sligh, J. Cai, D.P. Jones, G.R. MacGregor, and D.C. Wallace, *The ADP/ATP translocator is not essential for the mitochondrial permeability transition pore.* Nature, 2004. **427**(6973): p. 461-5.
443. Alcala, S., M. Klee, J. Fernandez, A. Fleischer, and F.X. Pimentel-Muinos, *A high-throughput screening for mammalian cell death effectors identifies the mitochondrial phosphate carrier as a regulator of cytochrome c release.* Oncogene, 2008. **27**(1): p. 44-54.
444. Leung, A.W.C., P. Varanyuwatana, and A.P. Halestrap, *The Mitochondrial Phosphate Carrier Interacts with Cyclophilin D and May.* J Biol Chem, 2008. **283**(39): p. 26312-23.
445. Kwong, J.Q., J. Davis, C.P. Baines, M.A. Sargent, J. Karch, X. Wang, T. Huang, and J.D. Molkentin, *Genetic deletion of the mitochondrial phosphate carrier desensitizes the mitochondrial permeability transition pore and causes cardiomyopathy.* Cell Death Differ, 2014. **21**(8): p. 1209-17.
446. Tait, S.W. and D.R. Green, *Mitochondria and cell death: outer membrane permeabilization and beyond.* Nat Rev Mol Cell Biol, 2010. **11**(9): p. 621-32.
447. Karch, J., J.Q. Kwong, A.R. Burr, M.A. Sargent, J.W. Elrod, P.M. Peixoto, S. Martinez-Caballero, H. Osinska, E.H.Y. Cheng, J. Robbins, K.W. Kinnally, and J.D. Molkentin, *Bax and Bak function as the outer membrane component of the mitochondrial permeability pore in regulating necrotic cell death in mice.* eLife, 2013. **2**.
448. Whelan, R.S., K. Konstantinidis, A.C. Wei, Y. Chen, D.E. Reyna, S. Jha, Y. Yang, J.W. Calvert, T. Lindsten, C.B. Thompson, M.T. Crow, E. Gavathiotis, G.W. Dorn, B. O'Rourke, and R.N. Kitsis, *Bax regulates primary necrosis through mitochondrial dynamics.* Proc Natl Acad Sci U S A, 2012. **109**(17): p. 6566-71.
449. Giorgio, V., E. Bisetto, M.E. Soriano, F. Dabbeni-Sala, E. Basso, V. Petronilli, M.A. Forte, P. Bernardi, and G. Lippe, *Cyclophilin D modulates mitochondrial F0F1-ATP synthase by interacting with the lateral stalk of the complex.* J Biol Chem, 2009. **284**(49): p. 33982-8.
450. Giorgio, V., S. von Stockum, M. Antoniel, A. Fabbro, F. Fogolari, M. Forte, G.D. Glick, V. Petronilli, M. Zoratti, I. Szabo, G. Lippe, and P. Bernardi, *Dimers of mitochondrial ATP synthase form the permeability transition pore.* Proc Natl Acad Sci U S A, 2013. **110**(15): p. 5887-92.
451. Bonora, M., A. Bononi, E. De Marchi, C. Giorgi, M. Lebiedzinska, S. Marchi, S. Patergnani, A. Rimessi, J.M. Suski, A. Wojtala, M.R. Wieckowski, G. Kroemer, L. Galluzzi, and P. Pinton, *Role of the c subunit of the FO ATP synthase in mitochondrial permeability transition.* Cell Cycle, 2013. **12**(4): p. 674-83.

452. Alavian, K.N., G. Beutner, E. Lazrove, S. Sacchetti, H.A. Park, P. Licznerski, H. Li, P. Nabili, K. Hockensmith, M. Graham, G.A. Porter, and E.A. Jonas, *An uncoupling channel within the c-subunit ring of the F(1)F(O) ATP synthase is the mitochondrial permeability transition pore.* Proc Natl Acad Sci U S A, 2014. **111**(29): p. 10580-5.
453. Elustondo, P.A., M. Nichols, A. Negoda, A. Thirumaran, E. Zakharian, G.S. Robertson, and E.V. Pavlov, *Mitochondrial permeability transition pore induction is linked to formation of the complex of ATPase C-subunit, polyhydroxybutyrate and inorganic polyphosphate*. Cell Death Discov, 2016. **2**: p. 16070.
454. Fournier, N., G. Ducet, and A. Crevat, *Action of cyclosporine on mitochondrial calcium fluxes.* J Bioenerg Biomembr, 1987. **19**(3): p. 297-303.
455. Broekemeier, K.M., M.E. Dempsey, and D.R. Pfeiffer, *Cyclosporin A is a potent inhibitor of the inner membrane permeability transition in liver mitochondria.* J Biol Chem, 1989. **264**(14): p. 7826-30.
456. Crompton, M., H. Ellinger, and A. Costi, *Inhibition by cyclosporin A of a Ca2+-dependent pore in heart mitochondria activated by inorganic phosphate and oxidative stress.* Biochem J, 1988. **255**(1): p. 357-60.
457. Halestrap, A.P. and A.M. Davidson, *Inhibition of Ca2(+)-induced large-amplitude swelling of liver and heart mitochondria by cyclosporin is probably caused by the inhibitor binding to mitochondrial-matrix peptidyl-prolyl cis-trans isomerase and preventing it interacting with the adenine nucleotide translocase.* Biochem J, 1990. **268**(1): p. 153-60.
458. Nakagawa, T., S. Shimizu, T. Watanabe, O. Yamaguchi, K. Otsu, H. Yamagata, H. Inohara, T. Kubo, and Y. Tsujimoto, *Cyclophilin D-dependent mitochondrial permeability transition regulates some necrotic but not apoptotic cell death.* Nature, 2005. **434**(7033): p. 652-8.
459. Martin, L.J., B. Gertz, Y. Pan, A.C. Price, J.D. Molkentin, and Q. Chang, *The mitochondrial permeability transition pore in motor neurons: involvement in the pathobiology of ALS mice.* Exp Neurol, 2009. **218**(2): p. 333-46.
460. Ramachandran, A., M. Lebofsky, C.P. Baines, J.J. Lemasters, and H. Jaeschke, *Cyclophilin D deficiency protects against acetaminophen-induced oxidant stress and liver injury.* Free Radic Res, 2011. **45**(2): p. 156-64.
461. Davis, T.L., J.R. Walker, V. Campagna-Slater, P.J. Finerty, R. Paramanathan, G. Bernstein, F. MacKenzie, W. Tempel, H. Ouyang, W.H. Lee, E.Z. Eisenmesser, and S. Dhe-Paganon, *Structural and Biochemical Characterization of the Human Cyclophilin Family of Peptidyl-Prolyl Isomerases.* PLoS Biol, 2010. **8**(7).
462. Wang, P. and J. Heitman, *The cyclophilins.* Genome Biol, 2005. **6**(7): p. 226.
463. Johnson, N., A. Khan, S. Virji, J.M. Ward, and M. Crompton, *Import and processing of heart mitochondrial cyclophilin D.* Eur J Biochem, 1999. **263**(2): p. 353-9.
464. Connern, C.P. and A.P. Halestrap, *Purification and N-terminal sequencing of peptidyl-prolyl cis-trans-isomerase from rat liver mitochondrial matrix reveals the existence of a distinct mitochondrial cyclophilin.* Biochem J, 1992. **284 (Pt 2)**: p. 381-5.
465. Bergsma, D.J., C. Eder, M. Gross, H. Kersten, D. Sylvester, E. Appelbaum, D. Cusimano, G.P. Livi, M.M. McLaughlin, K. Kasyan, and et al., *The cyclophilin*

multigene family of peptidyl-prolyl isomerases. Characterization of three separate human isoforms. J Biol Chem, 1991. **266**(34): p. 23204-14.
466. Kajitani, K., M. Fujihashi, Y. Kobayashi, S. Shimizu, Y. Tsujimoto, and K. Miki, *Crystal structure of human cyclophilin D in complex with its inhibitor, cyclosporin A at 0.96-A resolution.* Proteins, 2008. **70**(4): p. 1635-9.
467. Elrod, J.W., R. Wong, S. Mishra, R.J. Vagnozzi, B. Sakthievel, S.A. Goonasekera, J. Karch, S. Gabel, J. Farber, T. Force, J.H. Brown, E. Murphy, and J.D. Molkentin, *Cyclophilin D controls mitochondrial pore-dependent Ca(2+) exchange, metabolic flexibility, and propensity for heart failure in mice.* J Clin Invest, 2010. **120**(10): p. 3680-7.
468. Menazza, S., R. Wong, T. Nguyen, G. Wang, M. Gucek, and E. Murphy, *CypD(-/-) hearts have altered levels of proteins involved in Krebs cycle, branch chain amino acid degradation and pyruvate metabolism.* J Mol Cell Cardiol, 2013. **56**: p. 81-90.
469. Tavecchio, M., S. Lisanti, M.J. Bennett, L.R. Languino, and D.C. Altieri, *Deletion of Cyclophilin D Impairs β-Oxidation and Promotes Glucose Metabolism.* Sci Rep, 2015. **5**.
470. Bernardi, P. and S. von Stockum, *The permeability transition pore as a Ca(2+) release channel: New answers to an old question.* Cell Calcium, 2012. **52**(1): p. 22-7.
471. Altschuld, R.A., C.M. Hohl, L.C. Castillo, A.A. Garleb, R.C. Starling, and G.P. Brierley, *Cyclosporin inhibits mitochondrial calcium efflux in isolated adult rat ventricular cardiomyocytes.* Am J Physiol, 1992. **262**(6 Pt 2): p. H1699-704.
472. Selivanov, V.A., F. Ichas, E.L. Holmuhamedov, L.S. Jouaville, Y.V. Evtodienko, and J.P. Mazat, *A model of mitochondrial Ca(2+)-induced Ca2+ release simulating the Ca2+ oscillations and spikes generated by mitochondria.* Biophys Chem, 1998. **72**(1-2): p. 111-21.
473. Ichas, F. and J.P. Mazat, *From calcium signaling to cell death: two conformations for the mitochondrial permeability transition pore. Switching from low- to high-conductance state.* Biochim Biophys Acta, 1998. **1366**(1-2): p. 33-50.
474. Ichas, F., L.S. Jouaville, and J.P. Mazat, *Mitochondria are excitable organelles capable of generating and conveying electrical and calcium signals.* Cell, 1997. **89**(7): p. 1145-53.
475. Korge, P., L. Yang, J.H. Yang, Y. Wang, Z. Qu, and J.N. Weiss, *Protective role of transient pore openings in calcium handling by cardiac mitochondria.* J Biol Chem, 2011. **286**(40): p. 34851-7.
476. Barsukova, A., A. Komarov, G. Hajnoczky, P. Bernardi, D. Bourdette, and M. Forte, *Activation of the mitochondrial permeability transition pore modulates Ca2+ responses to physiological stimuli in adult neurons.* Eur J Neurosci, 2011. **33**(5): p. 831-42.
477. Forte, M., B.G. Gold, G. Marracci, P. Chaudhary, E. Basso, D. Johnsen, X. Yu, J. Fowlkes, M. Rahder, K. Stem, P. Bernardi, and D. Bourdette, *Cyclophilin D inactivation protects axons in experimental autoimmune encephalomyelitis, an animal model of multiple sclerosis.* Proc Natl Acad Sci U S A, 2007. **104**(18): p. 7558-63.

478. Karlsson, J., K.S. Fong, M.J. Hansson, E. Elmer, K. Csiszar, and M.F. Keep, *Life span extension and reduced neuronal death after weekly intraventricular cyclosporin injections in the G93A transgenic mouse model of amyotrophic lateral sclerosis.* J Neurosurg, 2004. **101**(1): p. 128-37.
479. Gandhi, S., A. Wood-Kaczmar, Z. Yao, H. Plun-Favreau, E. Deas, K. Klupsch, J. Downward, D.S. Latchman, S.J. Tabrizi, N.W. Wood, M.R. Duchen, and A.Y. Abramov, *PINK1-Associated Parkinson's Disease Is Caused by Neuronal Vulnerability to Calcium-Induced Cell Death.* Mol Cell, 2009. **33**(5-3): p. 627-38.
480. Wang, H.L., A.H. Chou, T.H. Yeh, A.H. Li, Y.L. Chen, Y.L. Kuo, S.R. Tsai, and S.T. Yu, *PINK1 mutants associated with recessive Parkinson's disease are defective in inhibiting mitochondrial release of cytochrome c.* Neurobiol Dis, 2007. **28**(2): p. 216-26.
481. Brustovetsky, N., T. Brustovetsky, K.J. Purl, M. Capano, M. Crompton, and J.M. Dubinsky, *Increased susceptibility of striatal mitochondria to calcium-induced permeability transition.* J Neurosci, 2003. **23**(12): p. 4858-67.
482. Moreira, P.I., M.S. Santos, A. Moreno, and C. Oliveira, *Amyloid beta-peptide promotes permeability transition pore in brain mitochondria.* Biosci Rep, 2001. **21**(6): p. 789-800.
483. Morais Cardoso, S., R.H. Swerdlow, and C.R. Oliveira, *Induction of cytochrome c-mediated apoptosis by amyloid beta 25-35 requires functional mitochondria.* Brain Res, 2002. **931**(2): p. 117-25.
484. Ferreiro, E., C.R. Oliveira, and C.M. Pereira, *The release of calcium from the endoplasmic reticulum induced by amyloid-beta and prion peptides activates the mitochondrial apoptotic pathway.* Neurobiol Dis, 2008. **30**(3): p. 331-42.
485. Chin, J.H., F.W. Tse, K. Harris, and J.H. Jhamandas, *Beta-amyloid enhances intracellular calcium rises mediated by repeated activation of intracellular calcium stores and nicotinic receptors in acutely dissociated rat basal forebrain neurons.* Brain Cell Biol, 2006. **35**(2-3): p. 173-86.
486. Mattson, M.P., B. Cheng, D. Davis, K. Bryant, I. Lieberburg, and R.E. Rydel, *beta-Amyloid peptides destabilize calcium homeostasis and render human cortical neurons vulnerable to excitotoxicity.* J Neurosci, 1992. **12**(2): p. 376-89.
487. Brewer, G.J., A. Lim, N.G. Capps, and J.R. Torricelli, *Age-related calcium changes, oxyradical damage, caspase activation and nuclear condensation in hippocampal neurons in response to glutamate and beta-amyloid.* Exp Gerontol, 2005. **40**(5): p. 426-37.
488. Schoneich, C., D. Pogocki, G.L. Hug, and K. Bobrowski, *Free radical reactions of methionine in peptides: mechanisms relevant to beta-amyloid oxidation and Alzheimer's disease.* J Am Chem Soc, 2003. **125**(45): p. 13700-13.
489. Du, H., L. Guo, X. Wu, A.A. Sosunov, G.M. McKhann, J.X. Chen, and S.S.D. Yan, *Cyclophilin D deficiency rescues Aβ-impaired PKA/CREB signaling and alleviates synaptic degeneration.* Biochim Biophys Acta, 2014. **1842**(12 0 0): p. 2517-27.
490. Du, H., L. Guo, W. Zhang, M. Rydzewska, and S. Yan, *Cyclophilin D deficiency improves mitochondrial function and learning/memory in aging Alzheimer disease mouse model.* Neurobiol Aging, 2011. **32**(3): p. 398-406.

491. Guo, L., H. Du, S. Yan, X. Wu, G.M. McKhann, J.X. Chen, and S.S.D. Yan, *Cyclophilin D Deficiency Rescues Axonal Mitochondrial Transport in Alzheimer's Neurons.* PLoS One, 2013. **8**(1).
492. Fujimoto, K., Y. Chen, K.S. Polonsky, and G.W. Dorn, 2nd, *Targeting cyclophilin D and the mitochondrial permeability transition enhances beta-cell survival and prevents diabetes in Pdx1 deficiency.* Proc Natl Acad Sci U S A, 2010. **107**(22): p. 10214-9.
493. Feng, D., Y. Tang, H. Kwon, H. Zong, M. Hawkins, R.N. Kitsis, and J.E. Pessin, *High-fat diet-induced adipocyte cell death occurs through a cyclophilin D intrinsic signaling pathway independent of adipose tissue inflammation.* Diabetes, 2011. **60**(8): p. 2134-43.
494. Taddeo, E.P., R.C. Laker, D.S. Breen, Y.N. Akhtar, B.M. Kenwood, J.A. Liao, M. Zhang, D.J. Fazakerley, J.L. Tomsig, T.E. Harris, S.R. Keller, J.D. Chow, K.R. Lynch, M. Chokki, J.D. Molkentin, N. Turner, D.E. James, Z. Yan, and K.L. Hoehn, *Opening of the mitochondrial permeability transition pore links mitochondrial dysfunction to insulin resistance in skeletal muscle.* Mol Metab, 2014. **3**(2): p. 124-34.
495. Keep, M., E. Elmér, K.S. Fong, and K. Csiszar, *Intrathecal cyclosporin prolongs survival of late-stage ALS mice.* Brain research, 2001. **894**(2): p. 327-331.
496. Gold, B.G., J. Voda, X. Yu, G. McKeon, and D.N. Bourdette, *FK506 and a nonimmunosuppressant derivative reduce axonal and myelin damage in experimental autoimmune encephalomyelitis: Neuroimmunophilin ligand-mediated neuroprotection in a model of multiple sclerosis.* Journal of neuroscience research, 2004. **77**(3): p. 367-377.
497. Kumar, P. and A. Kumar, *Neuroprotective effect of cyclosporine and FK506 against 3-nitropropionic acid induced cognitive dysfunction and glutathione redox in rat: possible role of nitric oxide.* Neuroscience research, 2009. **63**(4): p. 302-314.
498. Forte, M., B.G. Gold, G. Marracci, P. Chaudhary, E. Basso, D. Johnsen, X. Yu, J. Fowlkes, P. Bernardi, and D. Bourdette, *Cyclophilin D inactivation protects axons in experimental autoimmune encephalomyelitis, an animal model of multiple sclerosis.* Proceedings of the National Academy of Sciences, 2007. **104**(18): p. 7558-7563.
499. *Cyclosporine: A Review.* Journal of Transplantation, 2012. **2012**.
500. Khaspekov, L., H. Friberg, A. Halestrap, I. Viktorov, and T. Wieloch, *Cyclosporin A and its nonimmunosuppressive analogue N-Me-Val-4-cyclosporin A mitigate glucose/oxygen deprivation-induced damage to rat cultured hippocampal neurons.* Eur J Neurosci, 1999. **11**(9): p. 3194-8.
501. Clarke, S.J., G.P. McStay, and A.P. Halestrap, *Sanglifehrin A acts as a potent inhibitor of the mitochondrial permeability transition and reperfusion injury of the heart by binding to cyclophilin-D at a different site from cyclosporin A.* J Biol Chem, 2002. **277**(38): p. 34793-9.
502. Zenke, G., U. Strittmatter, S. Fuchs, V.F. Quesniaux, V. Brinkmann, W. Schuler, M. Zurini, A. Enz, A. Billich, J.J. Sanglier, and T. Fehr, *Sanglifehrin A, a novel cyclophilin-binding compound showing immunosuppressive activity with a new mechanism of action.* J Immunol, 2001. **166**(12): p. 7165-71.

503. Muramatsu, Y., Y. Furuichi, N. Tojo, A. Moriguchi, T. Maemoto, H. Nakada, M. Hino, and N. Matsuoka, *Neuroprotective efficacy of FR901459, a novel derivative of cyclosporin A, in in vitro mitochondrial damage and in vivo transient cerebral ischemia models.* Brain Res, 2007. **1149**: p. 181-90.
504. Azzolin, L., N. Antolini, A. Calderan, P. Ruzza, M. Sciacovelli, O. Marin, S. Mammi, P. Bernardi, and A. Rasola, *Antamanide, a Derivative of Amanita phalloides, Is a Novel Inhibitor of the Mitochondrial Permeability Transition Pore.* PLoS One, 2011. **6**(1).
505. Vorhees, C.V. and M.T. Williams, *Morris water maze: procedures for assessing spatial and related forms of learning and memory.* Nat Protoc, 2006. **1**(2): p. 848-58.
506. Gan, X., S. Huang, L. Wu, Y. Wang, G. Hu, G. Li, H. Zhang, H. Yu, R.H. Swerdlow, J.X. Chen, and S.S. Yan, *Inhibition of ERK-DLP1 signaling and mitochondrial division alleviates mitochondrial dysfunction in Alzheimer's disease cybrid cell.* Biochim Biophys Acta, 2014. **1842**(2): p. 220-31.
507. Yan, S., F. Du, L. Wu, Z. Zhang, C. Zhong, Q. Yu, Y. Wang, L.F. Lue, D.G. Walker, J.T. Douglas, and S.S. Yan, *F1F0 ATP Synthase-Cyclophilin D Interaction Contributes to Diabetes-Induced Synaptic Dysfunction and Cognitive Decline.* Diabetes, 2016. **65**(11): p. 3482-3494.
508. Eliseev, R.A., G. Filippov, J. Velos, B. VanWinkle, A. Goldman, R.N. Rosier, and T.E. Gunter, *Role of cyclophilin D in the resistance of brain mitochondria to the permeability transition.* Neurobiol Aging, 2007. **28**(10): p. 1532-42.
509. Hajnóczky, G. and J.B. Hoek, *Mitochondrial Longevity Pathways.* Science, 2007. **315**(5812): p. 607-609.
510. Wang, Y., L. Wu, J. Li, D. Fang, C. Zhong, J.X. Chen, and S.S. Yan, *Synergistic exacerbation of mitochondrial and synaptic dysfunction and resultant learning and memory deficit in a mouse model of diabetic Alzheimer's disease.* J Alzheimers Dis, 2015. **43**(2): p. 451-63.
511. Halestrap, A.P., *The C Ring of the F1Fo ATP Synthase Forms the Mitochondrial Permeability Transition Pore: A Critical Appraisal.* Front Oncol, 2014. **4**.
512. Giorgio, V., E. Bisetto, M.E. Soriano, F. Dabbeni-Sala, E. Basso, V. Petronilli, M.A. Forte, P. Bernardi, and G. Lippe, *Cyclophilin D Modulates Mitochondrial F(0)F(1)-ATP Synthase by Interacting with the Lateral Stalk of the Complex.* J Biol Chem, 2009. **284**(49): p. 33982-8.
513. Chinopoulos, C., C. Konràd, G. Kiss, E. Metelkin, B. Töröcsik, S.F. Zhang, and A.A. Starkov, *Modulation of F(0)F(1)-ATP synthase activity by cyclophilin D regulates matrix adenine nucleotide levels.* Febs j, 2011. **278**(7): p. 1112-25.
514. Currais, A., M. Prior, D. Lo, C. Jolivalt, D. Schubert, and P. Maher, *Diabetes exacerbates amyloid and neurovascular pathology in aging-accelerated mice.* Aging Cell, 2012. **11**(6): p. 1017-26.
515. Jolivalt, C.G., R. Hurford, C.A. Lee, W. Dumaop, E. Rockenstein, and E. Masliah, *Type-1 diabetes exaggerates features of Alzheimer's disease in APP transgenic mice.* Exp Neurol, 2010. **223**(2): p. 422-31.
516. Macauley, S.L., M. Stanley, E.E. Caesar, S.A. Yamada, M.E. Raichle, R. Perez, T.E. Mahan, C.L. Sutphen, and D.M. Holtzman, *Hyperglycemia modulates*

extracellular amyloid-beta concentrations and neuronal activity in vivo. J Clin Invest, 2015. **125**(6): p. 2463-7.
517. Yang, Y., Y. Wu, S. Zhang, and W. Song, *High glucose promotes Abeta production by inhibiting APP degradation.* PLoS One, 2013. **8**(7): p. e69824.
518. Burdo, J.R., Q. Chen, N.A. Calcutt, and D. Schubert, *The pathological interaction between diabetes and presymptomatic Alzheimer's disease.* Neurobiol Aging, 2009. **30**(12): p. 1910-7.
519. Mehla, J., B.C. Chauhan, and N.B. Chauhan, *Experimental induction of type 2 diabetes in aging-accelerated mice triggered Alzheimer-like pathology and memory deficits.* J Alzheimers Dis, 2014. **39**(1): p. 145-62.
520. Takeda, S., N. Sato, K. Uchio-Yamada, K. Sawada, T. Kunieda, D. Takeuchi, H. Kurinami, M. Shinohara, H. Rakugi, and R. Morishita, *Diabetes-accelerated memory dysfunction via cerebrovascular inflammation and Aβ deposition in an Alzheimer mouse model with diabetes.* Proc Natl Acad Sci U S A, 2010. **107**(15): p. 7036-41.
521. Lam, C.K., W. Zhao, G.S. Liu, W.F. Cai, G. Gardner, G. Adly, and E.G. Kranias, *HAX-1 regulates cyclophilin-D levels and mitochondria permeability transition pore in the heart.* Proc Natl Acad Sci U S A, 2015. **112**(47): p. E6466-75.